INFORMATION TO USERS

This manuscript has been reproduced from the microfilm master. UMI films the text directly from the original or copy submitted. Thus, some thesis and dissertation copies are in typewriter face, while others may be from any type of computer printer.

The quality of this reproduction is dependent upon the quality of the copy submitted. Broken or indistinct print, colored or poor quality illustrations and photographs, print bleedthrough, substandard margins, and improper alignment can adversely affect reproduction.

In the unlikely event that the author did not send UMI a complete manuscript and there are missing pages, these will be noted. Also, if unauthorized copyright material had to be removed, a note will indicate the deletion.

Oversize materials (e.g., maps, drawings, charts) are reproduced by sectioning the original, beginning at the upper left-hand corner and continuing from left to right in equal sections with small overlaps.

UMI®

Volcanology, Geochemistry, and Tectonic Setting of Late Paleozoic Volcanic
Formations in the Northern Canadian Cordillera: a Key to Understanding
the Evolution of Pericratonic Terranes

by

Renée-Luce Simard

Submitted in partial fulfillment of the requirements
for the degree of Doctor of Philosophy

at

Dalhousie University
Halifax, Nova Scotia
July, 2005

DALHOUSIE UNIVERSITY

To comply with the Canadian Privacy Act the National Library of Canada has requested that the following pages be removed from this copy of the thesis:

Preliminary Pages
Examiners Signature Page (pii)
Dalhousie Library Copyright Agreement (piii)

Appendices
Copyright Releases (if applicable)

Table of Contents

List of Figures

List of Tables

List of Plates

Abstract

This thesis presents geochemical and volcanological studies of two late Paleozoic sequences of the pericratonic Yukon-Tanana terrane of the northern Canadian Cordillera, the Mississippian to mid-Pennsylvanian Little Salmon formation and the Mississippian to Permian Klinkit Group. It provides insights that unravel the tectonic evolution of the western margin of Laurentia in late Paleozoic time.

Rocks of the Little Salmon formation are well exposed in central Yukon. The lower part of the Little Salmon magmatic sequence consists of Mississippian quartz-feldspar phyric felsic rocks. These calc-alkaline rocks probably represent high-level intrusions formed by crustal melting in a continental arc setting, the Little Kalzas-Little Salmon arc. Conformably overlying these felsic rocks is a thick pile of asthenosphere-derived alkali basalts ($\varepsilon_{Nd}=+7.5$) showing both proximal and distal volcanic lithofacies. It records seamount formation atop an extensional synvolcanic fault associated with the development of a rift basin(s) during the rifting of the Little Kalzas-Little Salmon continental arc system. This rifting resembles that of the modern Izu-Bonin-Mariana arc and the proto-Japan island arc extension and thinning.

The Klinkit Group is well exposed in northern British Columbia and southern Yukon. It is characterized at its base by a thick Mississippian to Early Pennsylvanian carbonate unit and overlain by abundant Permian primitive arc-derived volcaniclastic rocks ($\varepsilon_{Nd}=+6.7$ to 7.4). These thick volcaniclastic sequences represent megaturbidite deposits emplaced in a subsiding basin near active volcano(es), the Klinkit arc. Localized alkali basalts suggest intra-arc rifting event(s). The Klinkit Group closely resembles the basement of the Mesozoic Quesnel arc terrane; however, it also has characteristics similar to sequences of the pericratonic Yukon-Tanana terrane. The similarity suggests that the basement of the Mesozoic arc of the Quesnel terrane is the pericratonic Yukon-Tanana terrane or its southern equivalent.

Tectonic pulses along the late Paleozoic western margin of Laurentia have been driven by oblique continent-continent collisions on the other margins of the continent, first in Late Silurian-Early Devonian time, then in Carboniferous time. These collisions affected the translation and rotation of Laurentia, forcing plate boundary reorganization along its west margin, hence controlling the formation and tectonic evolution of the pericratonic systems throughout late Paleozoic time.

Acknowledgements

Chapter 1

Introduction

This thesis studies the tectono-magmatic evolution of two arc systems within the pericratonic Yukon-Tanana terrane, northern Canadian Cordillera, as a means to better understand the tectonic evolution of the late Paleozoic pericratonic systems of the west margin of Laurentia. Using field mapping, detailed stratigraphic and physical volcanology work and geochemical and isotopic analyses, this thesis presents evidence that the late Paleozoic pericratonic arc systems of the Yukon-Tanana terrane represent complex arc/backarc/basin systems that evolved from rifted continental arc (Little Salmon – Little Kalzas; Chapters 2-3) to island-arc (Klinkit; Chap. 4), from Mississippian to Permian time, in relative proximity to Laurentia. These systems formed during a period of major extension along the west coast of Laurentia at a time of major collisions on the other margins of the continent. Chapter 5 explores the potential tectonic links between these events.

1.1 Late Paleozoic island-arc systems on the west coast of Laurentia

The west margin of the Laurentia (now the North American continent) was characterized by active subduction processes since the mid-Devonian time (Engebretson et al., 1992; Monger, 1999). At first Laurentia was relatively static with respect to the subduction zone (continental arc magmatism) or moved away from it (island arc magmatism; Monger, 1999). This situation lasted until a major plate reorganization in Early Mesozoic time after which the newly formed North American continent started moving toward and over the subduction zone (North American Cordilleran Orogen; opening of the Atlantic Ocean; Monger, 1999).

Despite the relative immobility of the Laurentia in late Paleozoic time with reference to the subduction zone on its west margin, this margin was far from being passive. The rocks of the inner part of the North American Cordillera, especially in the northern Canadian Cordillera, recorded a complex sequence of extensional and compressional events most likely involving part of the Proterozoic-Cambrian passive margin of the continent, as well as formation of arc-back-arc systems in close proximity to the margin (pericratonic terranes; Monger, 1999).

These arc systems and their associated basins were accreted to the west margin of the newly formed North American continent in Early Mesozoic following the break-up of Pangea and the opening of the Atlantic Ocean; they now form the pericratonic terrane belt of the northern Canadian Cordillera. Important volcanogenic massive sulfide deposits occur within these systems (e.g. Kudz Ze Kayah; Piercey et al., 2001b).

1.2 Statement of problem

The tectono-magmatic evolution of the late Paleozoic pericratonic island-arc systems of the west margin of Laurentia is not well understood, particularly in the northern Canadian Cordillera, because of a strong metamorphic overprint, structural complexity and difficult access. Their respective volcanic stratigraphy as well as their tectonic relationship within each terrane are poorly known.

The Yukon-Tanana terrane of the northern Canadian Cordillera (Yukon Territory and northern British Columbia) is one of the best areas for unravelling the tectonic evolution of this dynamic stage of the western margin of Laurentia. The Yukon-Tanana terrane records the development of a series of Devono-Carboniferous arc edifices built in places upon metasedimentary basement, and punctuated by episodic arc rifting magmatism, back-arc formation, intra-arc deformation and local uplift and erosion (Colpron et al., in press; Piercey et al., 2002; Piercey et al., 2001a; Piercey et al., 2001b). Despite important metamorphic and structural overprints, these rocks are very well-preserved and exposed

2

in parts of the Yukon-Tanana terrane. This preservation and exposure allow for detailed studies of one or more of the late Paleozoic volcano-sedimentary sequences.

1.3 Objectives

i)   To document the geochemistry, petrography and volcanology of two late Paleozoic volcano-sedimentary sequences of the pericratonic Yukon-Tanana terrane, northern Canadian Cordillera;

ii) To determine their respective magmatic evolution and original tectonic setting;

iii) To evaluate their tectonic relationship.

iv) To document the evolution through time of the pericratonic systems of the Yukon-Tanana terrane;

v)   To unravel the late Paleozoic tectonic evolution of the pericratonic systems of the west margin of Laurentia in the northern Canadian Cordillera;

vi) To assess tectonic events that might have triggered the tectonic pulses observed on the west coast of Laurentia throughout the late Paleozoic.

1.4 Methodology and thesis organization

This thesis presents geochemical and volcanological studies of two late Paleozoic sequences of the Yukon-Tanana terrane, the Mississippian to mid-Pennsylvanian Little Salmon formation, central Yukon, and the Mississippian to Permian Klinkit Group, southern Yukon and northern British Columbia. It discusses their respective magmatic evolution and original tectonic setting. It also evaluates their tectonic relationship, and their evolution through time with respect to other coeval arc-backarc systems of the Yukon-Tanana terrane and of other parts the North American Cordillera.

Chapter 2 documents the stratigraphy and geochemistry of the Little Salmon formation and suggests interpretations on its depositional and tectonic setting. Chapter 3 consists of a lithofacies analysis of the upper succession of the Little Salmon formation, and provides important information about the eruption styles and type of volcanic edifices present at that time within the Little Salmon arc system. Chapter 4 establishes the Klinkit Group stratigraphy, describes its geochemistry and defines its original tectonic setting within the Canadian Cordillera. Chapter 5 presents an overall of the tectonic history of Laurentia in Paleozoic time and its potential effects on the evolution of its western margin.

Detailed lithofacies mapping was conducted at a scale of roughly 1:5 000 for the Little Salmon formation with the collaboration of the Yukon Geological Survey under the Ancient Pacific Margin NATMAP Project in the Glenlyon area, central Yukon. Extensive sampling was conducted throughout the mapping campaign. Representative samples from major/characteristic units were analyzed for major, trace, and rare earth elements, as well as Nd, and Sr isotopes to further characterize these units (see Chapter 2 for details on analytical techniques). Appendix 1 presents descriptions of representative rock types from the Little Salmon formation.

For the Klinkit Group, regional mapping was conducted at a scale of 1:50 000 under the Ancient Pacific Margin NATMAP Project in northern British Columbia and southern Yukon in collaboration with the Geological Survey of Canada, in order to evaluate its regional extent and define its stratigraphy. Specific localities were chosen for detailed stratigraphic analyses where preservation state and exposures were optimal. Just as for the Little Salmon formation, extensive sampling was conducted throughout the mapping campaign. Representative samples from major/characteristic units were analyzed for major, trace, and rare earth elements, as well as Nd isotopes to further characterize these units (see Chapter 4 for details on analytical techniques). Appendix 4 presents descriptions of representative rock types from the Klinkit Group.

Chapters 2 and 3 are manuscripts that document the Little Salmon formation and are ready for submission to peer-reviewed journals. Chapter 4 is the manuscript of Simard et al. (2003) published in Canadian Journal of Earth Sciences in July 2003 that documents the Klinkit Group. These three chapters raised questions about the tectonic diversity observed within all the pericratonic terranes in late Paleozoic time along the west coast of Laurentia. Chapter 5, with its review of the tectonic history of Laurentia in Paleozoic time and its implication for the tectonic evolution of its west coast, discusses some of these questions. This last chapter is intended to be the base of a future manuscript on the formation and evolution of the late Paleozoic pericratonic terranes of the west coast of Laurentia.

Chapter 2

Intra-arc rift basin development within a Mississippian continental arc system; example from the pericratonic terranes of the northern Canadian Cordillera, Yukon Territory, Canada[1]

2.1 Introduction

In early Mesozoic time, numerous arcs and basins accreted to the western margin of Laurentia, however, little is known about their initial distribution, geometry, extent, and nature. The oldest of these arc-basin systems were the first to accrete to the continent, and form the pericratonic terrane belt (Fig. 2-1). One of the most prominent of these pericratonic terranes, the Yukon-Tanana terrane in the northern Canadian Cordillera (Fig. 2-1), records the development of a series of Devono-Carboniferous arc edifices built in places upon metasedimentary basement, and punctuated by episodic arc rifting magmatism, back-arc formation, intra-arc deformation and local uplift and erosion (Colpron et al., in press-b; Piercey et al., 2002; Piercey et al., 2001a; Piercey et al., 2001b). Important volcanogenic massive sulfide deposits occur within these arc-backarc systems (e.g. Kudz Ze Kayah; Piercey et al., 2001b).

An understanding of the original tectonic setting of these complex arc systems is essential for unravelling the late Paleozoic tectonic evolution of the western margin of Laurentia. One of the best places to study the evolution of these systems is the Glenlyon area, central Yukon Territory, Canada, where the Yukon-Tanana terrane geology provides a unique opportunity to document the rifting of two Early Carboniferous arc systems, the Little Kalzas and Little Salmon arcs.

---

[1] Simard, R.L., Dostal, J., and Colpron, M. in prep. Manuscript ready to be submitted to Journal of Geology in August 2005. At this stage, as the first author, RL Simard wrote the entire manuscript and drafted most of the figures. The coauthors suggested corrections to the manuscript.

6
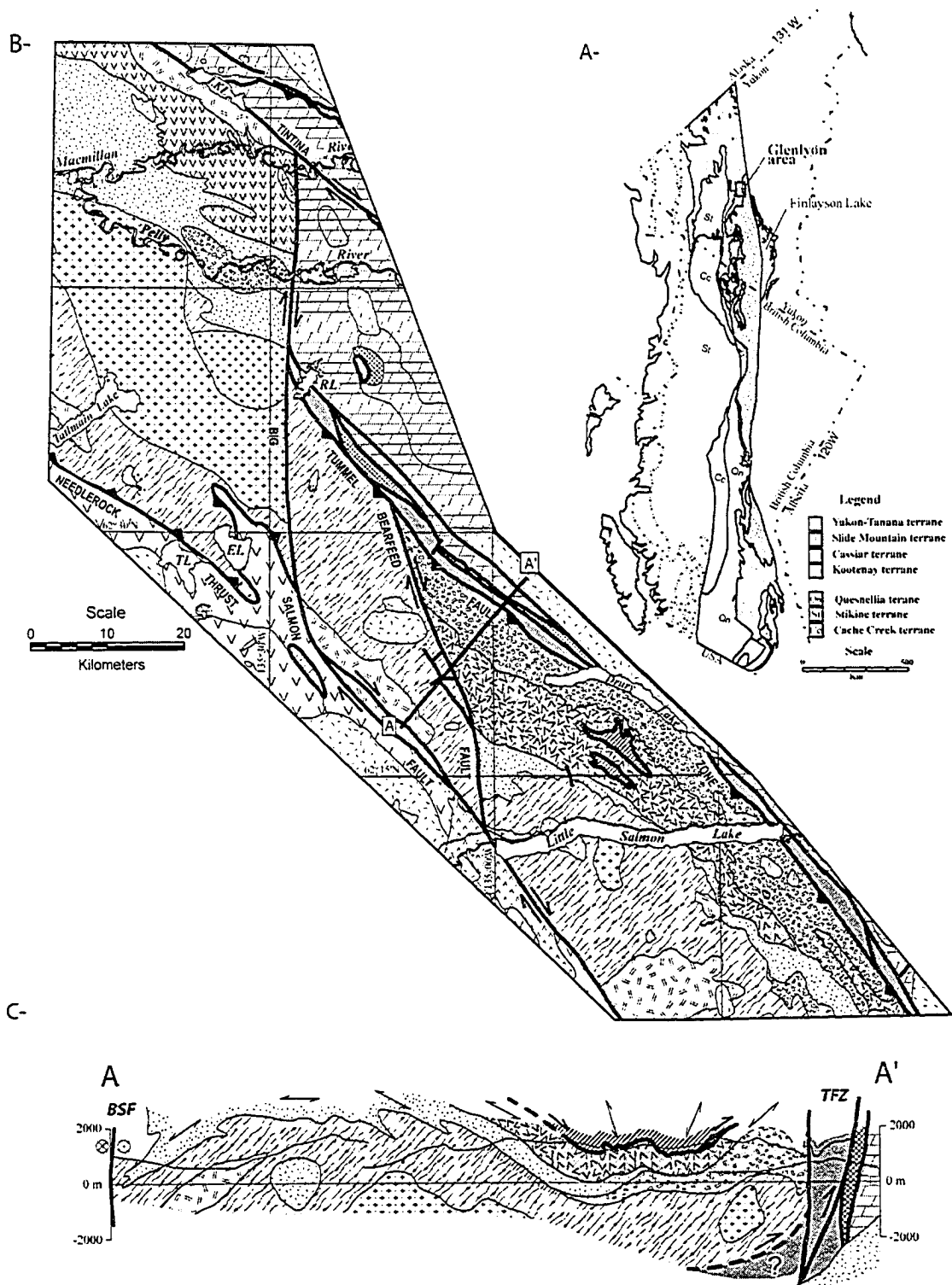
Figure 2-1 – Location map. A- Generalized terrane map of the eastern Canadian Cordillera, showing the pericratonic terrane belt (modified from Wheeler, 1991), B- Generalized geological map of the Yukon-Tanana terrane in the Glenlyon area, central Yukon (modified from Colpron et al., 2003; see next page for legend), C- Cross-section of the Yukon-Tanana rocks of the Glenlyon area showing the broad synclinorium structure in the area (modified from Colpron et al., in press-a). BSF: Big Salmon Fault, TFZ: Tummel Fault Zone

LEGEND

Late Cretaceous - Tertiary volcanic rocks

Mesozoic pluton

Permian - Triassic (?) synorogenic clastic rocks

SLIDE MOUNTAIN ASSEMBLAGE

Pennsylvanian - Permian chert & volcanic rocks: gabbro

SEMENOF BLOCK

Pennsylvanian granodiorite / tonalite / volcanic rocks

BEARFEED ALLOCHTONS

Paleozoic ? turbidite

NORTH AMERICAN MIOGEOCLINE

Early to Late Paleozoic sandstone, carbonate, shale, conglomerate

YUKON-TANANA TERRANE

Little Salmon Formation

Little Kalzas Formation

Pelmac Formation

Drury Formation

Snowcap Complex

Little Salmon plutonic suite

Early Mississippian gabbro

Little Kalzas plutonic suite

This paper provides stratigraphic, geochemical and isotopic evidence that document the rifting of the Early Carboniferous Little Kalzas-Little Salmon continental arc system, and recognize for the first time the development of an intra-arc rift basin stratigraphy with structurally controlled alkali-basalt seamounts and hydrothermal field. Recognizing these elements is essential to the paleogeographic reconstruction of these complex and rapidly evolving environments, and helps to assess whether or not Paleozoic rifted arcs formed in settings similar to those of today.

2.2 Regional geology

The Canadian Cordillera is generally considered to be a tectonic collage that results from the last ca. 400 Ma of subduction along the west coast of the Laurentian/North American continent (e.g. Coney et al., 1980; Gabrielse and Yorath, 1991). It is composed of Paleozoic and Mesozoic accreted terranes of mainly island arc and ocean floor affinity to the west, and passive margin deposits to the east (Monger, 1999). These terranes accreted to the western margin of the continent starting in the Mesozoic (e.g. Gabrielse and Yorath, 1991) and were subsequently intruded by major late Mesozoic-early Tertiary magmatism as a result of the ongoing subduction (e.g. Monger, 1999; Monger et al., 1982).

The inner portion of the Canadian Cordillera is dominated by the Proterozoic to Paleozoic Laurentian continental margin and a belt of accreted, mainly pericratonic terranes (Gabrielse et al., 1991). In the Yukon Territory, this inner belt is mostly

8

composed of the Yukon-Tanana terrane, a package of variably metamorphosed sedimentary and volcanic successions of Devonian and Carboniferous ages (Colpron et al., 2003; Mortensen, 1992), Laurentian continental margin rocks, along with minor oceanic rocks of the Slide Mountain terrane.

The stratigraphy of the Yukon-Tanana terrane in the study area includes (Fig. 2-2): (1) a pre-Devonian metasedimentary basement complex, the Snowcap Complex, unconformably overlain by (2) Late Devonian-early Mississippian clastic rocks, the Drury and Pelmac formations, in turn conformably overlain by the (3) Carboniferous volcanic and sedimentary rocks, the Little Kalzas and Little Salmon formations (Colpron et al., in press-b; Colpron et al., 2003).

The *Snowcap complex* comprises predominantly polydeformed and metamorphosed schist, quartzite, and calc-silicate rocks, which typically have amphibolite-grade metamorphic mineral assemblages (Fig. 2-2; Colpron et al., in press; Colpron et al.,2003). Subordinate coarse-grained garnet amphibolites have geochemical characteristics of enriched mid-ocean ridge basalts (E-MORB) to transitional within-plate tholeiites (Colpron et al., 2003). The predominantly quartz-rich siliciclastic and pelitic nature of the metasedimentary rocks of this complex, as well as the geochemical character of the associated metavolcanic rocks, suggests a rifted continental margin setting (Colpron et al., in press-b).

The *Drury formation*, which unconformably overlies the Snowcap Complex, is an Upper Devonian to lower Mississippian (Fig. 2-2; Colpron et al., in press-b) immature clastic sequence (Colpron, 1999a; Colpron, 1999b; Colpron et al., 2003) capped by tuffaceous volcaniclastic rocks, and quartz-feldspar porphyry (dated ca. 350 Ma; Colpron et al., in press-b; Gladwin et al., 2003). Detrital zircons from the arkosic grit beds have yielded primarily Late Devonian U/Pb ages, suggesting the erosion of a Late Devonian magmatic arc source (Fig. 2-2; Colpron et al., in press-b).
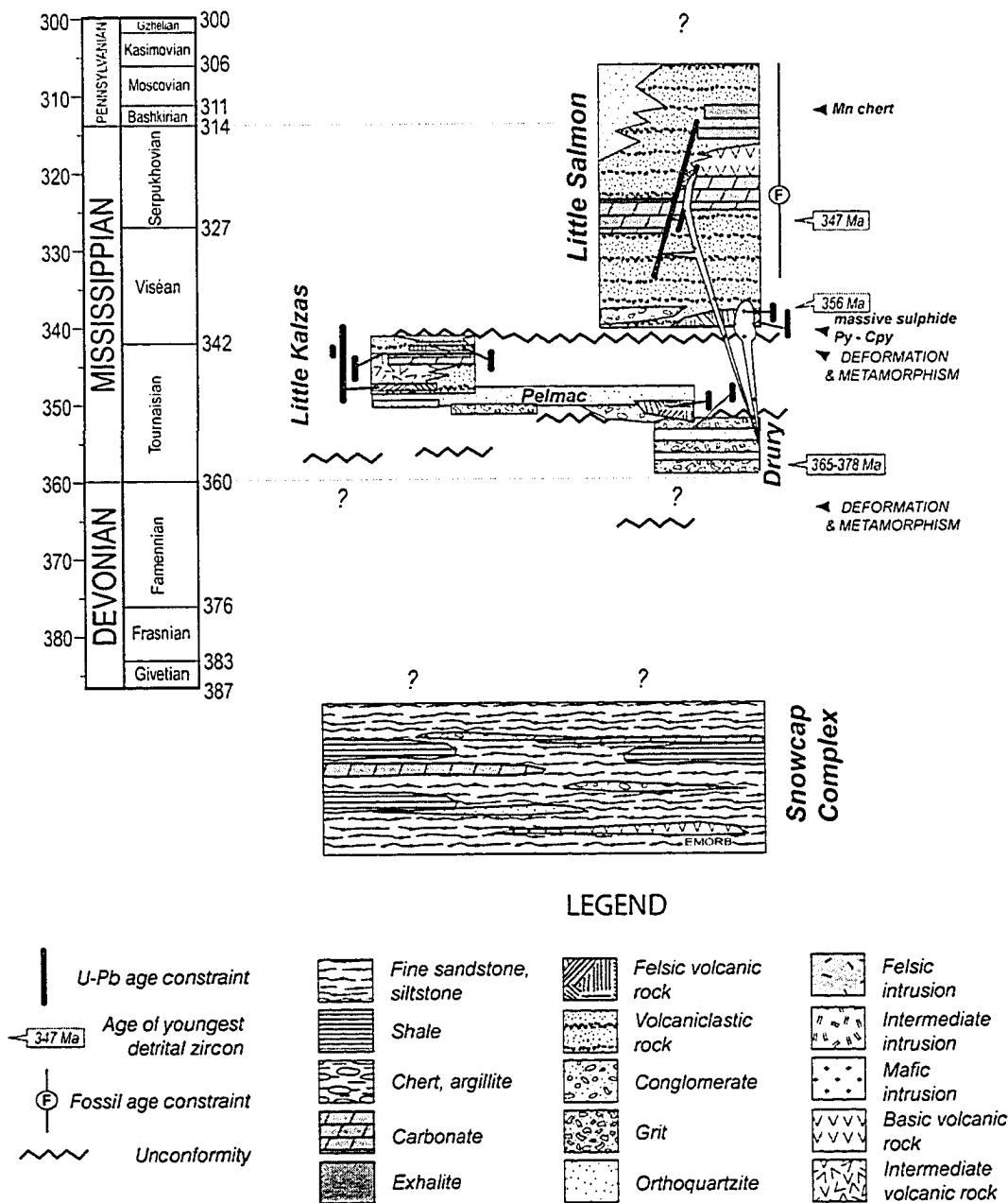
Figure 2-2 – Stratigraphic relations of Yukon-Tanana composite terrane in the Glenlyon area (modified from Colpron et al., in press-b)

The *Pelmac formation* unconformably overlies both the Drury formation and the Snowcap Complex (Fig. 2-2). The Pelmac formation consists of mature quartzarenite with minor alkali mafic volcanic rocks of within-plate affinity (Colpron, 2001). These

10

mature quartz-rich sediments likely represent mature shallow marine deposits (e.g. beaches) derived from recycled evolved continental source (Colpron et al., in press-b).

All of these siliciclastic rocks are conformably overlain by the Carboniferous volcanic and sedimentary rocks of the Little Kalzas and Little Salmon formations.

2.2.1 Stratigraphy and petrography of the Carboniferous volcanic sequences

2.2.1.1 Little Kalzas formation

The *Little Kalzas formation* is a lower Mississippian (345-346 Ma; Colpron et al., in press-b) arc-derived volcano-sedimentary sequence which conformably overlies the Pelmac formation (Fig. 2-2). It is composed, from bottom to top, of several meters of massive plagioclase-phyric andesite locally interbedded with minor rhyolite. The andesites pass both upward and laterally into sequences of volcaniclastic sandstone and argillite. A band of Early Carboniferous bioclastic limestone covers this lower volcanic package. Above the limestone, the Little Kalzas formation is dominated by clastic and volcaniclastic deposits with minor porphyritic andesites and alkali basalts (Fig. 2-2; Colpron, 1998; Colpron, 2001; Colpron et al., in press-b). Associated with these volcanic rocks is the widely distributed Little Kalzas plutonic suite of Early Mississippian age, interpreted as subvolcanic intrusions of the Little Kalzas arc, which consists predominantly of granodiorite, tonalite and diorite, with minor locally K-feldspar megacrystic granite (Colpron et al., in press-b).

The rocks of the Little Kalzas formation are heavily deformed at the outcrop scale and metamorphosed to amphibolite facies metamorphism. No primary mineralogy is preserved in these rocks and preservation of primary textures is minimal. This precludes further detailed lithofacies analyses of this sequence.

2.2.1.2 Little Salmon formation

The *Little Salmon formation* is a Mississippian to mid-Pennsylvanian (?) sequence of felsic and mafic volcanic rocks that sits unconformably on the Drury formation to the east, and on the Pelmac formation to the west (Figs. 2-2 and 2-3; Colpron, 2001; Colpron et al., 2003). It occupies a broad NW-SE synclinorium along Little Salmon Lake (Figs. 2-1 and 2-3). Rocks in the study areas are typically folded at the outcrop scale and display one to two well developed foliations that, in places, obscure the primary texture. The primary mineralogy is not preserved in the mafic volcanic rocks that have all been affected by low grade greenschist facies metamorphism as indicated by the mineral assemblage chlorite +muscovite +calcite ±actinolite ±biotite ±apatite ±quartz. Here the prefix 'meta' is omitted for simplicity.

The Little Salmon volcano-sedimentary sequence comprises a "lower succession" of felsic volcaniclastic and few massive volcanic rocks (Colpron et al., in press-b; Colpron et al., 2000), and an "upper succession" of mafic volcanic and volcaniclastic rocks (Figs. 2-3 and 2-4); a prominent late Mississippian to mid-Pennsylvanian bioclastic limestone unit separates the two successions (Figs. 2-3 and 2-4). Associated with the volcanic rocks of the Little Salmon formation, are dioritic, granodioritic, and gabbroic subvolcanic plutons of the mid-Mississippian Little Salmon plutonic suite (338-340 Ma; Colpron et al., in press-b) that intruded the Snowcap Complex and the Pelmac and Drury formations (Figs. 2-1B and 2-3).

Lower succession – On the west flank of the synclinorium the lower succession sits unconformably on the Pelmac formation (Figs. 2-1 and 2-2). Its base is characterized locally by a <5 m thick discontinuous conglomerate (Fig. 2-4; Colpron et al., in press-b; Gladwin et al., 2003). Ten to 150 m of coherent quartz-feldspar porphyritic felsic rocks mark the base of the volcanic pile (Figs. 2-3 and 2-4; ca. 340 Ma; Colpron et al., in press-b; Colpron et al., 2003), and host a small massive sulphide occurrence (Colpron, 1999b). These rocks are interpreted as flows or high-level intrusions, but the rocks are deformed and no margins are exposed so that flows or intrusive relationships are obscured. Above these felsic volcanic rocks is a 40 m – 300 m thick section of volcaniclastic sandstone and
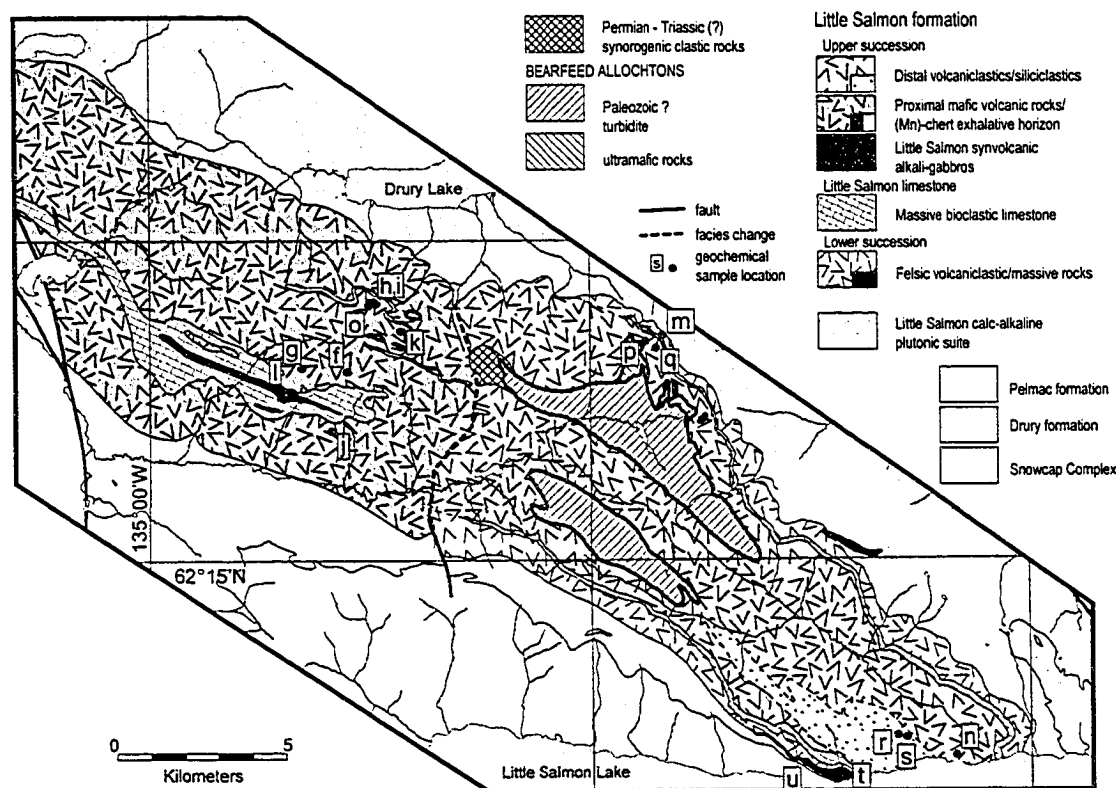
Figure 2-3 — Lithofacies distribution map of the Little Salmon formation. The rocks of the upper succession of the Little Salmon formation show an abrupt proximal versus distal volcanic facies change across a presumed syn-volcanic fault in the area (N-S dotted line). Table 2-1 presents geochemical data of the samples located on this map. Modified from Colpron (2000).

siltstone. Small cm-thick mafic dykes cross-cut the massive felsic rocks, most likely feeder dykes to the overlying mafic volcanism of the upper succession (see "Upper succession" for details).

On the east flank of the synclinorium the lower succession is thinner and not as well exposed and constrained. The exposed sections do not present any massive volcanic rocks, and the volcaniclastic rocks are interbedded with siliciclastic/epiclastic intervals very similar to the underlying Drury formation clastic units, making distinction between them difficult. A single sill of massive coarse grained gabbro is concordant within the stratigraphy of the lower succession at its northernmost exposure (sample location (m) on Fig. 2-3; Fig. 2-4).

13
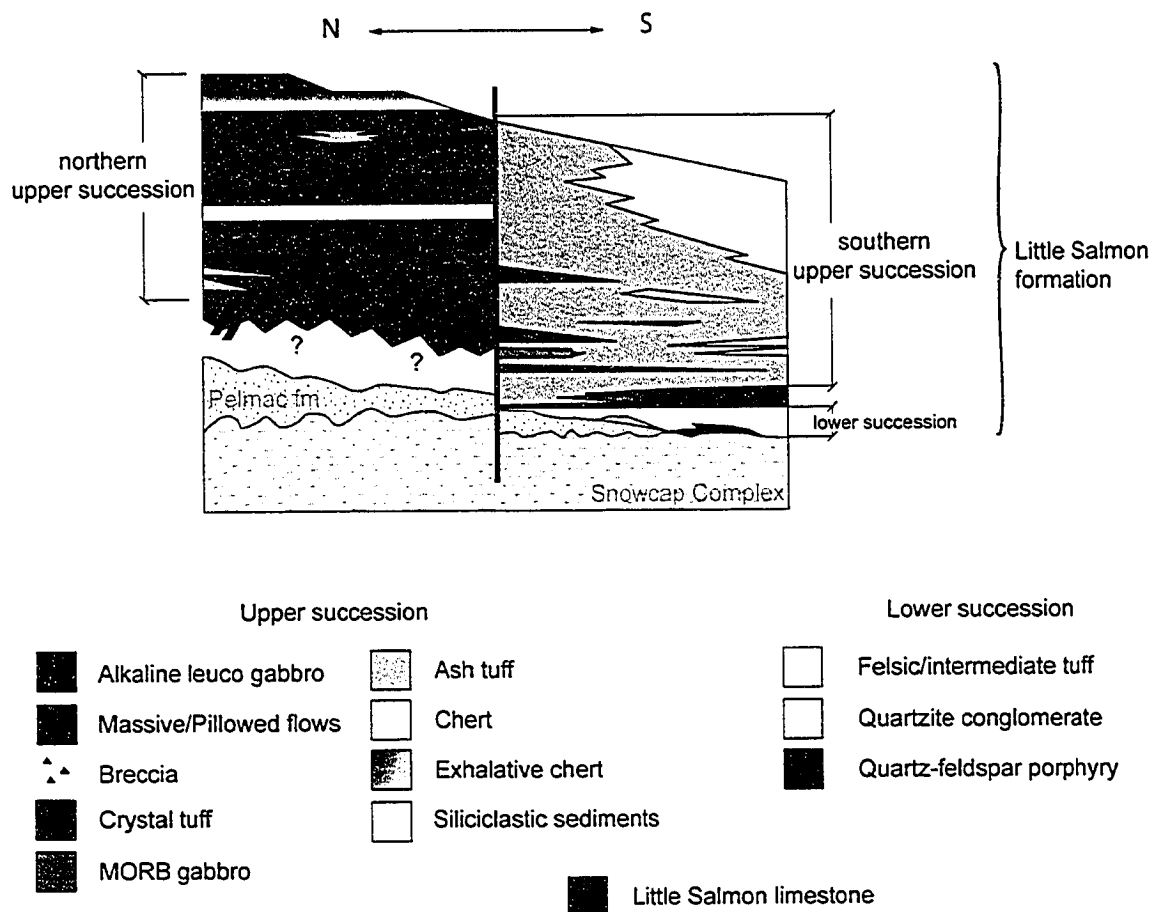
Figure 2-4 – Generalized stratigraphy of the Little Salmon formation.

Little Salmon limestone – A limestone unit conformably overlies the lower succession (Fig. 2-4). On the west side of the synclinorium. this limestone is mainly massive. and contains echinoderm columnals and corals of late Mississippian to mid-Pennsylvanian age (E.W. Bamber in Colpron and Reinecke. 2000). On the eastern flank of the synclinorium the base of the limestone is gradational from black calcareous shale. grading into shaly limestone interbedded with limestone granule and pebble conglomerate and finally massive limestone (calcarenite?) locally bioclastic. Northward the Little Salmon limestone thins or splits into several thinner beds of locally bioclastic limestone interbedded with tuffaceous layers (Figs. 2-3 and 2-4).

14

In the northern exposure of the Little Salmon formation the limestone occurs in the core of a secondary anticlinal structure; the limestone unit is highly recrystallized, does not preserve any primary texture, and is intruded by a leucocratic gabbro (Figs. 2-3 and 2-4).

Upper succession – Sitting conformably atop the Little Salmon limestone, the upper succession consists of a package of alkali basaltic rocks showing important facies changes along strike, from solely proximal in the north, to solely distal in the south (Figs. 2-3 and 2-4; Colpron, 2001; Chap. 3).

In the north (Fig. 2-3), the "northern" upper succession volcanic stratigraphy exposes highly porphyritic massive and pillowed lava flows with abundant associated breccia, crystal-tuff and ash-tuff volcaniclastic strata, localized exhalative strata and minor quartz-rich clastic strata (northern upper succession, Fig. 2-4). In the south, along the north shore of Little Salmon Lake, the "southern" upper succession volcanic stratigraphy consists of a thick pile of crystal and ash-tuff interbedded with abundant clastic strata, without any massive volcanic rock (southern upper succession, Fig. 2-4). These mafic rocks seem associated with one or more leucocratic gabbroic bodies, as well as sparse thin mafic dykes.

The boundary between the northern and the southern upper succession is abrupt and aligned with a small SW-NE fault of same attitude that cuts the underlying Little Salmon limestone, Little Salmon lower succession, Pelmac formation and Snowcap Complex on the west flank of the synclinorium (see "facies change" dashed-line on Fig. 2-3).

2.3 Geochemistry of the Carboniferous volcanic sequences

2.3.1 Analytical techniques, alteration, and sampling

Forty-six representative rock samples were selected for geochemical analyses from a suite of over 200 specimens collected during the mapping of the Little Salmon formation. Major and trace-element compositions of 13 representative samples from the Little

15

Salmon formation are given in Table 2-1; in addition, two samples from the Drury formation and three from the Little Kalzas formation are presented for reference. See Appendix 2 for additional analyses for the Little Salmon formation, as well as Colpron (2001) for more analyses of the Little Kalzas and Little Salmon formations. Where referred to in the text, all majors are reported as volatile-free (recalculated).

Major element concentrations in the samples used during this study were determined by X-ray fluorescence (XRF), trace elements and rare earth elements (REE) were analyzed by inductively coupled mass spectrometry (ICP-MS; using fusion for samples dissolution), and Sc was analyzed by instrumental neutron activation analysis (INAA) at Activation Laboratories Ltd., Ancaster, Ontario. Analytical error for the XRF method is <1% for major elements. For trace elements, precision is better than 6%, and analytical error is better than 5% (Young, 2002).

Twelve of these samples, eight from the Little Salmon formation, one from the Drury formation, and three from the Little Kalzas formation were subsequently selected for Nd and Sr isotope analysis. Sm and Nd concentrations and Sr and Nd isotopic compositions were analyzed using a multicollector Finnigan Mat 262 mass spectrometer at the Analytical Geochemistry Group laboratory, Memorial University of Newfoundland, St. John's, Newfoundland (Appendix 3). The epsilon Nd (ε_{Nd}) values are calculated using $^{147}Sm/^{144}Nd = 0.1967$ and $^{143}Nd/^{144}Nd = 0.512638$ values for the present-day chondrite uniform reservoir (CHUR). The ^{147}Sm decay constant is $6.54 \ 10^{-12} \ y^{-1}$ (Steiger and Jaeger, 1977). The model Nd ages are calculated with respect to a depleted mantle (DM) with an $\varepsilon_{Nd(0)}$ value of +10 isolated from the CHUR since 4.55 Ga following a linear evolution (T_{DM}; Table 2-2). In some cases, the Sr values seem affected by local alteration showing anomalous isotopic Sr ratios (Table 2-2); these results are therefore not considered here.

Although primary mineralogy is rarely preserved in the Little Salmon formation because of the low grade greenschist facies metamorphism, and is absent from the Little Kalzas formation because of the amphibolite facies metamorphism, most major elements, high

16

Table 2-1 - Representative analyses of the Drury, Little Kalzas and Little Salmon formations

	Drury formation		Little Kalzas formation			Little Salmon formation		
						Upper succession		
			Granodiorite	Rhyolite	Andesite	Volcaniclastic rocks		
						(f)	(g)	(h)
SAMPLE	RL02-1-1	RL02-17-10	98MC119	98MC125	98MC067	RL02-5-10	RL02-5-8D	RL02-4-7B
SiO_2 (%)	67.14	68.14	59.05	75.19	59.17	47.30	45.13	47.76
Al_2O_3	14.31	14.30	15.81	13.56	18.48	14.69	17.52	16.46
Fe_2O_3	4.35	5.05	7.94	1.31	5.84	9.25	8.15	11.17
MnO	0.09	0.07	0.14	-	0.17	0.19	0.20	0.23
MgO	2.26	1.19	4.28	0.85	1.84	2.45	4.17	4.90
CaO	2.29	5.32	7.59	0.04	4.55	9.79	12.67	9.89
Na_2O	4.64	2.32	2.13	0.09	3.82	6.49	3.28	2.96
K_2O	1.47	0.96	0.44	6.4	5.11	0.15	0.79	0.84
TiO_2	0.40	0.49	0.40	0.12	0.83	2.59	1.57	2.08
P_2O_5	0.07	0.09	0.04	0.04	0.34	0.64	0.32	0.74
LOI	2.94	1.55	3.01	1.79	0.70	6.83	6.21	2.88
TOTAL	99.95	99.49	100.82	99.39	100.86	100.36	100.01	99.88
Cr (ppm)	-	-	-	-	90	101	277	185
Ni	-	-	-	-	-	26	106	77
Co	10	8	26	-	24	29	39	36
V	75	61	184	-	214	268	215	170
Zn	80	53	72	21	242	133	114	113
Cu	66	56	-	-	75	111	192	113
Rb	42	30	11	151	127	2	16	19
Ba	403	505	160	2615	1786	24	135	269
Sr	125	222	170	20	318	224	437	628
Ga	15	15	16	17	22	14	19	20
Ta	0.62	0.52	0.14	1.09	0.88	2.71	1.51	4.55
Nb	6.17	8.32	2.30	13.00	13.00	42.14	28.83	73.20
Hf	3.30	3.60	1.60	4.30	3.70	4.97	2.79	3.73
Zr	115	122	48	154	148	244	142	172
Y	21.71	28.17	18.00	27.00	23.00	36.03	22.57	29.07
Th	9.49	5.71	2.14	14.7	7.28	3.29	1.96	4.81
U	3.48	1.54	0.51	3.11	2.04	0.57	0.54	1.33
Sc	13.90	15.40	-	-	-	22.20	25.40	18.50
La	24.72	17.02	6.73	36.20	25.40	32.77	19.95	49.38
Ce	44.81	33.76	15.10	66.40	48.80	62.49	39.17	87.21
Pr	4.37	3.78	1.90	6.99	5.67	6.70	4.19	8.51
Nd	17.63	16.30	8.26	25.70	23.50	29.60	18.06	34.79
Sm	3.64	4.01	2.10	4.95	4.89	6.84	4.40	7.10
Eu	0.79	0.96	0.62	0.67	1.22	2.24	1.58	2.46
Gd	3.07	3.97	2.54	4.50	4.32	6.13	4.04	5.81
Tb	0.55	0.77	0.43	0.73	0.68	1.10	0.72	0.97
Dy	3.50	4.92	2.75	4.31	3.84	6.28	4.08	5.33
Ho	0.73	1.05	0.59	0.87	0.75	1.28	0.81	1.03
Er	2.17	3.15	1.98	2.78	2.31	3.54	2.22	2.81
Tm	0.35	0.50	0.31	0.45	0.35	0.55	0.33	0.41
Yb	2.41	3.30	2.00	2.83	2.22	3.31	1.98	2.54
Lu	0.36	0.50	0.35	0.48	0.37	0.49	0.28	0.37
Th/Nb	1.54	0.69	0.93	1.13	0.56	0.08	0.07	0.07
La/Sm	6.79	4.25	3.20	7.31	5.19	4.79	4.54	6.95
Th/Yb	3.93	1.73	1.07	5.19	3.28	0.99	0.99	1.89
Nb/Yb	2.56	2.53	1.15	4.59	5.86	12.73	14.54	28.83
Nb/U	1.77	5.42	4.51	4.18	6.37	73.83	53.87	55.12
Zr/Y	5.30	4.34	2.67	5.70	6.43	6.78	6.28	5.92
Th/La	0.38	0.34	0.32	0.41	0.29	0.10	0.10	0.10
$(La/Yb)_N$	7.35	3.70	2.41	9.18	8.21	7.10	7.22	13.95
UTME*	530972	530970	466082	467119	459674	505864	504417	506684
UTMN*	6896573	6896550	6981130	6976327	6980284	6907585	6907591	6909613

Note: Samples are located on Figure 2-3 with lower case letter. RL02-1-1 and RL02-17-10: arkosic grits; 98MC119: granodiorite, 98MC125: rhyolite, 98MC067: andesite, RL02-5-10: ash tuff, RL02-5-8D: plagioclase-crystal tuff; RL02-4-7B: volcanic breccia;
*Zone 8, NAD 83

Table 2-1 (continued) - Representative analyses of the Drury, Little Kalzas and Little Salmon formations

SAMPLE	Massive volcanic rocks					Epiclastic rocks	Mn-chert
	(i) RL02-4-7A	(j) RL02-14-1	(k) RL02-6-5	(l) RL02-5-4A	(m) RL02-12-2	(n) RL02-17-1	(o) RL02-4-6
SiO2 (%)	44.78	49.93	49.79	46.26	46.79	56.05	90.70
Al2O3	14.66	15.69	16.46	17.39	14.06	12.32	3.45
Fe2O3	10.70	8.35	12.72	9.72	11.38	6.82	1.72
MnO	0.17	0.10	0.18	0.15	0.21	0.21	0.76
MgO	8.24	8.01	2.46	7.74	6.88	2.00	0.68
CaO	12.11	4.84	8.71	7.10	11.19	10.63	1.30
Na2O	1.48	4.40	2.39	3.01	2.16	3.66	0.06
K2O	1.21	0.16	1.23	1.98	0.35	0.97	0.56
TiO2	2.08	2.29	2.47	2.29	1.58	0.79	0.22
P2O5	0.48	0.51	1.16	0.37	0.14	0.24	0.08
LOI	3.12	5.89	2.67	4.18	4.18	6.60	0.70
TOTAL	99.05	100.15	100.24	100.19	98.91	100.29	100.22
Cr (ppm)	476	106	366	177	239	-	22
Ni	172	38	87	-	53	-	25
Co	47	23	41	36	36	11	20
V	233	238	218	297	355	123	10
Zn	117	141	210	128	98	110	81
Cu	127	118	154	88	84	108	159
Rb	25	3	26	32	7	24	17
Ba	516	29	270	783	80	701	1570
Sr	588	119	718	325	354	544	141
Ga	18	22	21	22	18	14	7
Ta	3.58	2.41	3.82	1.68	0.19	0.29	0.32
Nb	53.34	35.12	63.28	32.08	3.42	4.99	8.18
Hf	3.18	5.11	3.42	3.97	2.41	3.42	1.04
Zr	133	256	149	185	86	121	44
Y	24.19	34.42	46.18	29.41	38.36	27.41	10
Th	3.60	3.18	3.81	2.11	0.36	2.57	2.24
U	0.93	1.43	1.14	0.63	0.22	1.11	0.14
Sc	27.30	26.10	23.20	32.60	41.90	17.60	5.70
La	37.49	29.44	60.39	21.18	5.26	15.23	11.37
Ce	66.69	57.96	79.26	43.20	13.18	30.20	33.26
Pr	6.72	6.45	9.55	4.67	2.08	3.82	2.31
Nd	28.16	28.58	41.26	21.38	11.50	18.30	10.19
Sm	6.36	6.61	8.15	5.38	4.10	4.60	2.41
Eu	2.14	2.27	2.86	2.00	1.49	1.33	0.57
Gd	5.21	5.78	7.54	4.99	5.04	4.42	1.86
Tb	0.86	1.06	1.17	0.91	1.02	0.81	0.36
Dy	4.62	6.28	6.90	5.26	6.71	4.84	2.08
Ho	0.86	1.25	1.40	1.06	1.43	1.01	0.40
Er	2.26	3.53	4.01	2.92	4.09	2.90	1.08
Tm	0.33	0.54	0.60	0.44	0.65	0.45	0.17
Yb	1.93	3.35	3.70	2.68	4.01	2.90	1.05
Lu	0.26	0.48	0.57	0.39	0.59	0.45	0.16
Th/Nb	0.07	0.09	0.06	0.07	0.10	0.52	
La/Sm	5.90	4.46	7.41	3.94	1.28	3.31	
Th/Yb	1.87	0.95	1.03	0.79	0.09	0.89	
Nb/Yb	27.62	10.49	17.13	11.97	0.85	1.72	
Nb/U	57.10	24.60	55.51	50.58	15.50	4.51	
Zr/Y	5.48	7.42	3.23	6.29	2.25	4.42	
Th/La	0.10	0.11	0.06	0.10	0.07	0.17	
(La/Yb)N	13.92	6.31	11.72	5.67	0.94	3.77	
UTME*	506684	505360	507379	503784	515208	523540	506496
UTMN*	6909613	6905852	6909106	6906916	6908597	6896279	6909510

Note: Samples are located on Figure 2-3 with lower case letter. RL02-4-7A: massive porphyritic flow; RL02-6-5: massive porphyritic flow; RL02-14-1: massive flow; RL02-5-4A: leucogabbro; RL02-12-2: coarse grained gabbro sill; RL02-17-1: epiclastic sandstone;
*Zone 8, NAD 83

18

Table 2-1 (continued) - Representative analyses of the Drury, Little Kalzas and Little Salmon formations

	Little Salmon Formation					
	Upper succession				Lower succession	
	Sedimentary rocks				felsic volcanic rocks	
SAMPLE	(p) RL02-12-7	(q) RL02-12-5A	(r) RL02-16-2	(s) RL02-16-3B	(t) 99MC001c	(u) 99MC156
SiO2 (%)	60.53	64.09	82.50	64.81	68.82	68.55
Al2O3	14.54	15.04	7.38	14.62	14.67	13.68
Fe2O3	6.55	4.58	2.57	7.00	1.19	1.98
MnO	0.12	0.08	0.06	0.12	0.04	0.06
MgO	5.61	1.43	1.24	2.30	1.42	0.84
CaO	4.36	2.15	1.19	3.32	3.06	3.60
Na2O	3.12	1.91	2.02	1.08	0.71	2.73
K2O	1.88	6.67	0.83	3.08	4.30	2.70
TiO2	0.73	0.41	0.41	0.73	0.30	0.28
P2O5	0.17	0.14	0.10	0.19	0.08	0.07
LOI	2.72	3.29	1.68	2.79	4.30	4.06
TOTAL	100.32	99.79	99.96	100.04	98.86	98.56
Cr (ppm)	225	-	61	48	-	27
Ni	45	-	-	36	-	-
Co	25	7	4	12	-	2
V	156	32	63	84	30	44
Zn	128	129	80	149	-	-
Cu	68	84	66	97	-	-
Rb	56	302	29	96	129	79
Ba	831	1220	769	3340	771	838
Sr	365	176	76	444	92	101
Ga	19	20	8	19	16	10
Ta	0.63	2.63	0.52	0.85	0.9	1
Nb	16.43	34.00	6.48	11.10	11.1	11.5
Hf	3.37	6.08	2.14	5.09	4.3	4
Zr	140	255	81	185	164	157
Y	17.87	21.33	11.26	30.63	15	17
Th	8.85	60.24	4.61	12.58	8.49	8.11
U	1.82	15.88	1.42	3.76	1.71	1.83
Sc	20.80	5.00	6.30	14.90	-	-
La	22.77	77.43	13.15	34.72	26.5	19.9
Ce	40.47	126.93	23.85	67.55	49.1	40.6
Pr	4.19	11.62	2.81	7.37	5.23	4.76
Nd	17.20	40.28	11.52	31.59	18.4	18.2
Sm	3.59	6.59	2.45	6.88	3.44	3.56
Eu	1.05	1.17	0.61	1.59	1.02	0.891
Gd	3.15	4.34	2.03	5.57	2.89	3.06
Tb	0.51	0.68	0.34	0.97	0.47	0.54
Dy	3.01	3.70	2.07	5.78	2.66	2.92
Ho	0.60	0.71	0.42	1.14	0.53	0.58
Er	1.70	2.06	1.21	3.33	1.63	1.83
Tm	0.26	0.32	0.19	0.52	0.258	0.289
Yb	1.71	2.09	1.22	3.38	1.81	2.08
Lu	0.25	0.31	0.18	0.52	0.309	0.318
Th/Nb	0.54	1.77	0.71	1.13	0.76	0.71
La/Sm	6.35	11.75	5.38	5.05	7.70	5.59
Th/Yb	5.18	28.79	3.78	3.72	4.69	3.90
Nb/Yb	9.62	16.25	5.30	3.28	6.13	5.53
Nb/U	9.05	2.14	4.56	2.95	6.49	6.28
Zr/Y	7.85	11.94	7.23	6.04	10.86	9.02
Th/La	0.39	0.78	0.35	0.36	0.32	0.41
(La/Yb)N	9.56	26.55	7.72	7.36	10.50	6.86
UTME*	514460	514902	522607	522703	520300	520564
UTMN*	6908281	6908368	6896865	6897062	6895665	6897692

Note: Samples are located on Figure 2-3 with on lower case letter. RL02-16-2, and RL02-16-3B: quartz-rich sandstone; RL02-12-7: feldspar-grit; RL02-12-5A: K-feldspar grit; 99MC001c and 99MC156: quartz-feldspar porphyries
*Zone 8, NAD 83

Table 2-2 - Nd, Sm and Sr isotopic analyses of the Drury, Little Kalzas, and Little Salmon formations

Sample	Lithology	Nd (ppm)[1]	Sm (ppm)[1]	Sr (ppm)	$^{147}Sm/^{144}Nd$	$^{143}Nd/^{144}Nd$	±2σ	$f_{Sm/Nd}$[2]	$\varepsilon_{Nd(0)}$[2]	$\varepsilon_{Nd(340)}$[2]	T_{DM}[3] (Ma)	$^{87}Sr/^{86}Sr$	±2σ
Drury fm													
RL02-17-10	arkosic grit	15.951	3.841	222	0.1455	0.512146	±4	-0.26	-9.6	-7.4	2128	0.712674	±7
Little Kalzas fm													
98 MC-119	granodiorite	7.478	1.920	170	0.1552	0.512399	±5	-0.21	-4.7	-2.9	1823	0.710558	±9
98 MC-125	rhyolite	23.535	4.614	19.7	0.1185	0.512058	±5	-0.40	-11.3	-7.9	1667	0.776891	*±11
98 MC-067	andesite	22.424	4.711	318	0.1270	0.512418	±4	-0.35	-4.3	-1.3	1199	0.711808	±10
Little Salmon fm													
Upper succession													
RL02-5-10	ash tuff	29.275	6.387	224	0.1319	0.512878	±6	-0.33	4.7	7.5	414	0.704477	±9
RL02-5-8D	crystal tuff	18.672	4.164	437	0.1348	0.512869	±5	-0.31	4.5	7.2	448	0.703725	±10
RL02-4-7B	breccia	42.678	8.403	628	0.1190	0.512823	±3	-0.39	3.6	7.0	448	0.703825	±10
RL02-14-1	massive flow	28.569	6.509	119	0.1377	0.512883	±5	-0.30	4.8	7.3	436	0.705343	±10
RL02-17-1	epiclastic sdst	18.258	4.389	544	0.1453	0.512821	±5	-0.26	3.6	5.8	623	0.705579	±11
RL02-12-7	feldspar grit	18.021	3.730	365	0.1251	0.512091	±5	-0.36	-10.7	-7.6	1735	0.720333	±11
RL02-12-5A	K-feldspar grit	32.314	5.268	176	0.0985	0.511648	±6	-0.50	-19.3	-15.1	1917	0.732670	±8
RL02-12-2	gabbro sill	11.628	3.946	354	0.2052	0.513043	±5	0.04	7.9	7.5	1025	0.714756	*±11

[1] See Appendix A for analytical method
[2] Calculated using $^{143}Nd/^{144}Nd$ of chondrite uniform reservoir (CHUR)=0.512638 and $^{147}Sm/^{144}Nd$=0.1966 (Jacobsen and Wasserburg, 1980)
[3] TDM calculated using a linear evolution for a mantle separated from the CHUR at 4.55Ga and having a present day Epsilon value of +10
*The relative abundance of calcite in these samples suggests secondary alteration which would explain the anomalous Sr isotopic ratios.

field-strength element (HFSE), REE, Th, and transition elements are probably immobile under these metamorphic conditions (Winchester and Floyd, 1977). In addition, the consistency of various compositional trends using both mobile and immobile elements in the volcanic rocks of both the Little Salmon and Little Kalzas formations, and their similarities to those of modern igneous rocks suggest that most major and trace elements were not significantly affected by alteration/metamorphic processes, and that the distribution of these elements reflects their primary magmatic distribution.

2.3.2 Little Kalzas formation

The Little Kalzas volcanic rocks are composed primarily of massive porphyritic andesites (Fig. 2-5A), with SiO_2 content between 52.6-72.5% and moderate Nb/Y (0.35-0.75) and Zr/TiO_2 (104-238) values suggesting subalkaline affinity (Fig. 2-5A). The REE patterns (Fig. 2-6C) show a strong light REE (LREE) enrichment ($(La/Yb)_N$=6.50-10-91) with a slight depletion in heavy REE (HREE), suggesting that the source did contain residual garnet. These rocks were probably produced by partial melting of the mantle in the garnet peridotite field (e.g. Wilson, 1989). The pronounced negative Nb and Ti anomalies on the mantle normalized trace elements patterns (Fig. 2-6D) as well as their Ti/V ratio (Fig. 2-5C) and the distribution on the Zr-Ti-Y (Fig. 2-5B; Pearce and Cann, 1973) and Th-Hf-Nb (Fig. 2-5D; Wood et al., 1979) diagrams clearly indicate the subduction-related nature of these andesitic flows, and that they are the products of typical arc-derived calc-alkaline volcanism. The slightly negative ε_{Nd340} from one of these andesitic rocks (-1.3; Table 2-2) and moderate $^{87}Sr/^{86}Sr$ values (~0.711) are compatible with the mixing of a primitive mantle source with some continental crust (Fig. 2-8A). The very old depleted mantle model ages (T_{DM}) of these rocks (~1.199 Ga, Table 2-2) are typical of upper continental crust or its derivatives, supporting continental crust contamination of the magma.

The Little Kalzas formation also contains a minor component of felsic volcanics that are usually interbedded with the andesitic rocks. The Little Kalzas felsic rocks display very high SiO_2 content (SiO_2>76%) with moderate Nb/Y (0.48-0.58) and Zr/TiO_2 (1255-1283) values suggesting rhyolite of subalkaline affinity (Fig. 2-5A). The HFSE contents (Nb,
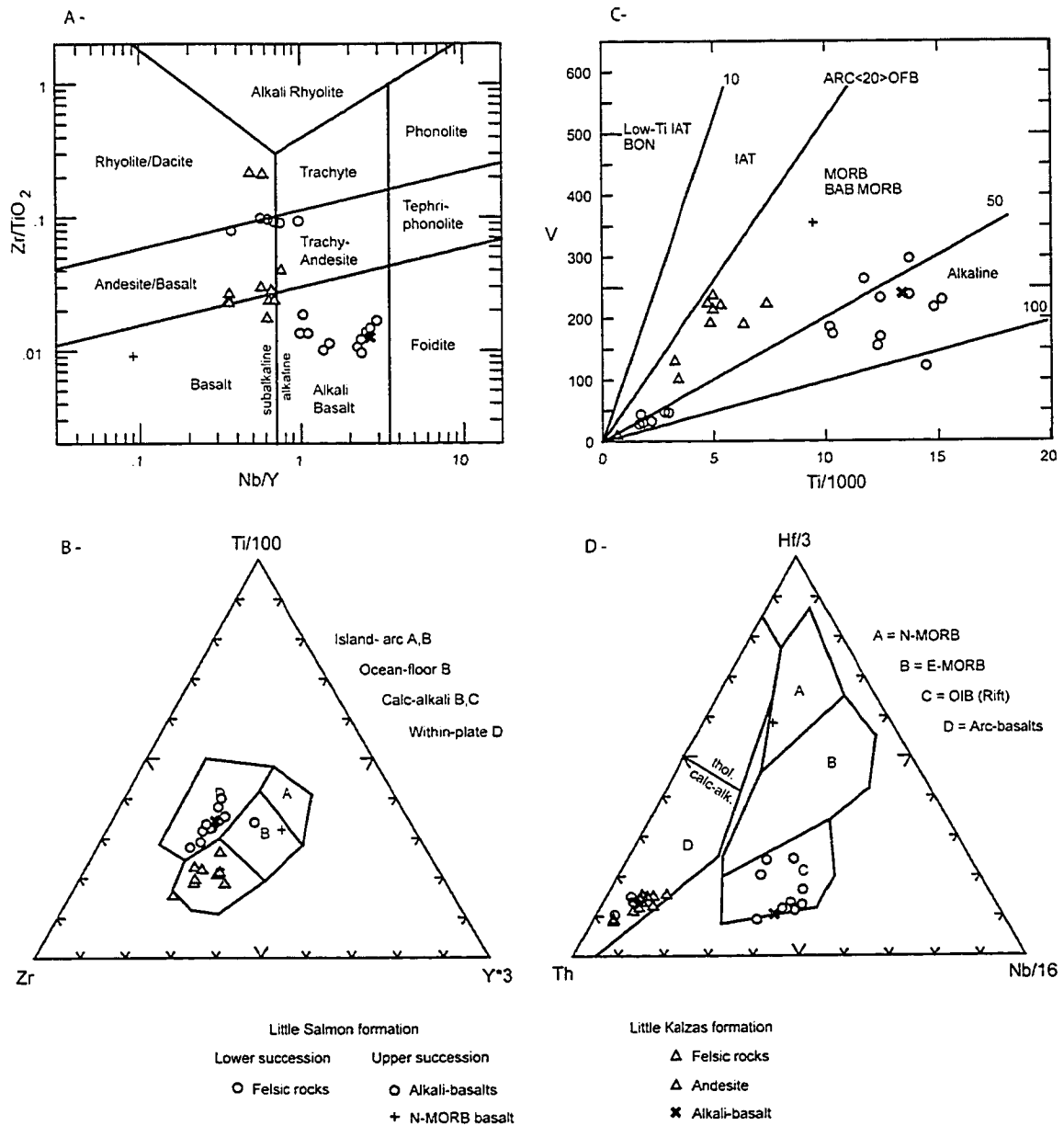
Figure 2-5 – Geochemical characteristics of the volcanic rocks of the Little Kalzas and Little Salmon formations. A- Zr/TiO_2 vs Nb/Y classification diagram (modified from Winchester and Floyd, 1976), B- Zr-$(Ti/100)$-$(Y*3)$ diagram of Pearce and Cann (1973), C- V-$(Ti/1000)$ diagram of Shervais (1982). $V/Ti < 20$ typical of arc, $V/Ti > 50$ typical of alkali magmatism. IAT-Island arc tholeiite, BAB-Back-arc basalts, MORB-Mid-ocean-ridge basalt and, OFB-Ocean-floor basalts, D- $Th/(Hf/3)/(Nb/16)$ diagram of Wood et al. (1979). Note that the Little Kalzas and Little Salmon formations include both calc-alkaline and alkaline volcanic rocks.

Ta, Ga, Zr, Hf, Y) relative to other incompatible elements within these rocks are moderate to low and are characteristic of volcanic-arc rocks (Fig. 2-5D). The REE and trace-element patterns of these rhyolitic rocks suggest a calc-alkaline to transitional nature (Zr/Y=5.7-7.3; Lentz, 1998; 1999). Like for the andesitic rocks, the moderately
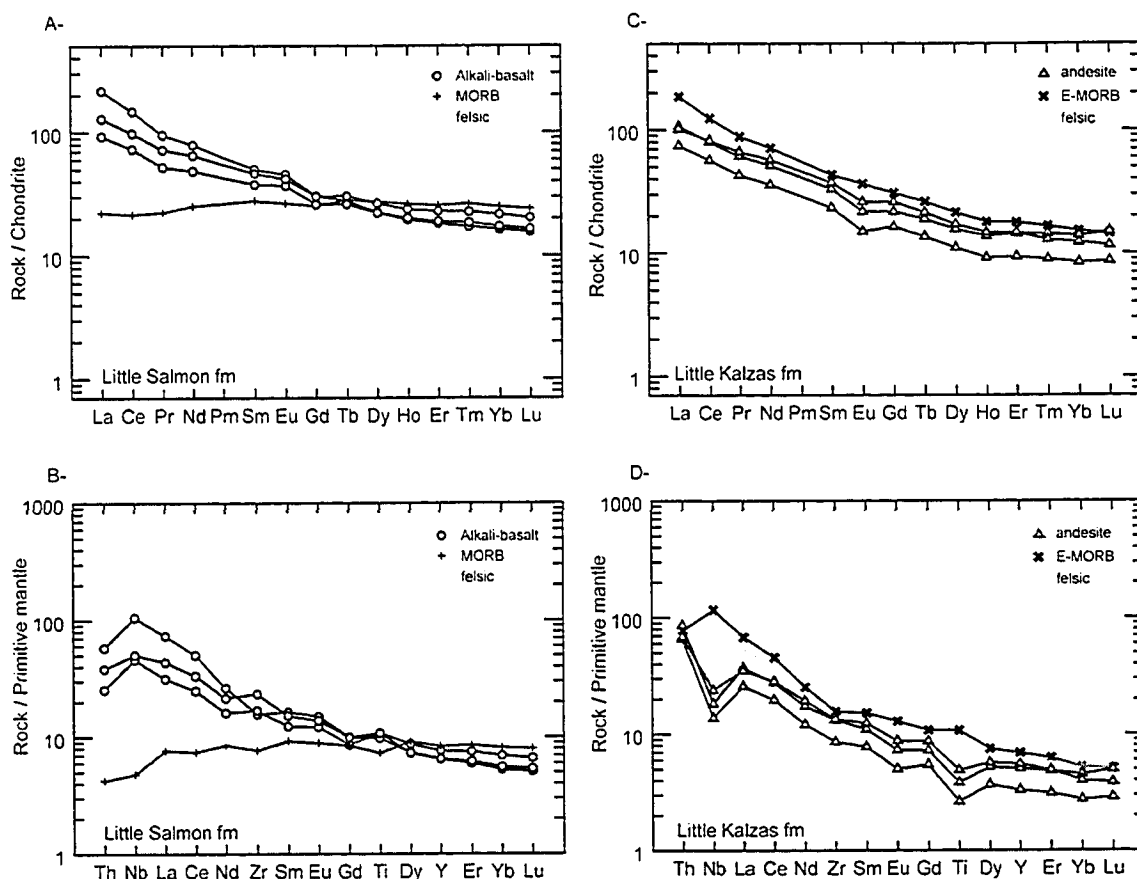
Figure 2-6 – Chondrite-normalized rare earth element patterns (A, C; normalization values from McDonough and Sun, 1995) and mantle-normalized incompatible trace element patterns (B, D; normalization values from Sun and McDonough, 1989) for the volcanic rocks of the Little Salmon and Little Kalzas formations.

negative ε_{Nd340} from one of these rhyolitic rocks (-7.9; Table 2-2) and its relatively old T_{DM} age (1.667 Ga; Table 2-2) suggest continental crust involvement with the magmas (Fig. 2-8A).

2.3.3 Little Salmon formation

2.3.3.1 Lower succession

The massive volcanic rocks of the lower succession are represented by the quartz-feldspar-phyric felsic lens on the west side of the synclinorium (Figs. 2-1B and 2-3). The analyzed samples have high SiO_2 content (SiO_2>72.5%) with moderate Nb/Y (0.6-0.9)
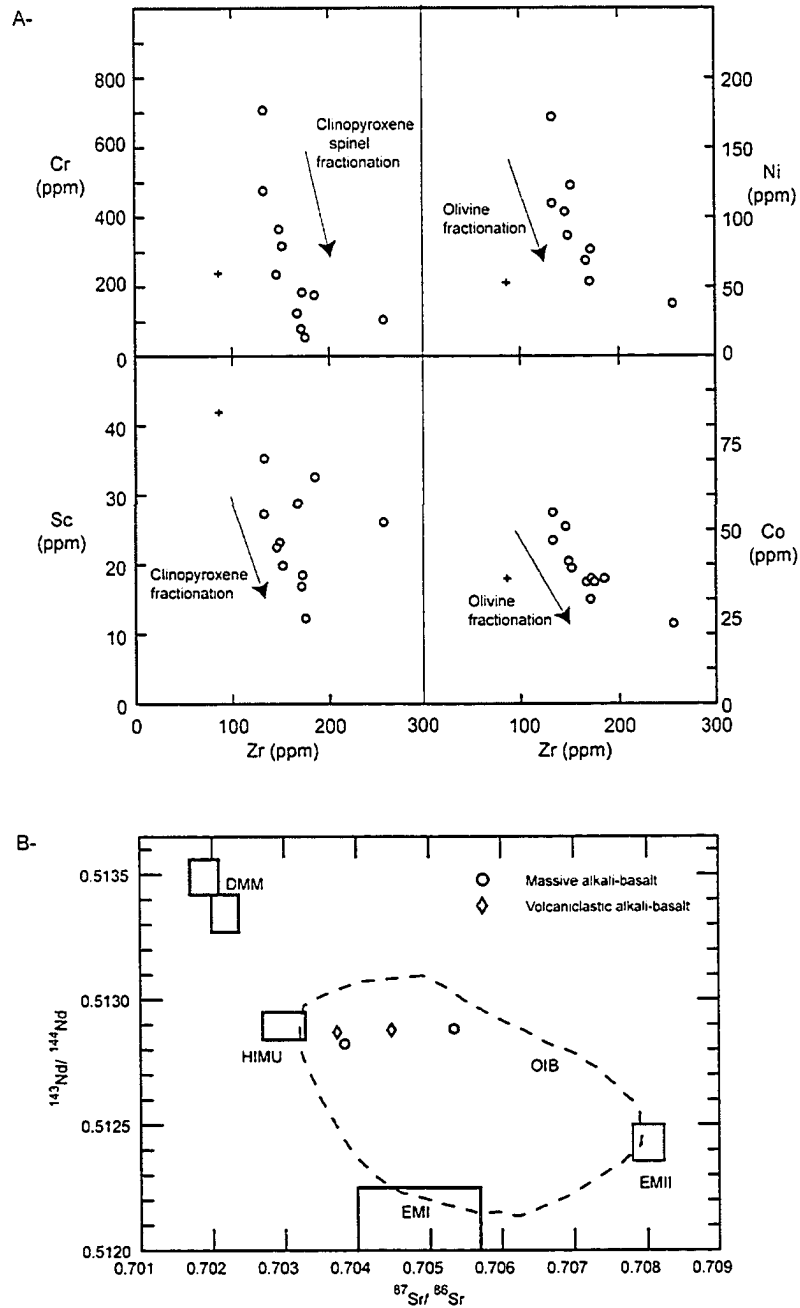
Figure 2-7A – Variation of Cr (ppm), Sc (ppm), Ni (ppm), and Co (ppm) relative to Zr (ppm) in the alkali-basalt volcanic rocks of the upper succession of the Little Salmon formation. The inverse relationships between Zr and Cr, Sc, Ni, and Co are consistent with clinopyroxene, olivine, ± spinel, fractionation, respectively.

Figure 2-7B – $^{143}Nd/^{144}Nd$ versus $^{87}Sr/^{86}Sr$ for the alkali-basalt rocks of the upper succession of the Little Salmon formation. Shown for comparison are the four principal end-member isotopic mantle source components in oceanic basalts (DMM:depleted MORB mantle, HIMU:high U/Pb mantle, EMI:Enriched mantle argued to be a slightly modified bulk-earth component and, EMII: Enriched mantle with a recycled (subducted) sediment protolith; Hart, 1988). The Little Salmon alkali-basalt mantle source is a mix of HIMU, EMI, and EMII, typical of oceanic island basalt (OIB) environment (OIB outlined area; Hart, 1988).

24

A-

DM

N-MORB
(RL02-12-2)

Dev-Jur miogeocline

Cambrian-Permian

C-Or miogeocline

Precambrian

PE miogeocline

RS92-567
Nd=14.78ppm
eND340=-24.4

ε_{Nd}

$^{147}Sm/^{144}Nd$

B-

0.5134

0.5129 — Little Salmon alkali-basalt

Little Kalzas andesite and granodiorite

0.5124

"young" sediments

Little Kalzas felsic

0.5119

"old" sediments

0.5114

craton

$^{143}Nd/^{144}Nd$

$^{87}Sr/^{86}Sr$

Little Salmon formation		Drury formation	Little Kalzas plutonic suite
+	MORB	☆ Arkosic sediments	◇ Granodiorite
◊	Volcaniclastic alkali-basalt	Little Kalzas formation	
O	Massive alkali-basalt		
✖	Epiclastic sediments	△ Rhyolite	
□	Siliciclastic sediments (grit)	△ Andesite	

Figure 2-8A – ε_{Nd} versus $^{147}Sm/^{144}Nd$ for the volcanic rocks of the Little Salmon and Little Kalzas formations. ε_{Nd} values were calculated at an age of 340 Ma. Shown for comparison are the Nd isotopic data for other crustally-derived miogeoclinal rocks from (1) southern British Columbia and Alberta (dotted outlines; Boghossian et al., 1996); (2) northern British Columbia, Yukon and the Northwest Territories (solid outlines; Garzione et al., 1997); and (3) the Nitsulin assemblage of the Yukon-Tanana terrane in southern Yukon (grey shaded areas; Creaser et al., 1997). Thick black mixing lines (according to Langmuir et al., 1978) are used to illustrate the impact of the input of various "continental crust" affinity sedimentary components to a primitive source. DM:depleted mantle, PE:Precambrian, C:Cambrian, Or:Ordivician, Dev:Devonian, Jur:Jurassic.

Figure 2-8B – $^{143}Nd/^{144}Nd$ versus $^{87}Sr/^{86}Sr$ for the volcanic rocks of the Little Salmon and Little Kalzas formations. Mixing lines (according to Langmuir et al., 1978) are used to characterize the impact of the input of various "continental crust" affinity sedimentary components to the local alkali-basalt source. Isotopic data for the "young" and "old" sedimentary component are from Goldstein (1988), and for the craton signature from Cameron and Hattori (1997).

and Zr/TiO_2 (542-564) values suggesting dacite-rhyolite of subalkaline affinity (Fig. 2-5A). The HFSE contents of these rocks, like those of the Little Kalzas felsic rocks, are moderate to low and are characteristic of volcanic-arc rocks (Fig. 2-5D). The REE patterns of the quartz-feldspar-phyric felsic rocks (Fig. 2-6A) show a strong LREE enrichment $((La/Yb)_N=5.49-10.5)$ with a fairly flat HREE pattern. The mantle-normalized trace-element patterns (Fig. 2-6B) display pronounced negative Nb and Ti anomalies, that are characteristic of subduction-related magmas (e.g. Hawkesworth et al., 1979; Pearce, 1983). The subduction-related nature of these rocks is also supported by their calc-alkaline nature (Fig. 2-5B; $Zr/Y>7$; Lentz, 1998; Lentz, 1999) and Th-Nb-Hf distribution (Fig. 2-5D).

2.3.3.2 Upper succession

Volcanic rocks - All analyzed samples of mafic volcanic rocks from the upper succession plot in the alkali-basalt field of Winchester and Floyd (1976; Fig. 2-5A) with low SiO_2 content (44.68 - 52.97 %). Their alkaline nature is supported by the high Nb/Y (>0.3, Fig. 2-5A) and high Ti/V (>50, Fig. 2-5C) ratios (Shervais, 1982; Winchester and Floyd, 1976). Zirconium, the incompatible trace element that is considered to be immobile during alteration processes (Winchester and Floyd, 1977), was used as an index of differentiation (Fig. 2-7). Some trace elements show systematic fractionation trends when plotted against Zr (Fig. 2-7); a decrease in Cr, Sc, Ni and Co values, while Zr increases, suggests fractionation of clinopyroxene, and olivine, ± spinel (Fig. 2-7A). The REE patterns (Fig. 2-6A) have a strong LREE enrichment $((La/Yb)_N \cong 13.7)$ and slight HREE depletion, typical of ocean-island basalts. The mantle normalized trace-element patterns (Fig. 2-6B) display a strong enrichment in the highly incompatible elements, with smooth profiles that increase with increasing element incompatibility and peak at Nb; these patterns are similar to those of ocean-island basalts (e.g. alkali basalts of Hawaii; Figs. 2-6A and 2-6B; Wilson, 1989). The HREE depletion suggests that these rocks were probably produced from partial melting of the mantle in the garnet peridotite field (e.g. Wilson, 1989). The highly positive ε_{Nd340} of these rocks (+7.3; Table 2-2) and the low

$^{87}Sr/^{86}Sr$ values (0.705; Table 2-2), suggest a primitive magma source (Fig. 2-7B) with little to no involvement of continental crust in the magma genesis (Figs. 2-8A and 2-8B). Considering the imprecise nature of the T_{DM}, the T_{DM} of one of the massive flow from the upper succession (436 Ma; Table 2-2) is consistent with the Paleozoic age of the rocks, supporting little continental crust contamination of the magma.

The undated leucocratic gabbroic intrusion that crosscuts the underlying limestone in the northern part of upper succession (Figs. 2-3 and 2-4) shows the same geochemical characteristic as the massive alkali-basalt flow, with high Nb/Y and Ti/V ratios (Figs. 2-5A and 2-5C). It also has the LREE and highly incompatible trace element enrichment on the REE and mantle-normalized trace-elements (Figs. 2-6A and 2-6B). A similar gabbroic body occurs on the east side of the synclinorium (ca. 339 Ma; Colpron et al., in press-b).

A massive coarse gabbro sill, just below the limestone in the northeastern part of the lower succession, plots in the basalt field of Winchester and Floyd (1976; Fig. 2-5A) with low SiO_2 content (49.39%) and a low Nb/Y ratio suggesting subalkaline affinity. Its HFSE contents (Nb, Ta, Ga, Hf, Y) are low. The rocks have a moderate Ti/V ratio (~25; Fig. 2-5C) which is typical of mid-ocean-ridge basalt (MORB). It plots in the ocean-floor field on the Zr-Ti-Y diagram of Pearce and Cann (1973; Fig. 2-5B), and in the N-MORB field of the Th-Hf-Nb diagram of Wood et al. (1979; Fig. 2-5D). The REE patterns show a slight LREE depletion ($(La/Yb)_N$=0.94) with a flat HREE pattern, suggesting partial melting in the spinel peridotite field, at <60 km depth (White et al., 1992). The mantle-normalized trace-element pattern is relatively flat and smoothly decreases to the more incompatible elements, including LREE and Th (Fig. 2-5A). It resembles modern N-MORB (Sun and McDonough, 1989), implying that it was derived from an asthenospheric mantle unaffected by subduction processes. The contrast between the alkaline rocks and this sample may reflect a difference in the depth and degree of partial melting; relatively high degrees of partial melting at low pressure for the MORB (spinel stability field), and lower degrees of partial melting at higher pressure (garnet stability

field) for the alkali basalts. The recalculated epsilon Nd value (ε_{Nd340}) of this sample is highly positive (+7.5; Table 2-2), which supports a primitive mantle source (Fig. 2-8A).

The red chert horizon interbedded within the alkali-basalt sequence in the northern part of the upper succession has >91% SiO_2 with high MnO (up to 0.76%) and Ba (up to 1570 ppm) contents (Table 2-1). The high MnO content is related to the abundant submicroscopic piemontite crystals (Mn-rich epidote) which give the red colour to this cherty bed.

Clastic rocks - Several samples of volcaniclastic and siliciclastic rocks from the upper succession and a few others from neighboring sedimentary sequences were also analyzed to characterize the effect of mixed siliciclastic and volcanic components on the geochemical composition of the various "clastic" rocks of the Little Salmon formation. The geochemical signatures can be use as source indicator. The relative increase of siliciclastic over volcaniclastic material in the volcaniclastic rocks of the upper succession is generally accompanied by higher SiO_2 values and Zr/TiO_2 ratios, along with lower TiO_2, MgO, CaO, Cr, Ni, V and Sc values and Nb/Th ratios (Table 2-1), and higher $^{87}Sr/^{86}Sr$ values (Table 2-2).

The abundant volcaniclastic rocks, tuff to breccia, closely associated with the massive alkali-basalt flows in the northern upper succession, present the same geochemical and isotopic signatures as the massive alkali-basalt flow from which they were derived (Tables 2-1 and 2-2; Fig. 2-9). Like the flows, the ε_{Nd340} values of these volcaniclastic rocks are highly positive (+7.0 to +7.5; Table 2-2), their $^{87}Sr/^{86}Sr$ values are low (~0.704; Table 2-2, Fig. 2-8B), and their T_{DM} average ~436 Ma, all of which suggest little to no sedimentary input from more evolved sources (Figs. 2-8A, 2-8B and 2-9).

The clastic rocks in the southern upper succession display three distinct geochemical signatures (Fig. 2-9). Most volcaniclastic rocks from the first 50 m above the limestone show very low La/Sc and Th/Sc ratios indicating a mafic-dominated provenance (Figs. 2-9A and 2-9B), and their trace-element content (La, Sc, Th, Zr) overlap those of the local
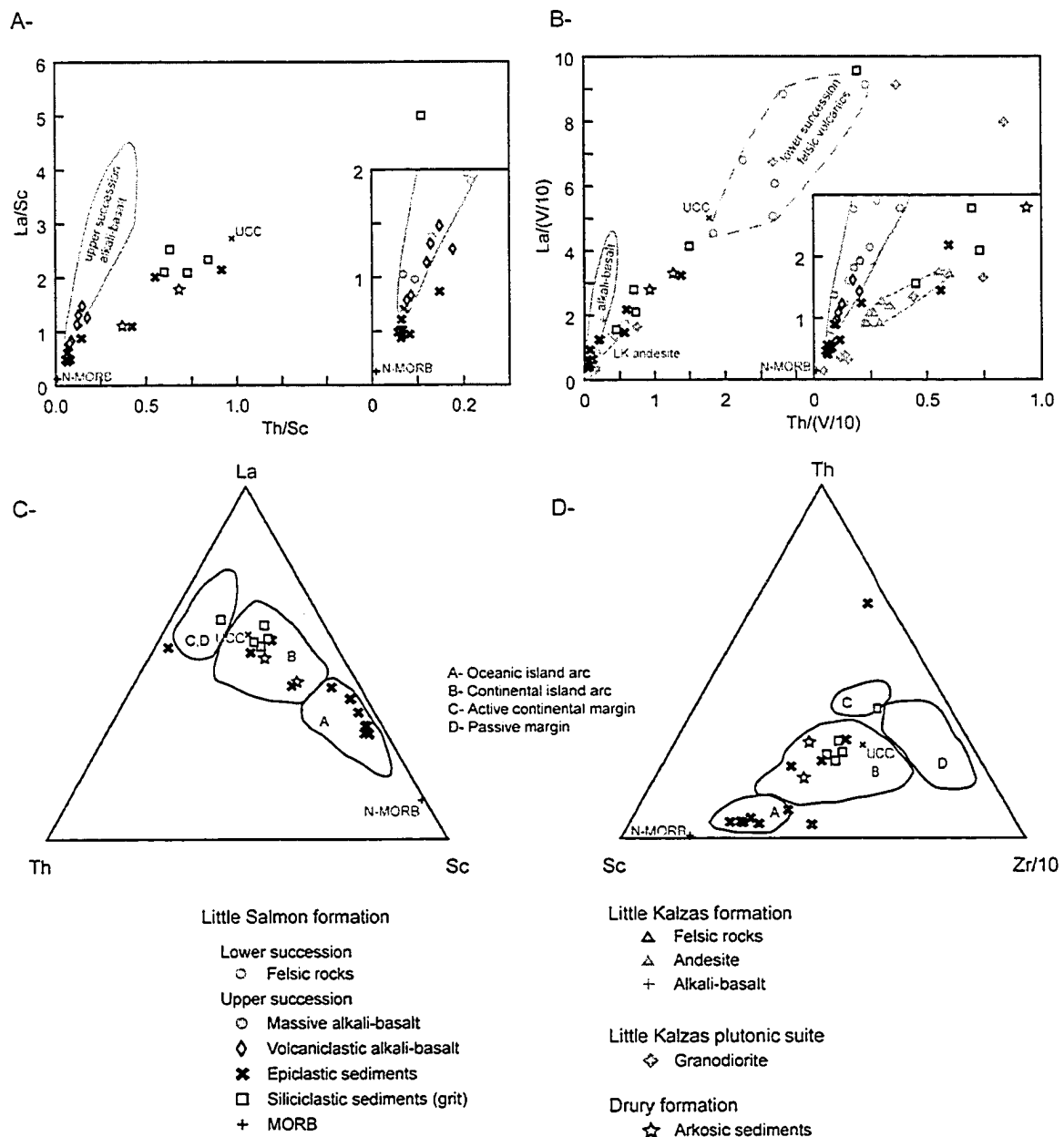
Figure 2-9 – Discrimination diagrams of sedimentary and volcanic rocks of the Little Salmon and Little Kalzas formations. A- La/Sc vs Th/Sc, B- La/(V/10) vs Th/(V/10), C- Th-La-Sc and D- Sc-Th-Zr/10 of Bhatia and Crook (1986). The volcanic and volcaniclastic rocks of the Little Salmon upper succession present a distinct geochemical signature compared to Upper Continental Crust (UCC) derived rocks, like the siliciclastic sediments or felsic rocks of the Little Salmon formation.

alkali-basalts (Figs. 2-9A and 2-9D).They also display high and positive ε_{Nd340} (+5.8; Table 2-2) and low $^{87}Sr/^{86}Sr$ values (~0.705; Table 2-2), similar to the alkali-basalt volcanic rocks of the northern upper succession. These rocks are interpreted as distal epiclastic deposits derived from the alkali-basalt volcanic centres observed in the

29

northern upper succession. However, their slightly lower ε_{Nd340} value, and slightly older T_{DM} age (623 Ma; Table 2-2) might suggest some sedimentary input from more evolved sources (Figs. 2-8B and 2-9).

The siliciclastic rocks on the other hand are strongly depleted in V (<85ppm) and Sc (<10ppm) compared with the volcanic rocks of upper succession; these low concentrations are typical of sedimentary rocks and, therefore, upper continental crust (V=60ppm and Sc=11ppm; Taylor and McLennan, 1985). Their high La/Sc and Th/Sc ratios suggest that they are derived from felsic rocks (Figs. 2-9A and 2-9B); however, their signature falls between the average felsic upper continental crust (LREE-enriched rocks; Taylor and McLennan, 1985) and chemically primitive rock compositions (N-MORB and/or OIB). This could reflect either input from both types provenance detritus or a separate source region (Figs. 2-9A and 2-9B). Most samples plot in the "continental island arc" field of both the Th-La-Sc and Sc-Th-Zr discriminant diagrams of Bhatia and Crook (1986; Figs. 2-9C and 2-9D); this is typical of eroding island arc formed on well developed continental crust or on thin continental margin. One sample plots in the "active continental margin" field, more indicative of eroding thick continental margin and/or crystalline basement.

Interbedded with the epiclastic deposits on the east side of the synclinorium are a few grit intervals showing moderate to high La/Sc and Th/Sc ratios, with moderate to strongly negative ε_{Nd340} (-7.6 to -15.1; Table 2-2), and very old T_{DM} ages (~1.7-1.9 Ga; Table 2-2), which implies source rock like old upper continental crust or its derivatives. Like the siliciclastic rocks, they plot in the "continental island arc" field of both Th-La-Sc and Sc-Th-Zr discriminant diagrams of Bhatia and Crook (1986; Figs. 2-9C and 2-9D), with the exception of the K-feldspar grit that plots toward the "active continental margin" field.

2.4 Petrogenesis of the Carboniferous volcanic sequences

2.4.1 Little Kalzas formation

The calc-alkaline andesitic and felsic volcanic rocks in the Little Kalzas formation with their strong negative Nb and Ti anomalies on the mantle-normalized trace-element patterns and negative ε_{Nd340} are typical of magmatism in a continental arc setting. The LREE enrichment, the high Th/La ratios (0.23-0.43), as well as old T_{DM} ages (1.2-1.7 Ga) for both the andesites and the felsic rocks, suggest influence from a crustal source with an extended history of LREE enrichment, typical of continental basement, or sedimentary rocks derived from such a source (Fig. 2-8A). The Little Kalzas andesites were probably generated by melting of the mantle wedge above the subduction zone and generation of a basaltic magma which accumulated under the continental crust, inducing partial melting of the latter and generating basaltic-crust hybrid magma. The negative ε_{Nd340} (-7.9; Table 2-2, Fig. 2-8A), very high Th/La ratios (0.41-0.43) and old T_{DM} of felsic volcanic rocks suggest a significant crustal residence time or crust-magma interaction for the felsic magmas, which is supported by the presence of inherited Archean to Paleoproterozoic zircons in the Little Kalzas rhyolitic rocks, as documented by Colpron et al. (in press-b).

Mixing lines (Fig. 2-8A) between primitive magmatic sources in the area (depleted mantle, DM, Hamilton et al., 1983; and Little Salmon MORB sample, RL02-12-2), and possible sedimentary end-members of known continental crust affinity in the area do not show a unique mixing solution. The isotopic composition of known rocks derived from the basement of Yukon-Tanana terrane (Nisutlin assemblage; Creaser et al., 1997) lies well within the compositional range of most other old sedimentary sequences of the Cordillera.

2.4.2 Little Salmon formation

Lower succession – Like for the Little Kalzas felsic rocks, the geochemical signature of the felsic volcanic rocks of the lower succession suggests that they represent crustal

melts. The calc-alkaline nature of the felsic rocks, coupled with the strong negative Nb and Ti anomalies on the mantle-normalized trace-element patterns, are similar to those of modern felsic rocks forming in arc environments (e.g. Pearce and Peate, 1995); however, this signature could be solely inherited from partial melting of crustal material without involvement of any subduction processes (e.g. decompression melting link to extension, Morris and Hooper, 1997; Morris et al., 2000). The high concentration of incompatible elements such as Th and Zr in these volcanic rocks, as well as their high Th/La (0.32-0.53) and low Nb/Ta (11.5-13.27) ratios are typical of upper continental crust and its derivatives. Typical upper continental crust has high Th/La (0.22) and low Nb/Ta (~11 to 12) ratios, whereas mantle and mantle-derived rocks typically have low Th/La (0.12) and high Nb/Ta (~17.5) ratios (Taylor and McLennan, 1995). Colpron et al. (in press-b) documented inherited Paleoproterozoic zircon in the *ca.* 340 Ma quartz-feldspar-phyric felsic rock at the based of the Little Salmon Formation. The crustal signature in these felsic rocks, as well as the inherited zircons, suggests an extensive interaction with continental crust. Although the Little Salmon formation lacks the andesitic volcanic rocks typical of continental arc, these quartz-feldspar porphyries, just like the felsic rocks of the neighboring Little Kalzas arc, most likely represent high-level intrusions of a arc system build on continental basement, or sedimentary rocks derived from such a source.

Upper succession – Concentrations of several trace elements in the alkali-basalts of the upper succession, as well as of the leucocratic alkali-gabbro intrusion, indicate that they could not have been derived from the same source or parental magma as those of the arc-derived rocks of the lower succession. Their geochemical and isotopic characteristics, including the lack of negative Nb and Ti anomalies, are consistent with an asthenospheric source unaffected by subduction processes. The leucocratic alkali-gabbro intrusions are interpreted as feeder dykes to the overlying alkalic volcanic system.

The Nd and Sr isotopic ratios of the alkali-basalts are typical of oceanic island-basalts (OIB; Hart, 1988; Fig. 2-7B) and show no sign of crustal contamination (Fig. 2-8B). The N-MORB coarse grained gabbro, although found within the lower succession of the Little Salmon formation, also show a very primitive source, very similar to modern depleted

mantle (DM, Fig. 2-8A). The data are consistent with progressive upwelling of the asthenospheric mantle during rifting of an arc system. During the ascent, melting of the asthenospheric mantle in the garnet stability field generated the alkali-basalts, while subsequently a larger degree of melting of the upwelling mantle at a shallower depth produced the MORB basalt. The MORB gabbro is likely a sill of the upper succession alkaline magmatism emplaced within the upper part of the lower succession stratigraphy.

The geochemical signature of the Mn-rich chert clearly demonstrates its exhalative nature. Its high SiO_2, MnO and Ba content are typical of hydrothermal chert horizons associated with low-temperature hydrothermal (off-axis?) plumes (Peter et al., 2003).

2.4.2.1 Provenance signatures for the "Upper succession" of the Little Salmon formation

The geochemical and isotopic signatures for the various clastic rocks of the southern upper succession clearly show at least two distinct provenances - one proximal source (the alkali-basalt volcanic centres of the northern upper succession), and one or several source(s) of siliciclastic sedimentary/upper continental crust affinity (Figs. 2-8A and 2-8B). Being able to determine the potential source(s) of these siliciclastic rocks will enable us to better constrain the paleodepositional environment of the upper succession of the Little Salmon formation.

Mixing lines (according to Langmuir et al., 1978) are used in figures 2-8A and 2-8B to characterize the impact of the input of various "continental crust" affinity sedimentary components to the local alkali-basalt source. These mixing lines calculated for the Nd isotopic ratios plotted against Sr isotopic ratios (Fig. 2-8B) demonstrate that there is no unique mixing solution that would encompass the upper succession "clastic" dataset, i.e. a line on which all the data lie upon indicative of a specific sedimentary contaminant, therefore suggesting multiple sources for the siliciclastic component. Moreover, these plots (Figs. 2-8A and 2-8B) indicate that the external sources must be evolved crustal material, either the craton itself or sediments derived from it.

On Figure 2-8A the various clastic rocks of upper succession, as well as a grit sample from the Drury formation, are plotted against other crustally-derived continental margin rocks of the Canadian Cordillera. This plot corroborates the multiple source hypothesis for the upper succession clastic rocks. All the analyzed grit samples, from both the upper succession and Drury formation on the eastern side of the synclinorium are, in part, derived from old continental margin rocks of Laurentian affinity, or their derivatives.

A multi-grain detrital zircon analysis from a K-feldspar grit interval along the eastern side of the synclinorium yielded a concordant age of *ca.* 346 Ma and Paleoproterozoic inheritance (Colpron et al., in press-b). This K-feldspar grit sample is stratigraphically and geographically very close to the other grit sample of the upper succession that show Nd isotopic signature very similar to the Little Kalzas felsic and intrusive rocks; several of the Little Kalzas synvolcanic intrusions, some K-feldspar-megacrystic, were dated at ca. 346 Ma (Colpron et al., in press-b). The similar ages and petrography suggest that parts of the Little Kalzas arc system, located just to the northwest of the Little Salmon arc system after restoration of the Big Salmon and Bearfeed faults (56 km dextral displacement; Colpron et al., 2003), were actively being eroded into the Little Salmon rift basin coeval with the alkali seamount volcanism.

According to their geochemical and isotopic signature the siliciclastic rocks of the Little Salmon upper succession are clearly derived from felsic rocks of continental crust affinity (Figs. 2-8A, 2-8B, and 2-9). The quartz-rich nature, the geochemical similarities, as well as the proximal setting of the Little Salmon and Little Kalzas arcs, strongly suggests that these arc rocks along with their underlying basement of "continental margin" and/or "continental crust" rocks are source material for siliciclastic rocks of the Little Salmon upper succession.

2.5 Reconstruction of the paleovolcanic environment of the Carboniferous Little Kalzas and Little Salmon formations

Reconstruction of the paleovolcanic environments is essential to understanding the tectonic environment within which the Little Kalzas and Little Salmon arcs formed (Fig. 2-10).

The association of abundant andesitic volcanics with minor felsic volcanic rocks at the base of the Little Kalzas formation is typical of proximal lithofacies of continental arc volcanoes. These massive volcanic rocks are associated, both upward and laterally, with abundant volcaniclastic and clastic rocks interbedded with bioclastic limestone(s) and argillite. These sequences resemble turbidite deposits in a subaqueous depositional setting (McPhie et al., 1993) typical of those found in subsiding basins near active volcano. The volcanic rocks of the Little Kalzas formation most likely represent part of a submerged (?) mid-Mississippian continental arc system (Fig. 2-10), active at around 349-343 Ma (Colpron et al., in press-b).

The quartz-feldspar porphyries and the thick section of felsic volcaniclastic sandstone and siltstone of the lower succession of the Little Salmon formation, just like the Little Kalzas rocks, are most likely the result of a pulse of magmatism at around 340 Ma (Colpron et al., in press-b) within the continental arc system (Fig. 2-10). This magmatic event was shortly followed by major extension of the arc system, and emplacement of the upper succession of the Little Salmon formation.

The volcanic facies of the upper succession of the Little Salmon formation show an important change along strike (Figs. 2-3 and 2-4). The northern portion of the upper succession is dominated by proximal volcanic lithofacies such as massive and pillowed lava flows associated with abundant polymictic volcanic breccia and coarse crystal-tuff, as well as an exhalative Mn-chert horizon (Figs. 2-3 and 2-4). This facies association, including minor flows and abundant volcaniclastic deposits, is consistent with submerged flank seamount stratigraphy (Corcoran, 2000; McPhie, 1995; Schmidt and Schmincke

Little Salmon
rift basin

Little Kalzas

Seamounts

Basin floor
sediments plain

Little Salmon

0   20   [1 km
km
VE=6

← Transfer zone
⇐ Primary sediment input
☐ Debris flow
☐ Basin floor sediments
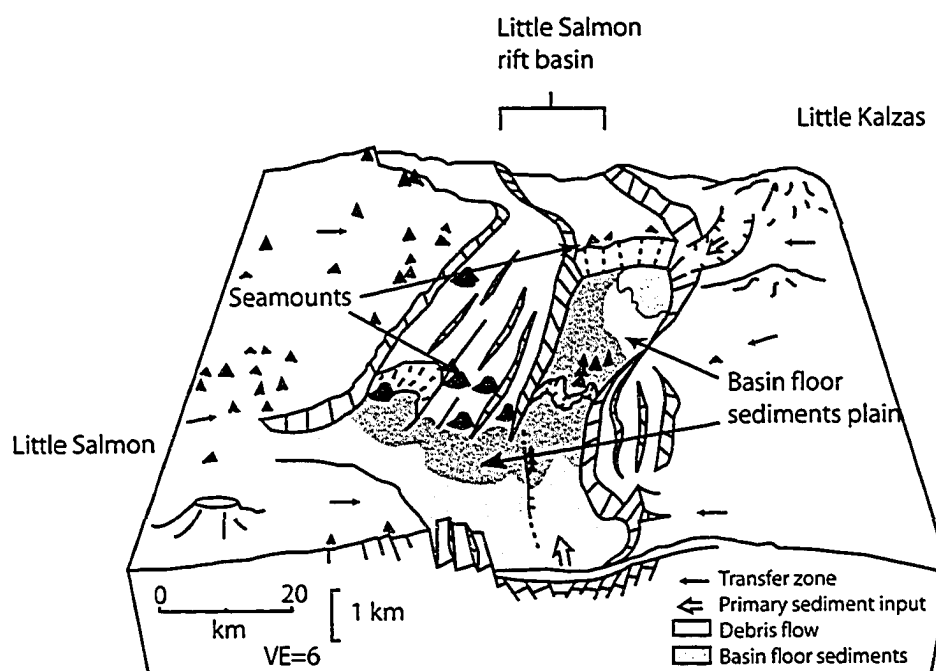
Figure 2-10 — Paleogeographic reconstruction of the Little Salmon rift basin within the Little Salmon-Little Kalzas arc system. This block diagram is a modified version of Klaus et al. (1992) block diagram of the Sumizu rift, SW Pacific, highlighting the clear resemblance between modern and ancient island arc systems. In solid yellow: Little Salmon and Little Kalzas felsic volcanic centres, in solid green: Little Salmon alkali-basalt seamounts, in light yellow: felsic crust-derived sediments, in light green: alkali-basalt volcaniclastic material, derived from the seamount volcanism. Water depth estimated to be <1000 m.

2000). The Mn-rich exhalative horizon records off-axis hydrothermal plume activities during a quiescent period in volcanic activity: such hydrothermal systems have been observed on several modern seamounts in arc-backarc systems (e.g. Fryer, 1995) and in rifted/rifting arcs (e.g. Taylor et al., 1990; Fig. 2-10).

The southern portion of the upper succession is characterized by abundant clastic deposits with a certain amount of fine grained alkali-basalt volcaniclastic and epiclastic deposits especially toward its base (Figs. 2-3 and 2-4). No lava flows or coarse volcanic material were observed in this portion of the upper succession. The pile of volcaniclastic/epiclastic material represents fallout and/or distal turbidite deposits derived from the alkali-basalt volcanic centres observed in the northern portion of the upper succession. The thick sequence of siliciclastic deposits atop the volcaniclastic deposits cannot be derived from the alkali-basalt centres: their quartz-rich content implies a felsic source of volcanic

origin (Little Kalzas and/or Little Salmon arcs) and/or recycled continental-crust-derived sediments (underlying basement; see previous section for details).

The boundary between the northern and the southern upper succession is abrupt and aligned with a small SW-NE fault of same attitude affecting the underlying Little Salmon limestone, Little Salmon lower succession, Pelmac Formation and Snowcap Complex on the west flank of the synclinorium (see "Facies change" dashed-line on Fig. 2-3).

Such an abrupt change in lithofacies aligned with normal fault suggests the presence of a synvolcanic fault scarp. Extensional synvolcanic faults are very common in rifting arc systems which develop series of asymmetric basins, half- to full-grabens, parallel to the arc front (e.g. Klaus et al., 1992; Taylor et al., 1992; Taylor et al., 1991). Volcanism is usually concentrated along these extensional faults and on highs between the rift basins (Taylor et al., 1992) forming relatively small volcanic centres, such as seamounts (northern upper succession stratigraphy; Fig. 2-10). Various amount of pyroclastic and volcaniclastic materials are shed from these volcanic centres in the rifted basins together with other sediments from the surroundings (southern upper succession stratigraphy).

The northern upper succession stratigraphy therefore records alkali-basalt seamount formation atop an extensional synvolcanic fault associated to the development of a rift basin during extension of the Little Salmon-Little Kalzas arc system. The southern upper succession stratigraphy represents the volcanogenic and clastic sediments deposited onto the rift-floor sediment plain(s) of this basin.

2.6 Tectonic significance and Conclusion

In early Mississippian time, several volcanic arcs were forming atop a strip of continental margin sediments, and possibly underlying fragment(s) of continental crust (Fig. 2-11), outboard of the western margin of Laurentia. Around 340 Ma, the Little Salmon continental island arc formed in close proximity to the Little Kalzas arc, an intermediate to felsic 349-343 Ma continental arc system (Colpron, 2001; Colpron et al., in press-b).
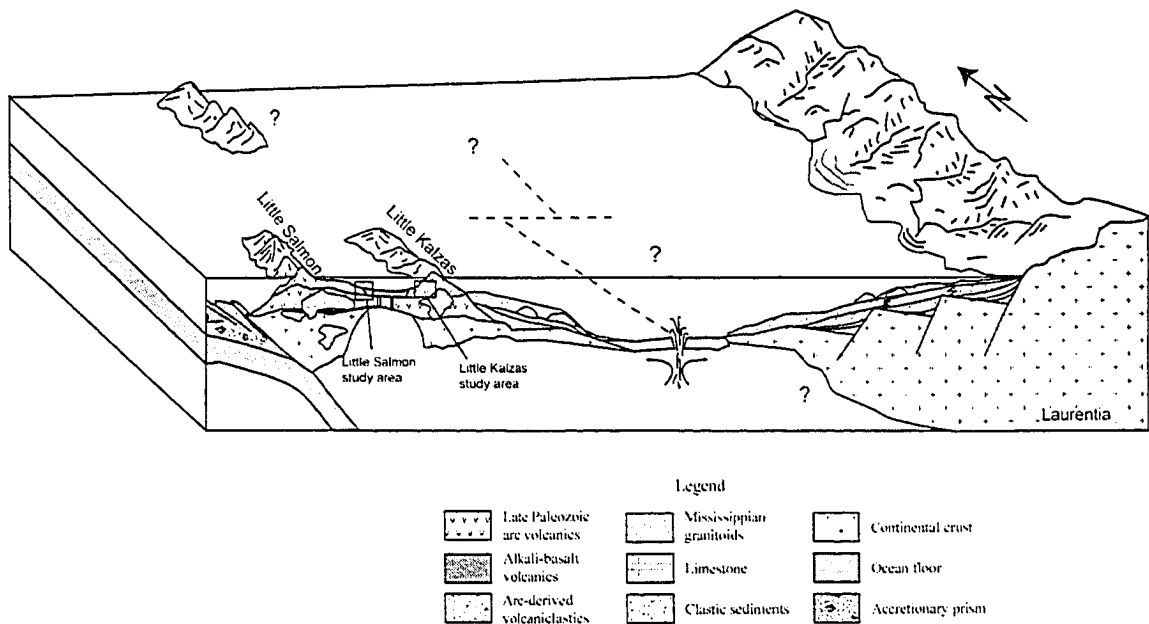
Figure 2-11 – Schematic reconstruction of volcanic arc complexes of the Yukon-Tanana terrane, northern Canadian Cordillera, along the west coast of Laurentia in Pennsylvanian time. The Little Salmon-Little Kalzas arc is inferred to have formed on thin rifted continental crust bloc west of Laurentia (modified from Simard et al., 2003). The Little Salmon-Little Kalzas arc system underwent extension which triggered the development of intra-arc rift basin(s). East-dipping subduction inferred from previous work on eclogite occurrences within the Yukon-Tanana terrane (e.g. Creaser et al., 1999; Nelson et al., in press).

This continental Little Kalzas-Little Salmon arc system, at some point after 340 Ma, underwent extension which triggered the development of intra-arc rift basin(s)(Fig. 2-11). One of these basins is floored by syn-rift volcanic rocks, the Little Salmon upper succession, that are geochemically distinct from their contemporary (?) front arc volcanic rocks, the Little Salmon lower succession. These lavas are alkali-basalt flows, the northern upper succession, formed on seamount flanks close to a normal fault at the margin of the basin. Turbidite sequences, as well as possible fall deposits generated by these volcanic centres, were deposited onto the rift-floor sediment plains, along with other epiclastic and siliciclastic deposits derived from the erosion of the surrounding Little Salmon and Little Kalzas volcanoes, as well as their "continental" basement. Hydrothermal deposits, such as Mn-chert, are unequivocal signs of an active hydrothermal system within that basin, meanwhile recording period(s) of volcanic quiescence in the area.

The rifted Little Salmon-Little Kalzas arc system resembles that of the modern Izu-Bonin-Mariana arc (e.g. Sumisu rift basin; Fig. 2-10; Klaus et al., 1992; Taylor et al., 1992), in which extension within the arc front has led to the development of rift basins of various sizes both in forearc and backarc settings. On the other hand, the presence of a "continental crust-derived" basement under parts of the Little Kalzas-Little Salmon arc system is more like the proto-Japan island arc extension and thinning (e.g. southern Japan Sea, Tamaki, 1995). These rift basins, whether formed in rifting oceanic or continental arc systems, are well-known to host important hydrothermal systems, and are well-accepted analogues to the settings where most major Phanerozoic volcanogenic massive sulphide deposits formed (e.g. Rona, 1988; Sawkins, 1971).

This study demonstrates that the Late Paleozoic arc-related volcano-sedimentary sequences that compose the Yukon-Tanana pericratonic terrane in the northern Canadian Cordillera today, formed in an extensional tectonic environment similar to modern arc environments with intra-arc rifting and hydrothermal activity.

2.7 References

Bhatia, M.R. and Crook, K.A.W., 1986. Trace element characteristics of greywackes and tectonic setting discrimination of sedimentary basins. Contributions to Mineralogy and Petrology, 92: 181-193.

Boghossian, N.D., Patchett, P.J., Ross, G.M. and Gehrels, G.E., 1996. Nd isotopes and the source of sediments in the miogeocline of the Canadian Cordillera. Journal of Geology, 104(3): 259-277.

Cameron, E.M. and Hattori, K., 1997. Strontium and neodynium isotope ratios in the Fraser River, British Columbia: a riverine transect across the Cordilleran orogen. Chemical Geology, 137(3-4): 243-253.

Colpron, M., 1998. Preliminary geological map of Little Kalzas Lake area, central Yukon (NTS 105L/13). Exploration and Geological Services Division, Yukon Region, Indian and Northern Affairs Canada.

Colpron, M., 1999a. Glenlyon Project: Preliminary stratigraphy and structure of Yukon-Tanana Terrane, Little Kalzas Lake area, central Yukon (105L/13). In: C.F. Roots and D.S. Emond (Editors), Yukon Exploration and Geology. Exploration and Geological Services Division, Yukon Region, Indian and Northern Affairs Canada, pp. 63-72.

Colpron, M., 1999b. A new mineral occurrence in Yukon-Tanana terrane near Little Salmon Lake, central Yukon (NTS 105L/2). In: C.F. Roots and D.S. Emond (Editors), Yukon Exploration and Geology. Exploration and Geological Services Division, Yukon Region, Indian and Northern Affairs Canada, pp. 255-258.

Colpron, M., 2000. Geological map of Little Salmon Lake (parts of NTS 105L/1, 2 & 7), central Yukon. Exploration and Geological Services Division, Yukon Region, Indian and Northern Affairs Canada.

Colpron, M., 2001. Geochemical characterization of Carboniferous volcanic successions from Yukon-Tanana terrane, Glenlyon map area (105L), central Yukon. In: D.S. Emond and L.H. Weston (Editors), Yukon Exploration and Geology 2000. Exploration and Geological Services Division, Yukon Region, Indian and Northern Affairs Canada, pp. 111-136.

Colpron, M., Gladwin, K., Johnston, S.T., Mortensen, J.K. and Gehrels, G.E., in press-a. Geology and juxtaposition history of Yukon-Tanana, Slide Mountain and Cassiar terranes in the Glenlyon area of central Yukon. Canadian Journal of Earth Sciences.

Colpron, M., Mortensen, J.K., Gehrels, G.E. and Villeneuve, M.E., in press-b. Basement complex, Carboniferous magmatic arcs and Paleozoic deformation in Yukon-Tanana terrane of central Yukon. In: M. Colpron, J.L. Nelson and R.I. Thompson (Editors), Paleozoic evolution and metallogeny of pericratonic terranes at the ancient Pacific margin of North America, Canadian and Alaskan Cordillera. Geological Association of Canada.

Colpron, M., Murphy, D.C. and Mortensen, J.K., 2000. Mid-Paleozoic tectonism in Yukon-Tanana Terrane, northern Canadian Cordillera: record of intra-arc deformation. Geological Society of America, Cordilleran Section, Abstracts with Programs, 32(6): A-7.

Colpron, M. et al., 2003. Yukon Targeted Geoscience Initiative, Part 1: Results of accelerated bedrock mapping in Glenlyon (105L/1-7, 11-14) and northeast Carmacks (115I/9,16) areas, central Yukon. In: D.S. Emond and L.L. Lewis (Editors), Yukon Exploration and Geology 2002. Exploration and Geological Services Division, Yukon Region, Indian and Northern Affairs Canada, pp. 85-108.

Colpron, M. and Reinecke, M., 2000. Glenlyon Project: Coherent stratigraphic succession from Little Salmon Range (Yukon-Tanana Terrane), and its potential for volcanic-hosted massive sulphide deposits. In: L.H. Weston (Editor), Yukon Exploration and Geology 1999. Exploration and Geological Services Division, Yukon Region, Indian and Northern Affairs Canada, pp. 87-100.

Coney, P.J., Jones, D.L. and Monger, J.W.H., 1980. Cordilleran suspect terranes. Nature, 288: 329-333.

Corcoran, P.L., 2000. Recognizing distinct portions of seamounts using volcanic facies analysis; examples from the Archean Slave Province, NWT, Canada. Precambrian Research, 101(2-4): 237-261.

Creaser, R.A., Erdmer, P., Stevens, R.A. and Grant, S.L., 1997. Tectonic affinity of Nisutlin and Anvil assemblage strata from the Teslin tectonic zone, northern Canadian Cordillera; constraints from neodymium isotope and geochemical evidence. Tectonics, 16(1): 107-121.

Creaser, R.A., Goodwin-Bell, J.-A.S. and Erdmer, P., 1999. Geochemical and Nd isotopic constraints for the origin of eclogite protoliths, northern Cordillera; implications for the Paleozoic tectonic evolution of the Yukon-Tanana Terrane. Canadian Journal of Earth Sciences = Revue Canadienne des Sciences de la Terre, 36(10): 1697-1709.

Fryer, P., 1995. Geology of the Mariana Trough. In: B. Taylor (Editor), Backarc basins; Tectonics and magmatism. Plenum Press, New York, pp. 237-280.

Gabrielse, H., Monger, J.W.H., Wheeler, J.O. and Yorath, C.J., 1991. Tectonic framework; Part A, Morphogeological belts, tectonic assemblages and terranes. In: H. Gabrielse and C.J. Yorath (Editors), Geology of the Cordilleran Orogen in

Canada. Geological Survey of Canada, Geology of Canada, (also Geological Society of America, v. G-2), pp. 677-705.

Gabrielse, H. and Yorath, C.J., 1991. Tectonic synthesis. In: H.G.a.C.J. Yorath (Editor), Geology of the Cordilleran Orogen in Canada. Geological Survey of Canada, Geology of Canada, (also Geological Society of America, v. G-2), pp. 677-705.

Garzione, C.N., Patchett, P.J., Ross, G.M. and Nelson, J., 1997. Provenance of Paleozoic sedimentary rocks in the Canadian Cordilleran miogeocline; a Nd isotopic study. Canadian Journal of Earth Sciences = Journal Canadien des Sciences de la Terre, 34(12): 1603-1618.

Gladwin, K., Colpron, M., Black, R. and Johnston, S.T., 2003. Bedrock geology at the boundary between Yukon-Tanana and Cassiar terranes, Truitt Creek map area (105L/1), south-central Yukon. In: D.S. Emond and L.L. Lewis (Editors), Yukon Exploration and Geology 2002. Exploration and Geological Services Division, Yukon Region, Indian and Northern Affairs Canada, pp. 135-148.

Goldstein, S.L., 1988. Decoupled evolution of Nd and Sr isotopes in the continental crust and the mantle. Nature, 336(6201): 733-738.

Hamilton, P.J., O'Nions, R.K., Bridgwater, D. and Nutman, A., 1983. Sm-Nd studies of Archaean metasediments and metavolcanics from West Greenland and their implications for the Earth's early history. Earth and Planetary Science Letters, 63: 263-273.

Hart, S.R., 1988. Heterogeneous mantle domains: signatures, genesis and mixing chronologies. Earth and Planetary Science Letters, 90(3): 272-296.

Hawkesworth, C.J. et al., 1979. $^{143}Nd/^{144}Nd$, $^{87}Sr/^{86}Sr$ and incompatible element variations in calc-alkaline andesites and plateau lavas from South America. Earth and Planetary Science Letters, 42: 45-57.

Jacobsen, S.B. and Wasserburg, G.J., 1980. Sm-Nd isotopic evolution of chondrites. Earth and Planetary Science Letters, 50: 139-155.

Klaus, A. et al., 1992. Structural and stratigraphic evolution of the Sumisu Rift, Izu-Bonin Arc. Proceedings of the Ocean Drilling Program, Scientific Results, 126: 555-573.

Langmuir, C.H., Vocke, R.D.J., Hanson, G.D. and Hart, S.R., 1978. A general mixing equation with applications to Icelandic basalts. Earth and Planetary Science Letters, 37: 380-393.

Lentz, D.R., 1998. Petrogenetic evolution of felsic volcanic sequences associated with Phanerozoic volcanic-hosted massive sulphide systems: the role of extensional geodynamics. Ore Geology Reviews, 12: 289-327.

Lentz, D.R., 1999. Petrology, geochemistry and oxygen isotopic interpretation of felsic volcanic and related rocks hosting the Brunswick 6 and 12 massive sulphide depostis (Brunswick Belt), Bathurst Mining Camp, New Brunswick, Canada. Economic Geology, 94: 57-86.

McDonough, W.F. and Sun, S.S., 1995. The composition of the Earth. In: W.F. McDonough, N.T. Arndt and S. Shirey (Editors), Chemical Geology. Elsevier, Amsterdam, pp. 223-253.

McPhie, J., 1995. A Pliocene shoaling basaltic seamount; Ba Volcanic Group at Rakiraki, Fiji. Journal of Volcanology and Geothermal Research, 64(3-4): 193-210.

McPhie, J., Doyle, M. and Allen, R., 1993. Volcanic texures: a huide to interpretation of textures in volcanic rocks. Centre for Ore Deposit and Exploration Studies, University of Tasmania, Tasmania, 198 pp.

Monger, J.W.H., 1999. Review of the geology and tectonics of the Canadian Cordillera. Short course notes, Sydney, 72 pp.

Monger, J.W.H., Price, R.A. and Tempelman-Kluit, D.J., 1982. Tectonic accretion and the origin of the two major metamorphic and plutonic welts in the Canadian Cordillera. Geology, 10(2): 70-75.

Morris, G.A. and Hooper, P.R., 1997. Petrogenesis of the Colville igneous complex, Northeast Washington; implications for Eocene tectonics in the northern U.S. Cordillera. Geology, 25(9): 831-834.

Morris, G.A., Larson, P.B. and Hooper, P.R., 2000. "Subduction style" magmatism in a non-subduction setting; the Colville igneous complex, NE Washington State, USA. Journal of Petrology, 41(1): 43-67.

Mortensen, J.K., 1992. Pre-mid-Mesozoic tectonic evolution of the Yukon-Tanana Terrane, Yukon and Alaska. Tectonics, 11(4): 836-853.

Nelson, J.L., Colpron, M. and Piercey, S.J., in press. Paleozoic tectonic and metallogenetic evolution of the pericratonic terranes in Yukon, northern British Columbia and eastern Alaska. In: M. Colpron, J.L. Nelson and R.I. Thompson (Editors), Paleozoic evolution and metallogeny of pericratonic terranes at the ancient Pacific margin of North America, Canadian and Alaskan Cordillera. Geological Association of Canada.

Pearce, J.A., 1983. Role of sub-continental lithopheric magma genesis at active continental margins. In: C.J. Hawkesworth and M.J. Norry (Editors), Continental flood basalts and mantle xenoliths. Shiva Publishing Ltd., Nantwich, pp. 230-249.

Pearce, J.A. and Cann, J.R., 1973. Tectonic setting of basic volcanic rocks determining using trace element analyses. Earth and Planetary Science Letters, 19: 290-300.

Pearce, J.A. and Peate, D.W., 1995. Tectonic implications of the composition of volcanic arc magmas. Annual Review of Earth and Planetary Sciences, 23: 251-285.

Peter, J.M., Mihalynuk, M.G., Colpron, M. and Nelson, J.L., 2003. Diverse examples of exhalative hydrothermal sediments in Yukon-Tanana Terrane, Yukon Territory and British Columbia, GAC-MAC 2003, Vancouver.

Piercey, S.J., Mortensen, J.K., Murphy, D.C., Paradis, S. and Creaser, R.A., 2002. Geochemistry and tectonic significance of alkalic mafic magmatism in the Yukon-Tanana Terrane, Finlayson Lake region, Yukon. Canadian Journal of Earth Sciences = Revue Canadienne des Sciences de la Terre, 39(12): 1729-1744.

Piercey, S.J., Murphy, D.C., Mortensen, J.K. and Paradis, S., 2001a. Boninitic magmatism in a continental margin setting, Yukon-Tanana Terrane, southeastern Yukon, Canada. Geology, 29(8): 731-734.

Piercey, S.J., Paradis, S., Murphy, D.C. and Mortensen, J.K., 2001b. Geochemistry and paleotectonic setting of felsic volcanic rocks in the Finlayson Lake volcanic-hosted massive sulfide district, Yukon, Canada. Economic Geology and the Bulletin of the Society of Economic Geologists, 96(8): 1877-1905.

Rona, P.A., 1988. Hydrothermal mineralization at oceanic ridges. Canadian Mineralogist, 26: 431-465.

Sawkins, F.J., 1971. Sulfide ore deposits in relation to geotectonics. Journal of Geology, 80: 377-397.

Schmidt, R. and Schmincke, H.-U., 2000. Seamounts and island building. In: H.
Sigurdsson, B.F. Houghton, S.R. McNutt, H. Rymer and J. Stix (Editors).
Academic Press, San Diego, pp. 383-402.

Shervais, J.W., 1982. Ti/V plots and the petrogenesis of modern and ophiolotic lavas.
Earth and Planetary Science Letters, 59: 101-118.

Simard, R.-L., Dostal, J. and Roots, C.F., 2003. Development of late Paleozoic volcanic
arcs in the Canadian Cordillera; an example from the Klinkit Group, northern
British Columbia and southern Yukon. Canadian Journal of Earth Sciences =
Revue Canadienne des Sciences de la Terre, 40(7): 907-924.

Steiger, R.H. and Jaeger, E., 1977. Subcommission on geochronology; convention on the
use of decay constants in geo- and cosmochronology. Earth and Planetary Science
Letters, 36(3): 359-362.

Sun, S.S. and McDonough, W.F., 1989. Chemical and isotopic systematics of oceanic
basalts; implications for mantle composition and processes. Geological Society
Special Publications, 42: 313-345.

Tamaki, K., 1995. Opening tectonic of the Japan Sea. In: B. Taylor (Editor), Backarc
basins: Tectonics and magmatism. Plenum Press, New York, pp. 407-420.

Taylor, B. et al., 1990. Alvin-Seabeam studies of the Sumisu Rift, Izu-Bonin Arc. Earth
and Planetary Science Letters, 100(1-3): 127-147.

Taylor, B. et al., 1992. Rifting and the volcanic-tectonic evolution of the Izu-Bonin-
Mariana Arc. Proceedings of the Ocean Drilling Program, Scientific Results, 126:
627-651.

Taylor, B. et al., 1991. Structural development of Sumisu Rift, Izu-Bonin Arc. Journal of
Geophysical Research, B, Solid Earth and Planets, 96(10): 16,113-16,129.

Taylor, S.R. and McLennan, S.M., 1985. The continental crust; its composition and
evolution; an examination of the geochemical record preserved in sedimentary
rocks. Geoscience texts. Blackwell Sci. Publ., Oxford, United Kingdom (GBR),
312 pp.

Taylor, S.R. and McLennan, S.M., 1995. The geochemical evolution of the continental
crust. Reviews of Geophysics, 33(2): 241-265.

Wheeler, J.O., Brookfiels, A.J., Gabrielse, H., Monger, J.W.H., tipper, H.W., and Woodsworth, G.J., 1991. Terrane map of the Canadian Cordillera, Geological Survey of Canada.

White, R.S., Mackenzie, D. and O'Nions, R.K., 1992. Oceanic crustal thickness from seismic measurement and REE inversions. Journal of Geophysical Research, 97: 19683-19715.

Wilson, M., 1989. Igneous Petrogenesis, a glodal tectonic approach. Chapman & Hall, London, 466 pp.

Winchester, J.A. and Floyd, P.A., 1976. Geochemical magma type discrimination; application to altered and metamorphosed basic igneous rocks. Earth and Planetary Science Letters, 28(3): 459-469.

Winchester, J.A. and Floyd, P.A., 1977. Geochemical discrimination of different magma series and their differentiation products using immobile elements. Chemical Geology, 20(4): 325-343.

Wood, D.A., Joron, J.L. and Treuil, M., 1979. A re-appraisal of the use of trace-elements to classify and discriminate between magma series erupted in different tectonic settings. Earth and Planetary Science Letters, 45(326-336).

Young, G.M., 2002. Geochemical investigation of a Neoproterozoic glacial unit; the Mineral Fork Formation in the Wasatch Range, Utah. Geological Society of America Bulletin, 114(4): 387-399.

Chapter 3

Mississippian alkali basalt seamounts and submarine pyroclastic activity in an intra-arc rift basin, Little Salmon formation, Yukon Territory, Canada[1]

3.1 Introduction

Seamounts[2] are the sites of most known modern active hydrothermal centres. Although there are more than one million on today's seafloor (Schmidt and Schmincke, 2000) and they occur throughout geological time in various tectonic settings (e.g. Corcoran, 2000; Sohn, 1995; Staudigel and Schmincke, 1984), seamounts are poorly studied because of their submarine setting. Uplifted subaerially exposed old subaqueous volcanic sequences are the best candidates for a thorough study of the internal stratigraphy of the most abundant volcanic edifice type on the Earth's surface.

The purpose of this paper is to document alkali basalt seamounts formation atop an extensional synvolcanic fault associated with the development of a rift basin during extension/rifting of a Mississippian continental arc system, the Little Kalzas-Little Salmon arc of northern Canadian Cordillera, central Yukon (Fig. 3-1).

Using detailed lithofacies analyses, this paper demonstrates that one part of the Little Salmon arc records explosive volcanic eruptions and associated pyroclastic flows during the build-up of several small alkali basalt seamounts, whereas another part represents various amounts of pyroclastic and volcaniclastic materials that were shed from the volcanic centres in the nearby rift basin and deposited together with other siliciclastic sediments from the surrounding areas.

---

[1] Simard, R.L., Dostal, J., and Colpron, M. in prep. Manuscript ready to be submitted to Journal of Volcanology and Geothermal Research in August 2005. At this stage, as the first author, RL Simard wrote the entire manuscript and drafted most of the figures, the coauthors suggested corrections to the manuscript.
[2] Seamounts: Volcanic edifices with elevations of more than 50-100 m above the surrounding seafloor (Schmidt and Schmincke, 2000).

47
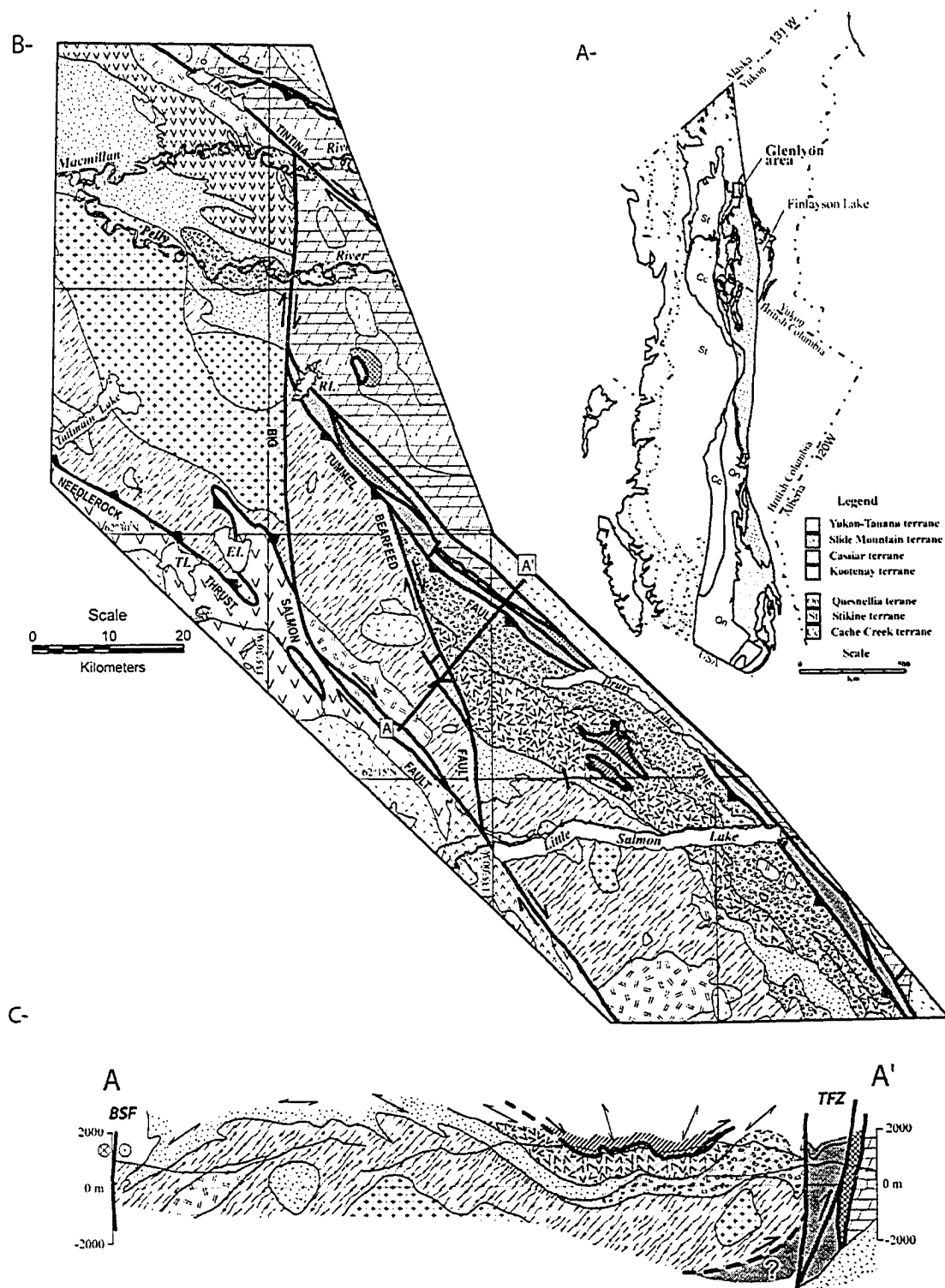
Figure 3-1 – Location map. A- Generalized terrane map of the eastern Canadian Cordillera, showing the pericratonic terrane belt (modified from Wheeler, 1991), B- Generalized geological map of the Glenlyon area, central Yukon (modified from Colpron et al., 2003; see next page for legend), C- Cross-section of the Yukon-Tanana rocks of the Glenlyon area showing the broad synclinorium structure in the area (modified from Colpron et al., in press-b).
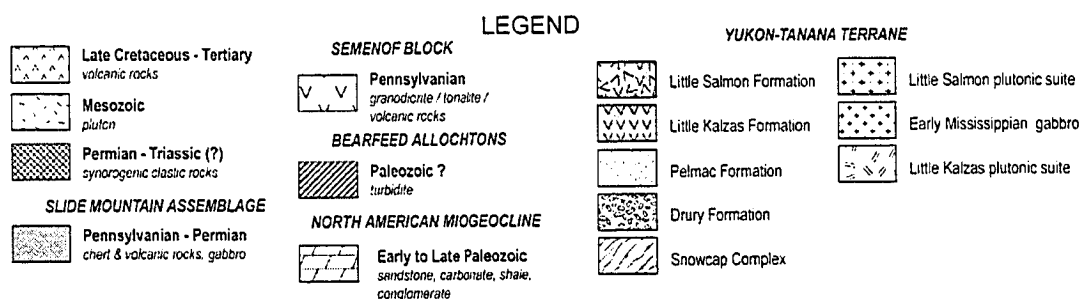
3.2 Northern Canadian Cordillera geology

The Canadian Cordillera was formed by the accretion of numerous arcs and basins to the western margin of Laurentia from Mesozoic to early Cenozoic time. The oldest of these arc-basin systems were the first to accrete to the continent, and form the pericratonic terrane belt (Fig. 3-1). The pericratonic terrane rocks record the pre-accretion late Paleozoic tectonic evolution of the western margin of Laurentia. One of the most prominent of these pericratonic terranes, the Yukon-Tanana terrane in the northern Canadian Cordillera (Fig. 3-1), records the development of a series of Devono-Carboniferous arc edifices built in places upon a metasedimentary basement, punctuated by episodic arc rifting magmatism, back-arc formation, intra-arc deformation and local uplift and erosion (Fig. 3-2; Colpron et al., in press-b; Piercey et al., 2002; Piercey et al., 2001a; Piercey et al., 2001b). Important volcanogenic massive sulfide deposits have been found within these arc-backarc systems (e.g. Kudz Ze Kayah; Piercey et al., 2001b).

3.2.1 Local Geology

The *Little Salmon formation* rocks, exposed in the Glenlyon area, central Yukon, are part of the Yukon-Tanana terrane (Figs. 3-1 and 3-2); they record the rifting of an Early Carboniferous continental arc system (Little Kalzas-Little Salmon arc; Chap. 2). The Little Salmon formation is a Mississippian to mid-Pennsylvanian sequence of felsic and mafic volcanic rocks that sits unconformably on basinal sedimentary sequences, the Drury and Pelmac formations, which were in turn deposited upon a metasedimentary basement of continental margin affinity, the Snowcap Complex (Figs. 3-2 and 3-3;
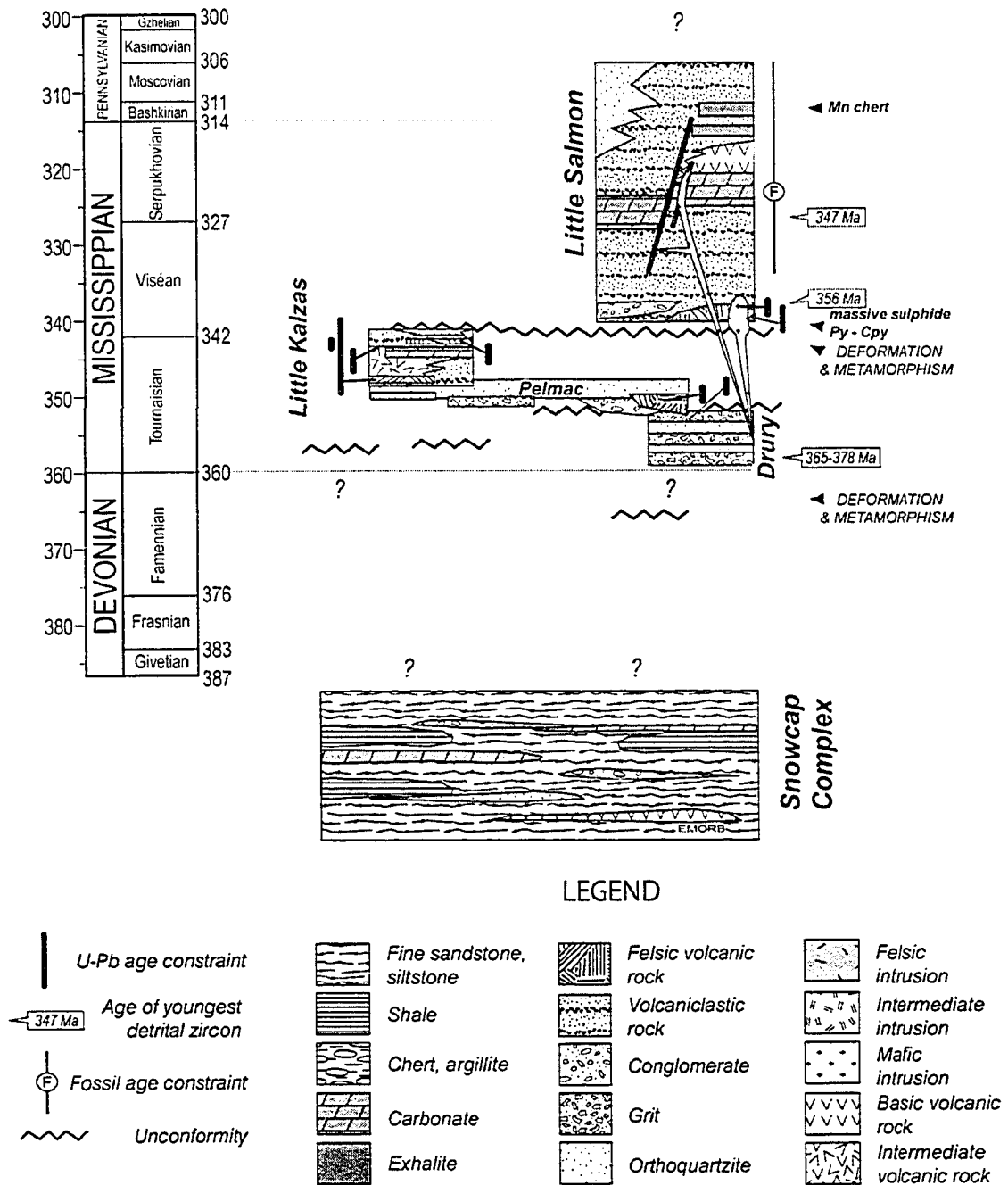
Figure 3-2 – Stratigraphic relations of Yukon-Tanana composite terrane in the Glenlyon area (modified from Colpron et al., in press-b)

Colpron, 2001; Colpron et al., 2003). This stratigraphy is exposed in a broad NW-SE synclinorium along Little Salmon Lake (Figs. 3-1 and 3-3). Little Salmon rocks are typically folded at the outcrop scale and display one to two well-developed foliations
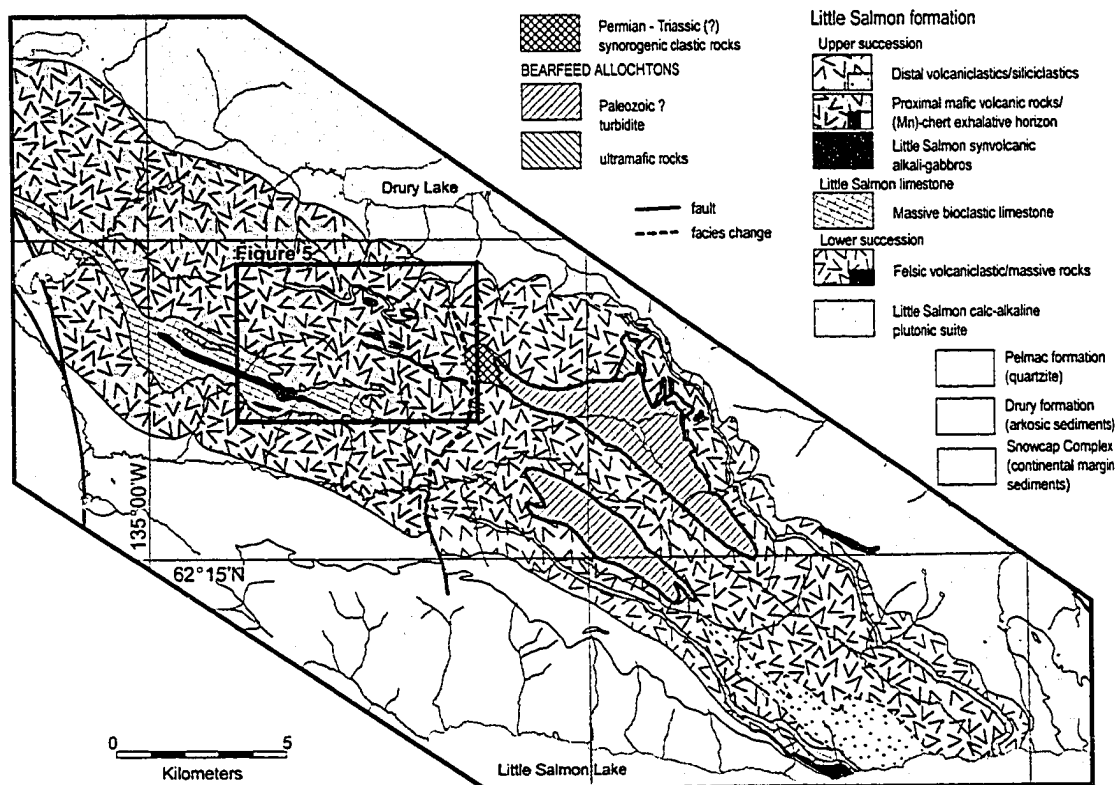
Figure 3-3 – Lithofacies distribution map of the Little Salmon formation. The rocks of the upper succession of the Little Salmon formation show an abrupt proximal versus distal volcanic facies change across a presumed syn-volcanic fault in the area (N-S dotted line).

that, in places, obliterate the primary texture. The primary mineralogy is not preserved in the mafic volcanic rocks that have all been affected by low-grade greenschist facies metamorphism as indicated by the mineral assemblage chlorite + muscovite + calcite ± actinolite ± biotite ± apatite ± quartz. However, the prefix 'meta' is omitted here for simplicity.

The Little Salmon formation comprises a "lower succession" of felsic volcaniclastic and volcanic rocks, and an "upper succession" of mafic volcanic and volcaniclastic rocks (Figs. 3-3 and 3-4; Colpron et al., in press-b; Colpron et al., 2000; Chap. 2); a late Mississippian to mid-Pennsylvanian bioclastic limestone unit separates the two successions (Figs. 3-3 and 3-4).

51

N ⟷ S

northern upper succession

southern upper succession

Little Salmon formation

Pelmac fm

lower succession

Snowcap Complex

Upper succession

- ■ Alkaline leuco gabbro
- ■ Massive/Pillowed flows
- ▲▲ Breccia
- ■ Crystal tuff
- ■ MORB gabbro

- ▨ Ash tuff
- □ Chert
- ▨ Exhalative chert
- □ Siliciclastic sediments

Lower succession

- □ Felsic/intermediate tuff
- □ Quartzite conglomerate
- ■ Quartz-feldspar porphyry

- ■ Little Salmon limestone

Figure 3-4 – Generalized stratigraphy of the Little Salmon formation.

The *lower succession* is a 40 m – 450 m thick section of coherent quartz-feldspar porphyritic felsic rocks and felsic volcaniclastic sandstone and siltstone. The calc-alkaline geochemical signature of these felsic volcanic rocks suggests that they formed in an arc environment, the Little Salmon arc, underlain by continental crust; they probably represent crustal melts (Chap. 2).

A limestone unit, the *Little Salmon limestone*, conformably overlies the lower succession (Figs. 3-3 and 3-4). This thick bioclastic limestone is typically massive and laterally interbedded with tuffaceous layers (Figs. 3-3 and 3-4).

Sitting conformably atop the Little Salmon limestone, the *upper succession* consists of a thick succession of alkali basalt, it shows important facies change along strike (Figs. 3-3 and 3-4). In the north (Fig. 3-3), east of Drury Lake, the "northern" upper succession

stratigraphy exposes highly porphyritic massive and pillowed lava flows with abundant associated breccia, crystal-tuff and ash-tuff volcaniclastic strata, localized exhalative strata and minor quartz-rich clastic strata (northern upper succession, Fig. 3-4). In the south (Fig. 3-3), along the north shore of Little Salmon Lake, the "southern" upper succession stratigraphy consists of a thick pile of crystal and ash-tuff interbedded with abundant clastic strata, without massive volcanic rocks (southern upper succession, Fig. 3-4). This alkali basalt volcanism is associated with one or more alkaline leucocratic gabbro bodies as well as sparse thin mafic dykes and sill(s) cross-cutting the underlying units; the latter most likely represent feeder dykes to the alkali basalt volcanism (Chap. 2). Their primitive alkaline geochemical and isotopic characteristics are consistent with an asthenospheric source unaffected by subduction processes. They represent intra-arc rifting mafic magmatism within the Little Salmon arc system (Chap. 2).

3.3 Lithofacies of the "upper succession" of the Little Salmon formation

Detailed stratigraphic work was conducted to constrain the lateral and vertical lithofacies distribution and to document the volcanic structure. Figure 3-5 presents simplified cross-sections of the northern upper succession stratigraphy and structure based on several traverses along well exposed ridges east of Drury Lake; Figure 3-6 shows a composite barrier diagram of the area. Table 3-1 gives complete descriptions of the volcanic and siliciclastic lithofacies observed in the upper succession of the Little Salmon formation.

The "northern" upper succession of the Little Salmon formation comprises abundant volcaniclastic lithofacies (polymictic volcanic breccia (15%; Plate 1H), monomictic volcanic breccia (5%; Plate 1G) , crystal-rich coarse-tuff (45%), crystal-rich tuff-breccia (5%; Plate 2A, 2B, and 2D), ash-tuff (20%; Plate 2C and 2E) which are interbedded with massive (5%; Plate 1A, 1B and 1C) and pillowed (5%; Plate 1D, 1E, and 1F) lava lithofacies and localized exhalative Mn-chert lithofacies (5%; Plates 2F, 3A and 3B). In contrast, the "southern" upper succession of the Little Salmon formation comprises solely clastic rocks, including interbedded volcaniclastic lithofacies [ash-tuff (15%; Plate 3D),
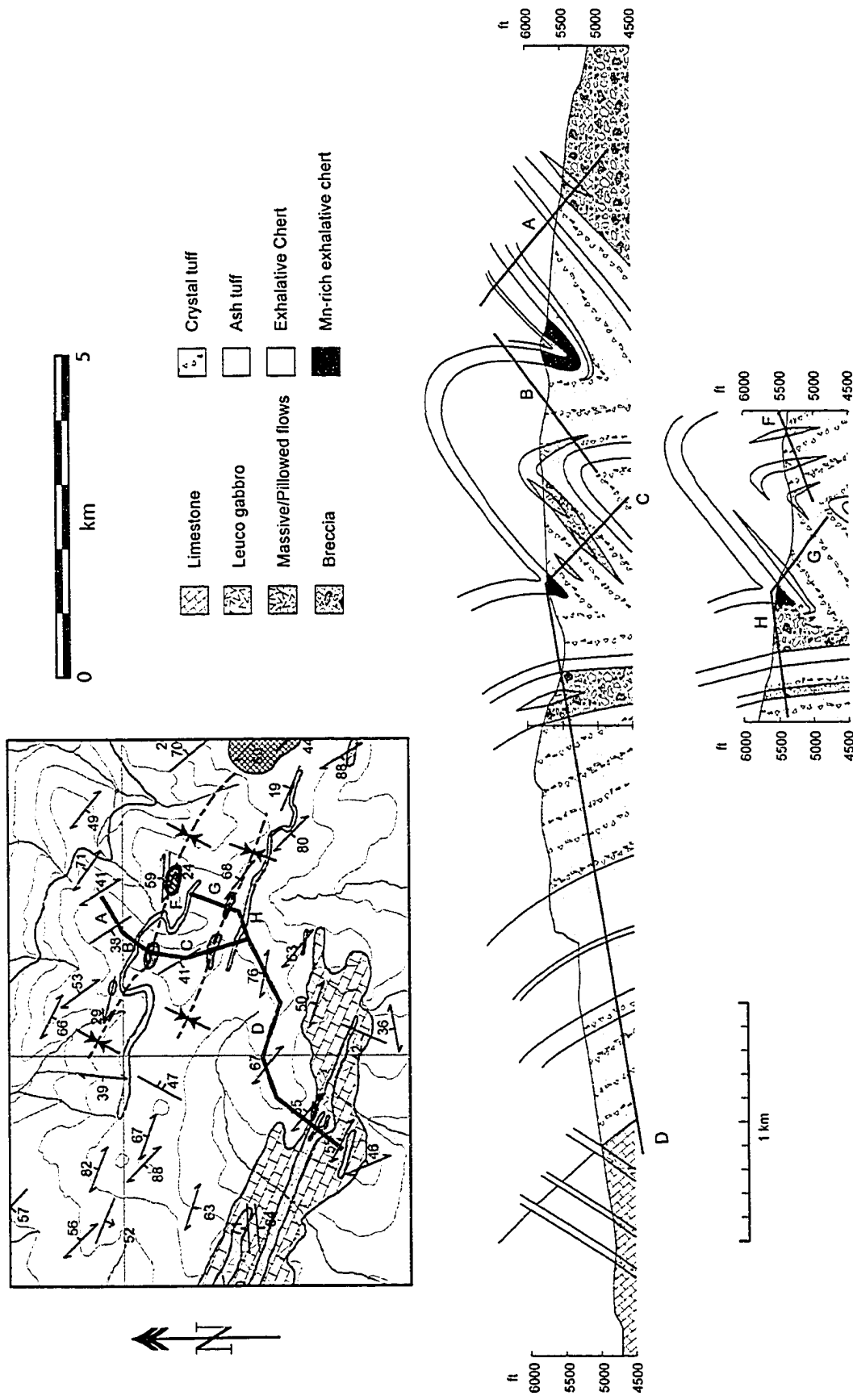
Figure 3-5 – Structural profiles of the northern upper succession. Profiles measured along well-exposed ridge, above tree-line. Vertical elevation in feet. Lines A-H refer to stratigraphic column, figure 3-6.

54
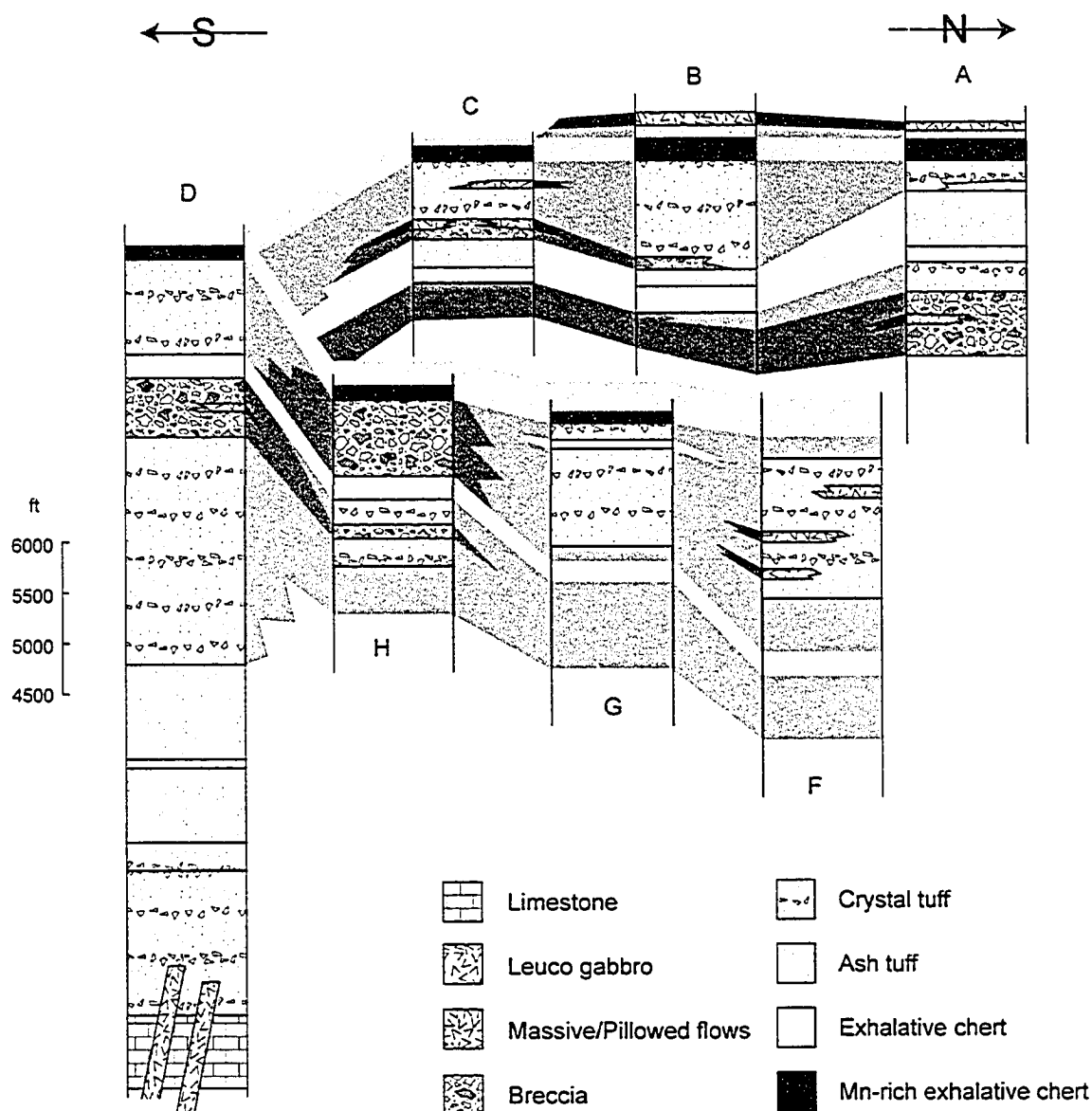
Figure 3-6 – Composite barrier diagram of the northern upper succession. Thickness measured in feet from the structural profiles. Total thickness of each lithofacies might include some structural thickening. Vertical elevation in feet.

volcaniclastic sandstone and siltstone (45%; Plate 3C)] and siliciclastic [quartz-rich sandstone and mudstone (35%; Plate 3E), arkosic grit (5%; Plate 3F)].

Throughout the study area, the cohesive lithofacies as well as the volcanic clasts in the volcaniclastic lithofacies are composed of alkali basalt. The alkali basalts are typically highly porphyritic, with about 10-20% plagioclase phenocrysts ranging up to 3 cm in size (Plate 1A); amygdules can be present but are neither abundant (<3%) nor large (<2mm).

Table 3-1 – Lithofacies description of the Little Salmon formation upper succession

Little Salmon formation - upper succession*	
Volcanic lithofacies**	**Description**
Massive basalt	5-15m-thick unit; purplish to dark green seriate porphyritic massive rock showing 10-20% euhedral to subhedral 0.2-3cm φ*** plagioclase phenocrysts; locally up to 3% of flatten chloritic disks (amygdules?)
Pillowed lava	5-30m-thick unit; dark purplish green ± porphyritic pillowed basaltic flow i) 25cm-1m φ closely-packed fine grained pillow tubes showing 3-5cm-thick altered rims, and locally up to 10% of calcite-filled amygdules <5mm φ in the core; ii) 30-50cm φ closely-packed pillow tubes showing in places highly porphyritic cores with 15% 2-13mm φ euhedral to subhedral plagioclase mega-phenocrysts in a very fine grained matrix with 10% of 0.5-1mm φ euhedral to subhedral plagioclase phenocrysts, 2-4cm- thick fine grained purple rim with 10% of 0.5-1mm φ euhedral to subhedral plagioclase phenocrysts, <15% flatten chloritic disks up to 2mm φ concentrated in the outer rim (amygdules) and <10% calcite-filled amygdules and hollows in the cores; iii) when pillows <30cm φ, not megaporphyritic, 10% of 0.5-1mm φ euhedral to subhedral plagioclase phenocrysts, not amygdaloidal, thin very fine grained rim (1-2cm-thick)
Monomictic volcanic breccia	>1m-thick unit; massive, monomictic pebble to cobble matrix-supported breccia showing up to 12 cm long dark purplish green porphyritic basaltic subangular clasts in a fine grained brownish carbonate-rich matrix; clasts: plagioclase-megaphyric basalt (pillow fragments?); associated with pillowed flows.
Polymictic volcanic breccia	2- >15m-thick unit; massive, poorly sorted, polymictic pebble breccia beds showing up to 6cm long stretched volcanic and minor limy clasts in a fine grained epidote-chlorite-calcite matrix; 80-90% volcanic component: plagioclase-megaphyric basalt, fine grained basalt (pillow rim fragments?), plagioclase crystals, volcanic ash (chlorite+epidote); 10-20% limy component: massive fine-grained grey limestone, potentially minor recrystallized corals and crinoids; commonly associated with massive or pillowed flows.
Bedded tuff	1cm- >10m-thick unit; massive to well-bedded medium-green tuff. i) crystal-rich coarse-tuff: coarse plagioclase-crystal-tuff showing up to 30% of 0.5-2mm φ euhedral to subhedral crystals in a epidote-chlorite-calcite fine grained matrix (recrystallized and metamorphosed ashes); formed massive 2cm-10m-thick layers, laterally continuous, locally graded; interbedded with very very coarse grained crystal-tuff and ash-tuff. ii) crystal-rich tuff-breccia: very very coarse plagioclase-crystal-tuff showing up to 70% of 2-15mm φ euhedral to subhedral crystals, commonly broken and/or fractured, in a epidote-chlorite-calcite fine grained matrix; formed massive 20cm->8m-thick poorly sorted layers, with rare inverse-graded base, and normal-graded top; normally laterally continuous over >30m, meter-long lenticular beds in places; interbedded with finer grained crystal- and ash-tuff; yielded Precambrian detrital zircons (G. Gehrels, pers. comm. 2003) iii) ash-tuff: medium to dark green massive to well-bedded chlorite-rich fine grained (metamorphosed ash) laterally continuous layers, commonly showing flatten chlorite-disks along bedding plane, and graded-beds; interbedded with coarser tuffaceous beds and flows.
Exhalative Mn-rich chert	5-30m-thick unit; pale green to pink to deep red finely bedded Mn-rich exhalative cherty layers; locally interbedded with ash-tuff layers
Volcaniclastic sandstone and siltstone	40-300 m-thick unit; light green, green, and beige well-bedded quartz-rich sandstone (quartz + muscovite ± carbonate ±chlorite ±magnetite) and siltstone (quartz +chlorite +muscovite ±carbonate ±magnetite) beds, commonly showing graded-beds; interpreted as epiclastic deposits

Siliciclastic lithofacies	Description
Quartzite-pebble to - boulder conglomerate	3 to 20m thick unit; quartzite-pebble to -boulder conglomerate of subangular to subrounded quartzite clasts, some of which contain a pre-depositional foliation, supported by a matrix of fine-grained quartz-rich sandstone (quartz +chlorite +muscovite +calcite; Gladwin et al., 2003). Detrital zircons of Early Mississippian age recovered from these rocks (Colpron et al., in press-a).
Quartz-rich sandstone and mudstone	5- >100m-thick unit; pale to medium green massive to well bedded quartz-rich sandstone to mudstone beds (quartz ±feldspar +muscovite +calcite ±epidote ±chlorite ±biotite ±apatite ±garnet), locally graded; interbedded with ash- and crystal-tuff layers in places; i) thinly bedded fine grained quartz-rich mudstone to siltstone, locally graded, locally showing faint ripple structures ii) massive to bedded quartz-rich sandstone, locally graded
Arkosic grits	15m-thick unit; massive K-feldspar-rich grit beds (perthitic orthoclase + quartz ±muscovite ±chlorite ±calcite ±opaque) showing 2-4mm-long twinned feldspar and 1-2mmϕ blue quartz eye crystals; very localized unit

*The rocks are typically folded at the outcrop scale and display one to two well developed foliations that, in places, obliterate the primary texture.

**No primary mineralogy is preserved in the mafic volcanic rocks. All are completely replaced by low grade greenschist facies minerals (chlorite +muscovite +calcite ±actinolite ±biotite ±apatite ±quartz).

*** ϕ:in diameter

except in some rare cases where massive flows present up to 30% vesicularity, with vesicles up to 8 mm in diameter (Plate 1C).

3.4 Interpretation of the lithofacies

3.4.1 Volcanic lithofacies

Massive lava - Thick massive flows are characteristic of higher effusion rates and temperatures (Yamagishi, 1991). When emplaced in a subaqueous environment, they represent channelized sheet flows that form during the initial stages of subaqueous eruption (Ballard et al., 1979; Cousineau and Dimroth, 1982), when the effusion rates are at their highest. Highly vesicular flows (~30%) showing large amygdules result from exsolution of high concentrations of magmatic volatiles, typical of alkaline magmas (Head and Wilson, 2003).

Pillowed lava – Pillowed lava forms when hot lava enters or erupts under water. Closely-packed pillows in the northern upper succession (Plate 1D) represent the normal, molded pillows of Dimroth et al. (1978) that are interpreted to develop when flow velocity and temperature have decreased compared to massive flows (Yamagishi, 1991). The presence

Plate 3-1 – Characteristics of the massive/pillowed flows, and volcanic breccia lithofacies of the Little Salmon upper succession. A) Massive plagioclase-megaporphyritic alkali basalt flow. Note the seriate texture with plagioclase phenocrysts up to 2.5cm long, hammer handle 1.5 cm wide for scale. B) Top of a massive plagioclase-megaporphyritic alkali basalt flow. Note the reduction in size of the plagioclase phenocrysts toward the top. C) Massive highly vesicular alkali basalt flow. D) Closely-packed 25cm - 1m ϕ fine grained pillow tubes showing 3-5cm-thick altered rims (carbonate-rich). E) Closely-packed <25cm ϕ stretched fine grained pillow tubes showing <1cm-thick altered rims. Magnet pen 0.7 cm wide for scale. F) Folded plagioclase-phyric 50cm ϕ pillow showing thick dark finer-grained rims. Dashed lines outline the folded pillow. Magnet pen 12 cm long for scale. G) Monomictic volcanic breccia (pillow breccia) showing subangular fragments of plagioclase-phyric alkali basalt in a carbonate- chlorite-rich matrix (metamorphosed hyaloclastites). Hammer head 15 cm long for scale. H) Deformed polymicitc volcanic breccia showing fragments of plagioclase-phyric alkali basalt and limy clasts, in a chlorite-rich matrix (metamorphosed volcanic ash).

58
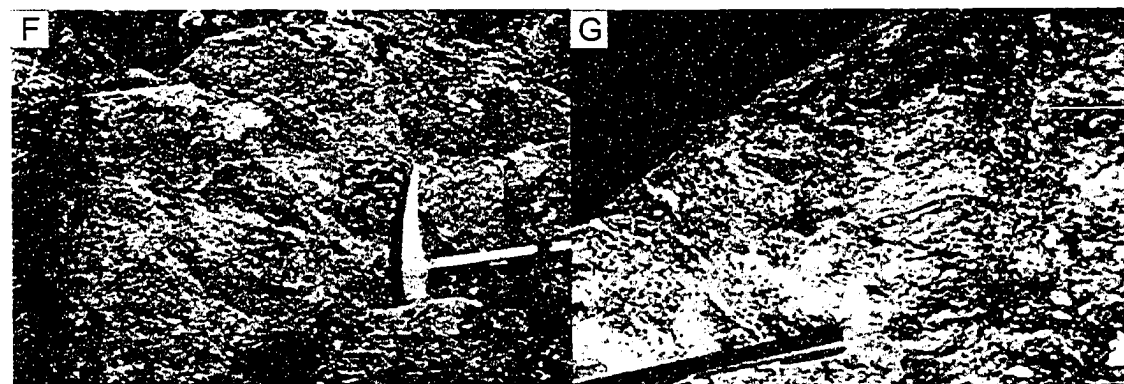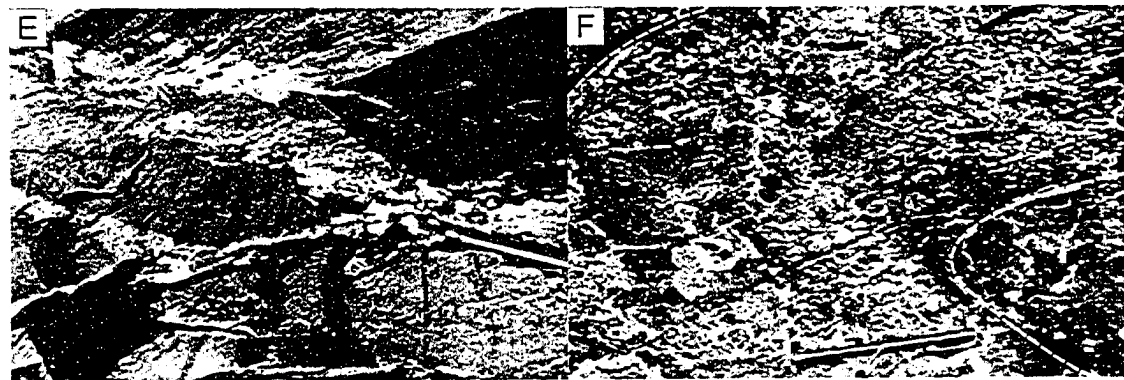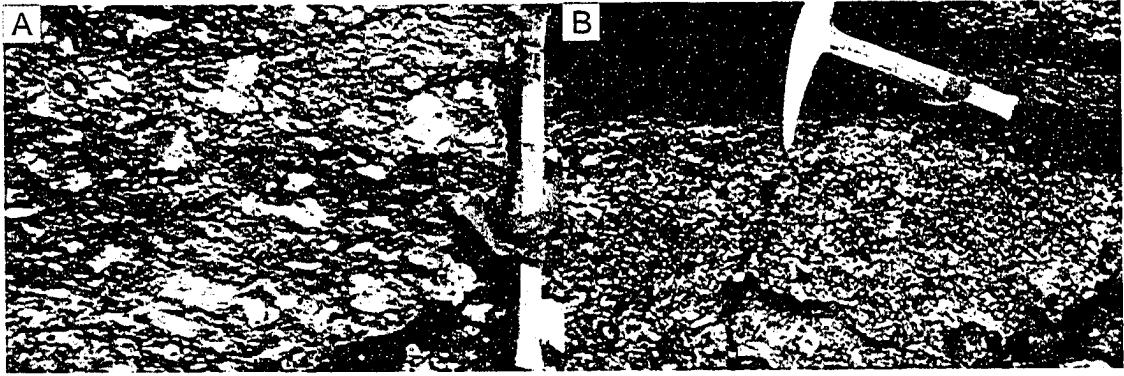
Plate 3-2 - Characteristics of the bedded tuff and exhalative lithofacies of the Little Salmon upper succession. **A)** Massive crystal-rich tuff-breccia hand sample showing a subrounded plagioclase-phyric fragment in a crystals- and chlorite-rich matrix. Photograph 10 cm wide. **B)** Close-up of a massive plagioclase crystal-rich tuff-breccia sample showing subangular broken plagioclase crystals (positive relief) in a chlorite-rich matrix (metamorphosed volcanic ash). **C)** Well bedded ash tuff (chlorite-rich fine grained rock) deposits showing graded beds. Magnet pen 12 cm long for scale. **D)** Close-up of a massive plagioclase crystal-rich tuff-breccia cut sample showing randomly oriented subangular broken plagioclase crystals in a chlorite-rich matrix (metamorphosed volcanic ash). **E)** Close-up of a well-bedded ash-tuff (chlorite-rich fine grained rock). **F)** 3 m-thick Mn-rich exhalative chert interval of the northern upper succession. Note the Mn concentration in the middle of the interval (deep-red colour) compared with the sides. Hammer 25 cm for scale.
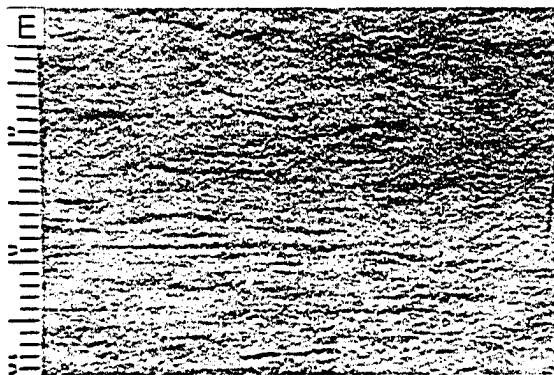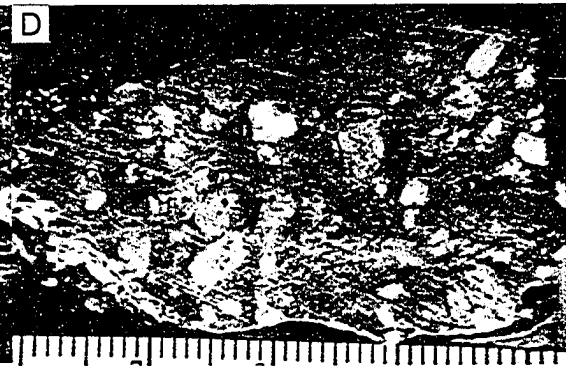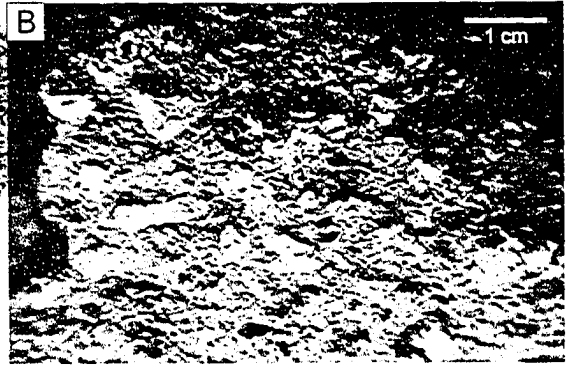
Plate 3-3 - Characteristics of the exhalative, volcaniclastic, and clastic lithofacies of the Little Salmon upper succession. **A)** Close-up of well-bedded Mn-rich exhalative chert showing hematite-rich mm-thick intervals (black layers). **B)** Close-up of Mn-poor exhalative chert sample showing thin <1 mm-thick chlorite-rich intervals (metamorphosed volcanic ash). **C)** Deformed well bedded volcaniclastic siltstone graded beds (epiclastic deposit). Lens cap 50 mm ϕ for scale. **D)** Massive to bedded crystal-rich tuff, distal fallout deposit. Photograph 12 cm wide. **E)** Massive to bedded quartz-rich sandstone to mudstone graded beds (quartz ± feldspar + muscovite + calcite ± epidote ± chlorite ± biotite ± apatite ± garnet). Photograph 8 cm wide. **F)** Deformed massive K-feldspar grit interval, with K-feldspar crystal up to 5 mm long. Photograph 6 cm wide.
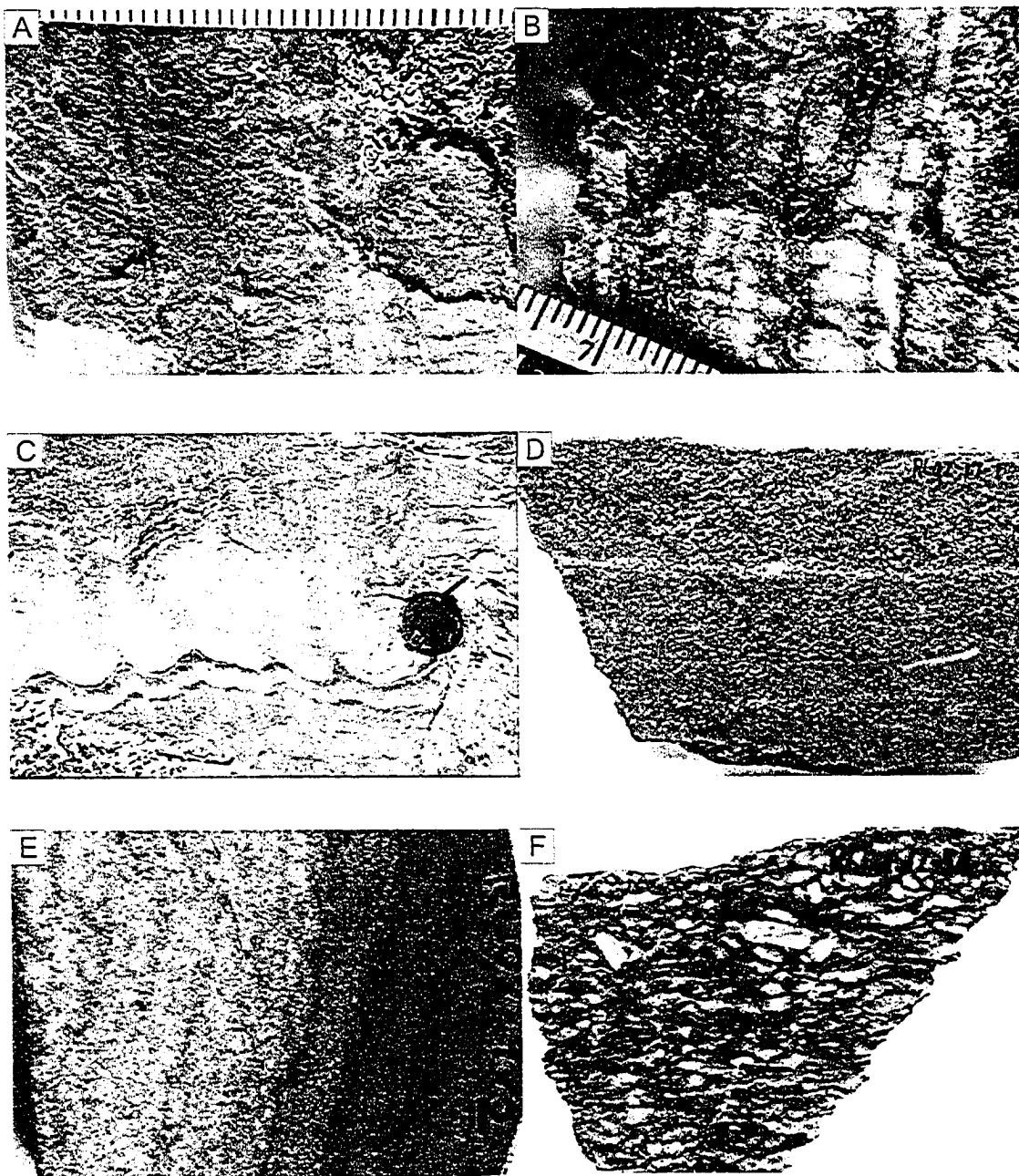
of small amygdules (<5 mm in diameter) in some of the pillowed flows and their low abundance (<10%) suggests an intermediate water depth, between 1000 m -700 m (Moore and Schilling, 1973).

Monomictic volcanic breccia – The monomictic nature of some of the volcanic breccia lithofacies (Plate 1G) in the northern upper succession as well as the angularity of the clasts indicate minimum post-depositional reworking. Considering that they are closely associated with pillowed flows, these volcanic breccias may represent "pillow breccia", which generally develops during quench fragmentation resulting from lava-water interactions (Dimroth et al., 1978; Yamagishi, 1991), or "pillow fragment breccia" which are the result of mechanical disintegration of pillow lava as a result of slumping.

Polymictic volcanic breccia – The polymictic nature of volcanic breccia lithofacies (abundant porphyritic alkali basalt clasts, plagioclase crystals, and minor limy clasts; Plate 1H) is either indicative of post-depositional reworking through mass-flow processes relatively close to a source of coarse clasts (McPhie, 1995), or represents a mix of juvenile and wall-rock fragments, products of an explosive eruption of part of the volcanic edifice and its underlying basement (White et al., 2000). Basaltic volcanism in the upper succession is alkaline in nature (Chap.2); alkaline basaltic magmas are typically volatile-rich (Wallace et al., 2000) which can trigger extensive magma fragmentation at a depth ≥780 m (Kokelaar, 1986; Staudigel and Schmincke, 1984). The close association of the polymictic volcanic breccia with alkali basalt lava, highly vesicular in places, suggests an explosive eruption style for the northern upper succession.

Bedded tuff – According to classifications of Fisher (1966) and Schmid (1981) based on grain size and pyroclastic fragment type, the pyroclastic rocks of the northern upper succession are crystal-rich coarse-tuff, crystal-rich tuff-breccia, and ash-tuff. The pyroclastic origin of these deposits is supported by the abundance of angular and broken crystals (e.g. Plate 2B and 2D; Fernandez, 1969; Fiske and Matsuda, 1964; Niem, 1977; Yamada, 1973). Non-welded subaqueous pyroclastic flow deposits characteristically have

64

a massive to poorly bedded and poorly sorted lower division and an upper thinly bedded division (Fisher and Schmincke, 1984). Unlike most turbidite sequences, the lower massive division forms 50% or more of the total sequence (Bond, 1973; Fiske and Matsuda, 1964; Niem, 1977), and massive sequences of up to 300 m thick are reported by Bond (1973). The thick crystal-rich coarse-tuff and crystal-rich tuff-breccia sequences (>300m thick; Fig. 3-6) of the northern upper succession are interpreted to be the lower division of subaqueous pyroclastic flows. Not all of these pyroclastic flows show the upper thinly bedded division that may indicate erosion (Yamada, 1973). Such erosional features are common on the flanks of seamounts; they are linked to the redeposition of parts of the pyroclastic deposits down-slope by debris-flows (Schmidt and Schmincke, 2000).

The two-division pyroclastic flows resut in terms of a waning, initially voluminous eruption (Fiske and Matsuda, 1964), which is supported by the inferred explosive nature of the northern upper succession alkali basalt volcanism. Where ash-tuff lithofacies occur (Plate 2C), they form thick, laterally continuous sequences, either forming the upper division of a subaqueous pyroclastic flow, or submarine fallout deposits from a neighbouring volcanic centre. Explosive eruptions effectively supply enormous volumes of particles instantaneously and have the potential to generate very large-scale, far-traveled turbidity currents; however, water-settled pyroclastic fall deposits would show very similar volcanic components, shards and crystal fragments and, like the turbidite sequences, show normally graded or massive beds of similar thicknesses (McPhie et al., 1993, and references therein).

Exhalative Mn-rich chert – Exhalative horizons are a common feature recognized in an active hydrothermal system associated with a submarine volcanic complex. The high SiO_2, MnO and Ba content of the Mn-chert of the northern upper succession (Plates 2F, 3A, and 3B) are typical of hydrothermal chert horizons associated with low-temperature hydrothermal (off-axis?) plumes (Peter et al., 2003; Chap. 2). Such hydrothermal systems occur on several modern seamounts in arc-backarc systems (e.g. Fryer, 1995) and in

rifted/rifting arcs (e.g. Taylor et al., 1990) during a period of temporary quiescence of the volcanic activity.

Volcaniclastic sandstone and siltstone – A thick pile of thinly bedded volcanogenic sandstone and siltstone, commonly showing graded beds, is typical of volcaniclastic turbidite sequences (e.g. Plate 3C). Despite uncertain origin, the volcaniclastic sandstone and siltstone lithofacies of the upper succession is most likely the result of the gradual post-eruptive readjustment of the sedimentary transport and depositional processes by means of mass-flow resedimentation (McPhie et al., 1993). This lithofacies occurs mainly in the southern upper succession in association with siliciclastic lithofacies.

3.4.2 Siliciclastic lithofacies

Quartzite-pebble to -boulder conglomerate – The massive quartzite-pebble to -boulder conglomerate shows subangular to subrounded quartzite clasts (Gladwin et al., 2003), suggesting minimum transport. Tightly folded foliation present in some boulders indicate derivation from a previously deformed source region (Gladwin et al., 2003).

Quartz-rich sandstone and mudstone – These well bedded quartz-rich sandstones and mudstones (Plate 3E) showing locally graded-beds and ripple structures are interpreted to be Bouma T_{a-c} divisions (Bouma, 1962), the result of turbidity current deposition.

Arkosic grits – These massive arkosic beds (Plate 3F) are interpreted to be S_3 beds (Lowe, 1982), also the result of turbidity current deposition.

The siliciclastic beds are generally massive, but are locally graded and show faint ripple structures in places; plane beds and ripple structures can indicate lower flow regime traction current. The petrography (Table 3-1) and geochemical and isotopic signatures (Chap. 2) of these siliciclastic rocks suggest external sedimentary input(s); their quartz-rich content suggests a felsic source, which could have been either felsic volcanics (continental arc), or recycled continental-crust-derived sediments. Detrital zircons of

Early Mississippian age were recovered from the quartzite-pebble to -boulder conglomerate matrix suggesting derivation from a source within Yukon-Tanana terrane for the base of the Little Salmon formation (Colpron et al., in press-b).

3.4.3 Vertical and lateral lithofacies transition

The *northern upper succession* stratigraphy is almost entirely composed of volcanic lithofacies accumulated subaqueously, as suggested by the presence of pillow lavas and exhalative horizons at different levels in the stratigraphy. Lithofacies transition generally ranges from massive and/or pillowed flows to volcanic breccia to bedded-tuff, both laterally and vertically; this is typical of a submarine volcanic sequence (Dimroth et al., 1978).

The northern upper succession shows multiple laterally discontinuous clusters of flows and their associated volcanic breccia at different levels through the stratigraphy, suggesting small and numerous overlapping volcanic centres, seamounts or pillow cones. These volcanic edifices were affected by gravitational collapse, slumping, of their flanks producing important fragmental deposits (McPhie et al., 1993) through a density current. Distinguishing between primary, redeposited, and reworked volcaniclastic deposits is often problematic, but the abundance of angular and broken large plagioclase crystals in addition to almost exclusively plagioclase-phyric alkali basalt lithic fragments in the northern upper succession tuffs argues for a primary or redeposited origin. Minor flows associated with abundant volcaniclastic deposits are consistent with submerged flank seamount stratigraphy (Corcoran, 2000; McPhie, 1995; Schmidt and Schmincke, 2000).

Massive polymictic volcanic breccia together with abundant angular and broken large plagioclase crystal beds close to submerged vents represent pyroclastic deposits fed directly from highly explosive eruption(s), typical of volatile-rich alkaline volcanism (Kokelaar, 1986; Staudigel and Schmincke, 1984).

Based on physical volcanology and geochemistry, the volcanic stratigraphy of the northern upper succession records explosive volcanic eruptions and associated pyroclastic flows during the formation of several small alkali basalt seamounts (Fig. 3-7).

In contrast the *southern upper succession* of the Little Salmon formation does not contain lava flow or any "proximal" volcanic lithofacies. It is entirely composed of interbedded volcaniclastic and siliciclastic lithofacies, most likely representing the distal deposits of an active volcanic complex. Structures observed in both the volcaniclastic and siliciclastic intervals clearly record a traction current typical of turbidites which are usually found in deep or subsiding basin(s) near the volcanic centre(s). However, the abundance of plagioclase crystals and the alkaline nature of some of these tuffaceous intervals might suggest a pyroclastic origin for some of the volcaniclastic beds, like submarine fallout deposits derived from the local alkali basalt volcanism.

3.5 Reconstruction of the paleovolcanic environment of the upper succession of the Little Salmon formation

The boundary between the northern upper succession seamount stratigraphy and the southern upper succession distal basinal deposits is abrupt and aligned with a SW-NE normal fault of the same attitude (see "Facies change" dashed-line on Fig. 3-3). This normal fault affects all the underlying units on the west flank of the synclinorium.

Although volcanic environments are characterized by abrupt and numerous lithofacies changes, they normally display a gradual evolution from the volcanic centre(s) (massive lavas, pillowed lavas, pillow fragment breccias, hyaloclastites), to the more distal deposits (reworked volcaniclastic beds) or clearly distal sequences (resedimented deposits, turbidites). Such an abrupt change in lithofacies aligned with a normal fault suggests the presence of a synvolcanic fault scarp. Extensional synvolcanic faults are common in rifted arc systems; they tend to develop series of asymmetric basins, half- to full-grabens, parallel to the arc front (e.g. Klaus et al., 1992; Taylor et al., 1992; Taylor et al., 1991). Volcanism is usually concentrated along these extensional faults and on highs

68

Pyroclastic subaqueous eruption

fallout

off-axis
hydrothermal
plume

exhalitive
horizon

wall-rock and
juvenile
fragments
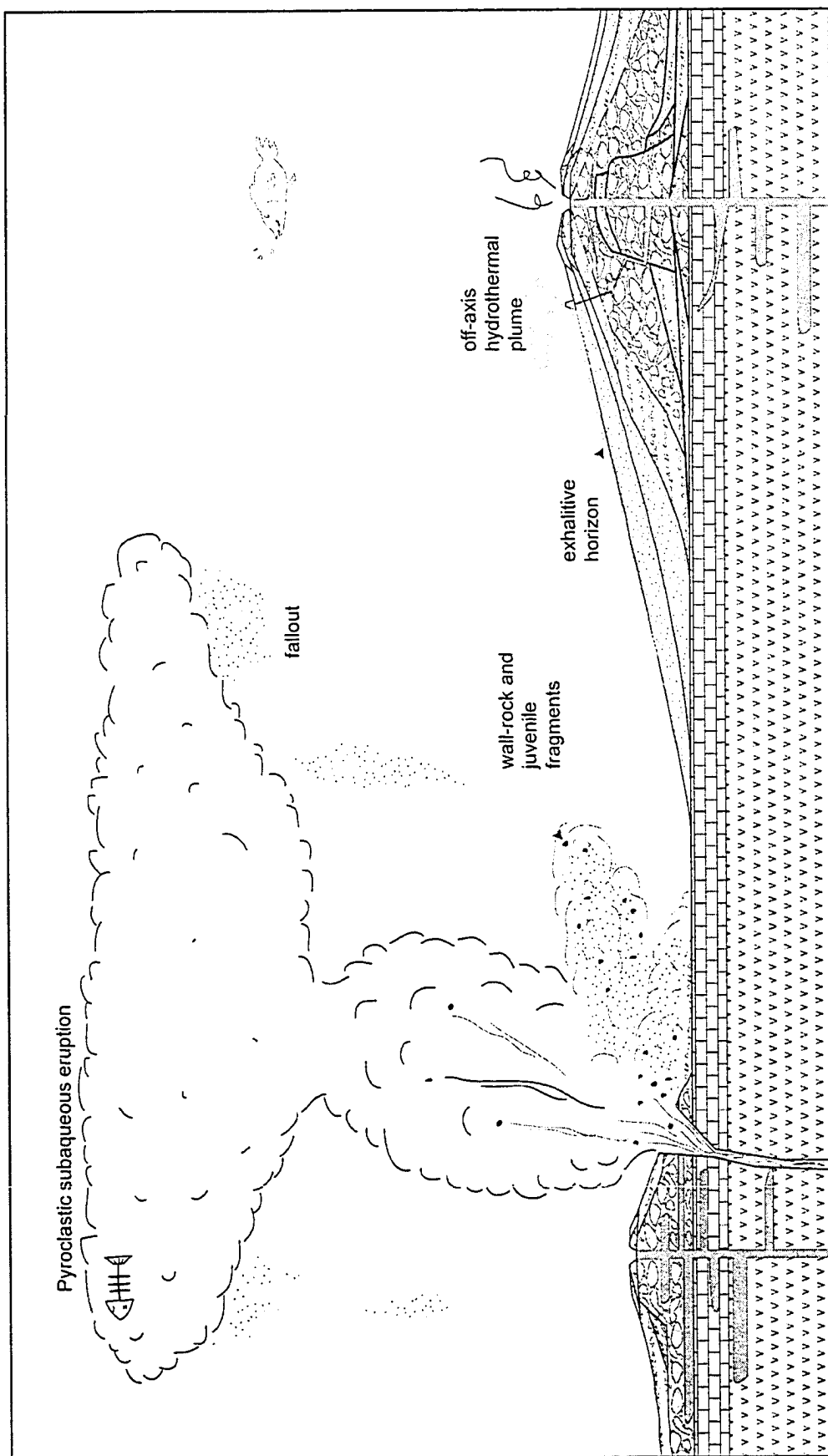
Figure 3-7 – Schematic seamounts and pyroclastic explosion model of the Little Salmon upper succession. Adapted from Mueller (2003), and Schmidt and Schmincke (2000). Diagram not to scale.

69

between the rift basins (Taylor et al., 1992) forming numerous relatively small volcanic centres, such as seamounts (northern upper succession stratigraphy). Pyroclastic and volcaniclastic materials are shed from these volcanic centres in the rift basins together with other sediments from the surroundings (southern upper succession stratigraphy).

The northern upper succession stratigraphy records the explosive eruption of alkali basalt on seamount flanks at an intermediate water depth atop an extensional synvolcanic fault associated with the development of a rift basin during extension/rifting of the Little Salmon arc system, whereas the southern upper succession stratigraphy represents the volcanogenic and siliciclastic sediments deposited onto the rift-floor sediment plain(s) of this basin (Fig. 3-8).

3.6 Modern analogues

Although formed in an intra-arc rift basin setting, the alkaline seamounts of the Little Salmon northern upper succession resemble Cenozoic seamounts in intraplate (e.g. Pliocene La Palma seamount; Staudigel and Schmincke, 1984) and "island-arc/back-arc" settings (e.g. Japan Sea; Sohn, 1995).

The volcanic lithofacies assemblages of the northern upper succession of the Little Salmon formation closely resemble those of the intra-plate alkaline Pliocene La Palma seamount, Canary Island, East Atlantic. The >300 m-thick dominantly crystal-rich coarse-tuff and crystal-rich tuff-breccia lithofacies interbedded with minor flows (~10%) of the northern upper succession is similar to the "intermediate water/shoaling stage, flank deposits" of the La Palma seamount which present an interval of 360 m of ~25% pillowed lavas, ~70% of fragment breccias and lapilli breccias, and about 5% hyaloclastites (Staudigel and Schmincke, 1984). However, unlike the La Palma seamount, the Little Salmon seamounts either did not develop an emergent stage, or that portion of these seamounts was not preserved.
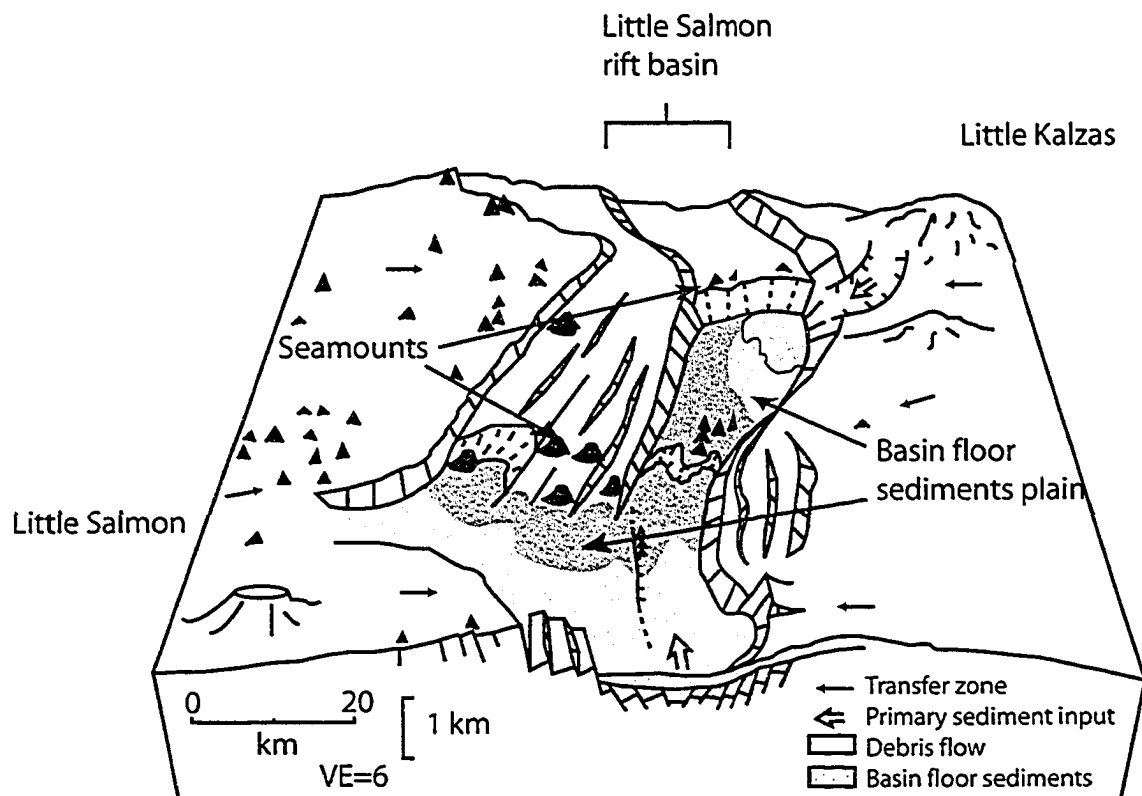
Figure 3-8 – Paleogeographic reconstruction of the Little Salmon rift basin within the Little Salmon-Little Kalzas arc system. This block diagram is a modified version of Klaus et al. (1992) block diagram of the Sumizu rift, SW Pacific, highlighting the clear resemblance between modern and ancient island arc systems (Chap. 2). In solid yellow: Little Salmon and Little Kalzas felsic volcanic centres; in solid green: Little Salmon alkali basalt seamounts; in light yellow: felsic crust-derived sediments; in light green: alkali basalt volcaniclastic material, derived from the seamount volcanism. Water depth estimated to be <1000 m.

The Little Salmon seamount stratigraphy is also similar to the Trachyte I unit, a mixture of coherent trachytic lavas and breccias that are interpreted to be subaqueous lavas and related hyaloclastites of the seamount succession at the base of the Tok island volcano, East Sea (Japan Sea), Korea (Sohn, 1995). Like the Little Salmon seamounts, the Tok island volcano formed in an extensional tectonic setting (Sohn, 1995). The Little Salmon seamounts formed in an intra-arc rift basin setting (Little Kalzas-Little Salmon arc, Fig. 3-8) whereas the Tok island volcano is in back-arc basin setting, the Sea of Japan.

The alkali basalt Little Salmon seamounts and hydrothermal system are a Late Paleozoic analogue for the recently discovered Nifonea hydrothermal vent field, Coriolis Troughs, Vanuatu, SW Pacific. Found in an "en echelon" intra-arc basin aligned subparallel to the New Hebrides volcanic arc ~50 km behind the volcanic front, this active Mn-rich

71

hydrothermal field presents recent alkali basalt volcanic activity with vesicular pillowed and sheet-flows associated with minor manganese deposits (McConachy et al., 2005). The Coriolis Troughs, which were previously considered intra-arc troughs, are now considered true back-arc basins (McConachy et al., 2005). The Little Salmon alkaline volcanism, like the Nifonea alkalic volcanism, might have been recording the onset of back-arc basin volcanism within the Little Salmon arc in Mississippian time.

3.7 Conclusions

Detailed lithofacies analyses of the upper succession of the Little Salmon formation, in the pericratonic terranes of the northern Canadian Cordillera, enable the identification of unequivocal signs of alkali basalt seamount formation atop an extensional synvolcanic fault associated with the development of a rift basin during extension/rifting of the Little Salmon arc system in Mississippian time. The northern upper succession of the Little Salmon records the explosive volcanic eruptions and associated pyroclastic flows during the formation of several small alkali basalt seamounts, whereas the southern upper succession represents various amount of pyroclastic and volcaniclastic materials shed from the volcanic centres into the nearby rift basin together with other siliciclastic sediments from the surroundings.

The Little Salmon alkali basalt seamount stratigraphy is similar to several well-studied Cenozoic seamounts formed both in intraplate and island-arc/back-arc settings, substantiating the abundance/importance of the seamount edifice in most subaqueous volcanic environment throughout the Phanerozoic.

The study of old subaerially exposed seamount stratigraphy in an inferred rifted island arc, like the Little Salmon seamounts, is an indirect look at one of the most abundant modern volcanic edifice types on Earth. It is a useful tool to help better understand poorly exposed, inaccessible modern examples, such as the Nifonea hydrothermal field, Vanuatu.

3.8 References

Ballard, R.D., Holcomb, R.T. and van Andel, T.H., 1979. The Galapagos Rift at 86'W: 3: sheet flows, collapse pits, and lava lakes of the rift valley. Journal of Geophysical Research, 84: 5407-5422.

Bond, G.C., 1973. A late Paleozoic volcanic arc in the eastern Alaska Range, Alaska. Journal of Geology, 81(5): 557-575.

Bouma, A.H., 1962. Sedimentology of some Flysch deposits; a graphic approach to facies interpretation. Elsevier, Amsterdam, 168 pp.

Colpron, M., 2001. Geochemical characterization of Carboniferous volcanic successions from Yukon-Tanana terrane, Glenlyon map area (105L), central Yukon. In: D.S. Emond and L.H. Weston (Editors), Yukon Exploration and Geology 2000. Exploration and Geological Services Division, Yukon Region, Indian and Northern Affairs Canada, pp. 111-136.

Colpron, M., Gladwin, K., Johnston, S.T., Mortensen, J.K. and Gehrels, G.E., in press-a. Geology and juxtaposition history of Yukon-Tanana, Slide Mountain and Cassiar terranes in the Glenlyon area of central Yukon. Canadian Journal of Earth Sciences.

Colpron, M., Mortensen, J.K., Gehrels, G.E. and Villeneuve, M.E., in press-b. Basement complex, Carboniferous magmatic arcs and Paleozoic deformation in Yukon-Tanana terrane of central Yukon. In: M. Colpron, J.L. Nelson and R.I. Thompson (Editors), Paleozoic evolution and metallogeny of pericratonic terranes at the ancient Pacific margin of North America, Canadian and Alaskan Cordillera. Geological Association of Canada.

Colpron, M., Murphy, D.C. and Mortensen, J.K., 2000. Mid-Paleozoic tectonism in Yukon-Tanana Terrane, northern Canadian Cordillera: record of intra-arc deformation. Geological Society of America, Cordilleran Section, Abstracts with Programs, 32(6): A-7.

Colpron, M. et al., 2003. Yukon Targeted Geoscience Initiative, Part 1: Results of accelerated bedrock mapping in Glenlyon (105L/1-7, 11-14) and northeast Carmacks (115I/9,16) areas, central Yukon. In: D.S. Emond and L.L. Lewis

(Editors), Yukon Exploration and Geology 2002. Exploration and Geological Services Division, Yukon Region, Indian and Northern Affairs Canada, pp. 85-108.

Corcoran, P.L., 2000. Recognizing distinct portions of seamounts using volcanic facies analysis; examples from the Archean Slave Province, NWT, Canada. Precambrian Research, 101(2-4): 237-261.

Cousineau, P. and Dimroth, E., 1982. Interpretation of the relations between massive, pillowed and brecciated faies in an Archean submarine andesite volcano; Amulet Andesite, Rouyn-Noranda area, Quebec, Canada. Canadian Journal of Earth Sciences = Journal Canadien des Sciences de la Terre, 15: 902-918.

Dimroth, E., Cousineau, P., Leduc, M. and Sanschagrin, Y., 1978. Structure and organization of Archean subaqueous basalt flows, Rouyn-Noranda area, Quebec, Canada. Canadian Journal of Earth Sciences = Journal Canadien des Sciences de la Terre, 15(6): 902-918.

Fernandez, H.E., 1969. Notes on the submarine ash flow tuff in Siargao island, Surigao del Norte. Philip. Geol., 23(1): 29-36.

Fisher, R.V., 1966. Rocks composed of volcanic fragments and their classification. Earth-Science Reviews, 1(4): 287-298.

Fisher, R.V. and Schmincke, H.-U., 1984. Pyroclastic rocks. Springer-Verlag, New York, 472 pp.

Fiske, R.S. and Matsuda, T., 1964. Submarine equivalents of ash flows in the Tokiwa Formation, Japan. American Journal of Science, 262(1): 76-106.

Fryer, P., 1995. Geology of the Mariana Trough. In: B. Taylor (Editor), Backarc basins; Tectonics and magmatism. Plenum Press, New York, pp. 237-280.

Gladwin, K., Colpron, M., Black, R. and Johnston, S.T., 2003. Bedrock geology at the boundary between Yukon-Tanana and Cassiar terranes, Truitt Creek map area (105L/1), south-central Yukon. In: D.S. Emond and L.L. Lewis (Editors), Yukon Exploration and Geology 2002. Exploration and Geological Services Division, Yukon Region, Indian and Northern Affairs Canada, pp. 135-148.

Head, J.W., III and Wilson, L., 2003. Deep submarine pyroclastic eruptions; theory and predicted landforms and deposits. Journal of Volcanology and Geothermal Research, 121(3-4): 155-193.

Klaus, A. et al., 1992. Structural and stratigraphic evolution of the Sumisu Rift, Izu-Bonin Arc. Proceedings of the Ocean Drilling Program, Scientific Results, 126: 555-573.

Kokelaar, P., 1986. Magma-water interactions in subaqueous and emergent basaltic volcanism. Bulletin of Volcanology, 48(5): 275-289.

Lowe, D.R., 1982. Sediment gravity flows; II, Depositional models with special reference to the deposits of high-density turbidity currents. Journal of Sedimentary Petrology, 52(1): 279-297.

McConachy, T.F. et al., 2005. New hydrothermal activity and alkalic volcanism in the backarc Coriolis Troughs, Vanuatu. Geology, 33(1): 61-64.

McPhie, J., 1995. A Pliocene shoaling basaltic seamount; Ba Volcanic Group at Rakiraki, Fiji. Journal of Volcanology and Geothermal Research, 64(3-4): 193-210.

McPhie, J., Doyle, M. and Allen, R., 1993. Volcanic texures: a huide to interpretation of textures in volcanic rocks. Centre for Ore Deposit and Exploration Studies, University of Tasmania, Tasmania, 198 pp.

Moore, J.G. and Schilling, J.-G., 1973. Vesicles, Water, and Sulfur in Reykjanes Ridge Basalts. Contributions to Mineralogy and Petrology, 41(2): 105-118.

Mueller, W.U., 2003. A subaqueous eruption model for shallow-water, small volume eruptions; evidence from two Precambrian examples. In: J.D.L. White, J.L. Smellie and D.A. Clague (Editors), Geophysical Monograph, vol.140. American Geophysical Union, Washington, pp. 189-203.

Niem, A.R., 1977. Mississippian pyroclastic flow and ash-fall deposits in the deep-marine Ouachita flysch basin, Oklahoma and Arkansas. Geological Society of America Bulletin, 88(1): 49-61.

Peter, J.M., Mihalynuk, M.G., Colpron, M. and Nelson, J.L., 2003. Diverse examples of exhalative hydrothermal sediments in Yukon-Tanana Terrane, Yukon Territory and British Columbia, GAC-MAC 2003, Vancouver.

Piercey, S.J., Mortensen, J.K., Murphy, D.C., Paradis, S. and Creaser, R.A., 2002. Geochemistry and tectonic significance of alkalic mafic magmatism in the Yukon-Tanana Terrane, Finlayson Lake region, Yukon. Canadian Journal of Earth Sciences = Revue Canadienne des Sciences de la Terre, 39(12): 1729-1744.

Piercey, S.J., Murphy, D.C., Mortensen, J.K. and Paradis, S., 2001a. Boninitic magmatism in a continental margin setting, Yukon-Tanana Terrane, southeastern Yukon, Canada. Geology, 29(8): 731-734.

Piercey, S.J., Paradis, S., Murphy, D.C. and Mortensen, J.K., 2001b. Geochemistry and paleotectonic setting of felsic volcanic rocks in the Finlayson Lake volcanic-hosted massive sulfide district, Yukon, Canada. Economic Geology and the Bulletin of the Society of Economic Geologists, 96(8): 1877-1905.

Schmid, R., 1981. Descriptive nomenclature and classification of pyroclastic deposits and fragments; recommendations of the IUGS Subcommission on the Systematics of Igneous Rocks. Geology, 9(1): 41-43.

Schmidt, R. and Schmincke, H.-U., 2000. Seamounts and island building. In: H. Sigurdsson, B.F. Houghton, S.R. McNutt, H. Rymer and J. Stix (Editors). Academic Press, San Diego, pp. 383-402.

Sohn, Y.K., 1995. Geology of Tok Island, Korea: eruptive and depositional processes of a shoaling to emergent island volcano. Bulletin of Volcanology (Historical Archive), 56(8): 660-674.

Staudigel, H. and Schmincke, H.-U., 1984. The Pliocene seamount series of La Palma/Canary Islands, JGR. Journal of Geophysical Research. B. American Geophysical Union, Washington, pp. 11,195-11,215.

Taylor, B. et al., 1990. Alvin-Seabeam studies of the Sumisu Rift, Izu-Bonin Arc. Earth and Planetary Science Letters, 100(1-3): 127-147.

Taylor, B. et al., 1992. Rifting and the volcanic-tectonic evolution of the Izu-Bonin-Mariana Arc. Proceedings of the Ocean Drilling Program, Scientific Results, 126: 627-651.

Taylor, B. et al., 1991. Structural development of Sumisu Rift, Izu-Bonin Arc. Journal of Geophysical Research, B, Solid Earth and Planets, 96(10): 16,113-16,129.

Wallace, P., Anderson, A.T., Jr. and Ballard, R.D., 2000. Volatiles in magmas. In: H. Sigurdsson, B.F. Houghton, S.R. McNutt, H. Rymer and J. Stix (Editors), Encyclopedia of volcanoes. Academic Press, San Diego.

Wheeler, J.O., Brookfiels, A.J., Gabrielse, H., Monger, J.W.H., tipper, H.W., and Woodsworth, G.J., 1991. Terrane map of the Canadian Cordillera, Geological Survey of Canada.

White, J.D.L., Houghton, B.F. and Ballard, R.D., 2000. Surtseyan and related phreatomagmatic eruptions. In: H. Sigurdsson, B.F. Houghton, S.R. McNutt, H. Rymer and J. Stix (Editors). Academic Press, San Diego.

Yamada, E., 1973. Subaqueous pumice flow deposits in the Onikobe Caldera, Miyagi Prefecture, Japan. Chishitsugaku Zasshi = Journal of the Geological Society of Japan, 79(9): 585-597.

Yamagishi, H., 1991. Morphological and sedimentological chracteristics of the Neogene submarine coherent lavas and hyaloclastites in Southwest Hokkaido, Japan. Sedimentary Geology, 74: 5-23.

Chapter 4

Development of Late Paleozoic volcanic arcs in the Canadian Cordillera: an example from the Klinkit Group, northern British Columbia and southern Yukon[1]

4.1 Abstract

The Late Paleozoic volcanic rocks of the northern Canadian Cordillera lying between Ancestral North America to the east, and the accreted terranes of the Omineca belt to the west, record early arc and rift magmatism along the paleo-Pacific margin of the North American craton. The Mississippian to Permian volcano-sedimentary Klinkit Group extends discontinuously over 250 km in northern British Columbia and southern Yukon. The two stratotype areas are: 1) in the Englishman Range, southern Yukon, the English Creek Limestone is conformably overlain by the volcano-sedimentary Mount McCleary Formation (Lower Clastic Member, Alkali-basalt Member and Volcaniclastic Member), and 2) in the Stikine Ranges, northern British Columbia, the Screw Creek Limestone is conformably overlain by the volcano-sedimentary Butsih Formation (Volcaniclastic Member and Upper Clastic Member). The calc-alkali nature of the basaltic volcaniclastic members of the Klinkit Group indicates a volcanic-arc setting ($(La/Yb)_N$=2.77-4.73), with little involvement of the crust in their genesis (ε_{Nd}=+6.7 to +7.4). Alkali basalts in the Mount McCleary Formation ($(La/Yb)_N$=12.5-17.8) suggest periodic intra-arc rifting events. Broadly coeval and compositionally similar volcano-sedimentary assemblages occur in the basement of the Mesozoic Quesnel arc, north-central British Columbia, and in the pericratonic Yukon-Tanana composite terrane, central Yukon, suggesting that they all represent pieces of a single long-lived, Late Paleozoic arc system that was

---

[1] Manuscript of Simard, Dostal and Roots (2003), "Development of Late Paleozoic volcanic arcs in the Canadian Cordillera: an example from the Klinkit Group, northern British Columbia and southern Yukon", Canadian Journal of Earth Sciences, v. 40, p. 907-924. As the first author, RL Simard wrote the entire manuscript and drafted all the figures, the coauthors suggested corrections to the manuscript prior to submission to the journal.

dismembered prior to its accretion onto Ancestral North America. Therefore, Yukon-Tanana terrane is possibly the equivalent to the basement of Quesnel terrane, and the northern Quesnel terrane has a pericratonic affinity.

4.2 Introduction

The Canadian Cordillera is generally considered to be a collage of allochthonous oceanic and pericratonic terranes that were accreted to the western margin of the North American craton during the Mesozoic (Coney et al., 1980; Gabrielse and Yorath, 1991; Monger and Irving, 1980; Monger et al., 1982). In the northern Canadian Cordillera, Late Paleozoic volcano-sedimentary sequences are an important part of these terranes. The magmatic sequences, as well as their surrounding stratigraphy, are well documented in intra-oceanic arc terranes such as Quesnel and Stikine (e.g. Monger et al., 1991), whereas those of pericratonic affinities, like in the Yukon-Tanana composite terrane, are ill-defined (Mortensen, 1992). Knowledge of the geological and geochemical evolution of Late Paleozoic magmatic sequences in pericratonic terranes is needed to make reasonable paleogeographic reconstruction of the northern Canadian Cordillera and to determine their tectonomagmatic history. Furthermore, age and compositional data may suggest a spatial, temporal or genetic relationship between pericratonic and intra-oceanic terranes in Late Paleozoic time.

The comparison and correlation of various time-correlative magmatic suites in northern British Columbia and southern Yukon is a fundamental step toward resolving the evolution of the northern Canadian Cordillera. The volcanic part of the Late Mississippian to Permian Klinkit Group represents one of these magmatic sequences. Previously linked to the oceanic Slide Mountain terrane and the pericratonic Dorsey and Yukon-Tanana terranes (Monger et al., 1991; Wheeler, 1991; see historical background in section 4.12.1 for details), this well preserved volcano-sedimentary sequence provides a rare opportunity to document the pre-accretion history of this part of the Canadian Cordillera.

The purpose of this paper is to define a new stratigraphic unit, the Klinkit Group, and to characterize its geological setting, stratigraphy, petrography and geochemistry; particularly with respect to its volcanic units. The distinct geochemical signature of these volcanic units can be used to discriminate indirectly between the allochtonous terranes in the area and to study their relationships. The data presented here are used to evaluate the petrogenesis and tectonic setting of these volcanic rocks and to compare the Klinkit Group with age-correlative volcano-sedimentary sequences of both pericratonic and intra-oceanic terranes in the northern Canadian Cordillera. The derived paleogeographic and tectonic reconstruction suggests that a major Paleozoic arc system developed atop a relatively thin continental crust and was structurally dismembered prior to, or at some stage during, its emplacement onto the western margin of North America.

4.3 Geological setting of the Klinkit Group

The Klinkit Group (proposed new Group name; see section 4.12) lies along the western side of the Omineca belt in the northern Canadian Cordillera (Fig. 4-1). Along its length, the Omineca belt is composed of complexly deformed and metamorphosed sedimentary and volcanic rocks intruded by Jurassic and Cretaceous plutons (Gabrielse et al., 1991; Monger, 1999). This belt is dominated by fragments of the Proterozoic to Paleozoic North American continental margin, together with terranes[2] of mostly pericratonic affinities (Gabrielse et al., 1991). However, in northern British Columbia and southern Yukon, the main terranes of this belt are the pericratonic[3] Yukon-Tanana composite terrane, the oceanic[4] Slide Mountain terrane and smaller exposures of the intra-oceanic[5] Quesnel terrane (Fig. 4-1).

---

[2] Terranes: Fault-bounded crustal blocks which have distinct lithologic and stratigraphic successions and which have geologic histories different from neighbouring terranes (Schermer et al. 1984).
[3] Pericratonic terrane: Terrane showing stratigraphic affinities with the margin of the craton (Gabrielse et al. 1991), in this case North America.
[4] Oceanic terrane: Terrane stratigraphy mainly records the evolution of an ocean.
[5] Intra-oceanic terrane: Terrane stratigraphy mainly records the evolution of an intra-oceanic arc.
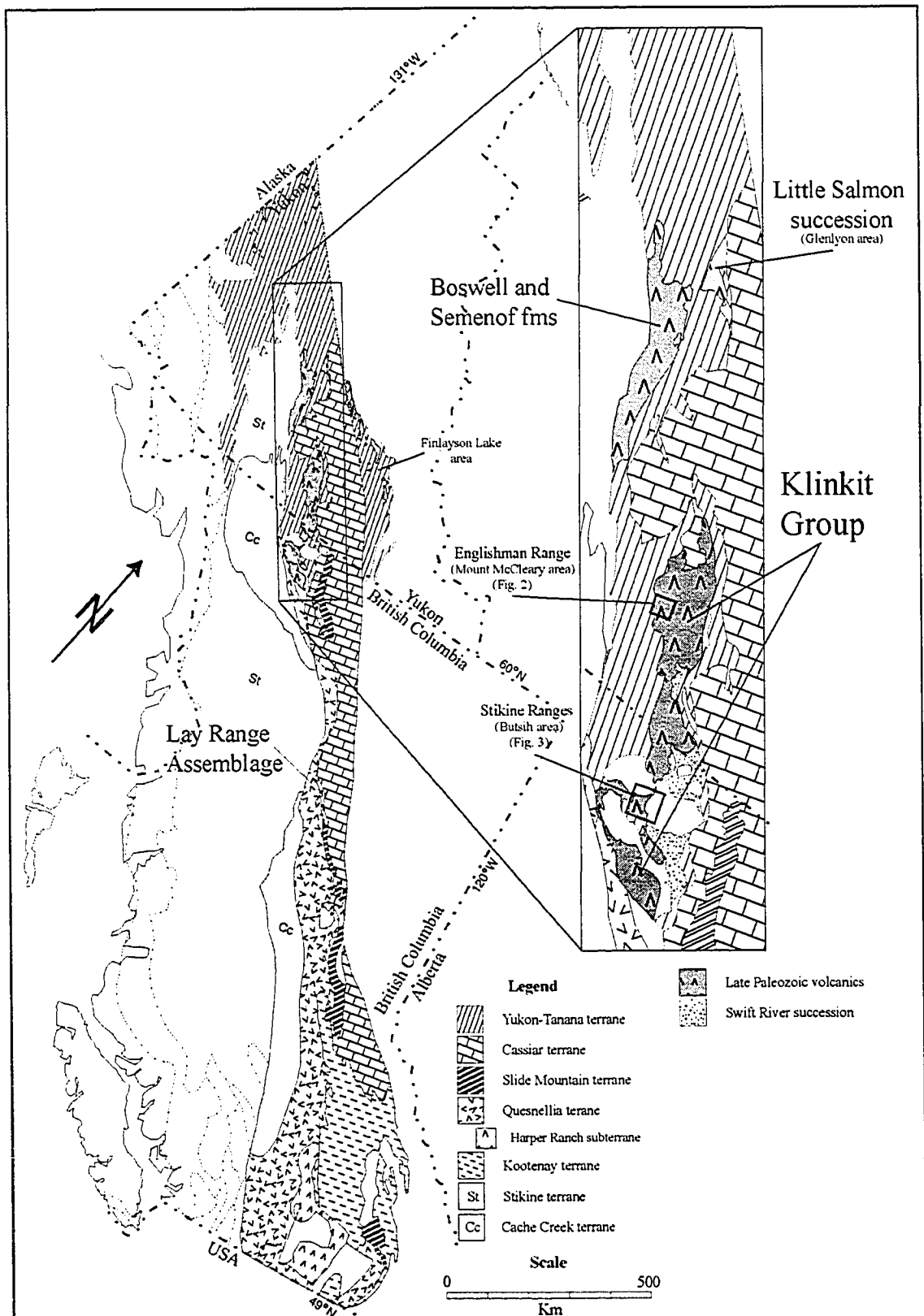
Figure 4-1 – Generalized terrane map of the eastern Canadian Cordillera. Modified after Wheeler et al. (1991). The inset shows the spatial relationship of the main Late Paleozoic volcano-sedimentary sequences of the northern Canadian Cordillera and the surrounding terranes.

The Klinkit Group is a part of the pericratonic Yukon-Tanana composite terrane, which structurally overlies rocks of the North American continental margin. In Yukon, the Yukon-Tanana terrane is composed of variably metamorphosed sedimentary and volcanic successions with abundant dioritic to granitic intrusions of dominantly Mississippian age (Mortensen, 1992).

The rocks of the Klinkit Group extend discontinuously from northern British Columbia into southern Yukon, a strike length of over 250 km (Fig. 4-1). This volcano-sedimentary sequence is characterized by the predominance of volcaniclastic rocks but includes carbonates of Visean to Bashkirian age (Mississippian to Early Pennsylvanian) in the lowermost part. Roots et al. (2002) reported an Early Permian age (U-Pb zircon; 281 ± 2 Ma) for the volcaniclastic rocks and inferred that Klinkit volcanism began in the Carboniferous and continued into Permian times. The group is unconformably overlain by the Triassic Teh Clastic succession (Fig. 4-2), a sedimentary unit of continental affinity (Colpron and Group, 2001; Creaser and Harms, 1998; Mihalynuk et al., 2000).

The Klinkit Group lies within a composite allochthon that has been thrust eastward onto the continental rocks of the North America (Nelson and Friedman, 2004; Nelson et al., 2000). To the west and north-west, the Klinkit Group is in inferred fault contact with the Late Devonian volcano-sedimentary Big Salmon Complex of the Yukon-Tanana composite terrane (Fig. 4-1; Mihalynuk et al., 1998; 2000). To the south-west, the Klinkit Group is faulted against Triassic arc strata of the Quesnel terrane.

The Klinkit Group shows important lithological changes along strike, including a variation in the relative abundance and stratigraphic position of the associated siliciclastic sediments. Two of the most continuous exposures reveal distinct stratigraphic successions within the group.

In the Englishman Range of southern Yukon, the Klinkit Group is subdivided into two formations (Figs. 4-2 and 4-3): the English Creek Limestone (proposed new Formation name; section 4.12) and the overlying volcano-sedimentary Mount McCleary Formation

Stikine Ranges
(northern British Columbia)

Englishman Range
(southern Yukon)

Teh Clastic
succession

KLINKIT GROUP

Butsih Formation

Upper Clastic
Member

Volcaniclastic
Member

Alkali-Basalt
Member

Lower Clastic
Member

Mount McCleary
Formation

Screw Creek
Limestone

English Creek
Limestone

?

?

Swift River
succession

Symbol	Description	Symbol	Description
	Alkali-basalt volcanism		Conglomerate
	Shale / Black argilite		Limestone / marble
	Quartzite / sandstone		Volcaniclastic rocks
	Deformed sediments		unconformity
	fault		deformation

Figure 4-2 – Schematic stratigraphic sections of the Klinkit Group. Left-hand section - Stikine Ranges, northern British Columbia; Right-hand section - Englishman Range, southern Yukon.

(proposed new Formation name; see section 4.12). The Mississippian English Creek Limestone is a light grey, finely crystalline, locally crinoidal limestone with minor dolostone, chert nodules and quartz arenite (Ml unit of Gordey and Stevens, 1994). It is conformably overlain by the Mount McCleary Formation, composed of three members

Klinkit Group
Mount McCleary Formation

	Volcaniclastic Member
	Alkali-Basalts Member
	Lower Clastic Member
	English Creek Limestone

| | Mid-Cretaceous granite |

0   0.5
km
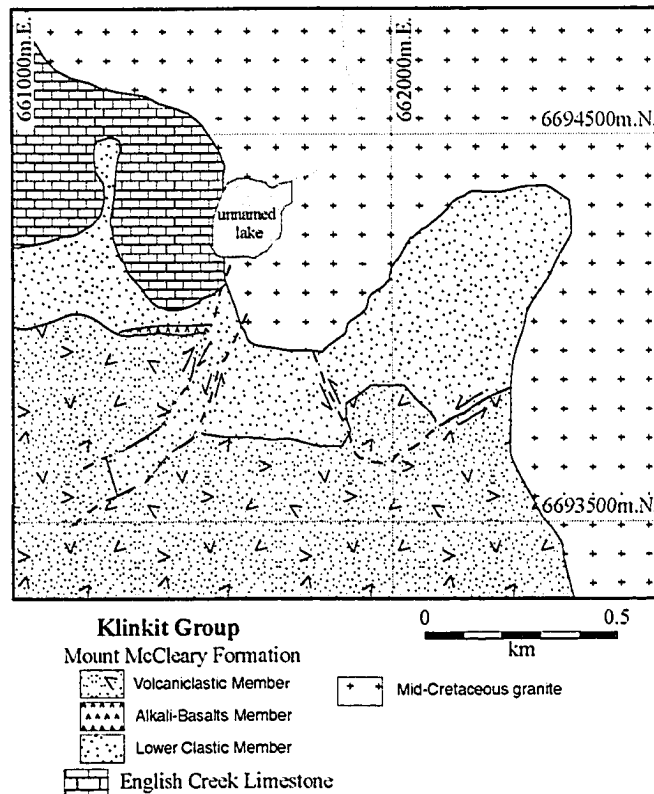
Figure 4-3 – Geological map of the Mount McCleary area, Englishman Range, southern Yukon. The Mount McCleary Formation conformably overlies the English Creek Limestone to the north. This coherent stratigraphy is truncated by mid-Cretaceous granite in the north-east.

(Figs. 4-2 and 4-3). From bottom to top these are: i) the Lower Clastic Member, a ~60-m-thick, dominantly siliciclastic sequence of interbedded sandstone, thin siltstone intervals, local conglomeratic lenses and carbonate beds, ii) the Alkali-Basalt Member, 5-10-m-thick lenses of dark-green mafic volcanic rocks, and iii) the Volcaniclastic Member, a >150-m-thick sequence of volcaniclastics and minor siliciclastic beds. In the Mount McCleary area, the Klinkit Group structurally overlies highly deformed siliciclastic sediments of probable continental affinity (Gordey, 1992; Gordey and Stevens, 1994).

In the second area, the Stikine Ranges of northern British Columbia (Figs. 4-2 and 4-4), the Klinkit Group includes the Screw Creek Limestone (Mihalynuk et al., 2000; Poole, 1956; Roots et al., 2002) conformably overlain by the volcano-sedimentary Butsih Formation (proposed new Formation name; see appendix; Roots et al., 2002). The Screw Creek Limestone is a prominent light-coloured reef and debris-flow carbonate of Visean

84
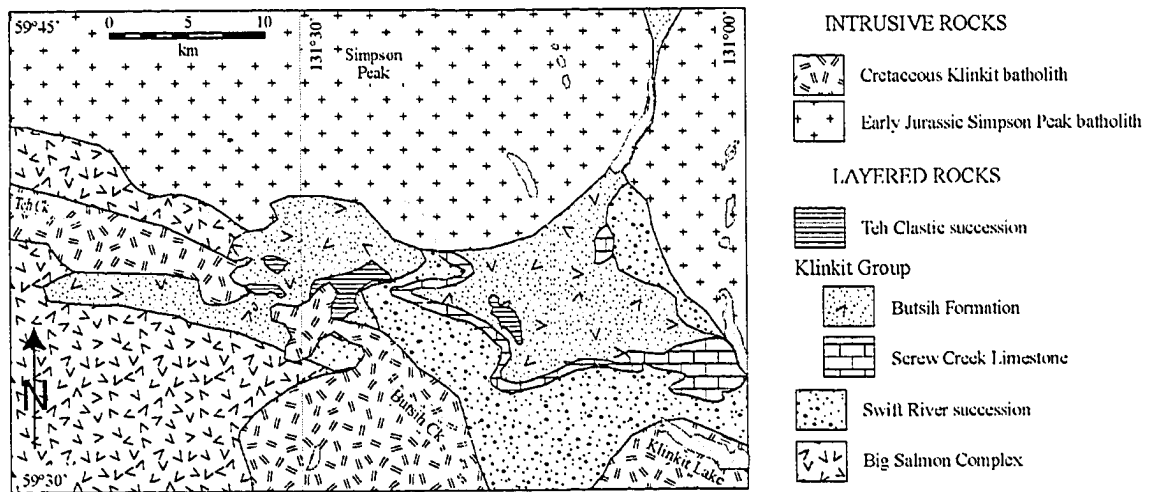
Figure 4-4 – Geological map of the Butsih Creek area, Stikine Ranges, northern British Columbia. The rocks of the Klinkit Group conformably overlie those of the Swift River succession and are disconformably overlain by the Triassic Teh Clastic succession.

to Bashkirian age (Mississippian to Early Pennsylvanian; Poole, 1956). The Butsih Formation is composed of two units: i) the Volcaniclastic Member, a >250-m-thick dominantly volcaniclastic sequence interbedded with sandstone, argillite, chert and minor limestone, and ii) the thin Upper Clastic Member, <100-m-thick, composed of siliciclastic and epiclastic rocks. In the Stikine Ranges, the Klinkit Group conformably overlies siliciclastic sedimentary rocks of continental affinity called the Swift River succession (Nelson, 2001). In at least one locality, the Triassic Teh Clastic succession (Roots et al., 2002) lies in angular unconformity on top of the Klinkit Group (Figs. 4-2 and 4-4; Simard et al., 2002).

4.4 Stratigraphy and petrography of the volcano-sedimentary formations of the Klinkit Group

4.4.1 Butsih Formation

The Volcaniclastic Member of the Butsih Formation is the thickest volcanic unit of the southern part of the Klinkit Group. It consists of several 100-m-thick fining-upward sequences of volcaniclastic beds ranging from lithic-tuff or breccia to crystal-tuff to ash-

85

deposits (Fig. 4-5A), together with minor interbedded siltstone beds. Its overall thickness is > 300 m (Simard et al., 2001).

Breccias at the base of some fining-upward sequences (Fig. 4-5A) are composed of plagioclase-phyric clasts (up to 4 cm in diameter) enclosed in a plagioclase crystal-rich quartzo-feldspathic matrix. This breccia facies is typically <8 m thick and grades upward into coarse tuff.

The main lithology of the Volcaniclastic Member is medium- to coarse-grained crystal- and lithic-tuffs. They are composed of variable proportions of crystals and lithic fragments enclosed in a fine devitrified quartzo-feldspathic matrix. The crystal fraction of those tuffs includes plagioclase, hornblende and in some cases clinopyroxene. The lithic fraction contains mainly plagioclase-phyric or plagioclase- and hornblende-phyric basaltic fragments, a lesser amount of relic plagioclase-phyric devitrified glass shards, and rare fine-grained siliciclastic and recrystallized quartz (chert?) clasts. The fine-grained volcaniclastic material (ash) includes small broken crystals (quartz and plagioclase) in a quartzo-feldspathic, carbonate or clay-rich matrix. The clasts are usually subrounded and present low sphericity. Towards the top of each sequence, volcaniclastic beds become progressively more diluted by non-volcanic clastics such as chert clasts and subrounded quartz grains, and the matrix becomes more clay-rich.

The Upper Clastic Member, which upwards contains increasing amounts of sandstone, carbonate and dark argillite over the volcaniclastic beds, reflects a gradual decrease in volcanic input. Meters-thick sequences of massive and cross-bedded layers of epiclastic and siliciclastic sediments have been observed in places (Fig. 4-5B). In contrast, the overlying Triassic sedimentary rocks of the Teh Clastic succession are composed of interbedded black argillite, dark siltstone, sandstone and chert, with minor pebble conglomerate and limestone beds.
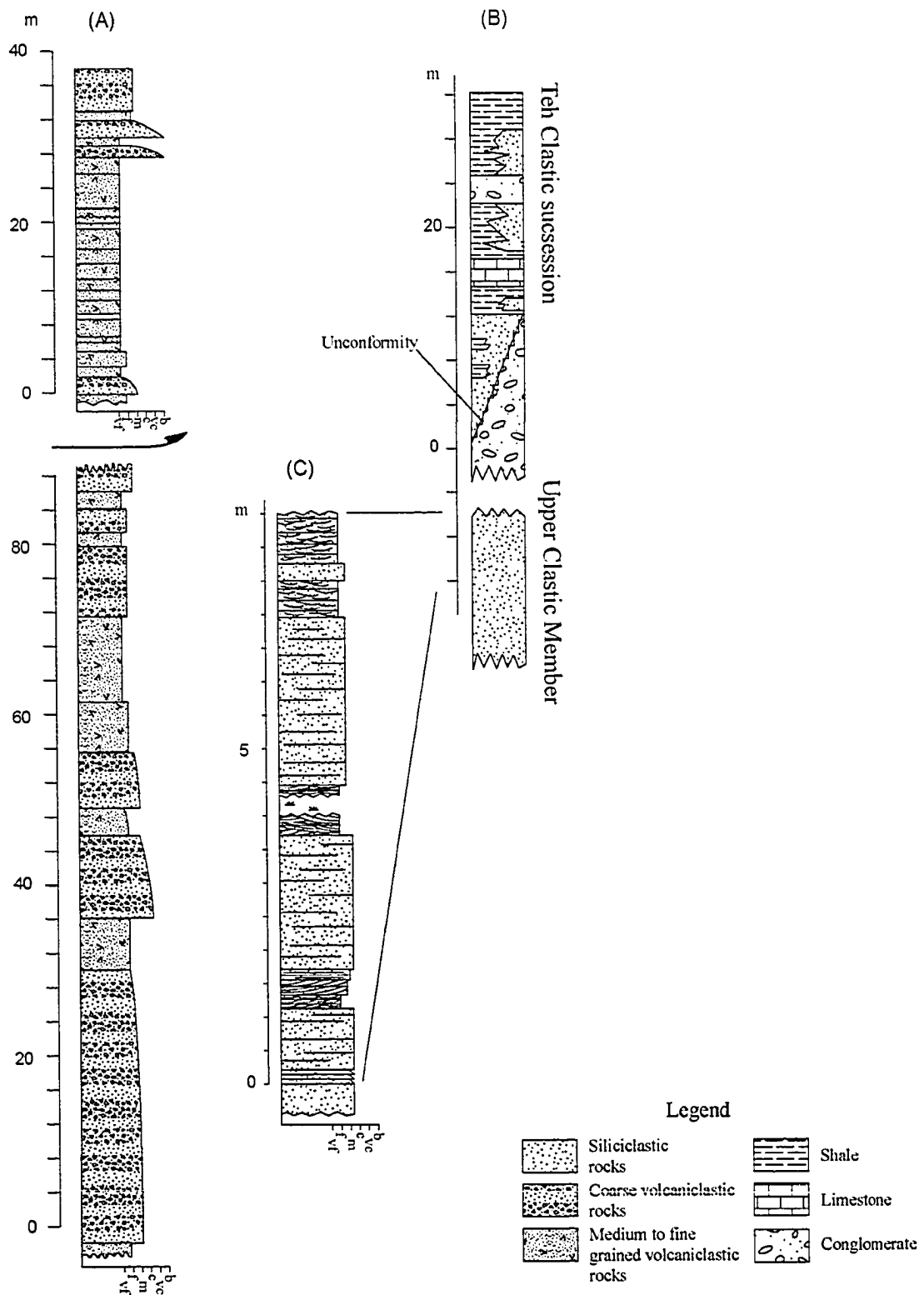
Figure 4-5 – Detailed stratigraphic sections of the Butsih Formation. (A) Measured section of the Butsih Formation Volcaniclastic Member in the Stikine Ranges, and (B) section showing the unconformity between the Upper Clastic Member of the Butsih Formation and the Teh Clastic succession, and (C) detailed of the Upper Clastic Member just below the unconformity. Grain-size scale indicates v (very), f (fine), m (medium), c (coarse), b (breccia).

4.4.2 Mount McCleary Formation

The Mount McCleary Formation is composed of three members (Fig. 4-2).

(i) The *Lower Clastic Member* is composed of quartz-rich sandstone interbedded with minor siltstone horizons and local conglomerate lenses. It displays an increase in volcaniclastic beds and limestone lenses towards the top.

(ii) The *Alkali-Basalt Member* is a laterally discontinuous unit of finely bedded volcaniclastic beds and massive porphyritic lava flows. The volcaniclastic beds are composed of intercalated plagioclase-rich crystal-tuff and ash-tuff layers. Although primary mineralogy has been obliterated by low-grade metamorphism, original magmatic textures are preserved in the lava flows. Phenocrysts, probably of clinopyroxene and/or hornblende originally, are replaced by actinolite and are set in a chlorite-actinolite groundmass.

(iii) The *Volcaniclastic Member* of the Mount McCleary Formation is petrographically indistinguishable from equivalent rocks of the Butsih Formation. It is a thick pile of massive, coarse crystal- and lithic-tuff beds, characterized by abundant plagioclase and hornblende crystals, basaltic clasts together with minor rounded quartz grains and other exotic clasts. A very fine recrystallized quartzo-feldspathic matrix is observed throughout this member.

4.5 Geochemistry

4.5.1 Analytical techniques, alteration and sampling

Forty-eight representative rock samples were selected for geochemical analyses from a suite of over two hundred specimens collected during the mapping of the Klinkit Group.

Major and trace element compositions of 13 representative samples from the Klinkit Group are given in Table 4-1.

Major and some trace (Rb, Sr, Ba, Zr, Y, Cr, Ni, V, Cu and Zn) elements were determined by X-ray fluorescence at the Geochemical Centre of Saint Mary's University, Halifax, Nova Scotia. The major elements along with V, Cr, Ba, Ni, Zn, Sr, and Zr are measured on fused glass beads. Other trace elements are determined on pressed pellets. Analytical error for this method for silica is within 0.5%. The analytical error is less than 1% for the other major elements. For trace elements, the precision is within 5%.

Additional trace elements (the rare earth elements [REEs], Ta, Hf, Nb and Th) were analyzed by inductively coupled plasma mass spectrometry (ICP MS) at the Activation Laboratories Ltd., Ancaster, Ontario, involving fusion using lithium borate-lithium tetraborate to insure total dissolution of the sample. Precision is better than 6% for trace elements, and analytical error is better than 5% (Young, 2002).

Four of these samples from the Butsih Formation were subsequently selected for Nd isotope analysis. Sm and Nd abundances were determined by isotope dilution mass spectrometry at the Department of Earth Sciences of Carleton University, Ontario. Analytical technique, as well as accuracy and precision for the technique, is described by Cousens (1996; 2000). In general, the $^{147}Sm/^{144}Nd$ ratios are reproducible to 1% (Cousens, 2000). Measured $^{143}Nd/^{144}Nd$ values were normalized to a natural $^{146}Nd/^{144}Nd$ ratio of 0.72190. Epsilon values (ε_{Nd}) (Table 4-2) were calculated assuming an age of 281 Ma for the Butsih Formation (Roots et al., 2002).

After careful field screening and petrographic analyses, only the least altered and metamorphosed samples from the volcanic rocks of the Klinkit Group were selected for geochemical analyses. Most major elements, high field strength elements (HFSE), rare earth elements (REE), Th and transition elements are thought to be immobile under low grade metamorphism (Winchester and Floyd, 1977). The consistency of various compositional trends using both mobile and immobile elements in the volcanic rocks of the Klinkit Group, and their similarities to those of modern igneous rocks, suggest that

Table 4-1 – Representative analyses of the Klinkit Group rocks.

| | Butsih Formation | | | | | | | | | Mount McCleary Formation | | | |
| | Volcaniclastic member | | | | | | | Upper Clastic member | | Volcaniclastic member | | Alkali-Basalt member | |
Sample	33-2	36-1a2	36-A	S-A2	S-36-G	34-a21	35-5	28-2b	28-2c	S-15-3	S-16-4	S-16-11	S-15-4
SiO2 (wt.%)	50.74	51.72	51.17	49.49	50.00	50.79	50.20	55.02	56.64	55.84	55.87	48.02	45.08
TiO2	0.96	1.02	0.77	0.98	0.86	0.95	0.82	0.88	0.84	0.97	0.95	2.16	3.72
Al2O3	16.92	15.94	14.81	16.48	18.16	17.46	17.24	16.43	16.81	17.19	17.25	19.67	13.58
Fe2O3	9.22	9.35	9.20	9.67	9.09	9.23	8.34	7.91	7.72	9.04	8.61	12.75	12.82
MnO	0.15	0.17	0.18	0.18	0.16	0.14	0.14	0.14	0.13	0.137	0.137	0.278	0.299
MgO	6.24	6.40	7.31	7.41	6.35	6.26	6.85	3.60	3.35	4.42	3.84	2.58	7.72
CaO	10.23	8.49	11.97	10.52	10.53	10.63	11.44	6.38	6.52	6.66	8.08	7.42	14.55
Na2O	4.46	4.96	3.44	2.48	2.51	3.33	2.90	3.42	3.78	3.71	3.89	4.90	0.94
K2O	0.16	0.17	0.56	0.90	1.18	0.15	0.78	1.71	1.18	1.57	0.94	0.96	0.18
P2O5	0.22	0.20	0.15	0.22	0.18	0.19	0.19	0.19	0.19	0.21	0.21	0.90	0.48
LOI	0.64	0.40	0.71	0.75	0.68	0.37	0.78	3.49	2.26	0.47	0.26	0.08	0.46
Mg#	0.57	0.57	0.61	0.60	0.58	0.57	0.62	0.47	0.46	0.49	0.47	0.29	0.54
Total	99.94	98.82	100.26	99.08	99.70	99.49	99.68	99.17	99.42	100.22	100.03	99.72	99.83
Cr (ppm)	175	161	208	208	139	175	166	61	49	53	57	60	405
Ni	64	57	61	89	55	72	62	17	17	56	40	89	132
Co	37	37	35	38	34	34	34	30	30	23	21	25	33
V	187	192	175	200	192	194	176	158	159	221	205	155	375
Cu	134	79	91	79	97	78	6	81	90	78	46	72	26
Zn	87	82	79	81	77	74	56	81	77	94	87	168	186
Rb	1	2	8	12	20	2	9	38	28	37	47	47	12
Ba		20	174	263	261	22	282	842	447	838	822	1,050	121
Sr	205	122	409	484	352	439	544	482	308	223	307	1980	671
Ga	17	17	16	18	20	19	18	20	18	19	20	26	21
Ta		0.47		0.39		0.35				0.21	0.31	8.32	4.40
Nb	4.27	8.20	2.56	6.88	4.28	6.45	4.24	6.00	4.92	2.20	5.00	113.00	58.20
Hf	2.80	2.74	2.15	2.74	2.40	2.80	2.36		3.35	3.1	3.30	6.70	5.60
Zr	101	106	75	101	87	103	86	144	116	121	125	343	232
Y	20.57	20.84	18.20	20.20	18.57	20.25	18.32	22.00	20.72	23.20	22.90	40.90	26.20
Th	1.60	1.75	1.25	1.51	1.41	1.57	1.48	2.00	3.01	1.96	2.17	10.50	5.06
La	11.33	13.37	7.36	12.04	10.36	11.96	10.07	13.00	15.44	13.40	13.50	83.70	36.90
Ce	26.94	31.06	17.58	28.58	24.77	28.84	23.96		33.01	25.80	26.00	122.00	64.00
Pr	3.90	4.25	2.54	4.04	3.53	4.12	3.42		4.30	3.78	3.81	14.60	8.46
Nd	17.86	18.82	11.79	18.48	16.14	18.44	15.64	17.00	18.00	16.50	16.50	52.70	35.10
Sm	4.39	4.50	3.20	4.56	4.06	4.44	4.06		3.93	3.97	3.99	9.17	7.68
Eu	1.25	1.32	0.98	1.37	1.30	1.38	1.31		1.18	1.29	1.36	3.49	2.75
Gd	4.31	4.32	3.40	4.45	4.08	4.35	3.87		3.91	4.40	4.19	7.17	6.93
Tb	0.64	0.66	0.53	0.65	0.60	0.63	0.58		0.62	0.67	0.65	1.02	0.95
Dy	3.86	3.93	3.26	3.87	3.47	3.82	3.37		3.79	4.04	4.00	6.56	5.37
Ho	0.77	0.79	0.67	0.74	0.69	0.74	0.69		0.77	0.85	0.84	1.29	0.98
Er	2.24	2.18	2.00	2.10	1.95	2.09	1.95		2.20	2.45	2.46	3.73	2.60
Tm	0.31	0.32	0.29	0.30	0.29	0.30	0.30		0.33	0.37	0.36	0.51	0.35
Yb	2.00	2.03	1.91	2.02	1.86	1.94	1.87		2.09	2.31	2.31	3.38	2.12
Lu	0.33	0.31	0.29	0.30	0.28	0.30	0.28		0.33	0.35	0.35	0.52	0.28

Notes: 33-2, 36-1a2, 36-A, S-A2, S-36-G, 34-a21, 35-5, S-15-3 and S-16-4, coarse-grained crystal- and lithic-tuffs; 28-2b and 28-2c, epiclastic material with >20% non-volcanic material such as quartz grains and metamorphosed clays; S-15-4, porphyritic alkali-basalt; S-16-11, layered crystals- and ash-tuff. [a]Mg# = MgO/(MgO + FeO_tot) in mol %.

Table 4-2 – Nd isotopic composition of the Klinkit Group rocks*

Sample	Nd (ppm)	Sm (ppm)	$^{147}Sm/^{144}Nd$	$^{143}Nd/^{144}Nd^a$	ϵ_{Nd} (281 Ma)
S-A2	18.48	4.56	0.1486	0.51293	+ 7.4
S-28-2C	18.00	3.93	0.1352	0.512868	+ 6.7
S-34-A2	18.44	4.44	0.1497	0.512907	+ 6.9
S-35-5	15.64	4.06	0.1505	0.512928	+ 7.3
S-36A	11.79	3.20	0.1585	0.512929	+ 7.1

*Notes: S-A2, S-34-A2, S-35-3 and S-36A: Volcaniclastic Member of the Butsih Formation; S-28-2c, Upper Clastic Member of the Butsih Formation.

^{a} $^{143}Nd/^{144}Nd$ at present

most major and trace elements were not significantly affected by alteration processes, and that the distribution of these elements reflects their primary magmatic distribution.

Petrographic study of the samples selected for geochemical analyses was done in order to minimize the effect of their clastic nature; only the crystal- and lihic-tuff samples showing <3% of non-volcanic material were considered. In order to evaluate the effect of the presence of siliciclastic material on the geochemical compositions of volcaniclastic rocks, a few samples from the Upper Clastic Member of the Butsih Formation showing over 10% of non-volcanic material (e.g. chert clasts, rounded quartz grains) were processed along with the volcaniclastic samples of the Volcaniclastic Member (Table 4-1). The relative increase of siliciclastic over volcaniclastic material in the sample is characterized by higher SiO_2, Zr and loss on ignition (LOI) values, along with lower MgO, CaO, Cr, Ni values (Table 4-1; Figs. 4-6,4-7 and 4-8).

4.5.2 Butsih Formation

The volcanic rocks of the Butsih Formation plot entirely within the subalkaline field of Winchester and Floyd (1977; Fig. 4-6), with SiO_2 contents between 49.9 and 51.9 % (LOI-free). Their Mg# ($MgO/(MgO+FeO_{tot})$ in mol %) are typically around 0.60. This moderately low Mg# compared to primitive melts suggests that these rocks underwent moderate fractional crystallization. Although they exhibit a calc-alkaline affinity (Figs. 4-7A, 4-7B and 4-10), the rocks also display a tholeiitic fractionation trend (Fig. 4-7C) as shown by a slight increase of TiO_2 with differentiation, suggesting that the rocks are

Rhyolite (A)

Rhyodacite-Dacite

70

SiO₂ (wt.%)

T

60

Andesite TA

Ph

50

Sub-AB AB

BTN

Rhyolite (B)

70

Rhyodacite-Dacite

SiO₂ (wt.%)

T

60

Andesite TA

Ph

50

Sub-AB AB

BTN

.001 0.01 0.1

Zr/TiO₂*0.0001

Klinkit Group

Butsih Formation

▲ Volcaniclastic Member

△ Upper Clastic Member

Mount McCleary Formation

▼ Alkali-basalt Member

▽ Volcaniclastic Member

Lay Range assemblage

□ Upper Mafic Tuff division

Little Salmon succession

◇ Alkali basalts

● Calc-alkaline andesites

○ Calc-alkaline rhyodacites

Figure 4-6 – Zr/TiO2 vs SiO2 (wt.%) diagrams (Winchester and Floyd 1977). Note the similarity of (A) the Klinkit samples to (B) both the subalkaline rocks of the Lay Range Assemblage (from Ferri 1997) and to the alkaline basalts of the Little Salmon succession (from Colpron 2001). The Klinkit Group includes both subalkaline and alkaline mafic volcanic rocks. (Sub-AB : subalkaline basalt; AB: alkaline basalt; TA: trachyandesite; BTN: basanite, trachyte, nephenite; T: trachyte; Ph: phonolite)

transitional between tholeiitic and calc-alkaline. Zirconium, an incompatible trace element that is considered to be immobile during alteration processes (Winchester and Floyd 1977), was used as an index of differentiation (Figs. 4-7C and 4-8). The Ti content,
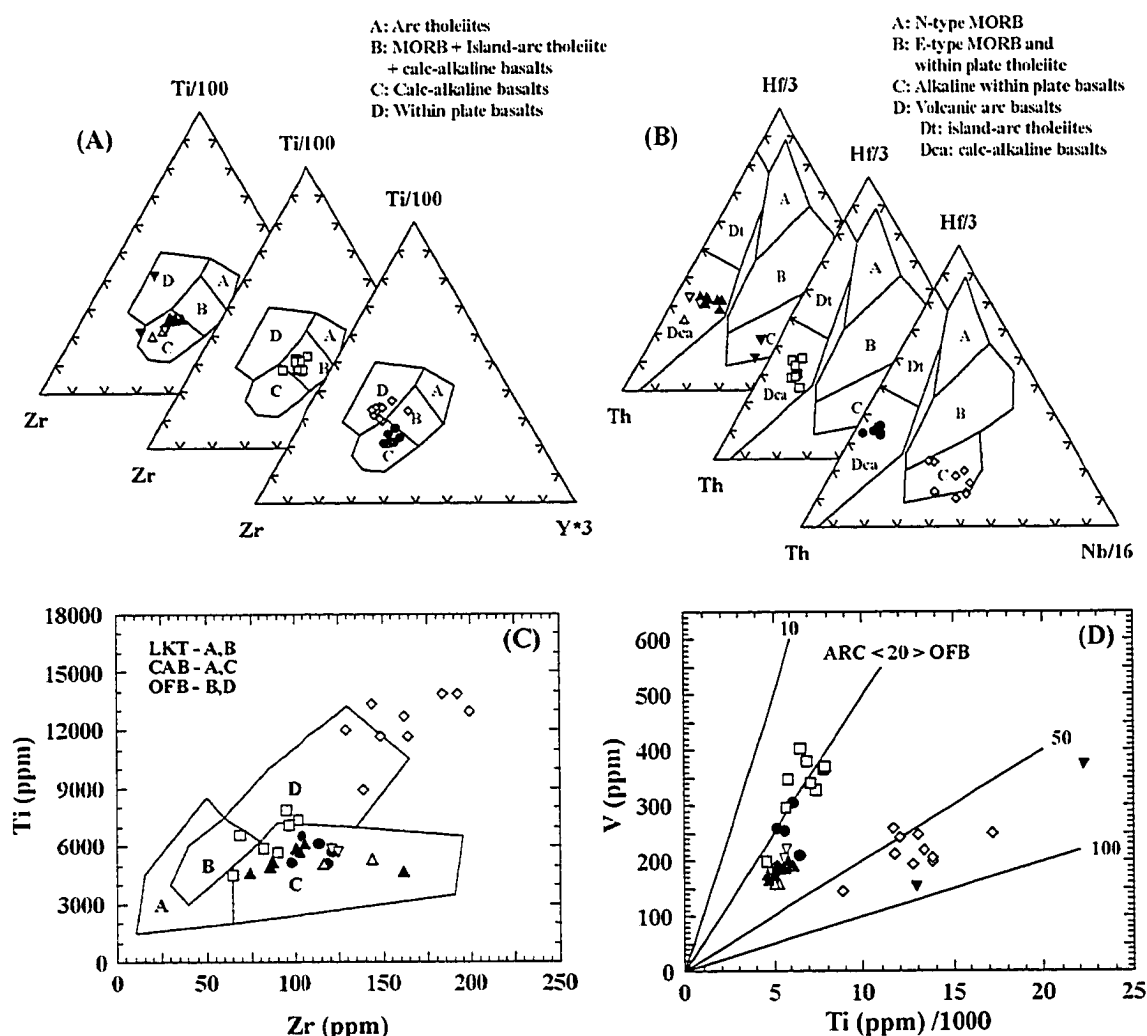
Figure 4-7 – Geochemical characteristics of the volcanic rocks of the Klinkit Group. (A) – Zr-(Ti/100)-(Y*3) diagram of Pearce and Cann (1973). (B) – Th/(Hf/3)/(Nb/16) diagram of Wood et al. (1979). (C) – Ti-Zr diagram of Winchester and Floyd (1977). LKT-Low-potassium tholeiites, CAB-Calc-alkaline basalts and, OFB-Ocean-floor basalts. This diagram also gives information on possible fractionation trends with differentiation of rock sequence. (D) – V-(Ti/1000) diagram of Shervais (1982). V/Ti < 20 typical of arc, V/Ti > 50 typical of alkaline magmatism. Representative analyses of the volcanic rocks of the Lay Range Assemblage (Ferri 1997) and the Little Salmon succession (Colpron 2001) are shown for comparison. Symbols as in Fig. 4-6.

as well as the Ti/Zr and Ti/V ratios (Figs. 4-7C and 4-7D), of the volcanic rocks resemble those of modern island-arc tholeiitic basalts (e.g. Gamble et al., 1995).

Some major and trace elements show systematic fractionation trends when plotted against Zr (eg. Figs. 4-7C and 4-8). A decrease of CaO, Mg, Cr, Ni and CaO/Al$_2$O$_3$ values while Zr increases suggests fractionation of clinopyroxene and plagioclase (Fig. 4-8). An
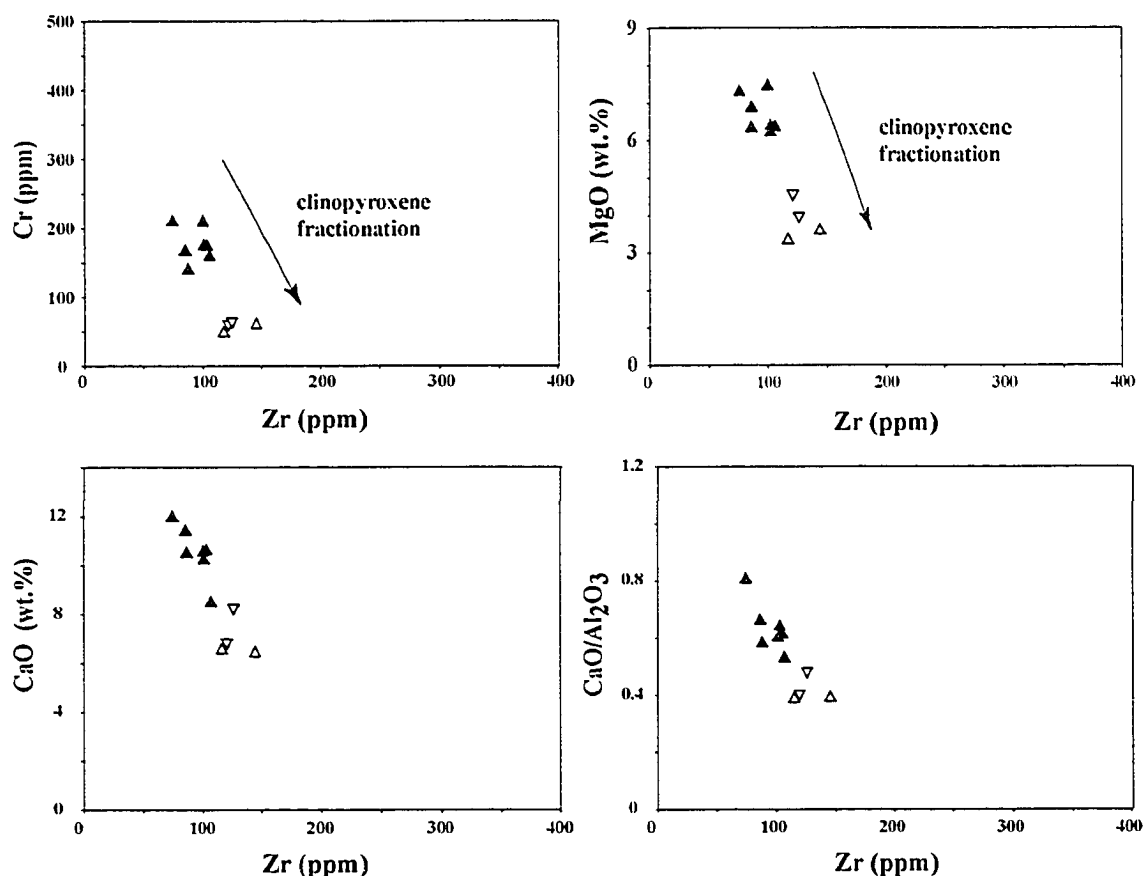
Figure 4-8 – Variation of (A) Cr (ppm), (B) MgO (wt.%), (C) CaO (wt.%), and (D) CaO/Al2O3 relative to Zr (ppm) in the volcaniclastic members of the Klinkit Group. Symbols as in Fig. 4-6.

increase of TiO_2 and V with increasing Zr argues against fractionation of Fe-Ti oxides (Fig. 4-7D).

The REE patterns of the Butsih Formation (Fig. 4-9) show a moderate light rare earth elements (LREE) enrichment ((La/Yb)$_N$=2.77-4.73) with a flat heavy rare earth elements (HREE) pattern, suggesting that the source did not contain residual garnet. The rocks were probably produced from partial melting in the spinel peridotite field, at < 60 km depth (White et al., 1992). The mantle-normalized trace element patterns (Fig. 4-10) display pronounced negative Nb and Ti anomalies, which are characteristic of subduction-related magmas (e.g. Hawkesworth et al., 1979; Pearce, 1983). The subduction-related nature of the rocks is also supported by their Th-Hf-Nb distribution (Fig. 4-7B), which is indicative of volcanic arc rocks.

Figure 4-9   **Figure 4-10**
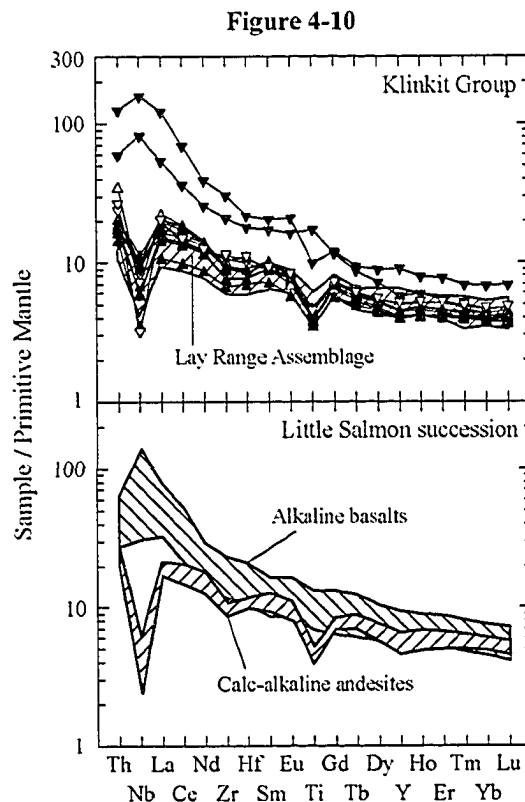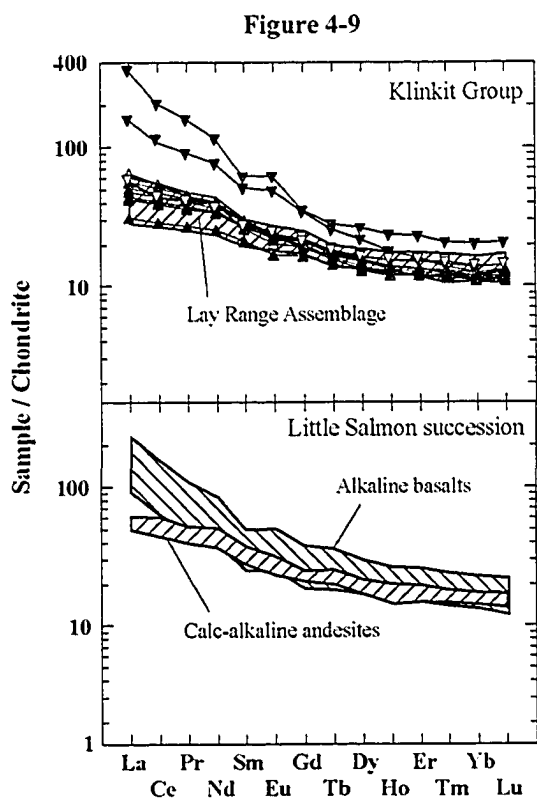
Figure 4-9 – Chondrite-normalized REE patterns for the volcanic rocks of the Klinkit Group. For comparison, shaded fields of representative analyses of the volcanic rocks of (A) the Lay Range Assemblage (Ferri 1997) and (B) the Little Salmon succession (Colpron 2001) are shown. Normalizing values from Sun (1982). Symbols as in Fig. 4-6.

Figure 4-10 – Mantle-normalized incompatible trace element patterns for the volcanic rocks of the Klinkit Group. For comparison, shaded fields of representative analyses of the volcanic rocks of (A) the Lay Range Assemblage (Ferri 1997) and (B) the Little Salmon succession (Colpron 2001) are shown. Normalizing values from Sun and McDonough (1989). Symbols as in Fig. 4-6.

The ε_{Nd} values of these rocks (Table 4-2) are high and positive (from +6.7 to +7.4), suggesting a primitive magma source with at most only little involvement of continental crust in the magma genesis (Fig. 4-11). The ε_{Nd} value for the sample from the Upper Clastic Member (+ 6.7; Table 4-2) is similar to those of the Volcaniclastic Member, suggesting derivation from the same source.
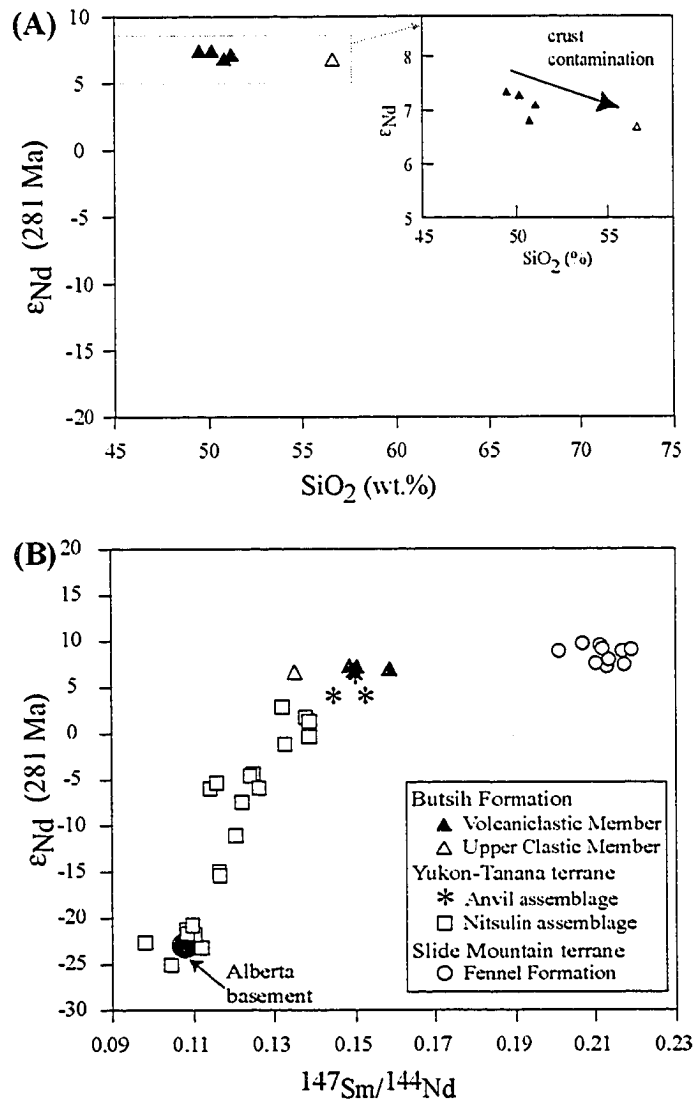
Figure 4-11 – εNd vs. (A) SiO2 (wt.%) and (B) 147Sm/144Nd for the rocks of the Butsih Formation, Klinkit Group. ε_{Nd} values were calculated for an age of 281 Ma. Shown for comparison are the compositions of Slide Mountain oceanic basalts (Smith et al., 1995), mafic continental volcanic arc rocks of the Anvil Assemblage, and Nitsulin sedimentary rocks of the Yukon-Tanana composite terrane in Teslin area, Yukon (Creaser et al., 1997) and the average Alberta basement (Theriault and Ross, 1991).

4.5.3 Mount McCleary Formation

4.5.3.1 Volcaniclastic Member

The geochemical signature of the Volcaniclastic Member of the Mount McCleary Formation is very similar to the equivalent unit in the Butsih Formation, suggesting that

they were both subduction-related, and probably derived from the same sources. The Mount McCleary Volcaniclastic Member rocks plot in the andesite field of Winchester and Floyd (1977; Fig. 4-6), with SiO_2 contents around 55.8 % (LOI-free). Both volcaniclastic members of the Klinkit Group represent calc-alkaline magmatism as shown in the Zr-Ti-Y diagram of Pearce and Cann (1973; Fig. 4-7A). They also share the same moderate LREE enrichment $((La/Yb)_N=4.1-4.2)$ with a flat HREE pattern on the REE diagram (Fig. 4-9), as well as the same mantle-normalized trace element patterns (Fig. 4-10) with strongly negative Nb and Ti anomalies.

4.5.3.2 Alkali-Basalt Member

The two samples analysed from the volcanic rocks of the Alkali-basalt Member plot in the alkaline basalt and basanite fields of Winchester and Floyd (1977; Fig. 4-6) with SiO_2 ranging between 45.4 and 48.2 % (LOI-free). The samples also plot in the alkaline within-plate basalts field of Th-Hf-Nb diagram (Fig. 4-7B). Their alkaline nature is supported by the high Ti/V ratio (Fig. 4-7D), as well as by the high content of incompatible elements like Th, Nb and Zr.

The REE patterns (Fig. 4-9) have a strong LREE enrichment $((La/Yb)_N=12.5-17.8)$, typical of ocean island basalts. The mantle-normalized trace element patterns (Fig. 4-10) display a strong enrichment in the highly incompatible elements. Mantle-normalized incompatible trace element patterns (Fig. 4-10) show smooth profiles that increase with increasing element incompatibility and peak at Nb. These patterns are similar to those of ocean-island basalts (e.g. alkali basalts of Hawaii; Figs. 4-9 and 4-10; Wilson, 1989). Geochemically, these rocks closely resemble the alkaline basalts of the Little Salmon succession of the Yukon-Tanana terrane in central Yukon (Figs. 4-1, 4-6, 4-7 and 4-9; Colpron 2001).

4.6   Petrogenesis of the Klinkit Group

The volcanic rocks of the Klinkit Group are mostly arc-derived. The similarities in relative element abundances of the volcaniclastic members of the Butsih and Mount McCleary formations, as well as their similar temporal and stratigraphic associations with Carboniferous limestones, suggest that they are genetically related, despite being 200 km apart at present.

Both volcaniclastic members show similar calc-alkaline magmatism with relatively low abundance of highly incompatible elements. The relatively high Mg#, as well as the moderate values of Cr (between 100 and 200 ppm) and Ni (<100 ppm) indicate that these basaltic rocks are moderately differentiated.

The low concentration of incompatible elements such as Th and Zr in these volcanic rocks, as well as their relatively low SiO_2 content and their highly positive ε_{Nd} values suggest no significant crust contamination. The Th/La ratio is a sensitive indicator of crustal contamination for which the average primitive mantle and the total continental crust values are 0.12 and 0.22, respectively (Taylor and McLennan, 1985). Both Volcaniclastic members of the Butsih and the Mount McCleary formation present Th/La ratios ranging from 0.13 to 0.17, which suggest crustal contamination. Higher Th/La ratio values of the Upper Clastic Member (0.15-0.2) could have been caused by the addition of continentally-derived siliciclastic sediments to the volcaniclastic rocks; however, the highly positive ε_{Nd} values of the Upper Clastic Member, as well as its position just outside the mixing line between the depleted mantle (Slide Mountain ocean; Fig. 4-11) and the crustal material (Alberta basement; Fig. 4-11) formed by the continentally-derived sediments of the Yukon-Tanana terrane (Nitsulin Assemblage; Creaser et al., 1997; Fig. 4-11) argue against significant crust interaction with old crustal material.

Based on geochemical and geological evidence, the volcaniclastic members of the Klinkit Group can be interpreted as part of a primitive arc erupted either through relatively young crust that consists of slightly older arc basement, or that was rapidly emplaced through

coated conduits and/or relatively thin continental crust without significant crust contamination. Similar interpretations have been proposed for mafic volcanic rocks of the Anvil Assemblage (Creaser et al., 1997), Little Salmon succession (Colpron, 2001) of the Yukon-Tanana terrane, and the Upper Mafic Tuff of the Lay Range Assemblage of the Harper Ranch sub-terrane, basement to Quesnel terrane (Ferri, 1997).

Concentrations of several trace elements in the basalts of the Alkali-Basalt Member of the Mount McCleary Formation are such that they cannot be derived from the same source or parental magma as those of the Volcaniclastic Member. Their geochemical characteristics, including the lack of negative Nb and Ti anomalies, are consistent with their derivation from asthenospheric sources; possibly during episodic intra-arc rifting events.

4.7 Reconstruction of the paleovolcanic environment of the Klinkit Group

In the Butsih Creek area, the Klinkit volcanics were deposited atop continentally derived siliciclastic sediments of the Swift River succession which represents sedimentation into a marginal basin older than the Late Carboniferous-Pennsylvanian Screw Creek Limestone.

The fining-upward sequences within the Volcaniclastic Member (Fig. 4-5A) resemble megaturbidite deposits typical of subaqueous, below-wave-base depositional setting of voluminous volcaniclastic turbidity currents. Volcaniclastic megaturbidite sedimentary units can be in the order of 100-m-thick and include abundant coarse, dense components (McPhie et al., 1993), which are a typical feature of the volcaniclastic members of the Klinkit Group. These currents are responsible for resedimentation of a wide variety of unconsolidated, primary volcaniclastic and volcanogenic sedimentary deposits, or can be directly fed by syn-eruptive pyroclastic flows, volcanic debris avalanches, volcaniclastic debris flows and lahars (McPhie et al., 1993). In some cases, such syn-eruptive deposits

are overlain by thinner bedded volcaniclastic turbidite sequences (Bull and Cas, 1991). The succession of massive and cross-bedded layers of volcaniclastic and siliciclastic sediments of the Upper Clastic Member rocks of the Butsih Formation can be interpreted as these. Despite uncertain origin, the latter clearly represents the gradual post-eruptive re-adjustement of the sedimentary transport and depositional processes by means of mass-flow resedimentation (McPhie et al., 1993). The significant thickness of volcaniclastic sediments covering the reef/debris-flow limestone suggests a deep or constantly subsiding basin near an active volcano. The absence of intrusions, lava flows and very coarse volcanic breccias in this arc-related volcanic sequence further supports the distal nature of the volcaniclastic rocks of the Klinkit Group.

Arc volcanism was active in the Early Permian but ceased by Triassic time as the volcaniclastic rocks were covered by the non-volcanic, continentally-derived deep water sediments of the Triassic Teh Clastic succession (Roots et al., 2002).

The northern part of the Klinkit Group, and possibly other parts of the Klinkit arc that were not preserved, experienced alkaline basalt magmatism. The scarcity of those lavas suggests that they accompanied episodic intra-arc rifting events.

4.8 Klinkit age-correlative successions

The Klinkit Group is one of several late Paleozoic volcanic successions that form a linear belt within Yukon-Tanana terrane (Figs. 4-1 and 4-12). Representative analyses from some of these are shown in the discriminant diagrams (Figs. 4-6 to 4-10).

The Late Paleozoic volcano-sedimentary sequence most similar to the Klinkit Group in the eastern part of the Cordillera is the Lay Range Assemblage (Ferri, 1997), 400 km to the south in northern central British Columbia (Figs. 4-1 and 4-12; Harms and Stevens, 1996b; Nelson, 1997). It is a tectonically dismembered volcanic complex that could be a

displaced fragment from the Klinkit arc, as their general stratigraphy and petrochemical nature are very similar (Figs. 4-6 to 4-10, 4-12).

The Lower Sedimentary Division of the Lay Range Assemblage resembles the siliciclastic Swift River succession which conformably underlies the Klinkit Group. Both are characterized by heterogeneous siliciclastic lithologies and the probable continental derivation of at least some of the rocks (Creaser et al., 1997; Creaser and Harms, 1998; Ferri, 1997).

Mid-Mississippian to Early Pennsylvanian limestone forms an important marker just above both of these sedimentary sequences (Fig. 4-12). It marks the change from deep basin sedimentation with sporadic siliciclastic influx to an active volcanic island-arc environment (Nelson, 2001).

Like the volcaniclastic members of the Klinkit Group, the Upper Mafic Tuff Division of the Lay Range Assemblage is composed mainly of mafic crystal-lithic and lapilli tuffs with minor siliciclastic input. However, the Upper Mafic Tuff Division also contains several volcanic flows suggesting more proximal facies than what is preserved within the Klinkit volcaniclastic members. The volcanism of the Upper Mafic Tuff Division is interpreted to be of Permian age (Ferri, 1997), consistent with the Early Permian age obtained from the Volcaniclastic Member of the Butsih Formation. The geochemical signature of the Upper Mafic Tuff Division is almost identical to the signature of the volcaniclastic members of the Klinkit Group (Figs. 4-6 to 4-10). This geochemical resemblance, as well as their age correlation and their stratigraphic similarities (Fig. 4-12), implies that they were both formed in the same subduction-related environment, probably derived from the same sources.

Unlike the Klinkit Group, which is unconformably overlain by the Triassic Teh Clastic succession of continental affinity, the volcanics of the Lay Range Assemblage are conformably overlain by a thick limestone straddling the Permo-Triassic boundary and Mesozoic volcanic rocks of the Quesnel arc (Fig. 4-12; Ferri 1997; Gabrielse and Yorath

Figure 4-12 – Stratigraphic correlation chart of selected Late Paleozoic volcano-sedimentary sequences of the northern Canadian Cordillera (modified from Colpron and Group, 2001). Note the presence of older siliciclastic basement and Late Mississippian to Early Pennsylvanian limestones in each sequence. Quesnel terrane/Lay Range Assemblage data from Ferri (1997).

DEVONIAN | MISSISSIPPIAN | PENNSYLVANIAN | PERMIAN | TRIASSIC

Frasnian 382.5 | Famennian 376.5 | Tournaisian 362 | Viséan 349.5 | Serpukhovian 333 | Bashkirian 323 | Moscovian 311.5 | Kasimovian 303 | Gzhelian 299 | Asselian 295 | Sakmarian 285 | Artinskian 280 | Kungurian 272 | Ufimian/Kazanian 269 | Tatarian 264 | Induan 251 | Olenekian 247 | Anisian 244 | Ladinian 240.6 | Carnian 227 | Norian 221 | Rhaetian 210

Quesnel terrane (QN) /
Lay Range Assemblage (LRA)
(northern central British Columbia)

Takla Group (QN)
Upper Mafic Tuff Division (LRA)
Lower Sedimentary Division (LRA)

Stikine Ranges and Englishman Range
(northern British Columbia and southern Yukon)

Teh clastic

Klinkit Group
Lower Mount McCleary clastic
Englishman
Deformation
Upper clastic
Bush
Screw Creek
Swift River succ.

Big Salmon Complex
Deformation
Mn chert

Glenlyon area
(central Yukon)

Boswell / Semenof
Little Kalzas
Little Salmon
Snowcap
Mn chert
UNCONFORMITY Deformation metamorphism
ultramafic

Yukon-Tanana terrane

400 km
200 km

Pericratonic basin
Mafic/ultramafic intrusion
Ultramafic/gabbro basal contact
Basic volcanic rocks
Intermediate volcanic rocks
Felsic volcanic rocks
Volcaniclastic rocks
Chert
Quartzite

Clast-rich conglomerate
Grit
Siliceous phyllite
Carbonaceous clastic rocks
Argillaceous siliceous clastic material?
Marble
Chlor. or grn. phyllite
Psammite

U-Pb geochronological age constraint
Fossil age constraint

103

1991). This conformable sequence demonstrates that the Lay Range Assemblage is the basement of the Mesozoic Quesnel arc (Ferri, 1997).

In addition, detrital quartz and zircons of Proterozoic age were recovered from the Upper Mafic Tuff division of the Lay Range Assemblage (Ferri, 1997), suggesting that continental crust was supplying detritus. Early Proterozoic and Paleozoic inheritence in zircon fractions recovered from Early Permian felsic volcanics of the Upper Mafic Tuff Division indicates that Lay Range magma erupted through older continental crust (F. Ferri, 2002). In contrast, the primitive nature of the Klinkit magma with little or no involvement of continental crust could have resulted from its rapid emplacement through thin continental crust.

Like in the Klinkit Group, Lay Range volcanic rocks include some alkaline flows at the base of the Upper Mafic Tuff division (F. Ferri, 2002[6]). Alkaline magmatism was also present in at least one other correlative Late Paleozoic volcanic sequence of the Yukon-Tanana composite terrane, the Little Salmon succession (Figs. 4-6 to 4-10, 4-12; Colpron, 2001).

4.9   Tectonic implications

In Late Devonian time, the western margin of North America had a thin and stretched continental edge (Monger, 1999). Outboard of the continent was a strip of continental sediments, and possibly an underlying fragment of continental crust, atop which volcanic arcs formed (Fig. 4-13). These are defined in the north as the Yukon-Tanana composite terrane (Colpron and Group, 2001; Mortensen, 1992), and in the south as the basement of the Mesozoic Quesnel arc (Ferri, 1997; Gabrielse and Yorath, 1991). These Late Devonian to Early Mississippian arc successions include the Big Salmon complex (Colpron and Group, 2001; Mihalynuk et al., 1998; 2000; Figs. 4-12 and 4-13) of northern British Columbia, the Little Kalzas succession of central Yukon (Colpron 2001;

---

[6] F.Ferri, written communication to the first author, 2002.
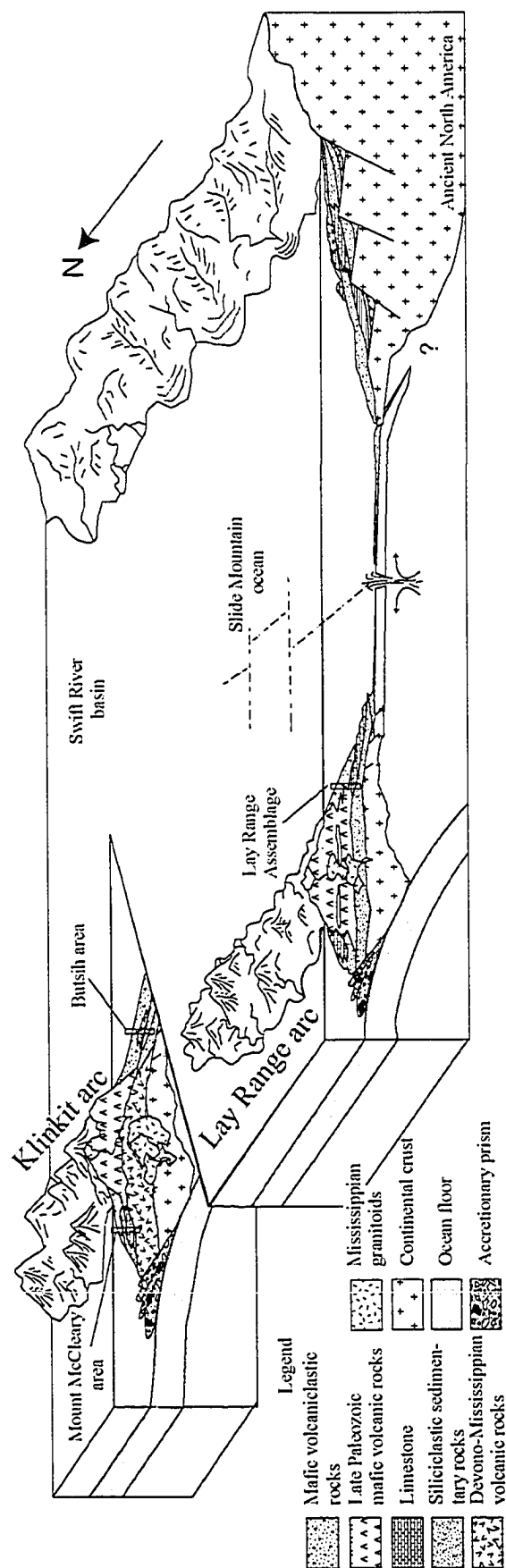
Figure 4-13 — Schematic drawing of volcanic arc complexes in Late Paleozoic time. The Klinkit arc is inferred to have formed on thin rifted continental crust west of ancestral North America. Lay Range volcanic rocks formed further south, possibly on the same arc system.

105

Colpron and Group, 2001) and the Fire Lake Unit of the Grass Lake Succession of the Finlayson Lake (Piercey et al., 2002) in the Yukon-Tanana composite terrane.

Between these Late Paleozoic arc-related rocks and the ancient North American cratonic rocks are discontinuous exposures of Slide Mountain rocks – remnant of a spreading ocean that probably developed as a marginal back-arc type basin throughout Early- and Mid-Mississippian time (Gabrielse, 1991; Nelson, 1993; Tempelman-Kluit, 1979). In the Stikine Ranges of northern British Columbia, the Butsih Formation rests on continentally-derived sediments of the Swift River succession, representing a marginal basin older than Late Carboniferous-Pennsylvanian to the east of the Klinkit arc (Colpron and Group, 2001; Nelson, 2000). The Swift River basin may be the northern precursor of the Slide Mountain ocean (Fig. 4-13). The northernmost exposure of the pericratonic belt is found in the Finlayson Lake region, southeastern Yukon, where the Kudz Ze Kayah Unit of the Grass Lake Succession and the Wolverine succession also recorded back-arc volcanic activity at that time (e.g. Piercey et al., 2003; 2002; 2001). Ocean-floor spreading in Pennsylvanian time is found in the Campbell Range Succession, Finlayson Lake region, southeastern Yukon, unconformably lying on the back-arc complex (Colpron and Group, 2001).

The Klinkit arc is part of another volcanic pulse developed atop this arc system from Pennsylvanian to Permian time (Fig. 4-13). Episodes of mafic arc volcanism at that time also occurred in the Little Salmon Lake area (Colpron, 2001), in the Boswell and Semenof hills in central Yukon, and in the Upper Mafic Tuff Division of the Lay Range Assemblage in central northern British Columbia (Ferri, 1997; Fig. 4-12). This belt of penecontemporaneous volcanism, which in its northern part is part of the Yukon-Tanana composite terrane and to the south forms the basement to the Quesnel terrane, suggests that the Yukon-Tanana composite terrane may be the northern extension of the basement of the Quesnel terrane. Therefore, the northern part of the Quesnel terrane may be considered pericratonic as it formed atop continentally derived rocks, instead of the former intra-oceanic interpretation.

Alkaline magmatic rocks are present in most of Late Paleozoic successions of the northern Canadian Cordillera (e.g. Colpron, 2001; Ferri, 1997), suggesting that intra-arc rifting may have occurred throughout this major arc system during Pennsylvanian time. However, only the southernmost sequence, the Lay Range assemblage, records the overlying Mesozoic arc volcanism of the Quesnel arc. In the Klinkit area, the continentally-derived Triassic Teh Clastic succession is preserved, and contemporaneous volcanic rocks either were not present or are not preserved. The continental signature of the Teh sediments suggests that this part of the arc system, and possibly the Yukon-Tanana composite terrane as a whole, was close to the North American craton in Triassic time.

4.10 Conclusion

The rocks of the Klinkit Group in northern British Columbia give new insights on the Late Paleozoic tectonic history of the northern Canadian Cordillera. The volcanic rocks were part of a mid-Mississippian and Permian arc system erupted possibly through thin continental crust that experienced some episodes of intra-arc rifting. This arc volcanism shed significant volcaniclastic debris into the surrounding basin, which constitutes the Klinkit Group. By Triassic time the Klinkit part of this arc system was proximal to North America as indicated by the continental nature of the sediments overlying the Klinkit rocks.

Volcanic rocks of the Klinkit Group strongly resemble those of the upper Lay Range Assemblage, the basement of the Quesnel terrane. The Late Paleozoic arc-related rocks of pericratonic Yukon-Tanana composite terrane may then be a northern equivalent to the basement of the southern Late Paleozoic to Mesozoic Quesnel arc. The northern Quesnel terrane therefore shows pericratonic affinity.

4.11 Acknowledgements

4.12 Appendix

4.12.1 Historical background

Regional mapping in northern British Columbia and southern Yukon in the last part of the century (Abbott, 1981; Gabrielse, 1969; Poole, 1956; Poole et al., 1961) set the basis of the Terrane Map of the Canadian Cordillera (Wheeler, 1991) in this area. Rocks of the new proposed Klinkit Group were there associated either with the Dorsey terrane to the east in the case of the sedimentary rocks, or with the Slide Mountain terrane to the west, on the basis of their mafic volcanic contents (Monger et al., 1991; Wheeler, 1991).

Subsequent mapping by Harms and Stevens of this area (Harms and Stevens, 1995; 1996b; Stevens, 1996; Stevens and Harms, 1995) eliminated the possibility of a fault separating the Slide Mountain terrane from the Dorsey terrane in the area (Harms and Stevens, 1995). They also proposed new nomenclature to replace the former Dorsey terrane based on both lithological and metamorphic/structural character, and related those new assemblages either to the pericratonic Yukon-Tanana composite terrane or to the intra-oceanic Quesnel terrane (Harms and Creaser, 1997; Harms and Stevens, 1995; Stevens and Harms, 2000).

The present paper proposed a revised nomenclature for this part of the northern Canadian Cordillera. The assemblages of Harms and Stevens (1995) are now subdivided into: (1) the Ram Creek assemblage (Harms and Stevens, 1995; 1996a; Stevens, 1996; Stevens and Harms, 1995; 1996), (2) the Dorsey assemblage (Harms and Stevens, 1995; Harms and Stevens, 1996a; Stevens, 1996; Stevens and Harms, 1995; Stevens and Harms, 1996), (3) the Klinkit Group (new proposed unit; see Stratotype information for previous work on these rocks) which includes two distinct stratigraphies (Fig. 4-4), i) the Butsih Formation (new proposed unit) and Screw Creek Limestone (Poole, 1956), from the Stikine Ranges, northern British Columbia, and ii) the Mount McCleary Formation (new proposed unit) and the English Creek Limestone (new proposed unit) from the Englishman Range, southern Yukon; (4) the Swift River succession (Nelson, 2001; Stevens and Harms, 1996), and (5) the Triassic Teh succession (Colpron and Group, 2001).

4.12.2 Stratotype information

Type areas for the different members of the Butsih Formation (Fig. 4-2) are located in the Stikine Ranges, northern British Columbia. The Volcaniclastic Member is best exposed in the headwaters of Butsih Creek and Teh Creek , about 15 km SSW of the Simpson Peak and 25 km northwest of Klinkit Lake (W 71°31'58", N 59°35'01"). It consists of steep sections ~100-200 m high on both sides of a prominent peak (Fig. 4-5A). This unit was previously included in "Klinkit Assemblage" of Harms and Stevens (1995), as "Tuffite" (Mihalynuk et al., 2000) and as "Butsih unit" by Roots et al. (2002). The Upper Clastic Member is best exposed about 5 km north on the same ridge (W71°30'48", N59°36'12"). It was described as the "Transitional Unit" by Mihalynuk et al. (2000) and "Bigfoot unit" by Roots et al. (2002).

The type area for the Mount McCleary Formation and the English Creek Limestone is well exposed on the northeast-facing cliff section beside a tarn 3 km south of the headwaters of English Creek and 5 km north of Mount McCleary in the Englishman

Range, southern Yukon (W66°04'26", N60°21'4"). The cliff exposes the entire

stratigraphy with the English Creek Limestone at the base overlain by the Mount

McCleary Formation and its four members. Rocks near the base are thermally

metamorphosed by the Mid-Cretaceous granite immediately to the east. These units have

not been previously named, but are shown as part of the Mv and Ml units respectively on

the map by Gordey and Stevens (1994).

4.13 References

Abbott, J.G., 1981. Geology of the Seagull tin district, Yukon Geology and Exploration.
Indian and Northern Affairs Canada, pp. 32-44.

Bull, S.W. and Cas, R.A.F., 1991. Depositional controls and characteristics of
subaqueous bedded volcaniclastics of the Lower Devonian Snowy River
Volcanics. Sedimentary Geology, 74(1-4): 189-215.

Colpron, M., 2001. Geochemical characterization of Carboniferous volcanic successions
from Yukon-Tanana terrane, Glenlyon map area (105L), central Yukon. In: D.S.
Emond and L.H. Weston (Editors), Yukon Exploration and Geology 2000.
Exploration and Geological Services Division, Yukon Region, Indian and
Northern Affairs Canada, pp. 111-136.

Colpron, M. and Group, Y.-T.W., 2001. Ancient Pacific Margin - An update on
stratigraphic comparison of potential volcanogenic massive sulphide hosting
successions of Yukon-Tanana terrane, northern British Columbia and Yukon. In:
D.S. Emond and L.H. Weston (Editors), Yukon Exploration and Geology.
Exploration and Geological Services Division, Yukon Region, Indian and
Northern Affairs Canada, pp. 97-110.

Coney, P.J., Jones, D.L. and Monger, J.W.H., 1980. Cordilleran suspect terranes. Nature,
288: 329-333.

Cousens, B., 1996. Magmatic evolution of Quaternary mafic magmas at Long Valley
Caldera and the Devils Postpile, California: effects of crustal contamination on
lithopheric mantl-derived magmas. Journal of Geophysical Research, 101: 27673-
27689.

Cousens, B.L., 2000. Geochemistry of the Archean Kam Group, Yellowknife greenstone belt, Slave Province, Canada. Journal of Geology, 108(2): 181-197.

Creaser, R.A., Erdmer, P., Stevens, R.A. and Grant, S.L., 1997. Tectonic affinity of Nisutlin and Anvil assemblage strata from the Teslin tectonic zone, northern Canadian Cordillera; constraints from neodymium isotope and geochemical evidence. Tectonics, 16(1): 107-121.

Creaser, R.A. and Harms, T.A., 1998. Lithological, geochemical and isotopic characterization of clastic units in the Klinkit and Swift River assemblages, northern British Columbia. In: F. Cook and P. Erdmer (Editors), Lithoprobe Report, Report: 64. University of British Columbia, Lithoprobe Secretariat for the Canadian Lithoprobe Program, pp. 239-242.

Ferri, F., 1997. Nina Creek Group and Lay Range Assemblage, north-central British Columbia; remnants of late Paleozoic oceanic and arc terranes. Canadian Journal of Earth Sciences = Journal Canadien des Sciences de la Terre, 34(6): 854-874.

Gabrielse, H., 1969. Geology of Jennings River map area, British Columbia (104/O), Paper 68-55. Geological Survey of Canada.

Gabrielse, H., 1991. Late Paleozoic and Mesozoic terrane interactions in north-central British Columbia. Canadian Journal of Earth Sciences = Journal Canadien des Sciences de la Terre, 28(6): 947-957.

Gabrielse, H., Monger, J.W.H., Wheeler, J.O. and Yorath, C.J., 1991. Tectonic framework; Part A, Morphogeological belts, tectonic assemblages and terranes. In: H. Gabrielse and C.J. Yorath (Editors), Geology of the Cordilleran Orogen in Canada. Geological Survey of Canada, Geology of Canada, (also Geological Society of America, v. G-2), pp. 677-705.

Gabrielse, H. and Yorath, C.J., 1991. Tectonic synthesis. In: H.G.a.C.J. Yorath (Editor), Geology of the Cordilleran Orogen in Canada. Geological Survey of Canada, Geology of Canada, (also Geological Society of America, v. G-2), pp. 677-705.

Gamble, J.A., Wright, I.C., Woodhead, J.D. and McCulloch, M.T., 1995. Arc and back-arc geochemistry in the southern Kermadec arc - Ngatoro Basin and offshore Taupo volcanic zone, SW Pacific. In: J.L. Smellie (Editor), Volcanism associated

with extension and consuming plate margins. Geological Society, Special Publication No. 81, pp. 193-212.

Gordey, S.P., 1992. Geological fieldwork in Teslin map area, southern Yukon Territory. 92-01A, Geological Survey of Canada, Ottawa.

Gordey, S.P. and Stevens, R.A., 1994. Tectonic framework of the Teslin region, southern Yukon Territory. 1994-A, Geological Survey of Canada, Ottawa.

Harms, T.A. and Creaser, R.A., 1997. Constraints on the geologic evolution and tectonic affinity of the Klinkit assemblage. In: F.A. Cook and P. Erdmer (Editors), Lithoprobe Report, vol.56. University of British Columbia, Lithoprobe Secretariat for the Canadian Lithoprobe Program, pp. 211-213.

Harms, T.A. and Stevens, R.A., 1995. Investigations in the Dorsey terrane; Part 2, Lithologies and structure of (?)Paleozoic stratified rocks in the Stikine Ranges, northern British Columbia. 1995-A, Geological Survey of Canada, Ottawa.

Harms, T.A. and Stevens, R.A., 1996a. Assemblage analysis of the Dorsey Terrane. In: F.A. Cook (Editor), Lithoprobe Report, Report: 50, vol.50. University of British Columbia, Lithoprobe Secretariat for the Canadian Lithoprobe Program, pp. 199-201.

Harms, T.A. and Stevens, R.A., 1996b. A working hypothesis for the tectonostratigraphic affinity of the Stikine Ranges and a portion of the Dorsey Terrane. In: F.A. Cook (Editor), Lithoprobe Report, Report: 50, vol.50. University of British Columbia, Lithoprobe Secretariat for the Canadian Lithoprobe Program, pp. 93-95.

Hawkesworth, C.J. et al., 1979. $^{143}Nd/^{144}Nd$, $^{87}Sr/^{86}Sr$ and incompatible element variations in calc-alkaline andesites and plateau lavas from South America. Earth and Planetary Science Letters, 42: 45-57.

McPhie, J., Doyle, M. and Allen, R., 1993. Volcanic textures: a huide to interpretation of textures in volcanic rocks. Centre for Ore Deposit and Exploration Studies, University of Tasmania, Tasmania, 198 pp.

Mihalynuk, M.G., Nelson, J., Friedman, R.M. and Smyth, W.R., 1998. Regional geology and mineralization of the Big Salmon Complex (104N NE and 1040 NW). 1998-1, British Columbia Geological Division, Victoria.

Mihalynuk, M.G. et al., 2000. Ancient Pacific Margin; Part III, Regional geology and mineralization of the Big Salmon Complex (NTS 104N/9E,16 & 104O 12,13,14W). 2000-1, British Columbia Geological Survey in cooperation with various British Columbia Ministries, Victoria.

Monger, J.W.H., 1999. Review of the geology and tectonics of the Canadian Cordillera. Short course notes, Sydney, 72 pp.

Monger, J.W.H. and Irving, E., 1980. Northward displacement of north-central British Columbia. Nature, 285: 289-294.

Monger, J.W.H., Price, R.A. and Tempelman-Kluit, D.J., 1982. Tectonic accretion and the origin of the two major metamorphic and plutonic welts in the Canadian Cordillera. Geology, 10(2): 70-75.

Monger, J.W.H. et al., 1991. Part B. Cordilleran terranes; Upper Devonian to Middle Jurassic assemblages. In: H. Gabrielse and C.J. Yorath (Editors), Geology of the Cordilleran Orogen in Canada. Geoligical Survey Canada, Ottawa, pp. 281-327.

Mortensen, J.K., 1992. Pre-mid-Mesozoic tectonic evolution of the Yukon-Tanana Terrane, Yukon and Alaska. Tectonics, 11(4): 836-853.

Nelson, J., 1997. Last seen heading south; extensions of the Yukon-Tanana Terrane into northern British Columbia. 1997-1, British Columbia Geological Division, Victoria.

Nelson, J., 2001. Geology of north-central Jennings River area (104O/14E, 15). 2001-1, Province of British Columbia, Ministry of Energy.

Nelson, J.L., 1993. The Sylvester Allochthon; upper Paleozoic marginal-basin and island-arc terranes in northern British Columbia. Canadian Journal of Earth Sciences = Journal Canadien des Sciences de la Terre, 30(3): 631-643.

Nelson, J.L., 2000. Ancient Pacific Margin; Part VI, Still heading south; potential VMS hosts in the eastern Dorsey Terrane, Jennings River (104O/1; 7, 8, 9, 10). 2000-1, British Columbia Geological Survey in cooperation with various British Columbia Ministries, Victoria.

Nelson, J.L. and Friedman, R.M., 2004. Superimposed Quesnel (late Paleozoic-Jurassic) and Yukon–Tanana (Devonian-Mississippian) arc assemblages, Cassiar

Mountains, northern British Columbia: field, U-Pb, and igneous petrochemical evidence. Canadian Journal of Earth Sciences, 41: 1201-1235.

Nelson, J.L. et al., 2000. Ancient Pacific Margin; Part II, A preliminary comparison of potential VMS-hosting successions of the Yukon Tanana Terrane, from Finlayson Lake District to northern British Columbia. 2000-1, British Columbia Geological Survey in cooperation with various British Columbia Ministries, Victoria.

Pearce, J.A., 1983. Role of sub-continental lithopheric magma genesis at active continental margins. In: C.J. Hawkesworth and M.J. Norry (Editors), Continental flood basalts and mantle xenoliths. Shiva Publishing Ltd., Nantwich, pp. 230-249.

Pearce, J.A. and Cann, J.R., 1973. Tectonic setting of basic volcanic rocks determining using trace element analyses. Earth and Planetary Science Letters, 19: 290-300.

Piercey, S.J., Mortensen, J.K. and Creaser, R.A., 2003. Neodymium isotope geochemistry of felsic volcanic and intrusive rocks from the Yukon-Tanana Terrane in the Finlayson Lake region, Yukon, Canada. Canadian Journal of Earth Sciences = Revue Canadienne des Sciences de la Terre, 40(1): 77-97.

Piercey, S.J., Mortensen, J.K., Murphy, D.C., Paradis, S. and Creaser, R.A., 2002. Geochemistry and tectonic significance of alkalic mafic magmatism in the Yukon-Tanana Terrane, Finlayson Lake region, Yukon. Canadian Journal of Earth Sciences = Revue Canadienne des Sciences de la Terre, 39(12): 1729-1744.

Piercey, S.J., Murphy, D.C., Mortensen, J.K. and Paradis, S., 2001. Boninitic magmatism in a continental margin setting, Yukon-Tanana Terrane, southeastern Yukon, Canada. Geology, 29(8): 731-734.

Poole, W.H., 1956. Geology of the Cassiar Mountains in the vicinity of the Yukon-British Columbia boundary. unpublished Ph.D. Thesis, Princeton University.

Poole, W.H., Roddick, J.A. and Green, L.H., 1961. Geology of Wolf Lake, Yukon Territory. Geological Survey of Canada, Map 10-1960.

Roots, C.F., Harms, T.A., Simard, R.L., Orchard, M.J. and Heaman, L., 2002. Constraints on the age of the Klinkit assemblage east of Teslin Lake, northern British Columbia. 2002-A7, Geological Survey of Canada.

Schermer, E.R., Howell, D.G. and Jones, D.L., 1984. The origin of allochthonous terranes. Annual Review of Earth and Planetary Sciences, 12: 107-131.

Simard, R.L., Roots, C.F. and Dostal, J., 2001. Tectonic implications of the geologic setting if the Klinkit assemblage (Yukon-Tanana Terrane), northern British Columbia. Geological Association of Canada - Mineralogical Association of Canada Abstract volume, 26: 138.

Simard, R.L., Roots, C.F. and Dostal, J., 2002. The pre-accretion history of the northern Canadian Cordillera: The Klinkit Formation, an example from northern British Columbia and southern Yukon. Geological Association of Canada - Mineralogical Association of Canada, Abstracts volume: 109.

Smith, A.D., Lambert, R.S.J., Brandon, A.D. and Goles, G.G., 1995. Nd, Sr, and Pb isotopic evidence for contrasting origins of late Paleozoic volcanic rocks from the Slide Mountain and Cache Creek terranes, south-central British Columbia. Canadian Journal of Earth Sciences = Journal Canadien des Sciences de la Terre, 32(4): 447-459.

Stevens, R.A., 1996. Dorsey assemblage; pre-Mid-Permian high temperature and pressure metamorphic rocks in the Dorsey Range, southern Yukon Territory, Lithoprobe Report, Report: 50, vol.50. University of British Columbia, Lithoprobe Secretariat for the Canadian Lithoprobe Program, pp. 70-75.

Stevens, R.A. and Harms, T.A., 1995. Investigations in the Dorsey terrane; Part 1, Stratigraphy, structure, and metamorphism in the Dorsey Range, southern Yukon Territory and northern British Columbia. 1995-A, Geological Survey of Canada, Ottawa.

Stevens, R.A. and Harms, T.A., 1996. Geology in the vicinity of the Dorsey Range, southern Yukon Territory and northern British Columbia; scale 1:50,000, Lithoprobe Report, Report: 50, vol.50. University of British Columbia, Lithoprobe Secretariat for the Canadian Lithoprobe Program, pp. 222-225.

Stevens, R.A. and Harms, T.A., 2000. Bedrock geology of the Dorsey Range, south Yukon Territory and Northern British Columbia, Geological Survey of Canada; Open File 3926, Calgary.

Sun, S.S., 1982. Chemical composition and origin of the Earth's primitive mantle. Geochimica et Cosmochimica Acta, 46: 176-192.

Sun, S.S. and McDonough, W.F., 1989. Chemical and isotopic systematics of oceanic basalts; implications for mantle composition and processes. Geological Society Special Publications, 42: 313-345.

Taylor, S.R. and McLennan, S.M., 1985. The continental crust; its composition and evolution; an examination of the geochemical record preserved in sedimentary rocks. Geoscience texts. Blackwell Sci. Publ., Oxford, United Kingdom (GBR), 312 pp.

Tempelman-Kluit, D., 1979. Transported cataclasite, ophiolite and granodiorite in Yukon: Evidence of arc-continent collision. Geolgicla Survey of Canada, Paper 79-14.

Theriault, R.J. and Ross, G.M., 1991. Nd isotopic evidence for crustal recycling in the ca. 2.0 Ga subsurface of Western Canada, Canadian Journal of Earth Sciences = Journal Canadien des Sciences de la Terre. National Research Council of Canada, Ottawa, pp. 1140-1147.

Wheeler, J.O., Brookfiels, A.J., Gabrielse, H., Monger, J.W.H., tipper, H.W., and Woodsworth, G.J., 1991. Terrane map of the Canadian Cordillera, Geological Survey of Canada.

White, R.S., Mackenzie, D. and O'Nions, R.K., 1992. Oceanic crustal thickness from seismic measurement and REE inversions. Journal of Geophysical Research, 97: 19683-19715.

Wilson, M., 1989. Igneous Petrogenesis, a glodal tectonic approach. Chapman & Hall, London, 466 pp.

Winchester, J.A. and Floyd, P.A., 1977. Geochemical discrimination of different magma series and their differentiation products using immobile elements. Chemical Geology, 20(4): 325-343.

Young, G.M., 2002. Geochemical investigation of a Neoproterozoic glacial unit; the Mineral Fork Formation in the Wasatch Range, Utah. Geological Society of America Bulletin, 114(4): 387-399.

Chapter 5

Late Paleozoic evolution of the western margin of Laurentia:
a global tectonic model

Note from the author: in contrast to the three previous chapters that were based on detailed field observations, mapping, stratigraphic analyses, geochemical and isotopic analyses, and physical volcanology of specific volcanic sequences in the northern Canadian Cordillera, what follows is an attempt, mainly based on a literature review, to integrate the data with published speculation about the late Paleozoic tectonic evolution of the west coast of Laurentia over ca. 400 Ma. It is partially speculative.

5.1 Introduction

Throughout the late Paleozoic the west margin of Laurentia underwent many pulses of extension and compression. Recent work by Colpron et al. (in press-a; in press-b), Nelson and Friedman (2004), Nelson et al. (in press), Simard et al. (Chapters 2 and 3; 2003), Piercey et al. (2003; 2002; 2004; 2001; in press), Ferri (1995) and others in the northern Canadian Cordillera has highlighted complex and rapidly evolving pericratonic arc/back-arc systems along the Late Paleozoic west margin of Laurentia which resulted from these tectonic pulses.

However, these Late Paleozoic tectonic disruptions, which include continental arc magmatism, back-arc extension, pericratonic island-arc/backarc formation, as well as opening of full size oceanic basins, are not accounted for in recent paleogeographic reconstructions for that period (e.g. Condie and Sloan, 1998; Lawver et al., 2002; Scotese, 2001).

This chapter presents evidence that the late Paleozoic tectonic activity along the western margin of Laurentia were driven by major oblique continent-continent collisions on the

other margins of the continent, first in Late Silurian-Early Devonian time then in Carboniferous time. These collisions affected the translation and rotation of Laurentia, forcing plate boundary reorganization along its western margin. The formation and tectonic evolution of the pericratonic systems along the west coast was most likely controlled by these collisions.

5.2 Laurentia tectonic evolution

5.2.1 Rodinia Break-up

The break-up of the supercontinent Rodinia in Late Proterozoic to Early Cambrian time has shaped the margins of Laurentia (Fig. 5-1; Hoffman, 1991); first to the west in the Neoproterozoic with the opening of the Panthalassic ocean (Fig. 5-1A), then to the east in the Early Cambrian with the opening of the Iapetus ocean (Fig. 5-1B). These major rifting events left behind irregular margins, characterized by promontories and embayments, like those on the modern margins of the Atlantic Ocean, which became the sites of multiple "collisions" in Paleozoic time.

These major rifting events, most likely resulting from the presence of mantle plumes beneath Rodinia in Meso- to Neoproterozoic time (Condie, 2003), fractured and weakened the crust of Laurentia (Kluth and Coney, 1981); major northwest-trending and north-trending extensional structures observed today in southwest United States reflect extension during the break-up of Rodinia in Proterozoic time (Fig. 5-1B; Karlstrom et al., 2000). These major faults were subsequently tectonically inverted during the formation of the Ancestral Rocky Mountains and the Laramide contraction and reactivated during Tertiary extension (see section below for details; Timmons et al., 2001).

Rifting on both sides of the future Laurentian continent is recorded in thick intracratonic rift basin sequences (e.g. Grand Canyon Supergroup, SW United States; Ocoee Supergroup, SE Unites States; Windemere Group, NW Canada; Gabrielse and Campbell,
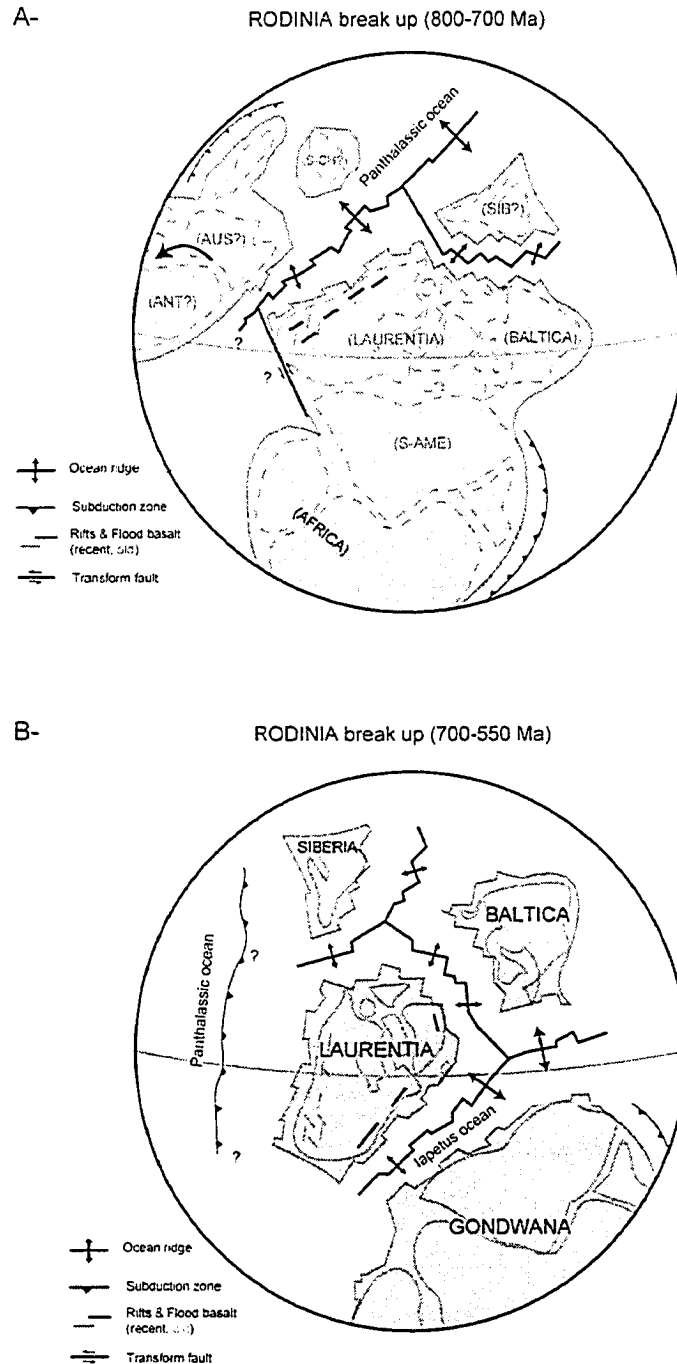
Figure 5-1 – Schematic reconstruction of Rodinia break-up. **A)** 800-700 Ma, first major rifting event of the supercontinent Rodinia with the opening of the Panthalassic Ocean on the west side of the future Laurentia craton (simplified from Condie, 2003). **B)** 700-550 Ma, final rifting of the supercontinent Rodinia with the opening of the Iapetus ocean on the east side of the future Laurentia craton (simplified from Condie, 2003). These Rodinia reconstructions are tentatively based on the AUSWUS model (Australia placed near southwestern Laurentia; Hoffman, 1991).

1991; Timmons et al., 2001; Tull and Holm, 2005), and is followed by passive margin sedimentation starting in Middle Cambrian time.

5.2.2 Closure of Iapetus Ocean/ Opening of the Rheic Ocean

By Late Cambrian time, the Iapetus Ocean was bordered by two or more subduction zones and began to close (e.g. Nance et al., 2002; Roberts, 2003). The Avalonia continental block rifted away from the west Gondwanian margin, opening the Rheic Ocean behind it (Fig. 5-2; Nance et al., 2002, and references therein). In the meantime, passive margin sedimentation was recorded all around Laurentia. These passive margins, at least on the west coast of Laurentia, underwent episodic extension and associated subsidence throughout the lower Paleozoic as recorded by the alkaline and ultrapotassic volcanism found intermittently within these sedimentary sequences (e.g. Selwin basin; Goodfellow et al., 1995). The southern margin of Laurentia from the Cambrian to the
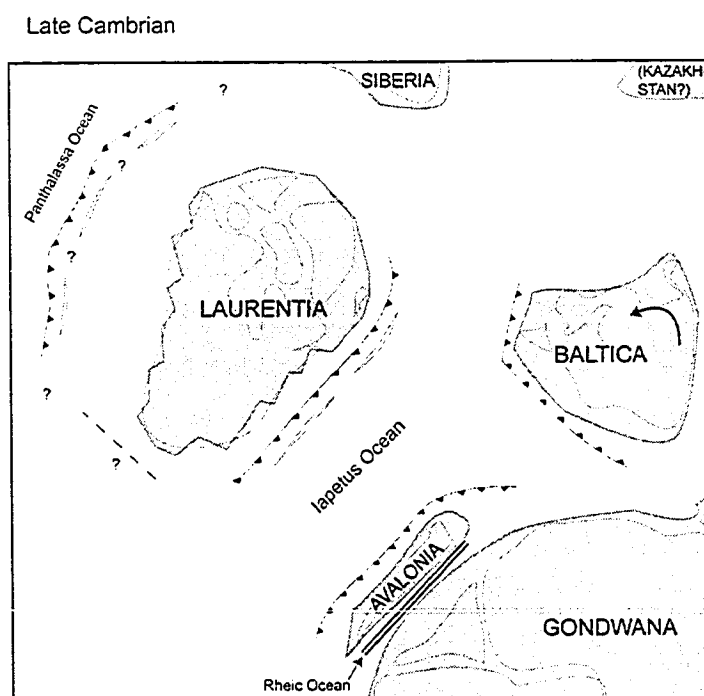
Late Cambrian

Figure 5-2 – Late Cambrian schematic plate reconstruction (simplified from Roberts, 2003; Torsvik and Rehnstrom, 2003). Iapetus Ocean is beginning to close, and the Avalonia continental block has rifted away from Gondwana, opening the Rheic Ocean. Passive margin sedimentation is recorded all around Laurentia at that time. Thick single-headed arrows indicate general plate motion directions relative to Laurentia but are not constrained.

120

Permian is of uncertain nature, either an east-dipping subduction zone or a sinistral

transform fault (dashed-line, Figs. 5-2 to 5-8); at present there are not enough data to

indicate which interpretation (or combination of them) might be correct (Burchfiel et al.,

1992).

By Late Ordovician time, the eastern margin of Laurentia was undergoing collision with

diverse arc complexes (Fig. 5-3; Taconic Orogeny of the Appalachian in Canada and

eastern United States, Hatcher, 1989; Taconic event of the Caledonides Orogeny in

Greenland, Roberts, 2003). To the east Avalonia had collided with Baltica (Grampian

Orogeny; Torsvik and Rehnstrom, 2003), inducing a northeastward movement to Baltica.

In the north, Siberia was slowly moving toward Laurentia, initiating the Innuitian

Orogeny, the collision of the Perya and other microcontinents with the northern passive
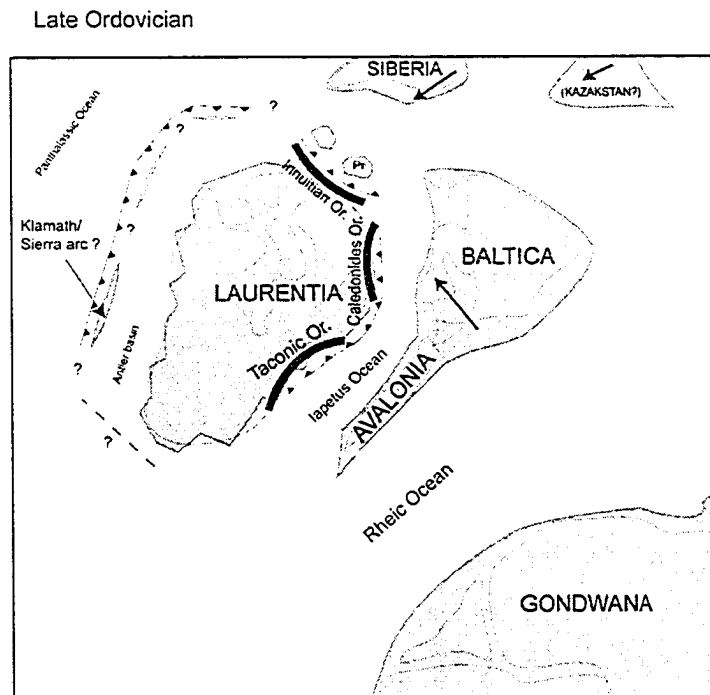
Late Ordovician

Figure 5-3 – Late Ordovician schematic plate reconstruction (simplified from Lawver et al., 2002; Roberts, 2003; Trettin, 1991). The east margin of Laurentia is undergoing collision with arc complexes (Taconic and Caledonides orogenies). The north margin of Laurentia was starting to be deformed by the collisions of microcontinental blocks (Pr=Perya); the Innuitian Orogeny begins. The west margin of Laurentia records passive margin sedimentation, although arc volcanics are present some distance offshore in the southwest (Klamath/Sierra arc?). Thick single-headed arrows indicate general plate motion directions relative to Laurentia but are not constrained.

121

margin of Laurentia (also known as M'Clintock Orogeny; Embry, 1991; Lawver et al., 2002). In the meantime, the western margin of Laurentia recorded passive margin sedimentation with episodic extensional events (Goodfellow et al., 1995), although arc volcanics are known to be present some distance offshore to the southwest (Klamath/Sierra arc?; Miller et al., 1992; Poole et al., 1992), and seamount volcanics are present in the Antler basin, southwest Laurentia (Watkins and Browne, 1989).

In Early Silurian the Iapetus ocean closed with the highly oblique collision of Avalonia with the eastern margin of Laurentia shortly followed by Baltica in mid-Silurian time (Fig. 5-4; Salinian/Acadian Orogeny of the Appalachian in Canada and eastern United States, Hatcher, 1989; van Staal et al., 1998; Castonguay and Tremblay, 2003; Scandian event of the Caledonides Orogeny in Greenland, Roberts, 2003). Evidence of
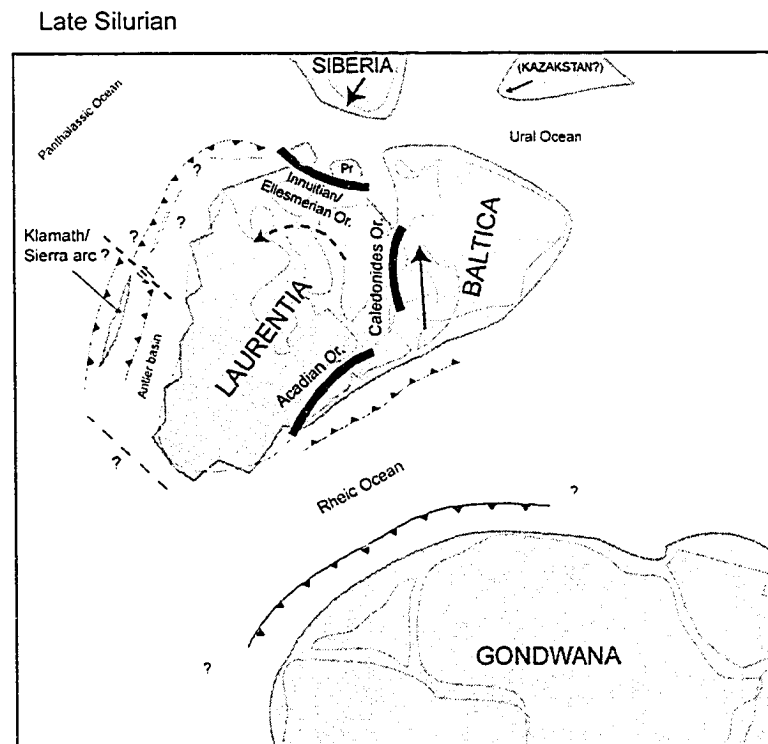
Late Silurian

Figure 5-4 – Late Silurian schematic plate reconstruction (simplified from Burchfiel et al., 1992; Lawver et al., 2002; Roberts, 2003). Baltica and Avalonia collided in Early to Mid-Silurian with the eastern margin of Laurentia at very high angle (Acadian and Caledonide orogenies). This oblique collision finalized the accretion of the microcontinental blocks (Pr=Perya) to the northern margin of Laurentia (Innuitian /Ellesmerian Orogeny). In Late Silurian, the west margin of Laurentia is still recording passive margin sedimentation, although the Antler marginal basin is beginning to close when the new west-dipping subduction zone started moving toward its foreland (Burchfiel et al., 1992). The oblique collision of Baltica and Avalonia with Laurentia most likely induced an anticlockwise rotation of the Laurentia craton, leading to disruption of the subduction system on the west coast. Thick single-headed arrows indicate general plate motion directions relative to Laurentia but are not constrained.

diachroneity is observed laterally and transversely throughout this orogeny reflecting oblique collisions between arcs, plate promontories or microcontinental blocks (Roberts, 2003). The final accretion of Perya and other microcontinental blocks at the northern margin of Laurentia was achieved in Late Silurian time by sinistral transpression accompanying the oblique collision of Baltica (Innuitian/Ellesmerian Orogeny; Lawver et al., 2002).

By Late Silurian, most of the west margin of Laurentia was still recording passive margin sedimentation with intermittent extension pulses (Goodfellow et al., 1995; Poole et al., 1992). However, the marginal basin between the offshore Klamath/Sierra arc system and the western margin of Laurentia (Antler basin, Fig. 5-4), was beginning to close as a new west-dipping subduction zone behind Klamath/Sierra arc began to move toward its foreland, eventually opening behind it the Havallah basin (Burchfiel et al., 1992; Gehrels et al., 2000).

5.2.3 Closure of Rheic Ocean / Opening of Slide Mountain Ocean

By Late Devonian time the east and north coasts of Laurentia were still undergoing the Acadian/Caledonides/Ellesmere Orogenies. The west dipping subduction zone along Avalonia, that obducted part of the continental margin in Late Silurian time (e.g. Meguma Group sediments, Nova Scotia; Mawer and White, 1987), induced major calc-alkaline magmatism all along the eastern margin (e.g. Late Devonian mafic intrusions and South Mountain batholith of the Meguma Zone, Nova Scotia; Nance et al., 2002; Tate and Clarke, 1995).

In the meantime in Late Devonian, the west coast of Laurentia was undergoing the change from a passive to an active margin. The Antler basin closed, driven by west-dipping subduction roll-back, thrusting part of the basin, the Robert Mountains Allochthon, onto Laurentia (Antler Orogeny; Fig. 5-5; Burchfiel et al., 1992). This roll-back movement of the subduction zone closing the Antler basin created extension in the overriding plate, and led to the opening of the Havallah basin (Burchfiel et al., 1992).

123
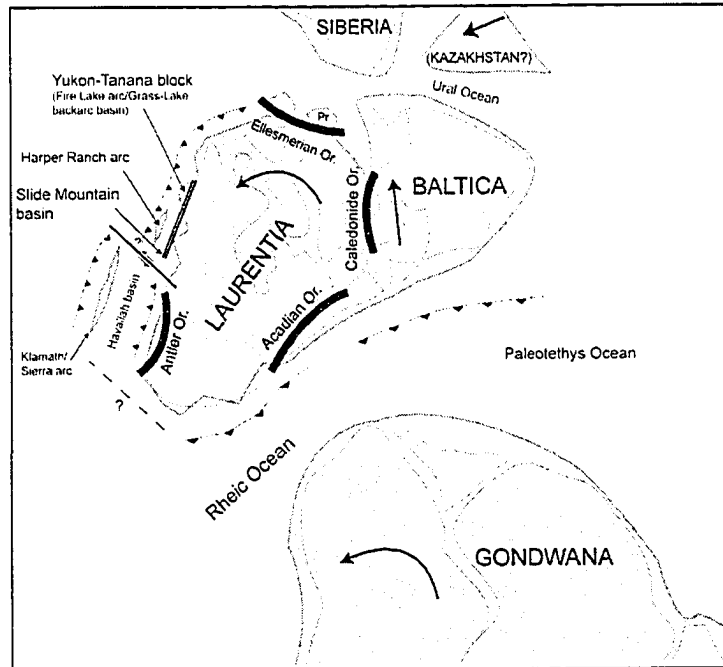
Late Devonian

Figure 5-5 – Late Devonian schematic plate reconstruction (adapted from Burchfiel et al., 1992; Gabrielse and Yorath, 1991; Roberts, 2003). The Acadian/Caledonides/ Ellesmerian Orogeny is still going strong on the east-northeast-north side of Laurentian, and the Rheic Ocean is beginning to close. Meanwhile, the west coast of Laurentia is undergoing major disruption with the closure of the Antler basin (Antler Orogeny) in the southwest, the opening of the Slide Mountain marginal basin to the west, and arc volcanism with associated backarc extension to the north. This extension event north of the Antler Orogeny will eventually lead to the opening of a full-size long-live oceanic basin, the Slide Mountain Ocean. Single-headed arrows indicate general plate motion directions relative to Laurentia but are not constrained.

The Klamath-Sierra arc system experienced intense volcanism starting in Late Devonian, which waxed and waned throughout the late Paleozoic (Burchfiel et al., 1992). The Antler Orogeny and the offshore Klamath-Sierra arc volcanism were restricted to southwest Laurentia.

During that same period, in west-northwest Laurentia (Fig. 5-5) extension began with the onset of the Slide Mountain basin/ocean to the south, and the opening of back-arc/marginal basins to the north (e.g. Grass Lakes back-arc, Swift River basin; Piercey et al., 2003; Chap. 4; Simard et al., 2003). Continental arc activity associated with back-arc extension was recorded in the Yukon-Tanana block in Late Devonian-Early Mississippian time (Fig. 5-5, Fire Lake arc; Piercey et al., 2003; Piercey et al., 2004). Further south, the Harper Ranch arc was also active at this time, but was already

separated from Laurentia by the Slide Mountain basin (Fig. 5-5; Monger, 1999; Monger et al., 1991); the Harper Ranch arc is interpreted as the basement of the future Mesozoic Quesnel arc (e.g. Monger et al., 1991). This extension eventually led to the opening of a full-size, long-lived oceanic basin, the Slide Mountain Ocean.

By mid-Mississippian time, the second major oblique continent-continent collision affecting the east coast of Laurentia was well underway with the final closing of the Rheic Ocean and the collision of Africa with east-southeast Laurentia (Fig. 5-6). This collision was dextral and laterally diachronous from northeast to southwest, from the
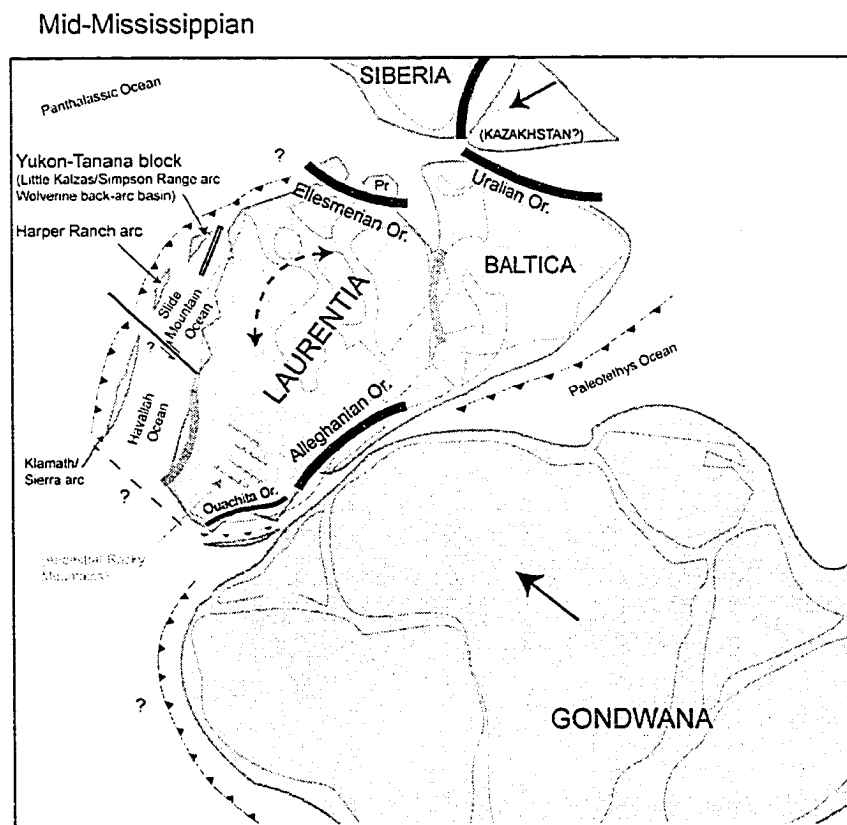
Mid-Mississippian

Figure 5-6 – Mid-Mississippian schematic plate reconstruction (modified and simplified from Brown et al., 2002; Burchfiel et al., 1992; Scotese, 2001; Torsvik and Cocks, 2004). The continent-continent collision between Laurentia and Gondwana started with the final closure of the Rheic Ocean (Alleghanian and Ouachita Orogenies). To the north, the collision of the Kazakhstan block with Siberia and Baltica might have caused the final stage of the Ellesmerian Orogeny. On the west coast of Laurentia, extension dominated with widening of the Havallah and Slide Mountain oceans and equivalent marginal basins to the north, and arc volcanism/magmatism to the west. Single-headed arrows indicate general plate motion directions but are not constrained.

Alleghanian Orogeny in eastern Canada and United States (Early Carboniferous; Hatcher, 1989) to the Ouachita Orogeny in the southern United States (late Mississippian-early Pennsylvanian; Thomas, 1989). This collision drove not only deformation along the eastern and southern coast of the Laurentian margins but also intraplate mountain building as far as 2500 km inboard, the Ancestral Rocky Mountains (Dickerson, 2003; Dickinson and Lawton, 2001; 2003; and references therein). In the north, the Kazakhstan block started to collide with Baltica and Siberia, closing the Uralian Ocean (Fig. 5-6; Uralian Orogeny; Brown et al., 2002; Lawver et al., 2002); far-field effects of this collision could have caused the Ellesmerian Orogeny on the northern Laurentian margin at this time (Lawver et al., 2002).

On the west coast, the Havallah and Slide Mountain oceans and equivalent marginal basins to the north widened (Fig. 5-6; Wolverine back-arc; Piercey et al., 2004), and arc magmatism was found all along (Fig. 5-6, Klamath/Sierra-Lay Range-Little Kalzas/Simpson Range arcs; Colpron et al., in press-a; Piercey et al., 2004).

By Pennsylvanian time (Fig. 5-7), the Alleghanian-Ouchita Orogeny was at its climax and generated important intraplate deformation once full collisional plate coupling had been achieved along the continental margin (Ziegler et al., 1998). The Ancestral Rocky Mountains basins and uplifts spread from north-central Mexico to southern British Columbia (Dickerson, 2003), reactivating Proterozoic rift structures (Fig. 5-1A; Karlstrom et al., 2000; Timmons et al., 2001). A sinistral transform fault was active at the southern margin of Laurentia and truncated part of the Antler Orogeny and early Paleozoic passive margin rocks (Burchfiel et al., 1992; Dickinson and Lawton, 2001; Trexler et al., 2004). In the north the collision between Siberia, Kazakhstan and Baltica was complete and the supercontinent Pangea was born. Large-scale rotations of Laurentia may have been induced by this orogenic episode (Dickerson, 2003).

Whereas most of Laurentia experienced compression/collision, its west margin was still undergoing extension. The western margin of Laurentia was now completely flanked by

Pennsylvanian

Figure 5-7 – Pennsylvanian schematic plate reconstruction (modified and simplified from Gabrielse and Yorath, 1991; Scotese, 2001). The Alleghenian-Ouachita Orogeny is at its climax which leads to major intraplate deformation throughout southern Laurentia, the formation of the Ancestral Rocky Mountains. To the north the final closure of the Uralian Ocean finalized the formation of the supercontinent Pangea. On the west coast of Laurentia extension is still going on with widening of the Slide Mountain Ocean, and even intra-arc rifting within the offshore arc system (Little Salmon arc, Yukon-Tanana block; Chapters 2 and 3). The southern margin of Laurentia is experiencing truncation through sinistral transform faulting. Thick single-headed arrows indicate general plate motion directions relative to Laurentia but are not constrained.

oceanic basins and even the arc systems to the west were showing signs of intra-arc rifting (e.g. Little Salmon arc; Chapters 2 and 3)

5.2.4 Closure of the Slide Mountain Ocean / Opening of the Atlantic Ocean

In Permian time, the tectonic regime of the west margin of Laurentia started changing. Primitive island-arc magmatism was progressively more important offshore and now flanked the entire continent on its west coast (Fig. 5-8; from Sierra-Klamath to Lay Range to Klinkit arc; Dickinson and Lawton, 2003; Ferri et al., 1995; Simard et al., 2003). There was no more truncation of the southern margin; an Andean setting had replaced it, which changed to an island-arc setting northward (Burchfiel et al., 1992). New west-dipping subduction along part of the west side of the oceanic basins retreated

Late Permian
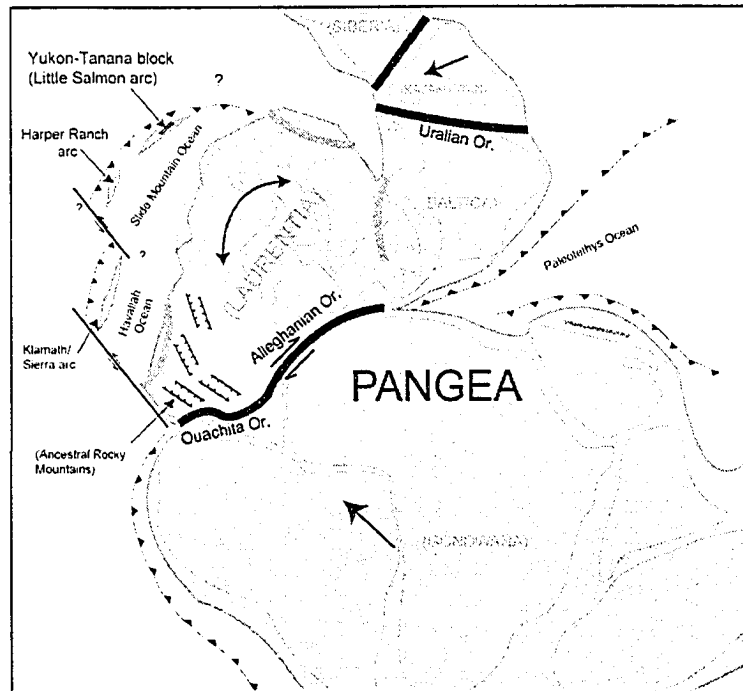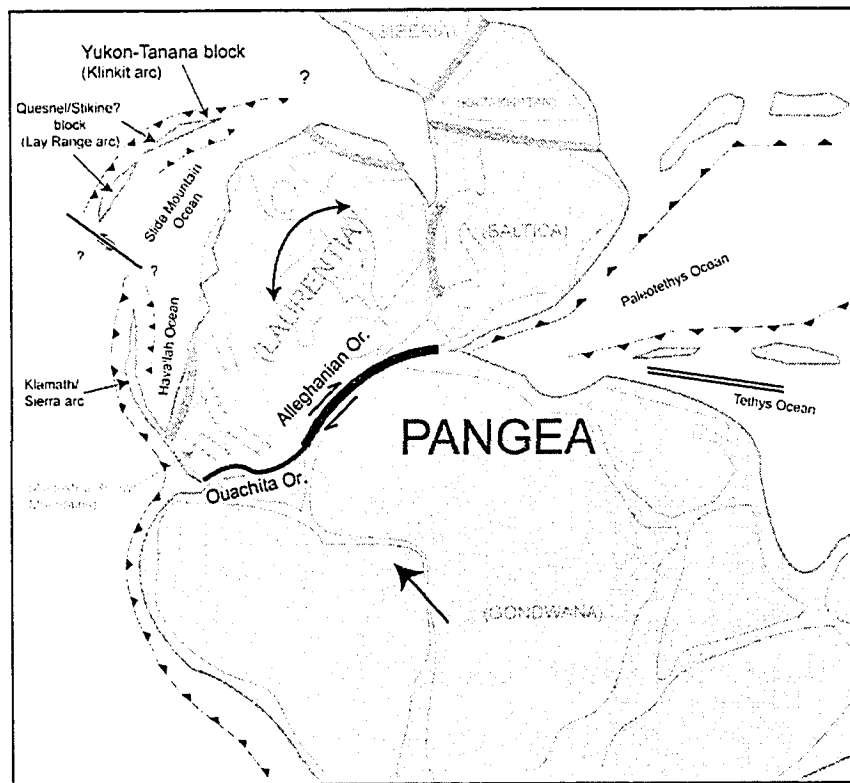

Figure 5-8 – Late Permian schematic plate reconstruction (modified and simplified from Gabrielse and Yorath, 1991; Scotese, 2001). Extension was slowing down on the west coast of Laurentia. The Havallah and Slide Mountain oceanic basins were slowly closing as newly formed west-dipping subduction zones on their western margins started retreating toward the craton. An Andean setting replaced the transform fault margin in southern Laurentia (Burchfiel et al., 1992). Single-headed arrows indicate general plate motion directions but are not constrained.

slowly toward the coast, closing diachronously the Havallah and Slide Mountain oceans (Fig. 5-8; Burchfiel et al., 1992; Tempelman-Kluit, 1979).

In Early Triassic time, the Havallah oceanic basin closed and was thrust in part onto the west margin of Laurentia (Sonora Orogeny; Fig. 5-9; Burchfiel et al., 1992). This roll-back movement of the west-dipping subduction zone closed the Havallah basin, and the Klamath-Sierra arc system eventually collided with the continent (Burchfiel et al., 1992). To the north, the Slide Mountain Ocean was in part closed between the Yukon-Tanana block and Laurentia; arc volcanism had ceased on the Yukon-Tanana block, and continentally-derived sedimentary sequences were overlapping it (Teh Clastic succession;

128
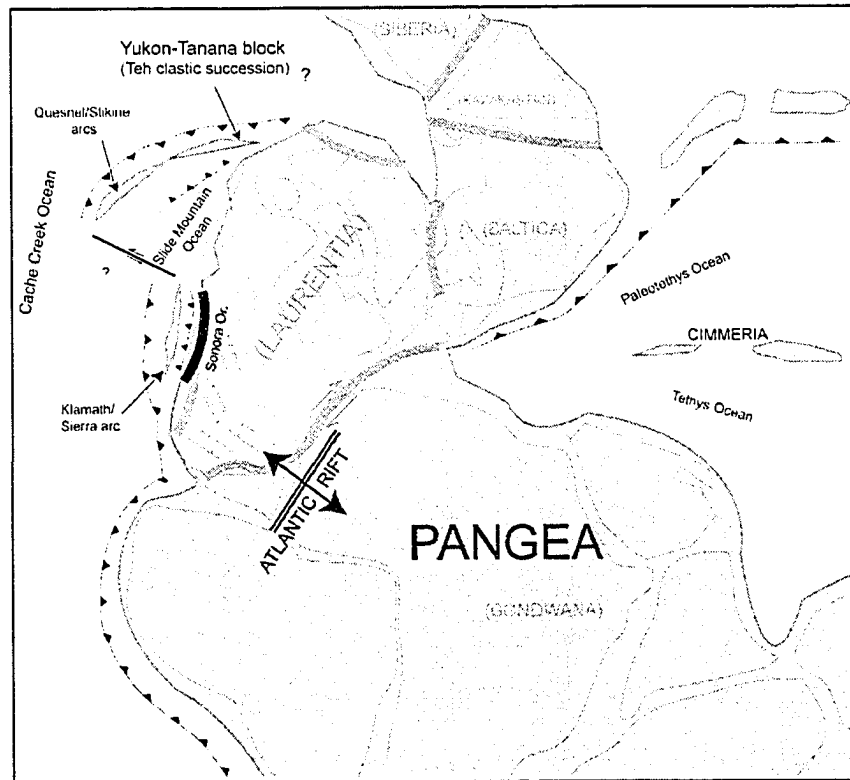
Triassic

Figure 5-9 – Triassic schematic plate reconstruction (modified and simplified from Gabrielse and Yorath, 1991; Scotese, 2001). The Havallah and Slide Mountain oceanic basins are in part closed (Sonora Orogeny, western United States; Teh clastic sequence, northern Canada). The Atlantic Ocean is beginning to open inducing westward movement of the North American continent.

Fig. 5-9; Chap. 4; Colpron and Group, 2001; Creaser and Harms, 1998; Simard et al., 2003).

The closure of the oceanic basins on the west coast of Laurentia accelerated in Late Triassic to Jurassic time with the opening of the central Atlantic Ocean (Fig. 5-9).The newly formed North American continent started moving westward then southwestward (Engebretson, 1982) towards and over the subduction zones (Monger, 1999), accreting the island arcs and oceanic basins to its west coast, marking the beginning of the North American Cordillera Orogeny.

5.3 Tectonic implications for the late Paleozoic west margin of Laurentia

The closure of Iapetus through highly oblique collision of Baltica and Avalonia with Laurentia in Silurian time (Salinian/Acadian/Caledonian Orogeny) was a major continent-continent collision that likely induced an anticlockwise rotation of Laurentia, as well as inducing a west-northwest translation of Laurentia over the Panthallassic plate. The correlation in timing of deformation/collision on the east coast (Salinian/Acadian/Caledonian Orogeny) with the disruption of the subduction system on the west coast is too close in time to be considered coincidental.

I propose that the west-northwest movement of Laurentia over the Panthallassic plate caused the continent to migrate closer to the offshore subduction zone in Late Silurian-Early Devonian time (Figs. 5-4 and 5-5), which, in addition to potential rotation of Laurentia, triggered plate reorganization in mid-Devonian time. The proximity of the subduction zone to the margin of the continent initiated continental arc magmatism and extension on the northwest part of Laurentia (e.g. Fire Lake arc/Grass Lake backarc; Fig. 5-5). In the southwest, plate readjustment seems to have induced subduction roll-back of a newly formed west-dipping subduction zone toward the coast, which closed the Antler basin (Antler Orogeny; Figs. 5-4 and 5-5).

The closure of the Rheic and Uralian oceans to the south, east, and north of Laurentia in Carboniferous time through one or more oblique continent-continent collisions (Figs. 5-6 to 5-8) likely induced new large-scale rotations within Laurentia, inducing more plate boundaries readjustments on its western margin (Fig. 5-7). These readjustments were mostly expressed as extension, such as the rifting of blocks from the continent (e.g. Yukon-Tanana block; Fig. 5-6), and the opening of the Slide Mountain Ocean and other coeval marginal basins all along the western margin of Laurentia.

This extensional tectonic regime dominated the western margin of Laurentia until Late Permian time, when the opening of the Atlantic Ocean put an end to it, by inducing prolonged westward, then southwestward movement, of the newly formed North

American continent over the Pacific plates (Engebretson, 1982). This marked the beginning of the North American Cordilleran Orogeny.

5.4 Conclusion

Throughout Paleozoic time, the west margin of Laurentia seems to have experienced a fairly simple evolution, from rifted to passive margin (Proterozoic to Cambrian time), through a mainly active divergent margin (Late Cambrian to Early Permian time), to a mainly convergent margin (Late Permian to modern time). However, when one looks through the rock record, each of these periods shows evidence for multiple complex tectonic pulses.

These tectonic pulses along the Paleozoic divergent west margin of Laurentia seem to have been driven by oblique continent-continent collisions on the opposite margin of the Laurentia, first in Late Silurian-Early Devonian time, then in Carboniferous time. These collisions produced the translation and rotation of Laurentia, forcing plate boundary reorganization along its west margin. The formation and tectonic evolution of the pericratonic blocks along the west coast, such as the Yukon-Tanana block, was most likely influenced by these collisions.

There are several well-documented modern examples of collided block/continent inducing surrounding plate readjustments, the best known probably being the India/Eurasia continent-continent collision and its complex effects on SE Asia tectonic. Although we do not have a full understanding of the large scale effects of these tectonic events, they play a very important role on the overall tectonic evolution the Earth, and have to be accounted for when trying to unravel the tectonic evolution of any part of the system.

Chapter 6

Conclusion

Recent work in the pericratonic terranes of the northern Canadian Cordillera, especially on the Yukon-Tanana terrane, Yukon and northern British Columbia, has highlighted a complex and dynamic tectonic evolution for the late Paleozoic west margin of Laurentia (e.g. Colpron et al., in press-a; Colpron et al., in press-b; Murphy et al., in press; Piercey et al., 2003; Piercey et al., 2002a; Piercey et al., 2001a; Piercey et al., in press; Roots et al., in press; Simard et al., 2003; Chapters 2, 3, and 4). At the time of major collisions on the eastern, northern and southern margins of the continent (Chap. 5), the western margin was undergoing major extension that led to the development of multiple arcs, back-arc/marginal basins, and oceanic basins.

Like most of the pericratonic terranes of the northern Canadian Cordillera, the Yukon-Tanana terrane is a complex assemblage of mid- to late Paleozoic continental margin, arc and marginal basins, which have, in places, isotopic and provenance ties to Archean and Proterozoic cratonic source regions, comparable to those of sedimentary strata from northwestern North America (Colpron et al., in press-b; Creaser et al., 1997; Gehrels et al., 1991; Mortensen, 1992; Patchett and Gehrels, 1998).

The oldest stratigraphic units of the Yukon-Tanana terrane in Yukon and northern B.C. consist predominantly of quartzite, psammitic, pelitic and calcsilicate schists, marble, and local amphibolite of continental margin affinity (Snowcap Complex in the Glenlyon area, Chapters 2 and 3; Dorsey Complex in northern British Columbia, Chap. 4). The rocks are typically polydeformed and metamorphosed to amphibolite facies, commonly occupy a low structural level in the terrane, and are generally intruded by early Mississippian plutons, in places late Devonian (Colpron et al., in press-b). These basement rocks most likely represent the rifted/thinned margin of Laurentia (e.g. Colpron et al., in press-b; Gehrels et al., 1991; Nelson et al., in press; Patchett and Gehrels, 1998). They are

overlain by Late Devonian to Permian volcano-sedimentary sequences that record the development of pericratonic arc/back-arc/marginal basin system(s) along the western margin of the Laurentia.

The Late Devonian continental arc magmatism of the Grass Lake and Wolverine groups of the Finlayson Lake area, SE Yukon (Fig. 2-1), records the onset of arc activity within the Yukon-Tanana terrane and the development of an ensialic back-arc in this part of the terrane (Piercey et al., in press; Piercey et al., 2001b; Piercey et al., 2002b). These back-arc rocks host some of the most significant massive sulphide deposits of the Yukon-Tanana terrane. This back-arc basin eventually evolved to a marginal basin in Permian time, the Campbell Range basin (Colpron et al., in press-b).

Shortly following this back-arc rifting, new pulses of continental arc magmatism are recorded within the Yukon-Tanana terrane, first in the mid-Mississippian with the Little Kalzas arc, then in the Late Mississippian with the Little Salmon arc, both in the Glenlyon area, central Yukon (Fig. 2-1; Chap. 2; Colpron et al., in press-a; Piercey et al., in press). This continental arc system underwent extension in the Pennsylvanian and led to the development of the Little Salmon rift basins and an alkali basalt seamount formation (Chapters 2-3). These rift basins were the sites of active hydrothermal systems, as revealed by the presence of Mn-rich exhalative chert horizons within the Little Salmon upper succession stratigraphy (Chapters 2 and 3; Colpron et al., in press-a; Peter et al., 2003).

Further south, northern British Columbia and southern Yukon display a similar geological evolution. The Late Devonian to Mississippian Ram Creek and Big Salmon arc magmatism also records continental arc activity (Fig. 4-12, Chap. 4; Piercey et al., in press; Roots et al., in press; Simard et al., 2003). This continental arc wss separated from Laurentia in Pennsylvanian time by a marginal basin, the Swift River basin, a northern equivalent of the Slide Mountain marginal/oceanic basin to the south (Fig. 4-13, Chap. 4; Simard et al., 2003, and references therein), and the Campbell Range basin to the north (Finlayson Lake area; Murphy et al., in press; Piercey et al., in press).

By Permian time, the Campbell Range basin (Finlayson Lake area), Swift River basin (northern British Columbia) and Slide Mountain basin formed a fully developed oceanic basin (Figs. 5-7 and 5-8, Chap. 5). In the meantime, the Klinkit island-arc developed atop the Big Salmon arc system, shedding important turbidite deposits on the western margin of the Swift River basin (Klinkit Group stratigraphy, Fig. 4-13, Chap. 4; Roots et al., in press; Simard et al., 2003). This new pulse of magmatism is not well developed elsewhere in the Yukon-Tanana terrane, but is found in north central British Columbia, in the Permian Lay Range island-arc (Figs. 4-12 and 4-13, Chap. 4; Ferri et al., 1995; Simard et al., 2003). The Lay Range island-arc in the south is interpreted to be the basement of the Mesozoic Quesnel arc, the Harper Ranch subterrane (Figs. 5-7, Chap. 5; Ferri, 1997; Gabrielse and Yorath, 1991).

This Permian belt of volcanism, which in its northern part is part of the Yukon-Tanana terrane and to the south forms the basement of the Quesnel terrane, suggests that the pericratonic Yukon-Tanana terrane may be the northern extension of the basement of the Quesnel terrane (Chap. 4; Simard et al., 2003, and references therein). Therefore, the northern part of the Quesnel terrane may be considered pericratonic and might have been part of the same arc system as the Yukon-Tanana one (Chap. 4; Figs. 5-7 and 5-8, Chap. 5; Simard et al., 2003).

This extensional tectonic regime, with arc/back-arc and marginal/oceanic basin development, dominated the western margin of Laurentia until Late Permian time, when the opening of the Atlantic Ocean most likely put an end to it, inducing prolonged westward then southwest movement of the newly formed North American continent over the Pacific plates (Fig. 5-8, Chap. 5; Engebretson, 1982). By Triassic time, the Yukon-Tanana arcs and basins were close to the North American continent, as suggested by the presence of the continentally-derived Triassic Teh clastic succession unconformably overlying the Klinkit Group, northern British Columbia (Chap. 4; Simard et al., 2003). By Late Triassic the pericratonic systems were accreted to the west coast of North

America, and now form the pericratonic terrane belt of the northern Canadian Cordillera (Fig. 2-1A); it was the beginning of the North American Cordilleran Orogeny.

Whether or not these various late Paleozoic pulses of arc magmatism along the west coast of Laurentia are directly linked to the major collisions occurring at the same time on the other coasts of the continent (Chap. 5) remain speculative; however, one must assess these possibilities when trying to understand the tectonic evolution through time of such major geologic systems.

References

Abbott, J.G., 1981. Geology of the Seagull tin district, Yukon Geology and Exploration. Indian and Northern Affairs Canada, pp. 32-44.

Ballard, R.D., Holcomb, R.T. and van Andel, T.H., 1979. The Galapagos Rift at 86'W: 3: sheet flows, collapse pits, and lava lakes of the rift valley. Journal of Geophysical Research, 84: 5407-5422.

Bhatia, M.R. and Crook, K.A.W., 1986. Trace element characteristics of greywackes and tectonic setting discrimination of sedimentary basins. Contributions to Mineralogy and Petrology, 92: 181-193.

Boghossian, N.D., Patchett, P.J., Ross, G.M. and Gehrels, G.E., 1996. Nd isotopes and the source of sediments in the miogeocline of the Canadian Cordillera. Journal of Geology, 104(3): 259-277.

Bond, G.C., 1973. A late Paleozoic volcanic arc in the eastern Alaska Range, Alaska. Journal of Geology, 81(5): 557-575.

Bouma, A.H., 1962. Sedimentology of some Flysch deposits; a graphic approach to facies interpretation. Elsevier, Amsterdam, 168 pp.

Brown, D., Juhlin, C. and Puchkov, V., 2002. Introduction, Mountain building in the Uralides:Pangea to the present. Geophysical Monograph. American Geophysical Union, pp. 1-7.

Bull, S.W. and Cas, R.A.F., 1991. Depositional controls and characteristics of subaqueous bedded volcaniclastics of the Lower Devonian Snowy River Volcanics. Sedimentary Geology, 74(1-4): 189-215.

Burchfiel, B.C., Cowan, D.S. and Davis, G.A., 1992. Tectonic overview of the Cordilleran orogen in the western United States. In: B.C. Burchfield, P.W. Lipman and M.L. Zoback (Editors), The Cordilleran Orogen: Conterminous U.S. Geological Society of America, The Geology of North America, v. G-3, Boulder, Colorado, pp. 407-479.

Cameron, E.M. and Hattori, K., 1997. Strontium and neodynium isotope ratios in the
    Fraser River, British Columbia: a riverine transect across the Cordilleran orogen.
    Chemical Geology, 137(3-4): 243-253.

Castonguay, S. and Tremblay, A., 2003. Tectonic evolution and significance of Silurian-
    Early Devonian hinterland-directed deformation in the internal Humber Zone of
    the southern Quebec Appalachians. Canadian Journal of Earth Sciences = Revue
    Canadienne des Sciences de la Terre, 40(2): 255-268.

Colpron, M. and Reinecke, M., 2000. Glenlyon Project: Coherent stratigraphic succession
    from Little Salmon Range (Yukon-Tanana Terrane), and its potential for
    volcanic-hosted massive sulphide deposits. In: L.H. Weston (Editor), Yukon
    Exploration and Geology 1999. Exploration and Geological Services Division,
    Yukon Region, Indian and Northern Affairs Canada, pp. 87-100.

Colpron, M. and Yukon-Tanana working Group, 2001. Ancient Pacific Margin - An
    update on stratigraphic comparison of potential volcanogenic massive sulphide
    hosting successions of Yukon-Tanana terrane, northern British Columbia and
    Yukon. In: D.S. Emond and L.H. Weston (Editors), Yukon Exploration and
    Geology. Exploration and Geological Services Division, Yukon Region, Indian
    and Northern Affairs Canada, pp. 97-110.

Colpron, M. et al., 2003. Yukon Targeted Geoscience Initiative, Part 1: Results of
    accelerated bedrock mapping in Glenlyon (105L/1-7, 11-14) and northeast
    Carmacks (115I/9,16) areas, central Yukon. In: D.S. Emond and L.L. Lewis
    (Editors), Yukon Exploration and Geology 2002. Exploration and Geological
    Services Division, Yukon Region, Indian and Northern Affairs Canada, pp. 85-
    108.

Colpron, M., Gladwin, K., Johnston, S.T., Mortensen, J.K. and Gehrels, G.E., in press-a.
    Geology and juxtaposition history of Yukon-Tanana, Slide Mountain and Cassiar
    terranes in the Glenlyon area of central Yukon. Canadian Journal of Earth
    Sciences.

Colpron, M., Mortensen, J.K., Gehrels, G.E. and Villeneuve, M.E., in press. Basement
    complex, Carboniferous magmatic arcs and Paleozoic deformation in Yukon-
    Tanana terrane of central Yukon. In: M. Colpron, J.L. Nelson and R.I. Thompson

(Editors), Paleozoic evolution and metallogeny of pericratonic terranes at the ancient Pacific margin of North America, Canadian and Alaskan Cordillera. Geological Association of Canada.

Colpron, M., Murphy, D.C. and Mortensen, J.K., 2000. Mid-Paleozoic tectonism in Yukon-Tanana Terrane, northern Canadian Cordillera: record of intra-arc deformation. Geological Society of America, Cordilleran Section, Abstracts with Programs, 32(6): A-7.

Colpron, M., Nelson, J.L. and Murphy, D.C., in press-b. A tectonostratigraphic framework for the pericratonic terranes of the northern Canadian Cordillera. In: M. Colpron, J.L. Nelson and R.I. Thompson (Editors), Paleozoic evolution and metallogeny of pericratonic terranes at the ancient Pacific margin of North America, Canadian and Alaskan Cordillera. Geological Association of Canada.

Colpron, M., 1998. Preliminary geological map of Little Kalzas Lake area, central Yukon (NTS 105L/13). Exploration and Geological Services Division, Yukon Region, Indian and Northern Affairs Canada.

Colpron, M., 1999a. Glenlyon Project: Preliminary stratigraphy and structure of Yukon-Tanana Terrane, Little Kalzas Lake area, central Yukon (105L/13). In: C.F. Roots and D.S. Emond (Editors), Yukon Exploration and Geology. Exploration and Geological Services Division, Yukon Region, Indian and Northern Affairs Canada, pp. 63-72.

Colpron, M., 1999b. A new mineral occurrence in Yukon-Tanana terrane near Little Salmon Lake, central Yukon (NTS 105L/2). In: C.F. Roots and D.S. Emond (Editors), Yukon Exploration and Geology. Exploration and Geological Services Division, Yukon Region, Indian and Northern Affairs Canada, pp. 255-258.

Colpron, M., 2000. Geological map of Little Salmon Lake (parts of NTS 105L/1, 2 & 7), central Yukon. Exploration and Geological Services Division, Yukon Region, Indian and Northern Affairs Canada.

Colpron, M., 2001. Geochemical characterization of Carboniferous volcanic successions from Yukon-Tanana terrane, Glenlyon map area (105L), central Yukon. In: D.S. Emond and L.H. Weston (Editors), Yukon Exploration and Geology 2000.

Exploration and Geological Services Division, Yukon Region, Indian and Northern Affairs Canada, pp. 111-136.

Condie, K.C. and Sloan, R.E., 1998. Origin and evolution of Earth. Prentice-Hall, Upper Saddle River, New Jersey, 498 pp.

Condie, K.C., 2003. Supercontinents, superplumes and continental growth; the Neoproterozoic record. Geological Society Special Publications, 206: 1-21.

Coney, P.J., Jones, D.L. and Monger, J.W.H., 1980. Cordilleran suspect terranes. Nature, 288: 329-333.

Corcoran, P.L., 2000. Recognizing distinct portions of seamounts using volcanic facies analysis; examples from the Archean Slave Province, NWT, Canada. Precambrian Research, 101(2-4): 237-261.

Cousens, B., 1996. Magmatic evolution of Quaternary mafic magmas at Long Valley Caldera and the Devils Postpile, California: effects of crustal contamination on lithopheric mantl-derived magmas. Journal of Geophysical Research, 101: 27673-27689.

Cousens, B.L., 2000. Geochemistry of the Archean Kam Group, Yellowknife greenstone belt, Slave Province, Canada. Journal of Geology, 108(2): 181-197.

Cousineau, P. and Dimroth, E., 1982. Interpretation of the relations between massive, pillowed and brecciated faies in an Archean submarine andesite volcano; Amulet Andesite, Rouyn-Noranda area, Quebec, Canada. Canadian Journal of Earth Sciences = Journal Canadien des Sciences de la Terre, 15: 902-918.

Creaser, R.A. and Harms, T.A., 1998. Lithological, geochemical and isotopic characterization of clastic units in the Klinkit and Swift River assemblages, northern British Columbia. In: F. Cook and P. Erdmer (Editors), Lithoprobe Report, Report: 64. University of British Columbia, Lithoprobe Secretariat for the Canadian Lithoprobe Program, pp. 239-242.

Creaser, R.A., Erdmer, P., Stevens, R.A. and Grant, S.L., 1997. Tectonic affinity of Nisutlin and Anvil assemblage strata from the Teslin tectonic zone, northern Canadian Cordillera; constraints from neodymium isotope and geochemical evidence. Tectonics, 16(1): 107-121.

Creaser, R.A., Goodwin-Bell, J.-A.S. and Erdmer, P., 1999. Geochemical and Nd isotopic constraints for the origin of eclogite protoliths, northern Cordillera; implications for the Paleozoic tectonic evolution of the Yukon-Tanana Terrane. Canadian Journal of Earth Sciences = Revue Canadienne des Sciences de la Terre, 36(10): 1697-1709.

Dickerson, W.P., 2003. Intraplate mountain building in response to continent-continent collision; the ancestral Rocky Mountains (North America) and inferences drawn from the Tien Shan (Central Asia). In: J.B. Murphy and J.D. Keppie (Editors), Tectonophysics, pp. 129-142.

Dickinson, W.R. and Lawton, T.F., 2001. Carboniferous to Cretaceous assembly and fragmentation of Mexico. GSA Bulletin, 113(9): 1142-1160.

Dickinson, W.R. and Lawton, T.F., 2003. Sequential intercontinental suturing as the ultimate control for Pennsylvanian ancestral Rocky Mountains deformation. Geology, 31(7): 609-612.

Dimroth, E., Cousineau, P., Leduc, M. and Sanschagrin, Y., 1978. Structure and organization of Archean subaqueous basalt flows, Rouyn-Noranda area, Quebec, Canada. Canadian Journal of Earth Sciences = Journal Canadien des Sciences de la Terre, 15(6): 902-918.

Embry, A.F., 1991. Middle-Upper Devonian clastic wedge of the Arctic Islands, Chapter 10. In: H.P. Trettin (Editor), Geology of the Innuitian Orogen and the ARctic PLatform fo Canada and Greenland. Geological Survey of Canada, Geology of Canada (also Geological Society of America, The Geology of North America), pp. 263-279.

Engebretson, D.C., 1982. Relative motions between oceanic and continental plates in the Pacific Basin. Ph.D. Thesis, Stanford University, 211 pp.

Engebretson, D.C., Kelley, K.P., Cashman, H.J. and Richards, M.A., 1992. 180 million years of subduction. GSA Today, 2(5): 93-100.

Fernandez, H.E., 1969. Notes on the submarine ash flow tuff in Siargao island, Surigao del Norte. Philip. Geol., 23(1): 29-36.

Ferri, F., 1997. Nina Creek Group and Lay Range Assemblage, north-central British Columbia; remnants of late Paleozoic oceanic and arc terranes. Canadian Journal of Earth Sciences = Journal Canadien des Sciences de la Terre, 34(6): 854-874.

Ferri, F., Rees, C. and Anonymous, 1995. Lay Range assemblage and Nina Creek Group, north-central British Columbia; remnants of upper Paleozoic arc and oceanic terranes, Program with Abstracts - Geological Association of Canada; Mineralogical Association of Canada; Canadian Geophysical Union, Joint Annual Meeting, vol.20. Geological Association of Canada, Waterloo, pp. 31.

Fisher, R.V. and Schmincke, H.-U., 1984. Pyroclastic rocks. Springer-Verlag, New York, 472 pp.

Fisher, R.V., 1966. Rocks composed of volcanic fragments and their classification. Earth-Science Reviews, 1(4): 287-298.

Fiske, R.S. and Matsuda, T., 1964. Submarine equivalents of ash flows in the Tokiwa Formation, Japan. American Journal of Science, 262(1): 76-106.

Fryer, P., 1995. Geology of the Mariana Trough. In: B. Taylor (Editor), Backarc basins; Tectonics and magmatism. Plenum Press, New York, pp. 237-280.

Gabrielse, H. and Campbell, R.B., 1991. Upper Proterozoic assemblages. In: H. Gabrielse and C.J. Yorath (Editors), Geology of the Cordilleran Orogen in Canada. Geological Survey of Canada, Geology of Canada (also Geological Society of America, The Geology of North America, v. G-2), pp. 125-150.

Gabrielse, H. and Yorath, C.J., 1991. Tectonic synthesis. In: H.G.a.C.J. Yorath (Editor), Geology of the Cordilleran Orogen in Canada. Geological Survey of Canada, Geology of Canada, (also Geological Society of America, v. G-2), pp. 677-705.

Gabrielse, H., Monger, J.W.H., Wheeler, J.O. and Yorath, C.J., 1991. Tectonic framework; Part A, Morphogeological belts, tectonic assemblages and terranes. In: H. Gabrielse and C.J. Yorath (Editors), Geology of the Cordilleran Orogen in Canada. Geological Survey of Canada, Geology of Canada, (also Geological Society of America, v. G-2), pp. 677-705.

Gabrielse, H., 1969. Geology of Jennings River map area, British Columbia (104/O), Paper 68-55. Geological Survey of Canada.

Gabrielse, H., 1991. Late Paleozoic and Mesozoic terrane interactions in north-central British Columbia. Canadian Journal of Earth Sciences = Journal Canadien des Sciences de la Terre, 28(6): 947-957.

Gamble, J.A., Wright, I.C., Woodhead, J.D. and McCulloch, M.T., 1995. Arc and back-arc geochemistry in the southern Kermadec arc - Ngatoro Basin and offshore Taupo volcanic zone, SW Pacific. In: J.L. Smellie (Editor), Volcanism associated with extension and consuming plate margins. Geological Society, Special Publication No. 81, pp. 193-212.

Garzione, C.N., Patchett, P.J., Ross, G.M. and Nelson, J., 1997. Provenance of Paleozoic sedimentary rocks in the Canadian Cordilleran miogeocline; a Nd isotopic study. Canadian Journal of Earth Sciences = Journal Canadien des Sciences de la Terre, 34(12): 1603-1618.

Gehrels, G.E. et al., 2000. Tectonic implications of detrital zircon data from Paleozoic and Triassic strata in western Nevada and Northern California. Special Paper - Geological Society of America, 347: 133-150.

Gehrels, G.E., McClelland, W.C., Samson, S.D., Patchett, P.J. and Ross, G.M., 1991. U-Pb geochronology of detrital zircons from a continental margin assemblage in the northern Coast Mountains, southeastern Alaska, Canadian Journal of Earth Sciences = Journal Canadien des Sciences de la Terre. National Research Council of Canada, Ottawa, pp. 1285-1300.

Gladwin, K., Colpron, M., Black, R. and Johnston, S.T., 2003. Bedrock geology at the boundary between Yukon-Tanana and Cassiar terranes, Truitt Creek map area (105L/1), south-central Yukon. In: D.S. Emond and L.L. Lewis (Editors), Yukon Exploration and Geology 2002. Exploration and Geological Services Division, Yukon Region, Indian and Northern Affairs Canada, pp. 135-148.

Goldstein, S.L., 1988. Decoupled evolution of Nd and Sr isotopes in the continental crust and the mantle. Nature, 336(6201): 733-738.

Goodfellow, W.D., Cecile, M.P. and Leybourne, M.I., 1995. Geochemistry, petrogenesis, and tectonic setting of lower Paleozoic alkalic and potassic volcanic rocks, northern Canadian Cordilleran miogeocline. Canadian Journal of Earth Sciences = Journal Canadien des Sciences de la Terre, 32(8): 1236-1254.

Gordey, S.P. and Stevens, R.A., 1994. Tectonic framework of the Teslin region, southern Yukon Territory. 1994-A, Geological Survey of Canada, Ottawa.

Gordey, S.P., 1992. Geological fieldwork in Teslin map area, southern Yukon Territory. 92-01A, Geological Survey of Canada, Ottawa.

Hamilton, P.J., O'Nions, R.K., Bridgwater, D. and Nutman, A., 1983. Sm-Nd studies of Archaean metasediments and metavolcanics from West Greenland and their implications for the Earth's early history. Earth and Planetary Science Letters, 63: 263-273.

Harms, T.A. and Creaser, R.A., 1997. Constraints on the geologic evolution and tectonic affinity of the Klinkit assemblage. In: F.A. Cook and P. Erdmer (Editors), Lithoprobe Report, vol.56. University of British Columbia, Lithoprobe Secretariat for the Canadian Lithoprobe Program, pp. 211-213.

Harms, T.A. and Stevens, R.A., 1995. Investigations in the Dorsey terrane; Part 2, Lithologies and structure of (?)Paleozoic stratified rocks in the Stikine Ranges, northern British Columbia. 1995-A, Geological Survey of Canada, Ottawa.

Harms, T.A. and Stevens, R.A., 1996a. Assemblage analysis of the Dorsey Terrane. In: F.A. Cook (Editor), Lithoprobe Report, Report: 50, vol.50. University of British Columbia, Lithoprobe Secretariat for the Canadian Lithoprobe Program, pp. 199-201.

Harms, T.A. and Stevens, R.A., 1996b. A working hypothesis for the tectonostratigraphic affinity of the Stikine Ranges and a portion of the Dorsey Terrane. In: F.A. Cook (Editor), Lithoprobe Report, Report: 50, vol.50. University of British Columbia, Lithoprobe Secretariat for the Canadian Lithoprobe Program, pp. 93-95.

Hart, S.R., 1988. Heterogeneous mantle domains: signatures, genesis and mixing chronologies. Earth and Planetary Science Letters, 90(3): 272-296.

Hatcher, R.D.J., 1989. Tectonic synthesis of the U.S. Appalachians. In: R.D.J. Hatcher, W.A. Thomas and G.W. Viele (Editors), The Appalachian-Ouachita Orogen in Unites States. The geology of North America. The Geological Society of America, Boulder, Colorado, pp. 511-535.

Hawkesworth, C.J. et al., 1979. 143Nd/144Nd, 87Sr/86Sr and incompatible element variations in calc-alkaline andesites and plateau lavas from South America. Earth and Planetary Science Letters, 42: 45-57.

Head, J.W., III and Wilson, L., 2003. Deep submarine pyroclastic eruptions; theory and predicted landforms and deposits. Journal of Volcanology and Geothermal Research, 121(3-4): 155-193.

Hoffman, P.F., 1991. Did the beakout of Laurentia turn Gondwanaland inside-out? Science, 252: 1409-1412.

Jacobsen, S.B. and Wasserburg, G.J., 1980. Sm-Nd isotopic evolution of chondrites. Earth and Planetary Science Letters, 50: 139-155.

Karlstrom, K.E. et al., 2000. Chuar Group of the Grand Canyon: Record of breakup of Rodinia, associated change in the global carbon cycle, and ecosystem expansion by 740 Ma. Geology, 28(7): 619-622.

Klaus, A. et al., 1992. Structural and stratigraphic evolution of the Sumisu Rift, Izu-Bonin Arc. Proceedings of the Ocean Drilling Program, Scientific Results, 126: 555-573.

Kluth, C.F. and Coney, P.J., 1981. Plate tectonics of the ancestral Rocky Mountains. Geology, 9(1): 10-15.

Kokelaar, P., 1986. Magma-water interactions in subaqueous and emergent basaltic volcanism. Bulletin of Volcanology, 48(5): 275-289.

Langmuir, C.H., Vocke, R.D.J., Hanson, G.D. and Hart, S.R., 1978. A general mixing equation with applications to Icelandic basalts. Earth and Planetary Science Letters, 37: 380-393.

Lawver, L.A., Grantz, A. and Gahagan, L.M., 2002. Plate kinematic evolution of the present Arctic region since the Ordovician. Geological Society of America Special Paper, 360: 333-358.

Lentz, D.R., 1998. Petrogenetic evolution of felsic volcanic sequences associated with Phanerozoic volcanic-hosted massive sulphide systems: the role of extensional geodynamics. Ore Geology Reviews, 12: 289-327.

Lentz, D.R., 1999. Petrology, geochemistry and oxygen isotopic interpretation of felsic volcanic and related rocks hosting the Brunswick 6 and 12 massive sulphide

depostis (Brunswick Belt), Bathurst Mining Camp, New Brunswick, Canada. Economic Geology, 94: 57-86.

Lowe, D.R., 1982. Sediment gravity flows; II, Depositional models with special reference to the deposits of high-density turbidity currents. Journal of Sedimentary Petrology, 52(1): 279-297.

Mawer, C.K. and White, J.C., 1987. Sense of displacement on the Cobequid-Chedabucto fault system, Nova Scotia, Canada. Canadian Journal of Earth Sciences, 24: 217-223.

McConachy, T.F. et al., 2005. New hydrothermal activity and alkalic volcanism in the backarc Coriolis Troughs, Vanuatu. Geology, 33(1): 61-64.

McDonough, W.F. and Sun, S.S., 1995. The composition of the Earth. In: W.F. McDonough, N.T. Arndt and S. Shirey (Editors), Chemical Geology. Elsevier, Amsterdam, pp. 223-253.

McPhie, J., 1995. A Pliocene shoaling basaltic seamount; Ba Volcanic Group at Rakiraki, Fiji. Journal of Volcanology and Geothermal Research, 64(3-4): 193-210.

McPhie, J., Doyle, M. and Allen, R., 1993. Volcanic texures: a huide to interpretation of textures in volcanic rocks. Centre for Ore Deposit and Exploration Studies, University of Tasmania, Tasmania, 198 pp.

Mihalynuk, M.G. et al., 2000. Ancient Pacific Margin; Part III, Regional geology and mineralization of the Big Salmon Complex (NTS 104N/9E,16 & 104O 12,13,14W). 2000-1, British Columbia Geological Survey in cooperation with various British Columbia Ministries, Victoria.

Mihalynuk, M.G., Nelson, J., Friedman, R.M. and Smyth, W.R., 1998. Regional geology and mineralization of the Big Salmon Complex (104N NE and 1040 NW). 1998-1, British Columbia Geological Division, Victoria.

Miller, E.L., Miller, M.M., Stevens, C.H., Wright, J.E. and Madrid, R.J., 1992. Late Paleozoic paleogeographic and tectonic evolution of the western U.S. Cordillera. In: B.C. Burchfield, P.W. Lipman and M.L. Zoback (Editors), The Cordilleran Orogen: Conterminous U.S. Geological society of America, The Geology of North America, v. G-3, Boulder, Colorado, pp. 57-106.

Monger, J.W.H. and Irving, E., 1980. Northward displacement of north-central British Columbia. Nature, 285: 289-294.

Monger, J.W.H. et al., 1991. Part B. Cordilleran terranes; Upper Devonian to Middle Jurassic assemblages. In: H. Gabrielse and C.J. Yorath (Editors), Geology of the Cordilleran Orogen in Canada. Geoligical Survey Canada, Ottawa, pp. 281-327.

Monger, J.W.H., Price, R.A. and Tempelman-Kluit, D.J., 1982. Tectonic accretion and the origin of the two major metamorphic and plutonic welts in the Canadian Cordillera. Geology, 10(2): 70-75.

Monger, J.W.H., 1999. Review of the geology and tectonics of the Canadian Cordillera. Short course notes, Sydney, 72 pp.

Moore, J.G. and Schilling, J.-G., 1973. Vesicles, Water, and Sulfur in Reykjanes Ridge Basalts. Contributions to Mineralogy and Petrology, 41(2): 105-118.

Morris, G.A. and Hooper, P.R., 1997. Petrogenesis of the Colville igneous complex, Northeast Washington; implications for Eocene tectonics in the northern U.S. Cordillera. Geology, 25(9): 831-834.

Morris, G.A., Larson, P.B. and Hooper, P.R., 2000. "Subduction style" magmatism in a non-subduction setting; the Colville igneous complex, NE Washington State, USA. Journal of Petrology, 41(1): 43-67.

Mortensen, J.K., 1992. Pre-mid-Mesozoic tectonic evolution of the Yukon-Tanana Terrane, Yukon and Alaska. Tectonics, 11(4): 836-853.

Mueller, W.U., 2003. A subaqueous eruption model for shallow-water, small volume eruptions; evidence from two Precambrian examples. In: J.D.L. White, J.L. Smellie and D.A. Clague (Editors), Geophysical Monograph, vol.140. American Geophysical Union, Washington, pp. 189-203.

Murphy, D.C., Mortensen, J.K., Piercey, S.J., Orchard, M.J. and Gehrels, G.E., in press. Mid-Paleozoic to Early Mesozoic tectonostratigraphic evolution of Yukon-Tanana and Slide Mountain terranes and affiliated overlap assemblages, Finlayson Lake massive sulphide district, southeasternYukon. In: M. Colpron, J.L. Nelson and R.I. Thompson (Editors), Paleozoic evolution and metallogeny of pericratonic terranes at the ancient Pacific margin of North America. Geological Association of Canada.

Nance, R.D., Murphy, J.B. and Keppie, J.D., 2002. A Cordilleran model for the evolution
of Avalonia. In: L. Eguiluz, J.B. Murphy and G. Zulauf (Editors),
Tectonophysics. Elsevier, Amsterdam, pp. 11-31.

Nelson, J., 1997. Last seen heading south; extensions of the Yukon-Tanana Terrane into
northern British Columbia. 1997-1, British Columbia Geological Division,
Victoria.

Nelson, J., 2001. Geology of north-central Jennings River area (104O/14E, 15). 2001-1,
Province of British Columbia, Ministry of Energy.

Nelson, J.L. and Friedman, R.M., 2004. Superimposed Quesnel (late Paleozoic-Jurassic)
and Yukon–Tanana (Devonian-Mississippian) arc assemblages, Cassiar
Mountains, northern British Columbia: field, U-Pb, and igneous petrochemical
evidence. Canadian Journal of Earth Sciences, 41: 1201-1235.

Nelson, J.L. et al., 2000. Ancient Pacific Margin; Part II, A preliminary comparison of
potential VMS-hosting successions of the Yukon Tanana Terrane, from Finlayson
Lake District to northern British Columbia. 2000-1, British Columbia Geological
Survey in cooperation with various British Columbia Ministries, Victoria.

Nelson, J.L., 1993. The Sylvester Allochthon; upper Paleozoic marginal-basin and island-
arc terranes in northern British Columbia. Canadian Journal of Earth Sciences =
Journal Canadien des Sciences de la Terre, 30(3): 631-643.

Nelson, J.L., 2000. Ancient Pacific Margin; Part VI, Still heading south; potential VMS
hosts in the eastern Dorsey Terrane, Jennings River (104O/1; 7, 8, 9, 10). 2000-1,
British Columbia Geological Survey in cooperation with various British
Columbia Ministries, Victoria.

Nelson, J.L., Colpron, M. and Piercey, S.J., in press. Paleozoic tectonic and
metallogenetic evolution of the pericratonic terranes in Yukon, northern British
Columbia and eastern Alaska. In: M. Colpron, J.L. Nelson and R.I. Thompson
(Editors), Paleozoic evolution and metallogeny of pericratonic terranes at the
ancient Pacific margin of North America, Canadian and Alaskan Cordillera.
Geological Association of Canada.

Niem, A.R., 1977. Mississippian pyroclastic flow and ash-fall deposits in the deep-marine Ouachita flysch basin, Oklahoma and Arkansas. Geological Society of America Bulletin, 88(1): 49-61.

Patchett, P.J. and Gehrels, G.E., 1998. Continental influence of Canadian Cordilleran terranes from Nd isotopic study, and significance for crustal growth processes. Journal of Geology, 106(3): 269-280.

Pearce, J.A. and Cann, J.R., 1973. Tectonic setting of basic volcanic rocks determining using trace element analyses. Earth and Planetary Science Letters, 19: 290-300.

Pearce, J.A. and Peate, D.W., 1995. Tectonic implications of the composition of volcanic arc magmas. Annual Review of Earth and Planetary Sciences, 23: 251-285.

Pearce, J.A., 1983. Role of sub-continental lithopheric magma genesis at active continental margins. In: C.J. Hawkesworth and M.J. Norry (Editors), Continental flood basalts and mantle xenoliths. Shiva Publishing Ltd., Nantwich, pp. 230-249.

Peter, J.M., Mihalynuk, M.G., Colpron, M. and Nelson, J.L., 2003. Diverse examples of exhalative hydrothermal sediments in Yukon-Tanana Terrane, Yukon Territory and British Columbia, GAC-MAC 2003, Vancouver.

Piercey, S.J. et al., in press. Paleozoic magmatism and crustal recycling along the ancient Pacific margin of North America, northern Cordillera. In: M. Colpron, J.L. Nelson and R.I. Thompson (Editors), Paleozoic evolution and metallogeny of pericratonic terranes at the ancient Pacific margin of North America, Canadian and Alaskan Cordillera. Geological Association of Canada.

Piercey, S.J., Mortensen, J.K. and Creaser, R.A., 2003. Neodymium isotope geochemistry of felsic volcanic and intrusive rocks from the Yukon-Tanana Terrane in the Finlayson Lake region, Yukon, Canada. Canadian Journal of Earth Sciences = Revue Canadienne des Sciences de la Terre, 40(1): 77-97.

Piercey, S.J., Mortensen, J.K., Murphy, D.C., Paradis, S. and Creaser, R.A., 2002. Geochemistry and tectonic significance of alkalic mafic magmatism in the Yukon-Tanana Terrane, Finlayson Lake region, Yukon. Canadian Journal of Earth Sciences = Revue Canadienne des Sciences de la Terre, 39(12): 1729-1744.

Piercey, S.J., Murphy, D.C., Mortensen, J.K. and Creaser, R.A., 2004. Mid-Paleozoic initiation of the northern Cordilleran marginal backarc basin; geologic,

geochemical, and neodymium isotope evidence from the oldest mafic magmatic rocks in the Yukon-Tanana Terrane, Finlayson Lake District, southeast Yukon, Canada. Geological Society of America Bulletin, 116(9-10): 1087-1106.

Piercey, S.J., Murphy, D.C., Mortensen, J.K. and Paradis, S., 2001. Boninitic magmatism in a continental margin setting, Yukon-Tanana Terrane, southeastern Yukon, Canada. Geology, 29(8): 731-734.

Piercey, S.J., Paradis, S., Murphy, D.C. and Mortensen, J.K., 2001. Geochemistry and paleotectonic setting of felsic volcanic rocks in the Finlayson Lake volcanic-hosted massive sulfide district, Yukon, Canada. Economic Geology and the Bulletin of the Society of Economic Geologists, 96(8): 1877-1905.

Piercey, S.J., Paradis, S., Peter, J.M. and Tucker, T.L., 2002b. Geochemistry of basalt from the Wolverine volcanichosted massive-sulphide deposit, Finlayson Lake district, Yukon Territory. Geological Survey of Canada, Current Research 2002-A3, 11 pp.

Poole, F.G. et al., 1992. Lates Precambrian to latest Devonian time; Development of a continental margin. In: B.C. Burchfield, P.W. Lipman and M.L. Zoback (Editors), The Cordilleran Orogen: Conterminous U.S. Geological Society of America, The Geologi of North America, v. G-3, Boulder, Colorado, pp. 9-56.

Poole, W.H., 1956. Geology of the Cassiar Mountains in the vicinity of the Yukon-British Columbia boundary. unpublished Ph.D. Thesis, Princeton University.

Poole, W.H., Roddick, J.A. and Green, L.H., 1961. Geology of Wolf Lake, Yukon Territory. Geological Survey of Canada, Map 10-1960.

Roberts, D., 2003. The Scandinavian Caledonides; event chronology, palaeogeographic settings and likely modern analogues. In: J.B. Murphy and J.D. Keppie (Editors), Tectonophysics, pp. 283-299.

Rona, P.A., 1988. Hydrothermal mineralization at oceanic ridges. Canadian Mineralogist, 26: 431-465.

Roots, C.F., Harms, T.A., Simard, R.L., Orchard, M.J. and Heaman, L., 2002. Constraints on the age of the Klinkit assemblage east of Teslin Lake, northern British Columbia. 2002-A7, Geological Survey of Canada.

Roots, C.F., Nelson, J.L., Simard, R.L. and Harms, T.A., in press. Continental fragments, Paleozoic arcs and overlapping arc and Triassic sediments in the pericratonic belt, northern British Columbia and southern Yukon. In: M. Colpron, J.L. Nelson and R.I. Thompson (Editors), Paleozoic evolution and metallogeny of pericratonic terranes at the Ancient Pacific Margin of North America. Geological Assosiation of Canada.

Sawkins, F.J., 1971. Sulfide ore deposits in relation to geotectonics. Journal of Geology, 80: 377-397.

Schermer, E.R., Howell, D.G. and Jones, D.L., 1984. The origin of allochthonous terranes. Annual Review of Earth and Planetary Sciences, 12: 107-131.

Schmid, R., 1981. Descriptive nomenclature and classification of pyroclastic deposits and fragments; recommendations of the IUGS Subcommission on the Systematics of Igneous Rocks. Geology, 9(1): 41-43.

Schmidt, R. and Schmincke, H.-U., 2000. Seamounts and island building. In: H. Sigurdsson, B.F. Houghton, S.R. McNutt, H. Rymer and J. Stix (Editors). Academic Press, San Diego, pp. 383-402.

Scotese, C.R., 2001. Atlas of Earth History. Paleogeography, PALEOMAP Project, vol. 1, (www. scotese.com), Arlington, Texas, 52 pp.

Shervais, J.W., 1982. Ti/V plots and the petrogenesis of modern and ophiolotic lavas. Earth and Planetary Science Letters, 59: 101-118.

Simard, R.-L., Dostal, J. and Roots, C.F., 2003. Development of late Paleozoic volcanic arcs in the Canadian Cordillera; an example from the Klinkit Group, northern British Columbia and southern Yukon. Canadian Journal of Earth Sciences = Revue Canadienne des Sciences de la Terre, 40(7): 907-924.

Simard, R.L., Roots, C.F. and Dostal, J., 2001. Tectonic implications of the geologic setting if the Klinkit assemblage (Yukon-Tanana Terrane), northern British Columbia. Geological Association of Canada - Mineralogical Association of Canada Abstract volume, 26: 138.

Simard, R.L., Roots, C.F. and Dostal, J., 2002. The pre-accretion history of the northern Canadian Cordillera: The Klinkit Formation, an example from northern British

Columbia and southern Yukon. Geological Association of Canada - Mineralogical Association of Canada, Abstracts volume: 109.

Smith, A.D., Lambert, R.S.J., Brandon, A.D. and Goles, G.G., 1995. Nd, Sr, and Pb isotopic evidence for contrasting origins of late Paleozoic volcanic rocks from the Slide Mountain and Cache Creek terranes, south-central British Columbia. Canadian Journal of Earth Sciences = Journal Canadien des Sciences de la Terre, 32(4): 447-459.

Sohn, Y.K., 1995. Geology of Tok Island, Korea: eruptive and depositional processes of a shoaling to emergent island volcano. Bulletin of Volcanology (Historical Archive), 56(8): 660-674.

Staudigel, H. and Schmincke, H.-U., 1984. The Pliocene seamount series of La Palma/Canary Islands, JGR. Journal of Geophysical Research. B. American Geophysical Union, Washington, pp. 11,195-11,215.

Steiger, R.H. and Jaeger, E., 1977. Subcommission on geochronology; convention on the use of decay constants in geo- and cosmochronology. Earth and Planetary Science Letters, 36(3): 359-362.

Stevens, R.A. and Harms, T.A., 1995. Investigations in the Dorsey terrane; Part 1, Stratigraphy, structure, and metamorphism in the Dorsey Range, southern Yukon Territory and northern British Columbia. 1995-A, Geological Survey of Canada, Ottawa.

Stevens, R.A. and Harms, T.A., 1996. Geology in the vicinity of the Dorsey Range, southern Yukon Territory and northern British Columbia; scale 1:50,000, Lithoprobe Report, Report: 50, vol.50. University of British Columbia, Lithoprobe Secretariat for the Canadian Lithoprobe Program, pp. 222-225.

Stevens, R.A. and Harms, T.A., 2000. Bedrock geology of the Dorsey Range, south Yukon Territory and Northern British Columbia, Geological Survey of Canada; Open File 3926, Calgary.

Stevens, R.A., 1996. Dorsey assemblage; pre-Mid-Permian high temperature and pressure metamorphic rocks in the Dorsey Range, southern Yukon Territory, Lithoprobe Report, Report: 50, vol.50. University of British Columbia, Lithoprobe Secretariat for the Canadian Lithoprobe Program, pp. 70-75.

Sun, S.S. and McDonough, W.F., 1989. Chemical and isotopic systematics of oceanic basalts; implications for mantle composition and processes. Geological Society Special Publications, 42: 313-345.

Sun, S.S., 1982. Chemical composition and origin of the Earth's primitive mantle. Geochimica et Cosmochimica Acta, 46: 176-192.

Tamaki, K., 1995. Opening tectonic of the Japan Sea. In: B. Taylor (Editor), Backarc basins: Tectonics and magmatism. Plenum Press, New York, pp. 407-420.

Tate, M.C. and Clarke, D.B., 1995. Petrogenesis and regional tectonic significance of Late Devonian mafic intrusions in the Meguma Zone, Nova Scotia. Canadian Journal of Earth Sciences, 32(11): 1883-1898.

Taylor, B. et al., 1990. Alvin-Seabeam studies of the Sumisu Rift, Izu-Bonin Arc. Earth and Planetary Science Letters, 100(1-3): 127-147.

Taylor, B. et al., 1991. Structural development of Sumisu Rift, Izu-Bonin Arc. Journal of Geophysical Research, B, Solid Earth and Planets, 96(10): 16,113-16,129.

Taylor, B. et al., 1992. Rifting and the volcanic-tectonic evolution of the Izu-Bonin-Mariana Arc. Proceedings of the Ocean Drilling Program, Scientific Results, 126: 627-651.

Taylor, S.R. and McLennan, S.M., 1985. The continental crust; its composition and evolution; an examination of the geochemical record preserved in sedimentary rocks. Geoscience texts. Blackwell Sci. Publ., Oxford, United Kingdom (GBR), 312 pp.

Taylor, S.R. and McLennan, S.M., 1995. The geochemical evolution of the continental crust. Reviews of Geophysics, 33(2): 241-265.

Tempelman-Kluit, D., 1979. Transported cataclasite, ophiolite and granodiorite in Yukon: Evidence of arc-continent collision. Geolgicla Survey of Canada, Paper 79-14.

Theriault, R.J. and Ross, G.M., 1991. Nd isotopic evidence for crustal recycling in the ca. 2.0 Ga subsurface of Western Canada, Canadian Journal of Earth Sciences = Journal Canadien des Sciences de la Terre. National Research Council of Canada, Ottawa, pp. 1140-1147.

Thomas, W.A., 1989. The Appalachian-Ouchiata orogen beneath the Gulf Coastal Plain between the outcrops in the Appalachian and Ouachita Mountains. In: R.D.J. Hatcher, W.A. Thomas and G.W. Viele (Editors), The Appalachian-Ouachita Orogen in the United States. Geological Socitey of America, The Geology of North America, v. F-2, Boulder, Colorado, pp. 537-553.

Timmons, J.M., Karlstrom, K.E., Dehler, C.M., Geissman, J.W. and Heizler, M.T., 2001. Proterozoic multistage (ca. 1.1 and 0.8 Ga) extension recorded in the Grand Canyon Supergroup and establishment of northwest- and north-trending tectonic grains in the southwestern United States. GSA Bulletin, 113(2): 163-181.

Torsvik, T.H. and Cocks, L.R.M., 2004. Earth geography from 400 to 250 Ma: a palaeomagnetic, faunal and facies review. Journal of the Geological Society of London, 161: 555-572.

Torsvik, T.H. and Rehnstrom, E.F., 2003. The Tornquist Sea and Baltica-Avalonia docking. Tectonophysics, 362: 67-82.

Trettin, H.P., 1991. The Proterozoic to Late Silurian record of Perya. In: H.P. Trettin (Editor), Geology of the Innuitian Orogen and Artic Platform of Canada and Greenland. Geological Survey of Canada, Geology of Canada (also Geological Society of America, The geology of North America, v. E), pp. 241-259.

Trexler, J.H.J., Cashman, P.H., Snyder, W.S. and Davydov, V.I., 2004. Late Paleozoic tectonism in Nevada; timing, kinematics, and tectonic significance. Geological Society of America Bulletin, 116(5-6): 525-538.

Tull, J.F. and Holm, C.S., 2005. Structural evolution of a major Appalachian salient-recess junction: Consequences of oblique collisional convergence across a continental margin transform fault. GSA Bulletin, 117(3/4): 482-499.

van Staal, C.R., Dewey, J.F., Mac Niocaill, C. and McKerrow, W.S., 1998. The Cambrian-Silurian tectonic evolution of the Northern Appalachians and British Caledonides; history of a complex, west and southwest Pacific-type segment of Iapetus. Geological Society Special Publications, 143: 199-242.

Wallace, P., Anderson, A.T., Jr. and Ballard, R.D., 2000. Volatiles in magmas. In: H. Sigurdsson, B.F. Houghton, S.R. McNutt, H. Rymer and J. Stix (Editors), Encyclopedia of volcanoes. Academic Press, San Diego.

Watkins, R. and Browne, Q.J., 1989. An Ordovician continental-margin sequence of turbidite and seamount deposits in the Roberts Mountains allochton, Indeoendence Range, Nevada. Geological Society of America Bulletin, 101: 731-741.

Wheeler, J.O., Brookfiels, A.J., Gabrielse, H., Monger, J.W.H., tipper, H.W., and Woodsworth, G.J., 1991. Terrane map of the Canadian Cordillera, Geological Survey of Canada.

White, J.D.L., Houghton, B.F. and Ballard, R.D., 2000. Surtseyan and related phreatomagmatic eruptions. In: H. Sigurdsson, B.F. Houghton, S.R. McNutt, H. Rymer and J. Stix (Editors). Academic Press, San Diego.

White, R.S., Mackenzie, D. and O'Nions, R.K., 1992. Oceanic crustal thickness from seismic measurement and REE inversions. Journal of Geophysical Research, 97: 19683-19715.

Wilson, M., 1989. Igneous Petrogenesis, a glodal tectonic approach. Chapman & Hall, London, 466 pp.

Winchester, J.A. and Floyd, P.A., 1976. Geochemical magma type discrimination; application to altered and metamorphosed basic igneous rocks. Earth and Planetary Science Letters, 28(3): 459-469.

Winchester, J.A. and Floyd, P.A., 1977. Geochemical discrimination of different magma series and their differentiation products using immobile elements. Chemical Geology, 20(4): 325-343.

Wood, D.A., Joron, J.L. and Treuil, M., 1979. A re-appraisal of the use of trace-elements to classify and discriminate between magma series erupted in different tectonic settings. Earth and Planetary Science Letters, 45(326-336).

Yamada, E., 1973. Subaqueous pumice flow deposits in the Onikobe Caldera, Miyagi Prefecture, Japan. Chishitsugaku Zasshi = Journal of the Geological Society of Japan, 79(9): 585-597.

Yamagishi, H., 1991. Morphological and sedimentological chracteristics of the Neogene submarine coherent lavas and hyaloclastites in Southwest Hokkaido, Japan. Sedimentary Geology, 74: 5-23.

Young, G.M., 2002. Geochemical investigation of a Neoproterozoic glacial unit; the Mineral Fork Formation in the Wasatch Range, Utah. Geological Society of America Bulletin, 114(4): 387-399.

Ziegler, P.A., van Wees, J.-D. and Cloetingh, S., 1998. Mechanical controls on collision-related compressional intraplate deformation. Tectonophysics, 300(1-4): 102-129.

Appendix 1

Little Salmon rock descriptions

Little Salmon formation[1]
upper succession

Massive alkali basalt flow

Purplish to dark green seriate porphyritic massive rock showing; locally up to 3% of flatten chloritic disks, or calcite pods (amygdules?)

Phenocrysts:
- plagioclase phenocrysts (10-20%, relict, euhedral to subhedral, 0.2-3cm ϕ*); partly to completely replaced by very fine grained epidote, muscovite and calcite.
- clinopyroxene and/or hornblende (<15%, relict, 0.5-4mm Φ); completely replaced by actinolite and epidote; fine coating of iron-oxides around relict margins (observed in <10% of the flow; e.g. RL02-4-7A)

Matrix:
- (Porphyritic rocks) The matrix is a very fine grained mix of epidote, iron-oxide (hematite?), chlorite, and +/- calcite, with scattered apatite grains. Pockets of calcite and chlorite (0.1-3mm Φ, irregularly shapes) are scattered through the rock (amygdules?).
- (Microporphyritic rocks) The matrix is composed of small relict plagioclase (0.1mm long; albite), fine chlorite, epidote, very fine quartzofeldspathic material. Scattered calcite spots, 0.3mm Φ, can be observed (10%).

Texture:

- Massive, +/- amygdaloidal, seriate porphyritic alkali basalt flow (RL02-4-7A, RL02-6-5)
- Massive, +/- amygdaloidal, microporphyritic alkali basalt flow (RL02-11-13, RL02-14-1)
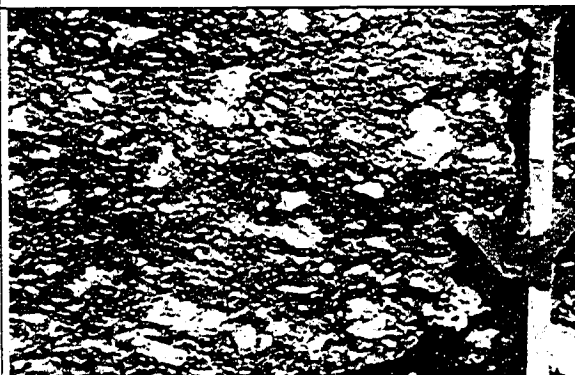
Massive porphyritic alkali basalt flow
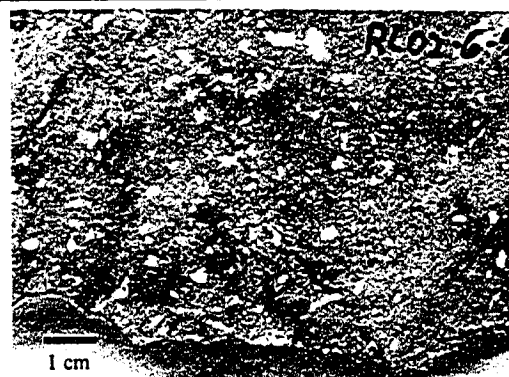
Massive porphyritic alkali basalt flow (RL02-6-5)

---

[1] See UTM coordinates in appendix 2 for sample location
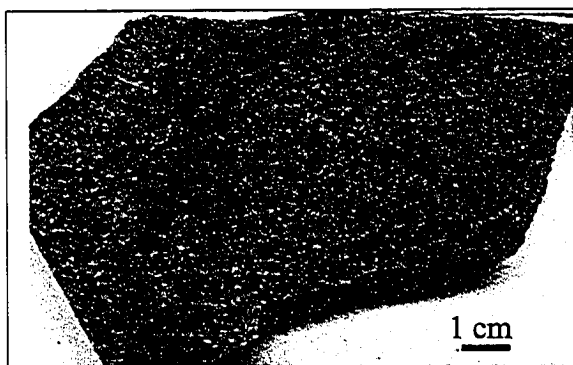
Microporphyritic alkali basalt flow (RL02-14-1)
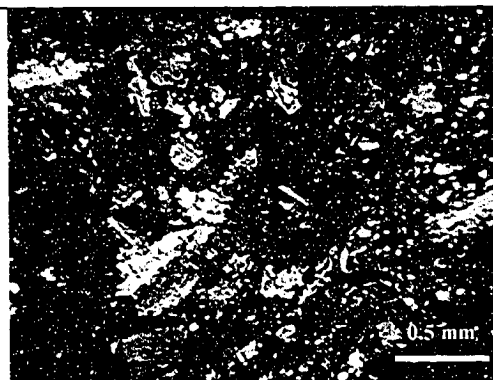
Microporphyritic alkali basalt flow (RL02-14-1)
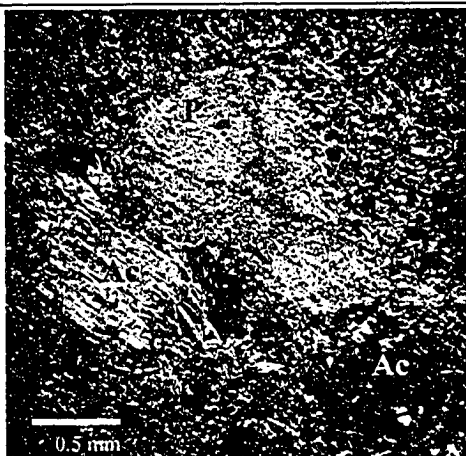
Massive porphyritic alkali basalt flow (RL02-4-7A. P:Plag., Ac:Actinolite)
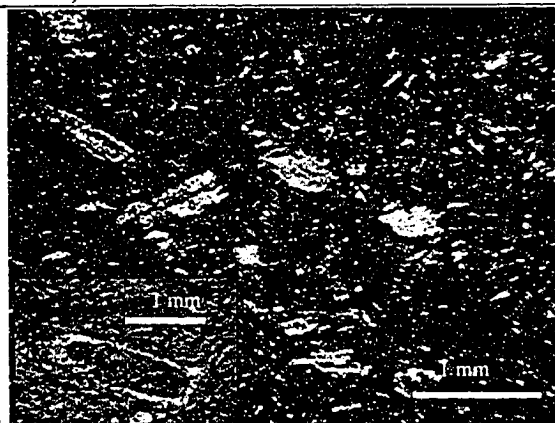
Microporphyritic alkali basalt flow (RL02-11-13; note calcite pods, and zoned plag. laths)

Vesicular massive microporphyritic lava flow

Cooked base of a lava flow (pencil) atop brecciated mafic rocks

158

Pillowed alkali basalt flow

dark purplish green ± porphyritic pillowed basaltic flow

i) 25cm-1m ϕ closely-packed fine grained pillow tubes showing 3-5cm-thick altered rims, and locally up to 10% of calcite-filled amygdules <5mmϕ in the core;

ii) 30-50cm ϕ closely-packed pillow tubes showing in places highly porphyritic cores with 15% 2-13mm ϕ euhedral to subhedral plagioclase mega-phenocrysts in a very fine grained matrix with 10% of 0.5-1mm ϕ euhedral to subhedral plagioclase phenocrysts. 2-4cm- thick fine grained purple rim with 10% of 0.5-1mm ϕ euhedral to subhedral plagioclase phenocrysts, <15% flatten chloritic disks up to 2mm ϕ concentrated in the outer rim (amygdules) and <10% calcite-filled amygdules and hollows in the cores;

iii) when pillows <30cm ϕ, not megaporphyritic, 10% of 0.5-1mm ϕ euhedral to subhedral plagioclase phenocrysts, not amygdaloidal, thin very fine grained rim (1-2cm-thick)

Large fine grained pillow tubes

Closely-packed fine grained pillow tubes

| Small closely-packed fine grained pillow tubes | **Folded** porphyritic amygdaloidal pillow tubes |
| Close up, porphyritic pillowed amygdaloidal alkali basalt flow (RL02-3-2; note flatten chlorite (arrow) pods) | Porphyritic pillowed amygdaloidal alkali basalt flow (RL02-3-2; note how all the plagioclase (P) are replaced) |
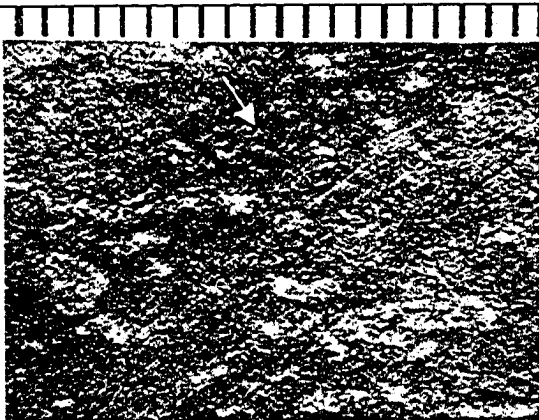
Massive alkali basalt intrusive rocks

Purplish to dark green coarse grained massive rock

Mineralogy

Large actinolite crystals overgrowing a fine grained quartzofelspathic epidote-rich matrix.

Texture

Massive coarse grained dyke/sill, +/- deformed
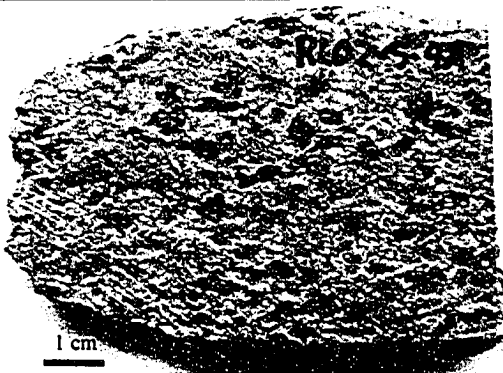
| Massive coarse grained dyke (RL02-5-4A) | Deformed mafic sill (RL02-12-2) |
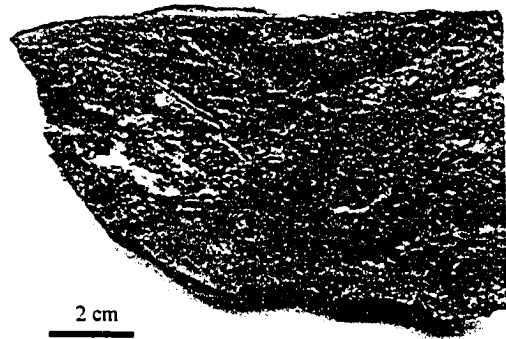
Volcanic breccia

Monomictic breccia / Brecciated flow (in situ)
- massive, pebble to cobble matrix-supported breccia showing up to 12 cm long dark purplish green porphyritic basaltic subangular clasts in a fine grained brownish carbonate-rich matrix;
- clasts: plagioclase-megaphyric basalt
- In places, the massive flows laterally/vertically become brecciated (in situ breccia)

Polymictic breccia
- massive, poorly sorted, polymictic pebble breccia beds showing up to 6cm long stretched volcanic and minor limy clasts in a fine grained epidote-chlorite-calcite matrix;
- volcanic component (80-90%): plagioclase-megaphyric basalt, fine grained basalt (pillow rim fragments?), plagioclase crystals, volcanic ash (chlorite+epidote);
- limy component (10-20%): massive fine-grained grey limestone, potentially minor recrystallized corals and crinoids
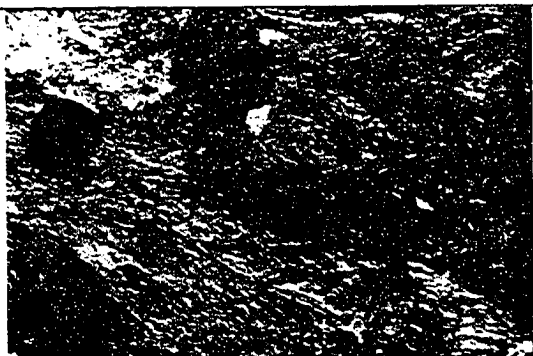
In situ brecciated porphyritic lava flow
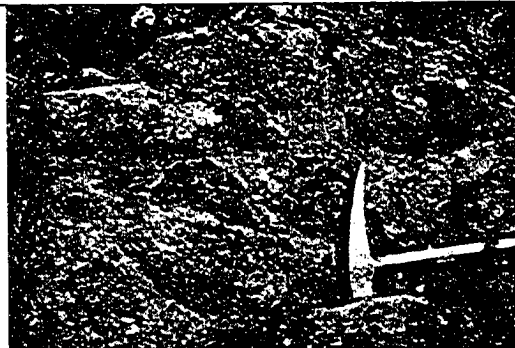
Monomictic volcanic breccia

Polymictic breccia showing stretched porphyritic fragments and limy fragments
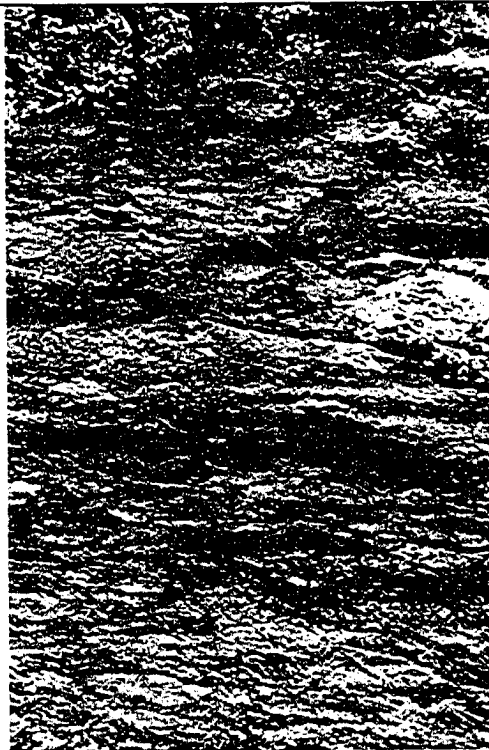
Polymictic breccia showing stretched mafic fragments and limy fragments

Massive crystal-rich volcanic breccia (RL02-8-8B).
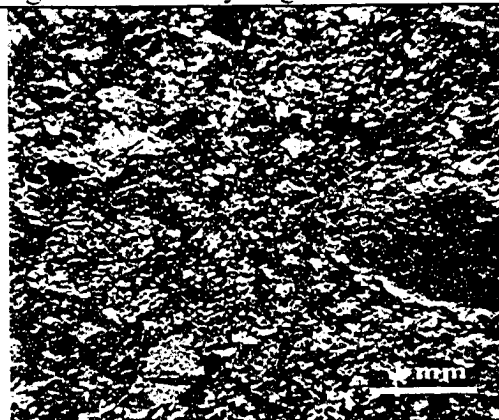
Close up massive crystal-rich volcanic breccia (RL02-8-8B).

Bedded tuff

massive to well-bedded medium-green tuff.

i) crystal-rich coarse-tuff: coarse plagioclase-crystal-tuff showing up to 30% of 0.5-2mm ϕ euhedral to subhedral crystals in a epidote-chlorite-calcite fine grained matrix (recrystallized and metamorphosed ashes); formed massive 2cm-10m-thick layers, laterally continuous, locally graded; interbedded with very very coarse grained crystal-tuff and ash-tuff.

ii) crystal-rich tuff-breccia: very very coarse plagioclase-crystal-tuff showing up to 70% of 2-15mm ϕ euhedral to subhedral crystals, commonly broken and/or fractured, in a epidote-chlorite-calcite fine grained matrix; formed massive 20cm->8m-thick poorly sorted layers, with rare inverse-graded base, and normal-graded top; usually laterally continuous over >30m, meter-long lenticular beds in places; interbedded with finer grained crystal- and ash-tuff; yielded Precambrian detrital zircons (G. Gehrels, pers. comm. 2003)

iii) ash-tuff: medium to dark green massive to well-bedded chlorite-rich fine grained (metamorphosed ash) laterally continuous layers, commonly showing flatten chlorite-disks along bedding plane, and graded-beds; interbedded with coarser tuffaceous beds and flows.

Well-bedded ash tuff

Well bedded ash tuff (chloritized)

Crystal-rich tuff-breccia
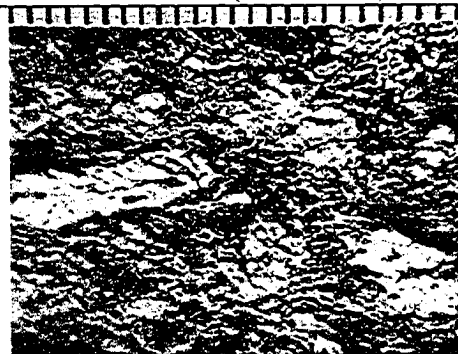
Close-up crystal-rich tuff-breccia (note broken crystal in lower right corner)

Exhalitive Mn-rich chert

pale green to pink to deep red finely bedded Mn-rich exhalative cherty layers; locally interbedded with ash-tuff layers
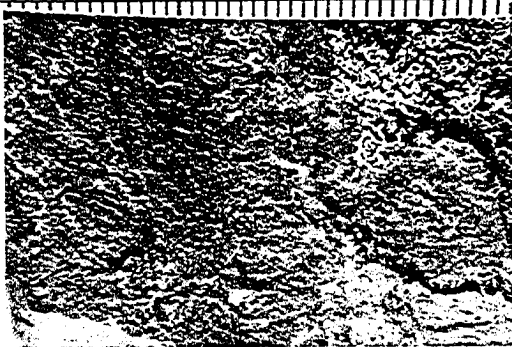
Mn-rich exhalative chert with fine hematite interbeds
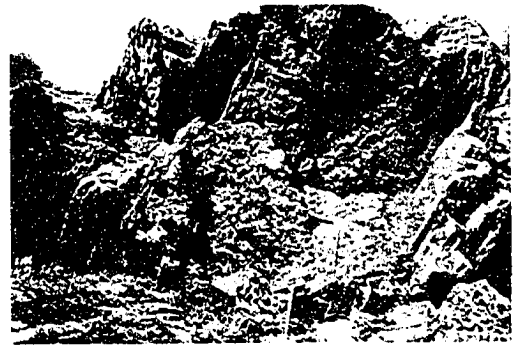
Mn-rich exhalative chert (hammer for scale)

Volcaniclastic sandstone and siltstone

light green, green, and beige well-bedded quartz-rich sandstone (quartz + muscovite ± carbonate ±chlorite ±magnetite) and siltstone (quartz +chlorite +muscovite ±carbonate ±magnetite) beds, commonly showing graded-beds; interpreted as epiclastic deposits
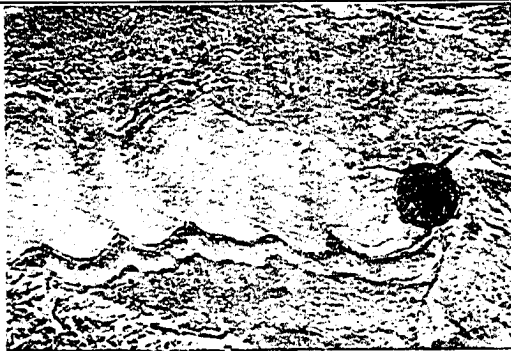
Well bedded volcaniclastic siltstone graded beds

Well bedded interbedded volcaniclastic sandstone and siltstone
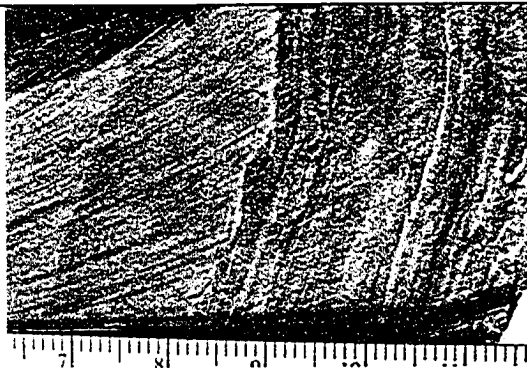
Well bedded siltstone and mudstone

Well bedded siltstone and mudstone

164
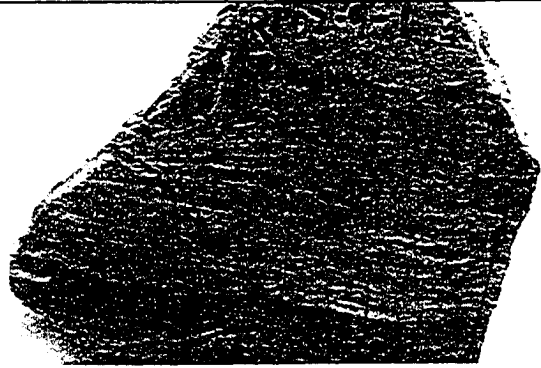
Quartzite-pebble to -boulder conglomerate

Quartzite-pebble to -boulder conglomerate of subangular to subrounded quartzite clasts, some of which contain a pre-depositional foliation, supported by a matrix of fine-grained quartz-rich sandstone (quartz +chlorite +muscovite +calcite; Gladwin et al., 2003). In places, beige to brown massive quartzite-pebble to- boulder matrix supported conglomerate interbedded with 50cm-3m-thick quartzite-rich conglomeratic sandstone and coarse sandstone beds; locally the sandstone beds show grading.

Quartzite pebbles and cobbles in a chloritic matrix. (Field of view is approximately 40 cm across; photo from Gladwin et al. 2003)

Quartz-rich sandstone and mudstone

Pale to medium green massive to well bedded quartz-rich sandstone to mudstone beds (quartz ±feldspar +muscovite +calcite ±epidote ±chlorite ±biotite ±apatite ±garnet), locally graded; interbedded with ash- and crystal-tuff layers in places;

i) thinly bedded fine grained quartz-rich mudstone to siltstone, locally graded, locally showing faint ripple structures

ii) massive to bedded quartz-rich sandstone, locally graded

Bedded quartz-rich sandstone to mudstone
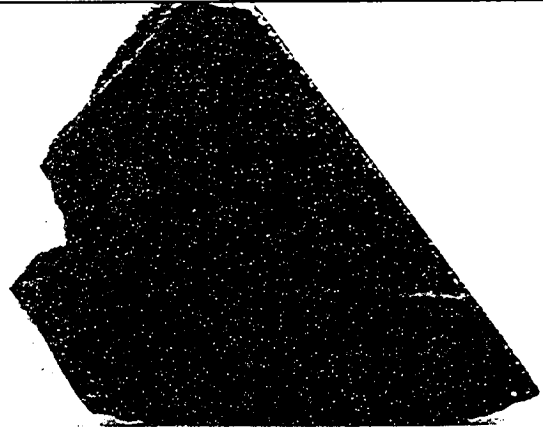
Bedded quartz-rich sandstone

Arkosic grit

Massive K-feldspar-rich grit beds (perthitic orthoclase + quartz ±muscovite ±chlorite ±calcite ±opaque) showing 2-4mm-long twinned feldspar and 1-2mmϕ blue quartz eye crystals

1 cm
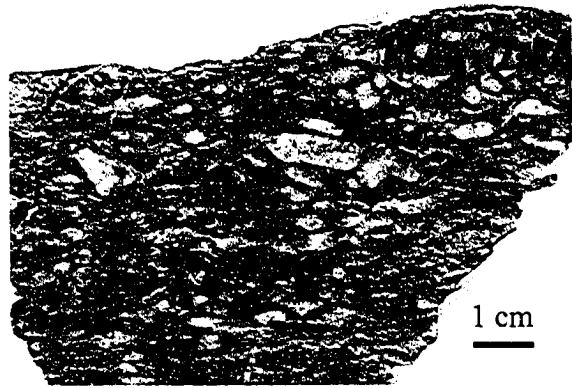
Little Salmon formation
lower succession

Felsic volcaniclastic sandstone and siltstone

Light green, green, and beige well-bedded quartz-rich sandstone (quartz +muscovite ±carbonate ±chlorite ±magnetite) and siltstone (quartz +chlorite +muscovite ±carbonate ±magnetite) beds

Finely bedded felsic volcaniclastic rocks

Finely bedded felsic volcaniclastic rocks

Quartz-feldspar porphyry

White to light pink massive quartz-feldspar porphyry, sheared.

*=in diameter

166

Challenges of the Little Salmon formation

Broadly folds in competent quartz-rich units

Kink-band folds, in places, in mafic unit

Appendix 2

Little Salmon formation geochemical analyses

Appendix 2 - Analyses of the Little Salmon formation

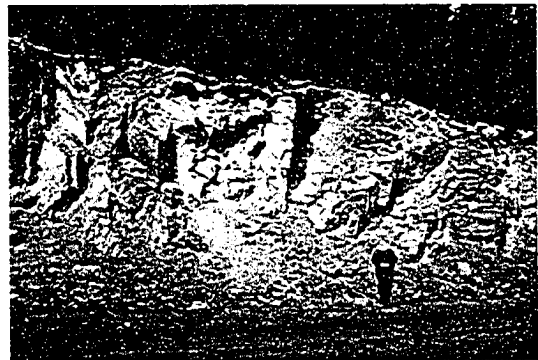|	Northern Upper succession								
	Massive volcanic rocks							Volcaniclastic rocks	
	(a) Massive porphyritic flow	(b) Massive porphyritic flow	(c) Massive porphyritic flow	(d) Pillowed porphyritic flow	(e) Massive flow	(f) Leucogabbro	(g) Sill	(h) Volcanic breccia	(i) Volcanic breccia
Lithology SAMPLE	RL02-4-7A	RL02-6-5	RL02-11-13	RL02-3-2	RL02-14-1	RL02-5-4A	RL02-12-2	RL02-4-7B	RL02-6-3
SiO_2 (%)	44.78	49.79	41.97	47.63	49.93	46.26	46.79	47.76	45.82
Al_2O_3	14.66	16.46	17.36	18.73	15.69	17.39	14.06	16.46	17.30
Fe_2O_3	10.70	12.72	12.68	8.89	8.35	9.72	11.38	11.17	13.23
MnO	0.17	0.18	0.17	0.16	0.10	0.15	0.21	0.23	0.22
MgO	8.24	2.46	8.93	2.53	8.01	7.74	6.88	4.90	5.95
CaO	12.11	8.71	6.53	9.56	4.84	7.10	11.19	9.89	6.62
Na_2O	1.48	2.39	3.01	2.41	4.40	3.01	2.16	2.96	2.79
K_2O	1.21	1.23	0.08	1.40	0.16	1.98	0.35	0.84	0.84
TiO_2	2.08	2.47	2.53	2.06	2.29	2.29	1.58	2.08	2.41
P_2O_5	0.48	1.16	0.68	0.48	0.51	0.37	0.14	0.74	1.01
LOI	3.12	2.67	6.30	6.25	5.89	4.18	4.18	2.88	3.91
TOTAL	99.05	100.24	100.23	100.08	100.15	100.19	98.91	99.88	100.09
Cr (ppm)	476	366	236	125	106	177	239	185	56
Ni	172	87	104	69	38	-	53	77	-
Co	47	41	51	35	23	36	36	36	35
V	233	218	230	155	238	297	355	170	122
Zn	117	210	150	167	141	128	98	113	130
Cu	127	154	134	61	118	88	84	113	87
Rb	25	26	2	27	3	32	7	19	13
Ba	515.60	270.25	58.51	184.43	29.01	782.90	80.12	269.49	615.38
Sr	588	718	823	487	119	325	354	628	504
Ga	18	21	21	18	22	22	18	20	19
Ta	3.58	3.82	4.37	2.23	2.41	1.68	0.19	4.55	4.88
Nb	53.34	63.28	63.51	28.67	35.12	32.08	3.42	73.20	77.36
Hf	3.18	3.42	3.49	3.46	5.11	3.97	2.41	3.73	3.82
Zr	133	149	146	167	256	185	86	172	175
Y	24	46	27	29	34	29	38	29	33
Th	3.60	3.81	4.67	2.73	3.18	2.11	0.36	4.81	5.03
U	0.93	1.14	1.16	0.58	1.43	0.63	0.22	1.33	1.29
Sc	27.30	23.20	22.50	28.80	26.10	32.60	41.90	18.50	12.30
La	37.49	60.39	44.29	28.19	29.44	21.18	5.26	49.38	54.73
Ce	66.69	79.26	78.03	52.16	57.96	43.20	13.18	87.21	98.94
Pr	6.72	9.55	8.15	5.49	6.45	4.67	2.08	8.51	9.89
Nd	28.16	41.26	33.35	23.63	28.58	21.38	11.50	34.79	41.35
Sm	6.36	8.15	6.98	5.55	6.61	5.38	4.10	7.10	8.51
Eu	2.14	2.86	2.35	2.05	2.27	2.00	1.49	2.46	2.86
Gd	5.21	7.54	5.77	5.17	5.78	4.99	5.04	5.81	6.81
Tb	0.86	1.17	0.93	0.90	1.06	0.91	1.02	0.97	1.14
Dy	4.62	6.90	5.21	5.07	6.28	5.26	6.71	5.33	6.06
Ho	0.86	1.40	1.00	0.99	1.25	1.06	1.43	1.03	1.16
Er	2.26	4.01	2.66	2.75	3.53	2.92	4.09	2.81	3.12
Tm	0.33	0.60	0.38	0.42	0.54	0.44	0.65	0.41	0.46
Yb	1.93	3.70	2.30	2.47	3.35	2.68	4.01	2.54	2.75
Lu	0.26	0.57	0.32	0.35	0.48	0.39	0.59	0.37	0.39
$^{147}Sm/^{144}Nd$	-	-	-	-	0.1377	-	0.2052	0.119	-
$^{143}Nd/^{144}Nd$	-	-	-	-	0.512883	-	0.513043	0.512823	-
$^{87}Sr/^{86}Sr$	-	-	-	-	0.705343	-	0.714756	0.703825	-
Th/Nb	0.07	0.06	0.07	0.10	0.09	0.07	0.10	0.07	0.07
La/Sm	5.90	7.41	6.35	5.08	4.46	3.94	1.28	6.95	6.43
Th/Yb	1.87	1.03	2.03	1.10	0.95	0.79	0.09	1.89	1.83
Nb/Yb	27.62	17.13	27.61	11.59	10.49	11.97	0.85	28.83	28.16
Nb/U	57.10	55.51	54.97	49.50	24.60	50.58	15.50	55.12	59.76
Zr/Y	5.48	3.23	5.39	5.68	7.42	6.29	2.25	5.92	5.34
Th/La	0.10	0.06	0.11	0.10	0.11	0.10	0.07	0.10	0.09
$(La/Yb)_N$	13.92	11.72	13.81	8.18	6.31	5.67	0.94	13.95	14.29
UTME*	506685	507422	509623	507060	505360	503785	515208	506685	507486
UTMN*	6909615	6908730	6906866	6910262	6905852	6906917	6908597	6909615	6908904

$(La/Yb)N$ - chondrite normalized values

*Zone 8, NAD 83

169

Appendix 2 - Analyses of the Little Salmon formation

	Northern Upper succession						Northern Upper succession		
	Volcaniclastic rocks						Volcaniclastic rocks		
	(j)	(k)	(l)	(m)	(n)	(o)	(p)	(q)	(r)
Lithology SAMPLE	Volcanic breccia RL02-7-4	Volcanic breccia RL02-8-8B	Plagioclase-crystal tuff RL02-5-7	Plagioclase-crystal tuff RL02-5-8A	Plagioclase-crystal tuff RL02-5-8D	Crystal-tuff RL02-8-7	Ash tuff RL02-3-2b	crystal tuff RL02-4-1c	Ash tuff RL02-4-9
SiO_2 (%)	50.91	44.27	42.73	42.18	45.13	46.86	45.79	54.55	47.45
Al_2O_3	18.04	16.10	14.62	15.11	17.52	17.17	17.30	16.03	17.23
Fe_2O_3	12.03	8.91	10.53	9.12	8.15	8.49	11.09	6.94	11.12
MnO	0.11	0.15	0.15	0.20	0.20	0.16	0.19	0.12	0.15
MgO	3.22	7.69	4.56	5.49	4.17	7.52	7.16	2.90	5.53
CaO	5.53	8.53	9.75	14.57	12.67	6.96	8.22	9.45	7.19
Na_2O	2.99	2.96	4.30	2.16	3.28	2.72	2.39	3.65	2.57
K_2O	1.94	1.01	0.42	0.11	0.79	3.04	0.38	0.67	2.33
TiO_2	1.96	1.72	2.84	1.96	1.57	1.70	2.27	0.77	1.86
P_2O_5	0.46	0.51	0.60	0.39	0.32	0.55	0.50	0.17	0.49
LOI	2.84	7.42	8.80	7.82	6.21	5.04	5.17	5.06	3.52
TOTAL	100.04	99.25	99.30	99.11	100.01	100.23	100.46	100.30	99.44
Cr (ppm)	707	318	51	260	277	80	355	58	379
Ni	110	123	23	91	106	54	146	28	122
Co	55	39	30	38	39	30	61	15	48
V	264	175	287	245	215	186	205	188	232
Zn	226	126	107	129	114	117	168	110	168
Cu	141	110	75	137	192	98	68	120	103
Rb	47	23	15	2	16	67	8	13	46
Ba	475.05	425.89	89.05	30.24	134.69	973.87	88.86	344.93	390.00
Sr	309	678	269	605	437	680	587	502	619
Ga	21	19	21	18	19	21	18	18	20
Ta	2.35	3.54	2.37	1.92	1.51	4.78	2.87	0.12	3.05
Nb	40.28	61.37	38.38	33.43	28.83	76.10	38.65	7.88	49.81
Hf	2.94	3.24	5.91	3.48	2.79	3.59	4.50	1.96	3.64
Zr	133	152	275	164	142	171	210	77	174
Y	27	23	46	26	23	26	29	17	25
Th	2.40	4.31	3.07	2.47	1.96	7.16	3.51	1.03	4.64
U	0.51	1.16	0.56	0.61	0.54	1.96	1.03	0.61	0.96
Sc	35.30	19.90	23.80	28.60	25.40	16.90	29.20	18.00	26.30
La	36.23	37.65	31.18	23.74	19.95	51.79	33.18	8.60	33.15
Ce	58.22	66.47	64.88	46.14	39.17	84.47	61.30	18.26	57.49
Pr	6.40	6.67	7.22	4.88	4.19	8.20	6.18	2.26	5.67
Nd	27.67	27.44	32.34	21.23	18.06	32.66	26.04	10.82	23.43
Sm	5.84	5.62	8.11	5.13	4.40	6.18	6.16	2.91	5.29
Eu	2.06	1.97	2.66	1.78	1.58	2.12	2.19	1.01	1.82
Gd	5.25	4.76	7.65	4.66	4.04	5.13	5.43	2.78	4.61
Tb	0.88	0.78	1.37	0.82	0.72	0.84	0.96	0.49	0.80
Dy	5.01	4.30	8.20	4.76	4.08	4.91	5.40	2.81	4.51
Ho	0.98	0.84	1.68	0.93	0.81	0.94	1.06	0.59	0.88
Er	2.67	2.25	4.78	2.53	2.22	2.60	2.85	1.67	2.39
Tm	0.40	0.34	0.70	0.37	0.33	0.39	0.41	0.26	0.36
Yb	2.45	2.12	4.39	2.33	1.98	2.42	2.46	1.60	2.19
Lu	0.34	0.30	0.63	0.34	0.28	0.35	0.36	0.24	0.31
$^{147}Sm/^{144}Nd$	-	-	-	-	0.1348	-	-	-	-
$^{143}Nd/^{144}Nd$	-	-	-	-	0.512869	-	-	-	-
$^{87}Sr/^{86}Sr$	-	-	-	-	0.703725	-	-	-	-
Th/Nb	0.06	0.07	0.08	0.07	0.07	0.09	0.09	0.13	0.09
La/Sm	6.20	6.70	3.84	4.63	4.54	8.37	5.39	2.96	6.26
Th/Yb	0.98	2.03	0.70	1.06	0.99	2.95	1.43	0.65	2.12
Nb/Yb	16.45	28.91	8.74	14.33	14.54	31.39	15.73	4.94	22.78
Nb/U	79.48	52.92	69.10	54.74	53.87	38.87	37.55	12.87	51.93
Zr/Y	4.85	6.54	5.96	6.27	6.28	6.53	7.27	4.43	7.02
Th/La	0.07	0.11	0.10	0.10	0.10	0.14	0.11	0.12	0.14
$(La/Yb)_N$	10.61	12.72	5.09	7.30	7.22	15.32	9.69	3.86	10.88
UTME*	506898	508361	504051	504418	504418	508255	507060	506876	506607
UTMN*	6908663	6907337	6907322	6907591	6907591	6907225	6910262	6909349	6909430

(La/Yb)N - chondrite normalized values

*Zone 8, NAD 83

170

	Northern Upper succession			Southern Upper succession				
	Volcaniclastic rocks	Exhalative chert		Epiclastic rocks				
	(s)	(t)	(u)	(v)	(w)	(x)	(y)	(z)
Lithology	Ash tuff	Mn-chert	Mn-chert	Arkosic sandstone	Epiclastic rock	Epiclastic rock	Fine grained green rock	qtz-rich sediments
SAMPLE	RL02-5-10	RL02-4-6	RL02-6-8	RL02-2-6	RL02-9-1	RL02-9-2	RL02-10-3	RL02-11-5
SiO2 (%)	47.30	90.70	94.15	52.20	60.38	70.27	61.48	62.04
Al2O3	14.69	3.45	2.25	16.00	14.47	11.72	12.71	14.54
Fe2O3	9.25	1.72	1.07	10.17	8.88	4.87	9.73	8.32
MnO	0.19	0.76	0.09	0.23	0.17	0.09	0.13	0.10
MgO	2.45	0.68	0.82	3.31	3.32	2.44	3.00	4.92
CaO	9.79	1.30	0.27	5.62	5.21	2.17	4.96	2.51
Na2O	6.49	0.06	0.06	5.61	3.99	2.20	2.81	2.01
K2O	0.15	0.56	0.33	0.58	0.69	2.23	0.48	1.56
TiO2	2.59	0.22	0.12	0.98	0.85	0.59	0.85	0.88
P2O5	0.64	0.08	0.04	0.24	0.18	0.13	0.17	0.23
LOI	6.83	0.70	0.70	4.00	2.22	3.06	3.73	3.27
TOTAL	100.36	100.22	99.90	98.94	100.36	99.77	100.05	100.39
Cr (ppm)	101	22	-20	24	-	111	-	-
Ni	26	25	-	-	-	39	-	-
Co	29	20	7	26	25	7	25	22
V	268	10	9	226	252	107	251	218
Zn	133	81	76	176	152	126	158	156
Cu	111	159	69	175	118	117	175	139
Rb	2	17	10	10	12	71	10	34
Ba	23.59	1570.00	1140.00	555.53	284.54	1330.00	285.55	1060.00
Sr	224	141	48	377	426	123	391	221
Ga	14	7	5	19	19	16	18	20
Ta	2.71	0.32	0.18	0.15	0.28	0.71	0.15	0.13
Nb	42.14	8.18	16.28	2.78	17.46	17.72	9.59	7.59
Hf	4.97	1.04	0.80	2.62	2.53	2.85	2.34	2.79
Zr	244	44	35	98	95	114	88	102
Y	36	10	5	26	22	21	21	26
Th	3.29	2.24	1.57	1.75	1.60	6.41	1.53	1.34
U	0.57	0.14	0.18	0.92	0.54	1.92	0.47	0.58
Sc	22.20	5.70	4.30	27.90	23.50	11.60	23.80	20.40
La	32.77	11.37	6.19	13.93	11.86	23.30	10.44	12.21
Ce	62.49	33.26	18.83	30.62	26.72	43.25	24.06	27.08
Pr	6.70	2.31	1.41	3.73	3.39	4.75	3.09	3.53
Nd	29.60	10.19	5.91	17.10	16.35	19.43	14.76	17.34
Sm	6.84	2.41	1.41	4.75	4.08	4.27	3.96	4.65
Eu	2.24	0.57	0.30	1.54	1.27	1.10	1.24	1.45
Gd	6.13	1.86	1.10	4.17	3.91	3.66	3.62	4.56
Tb	1.10	0.36	0.20	0.71	0.66	0.62	0.63	0.76
Dy	6.28	2.08	1.16	4.27	3.85	3.63	3.74	4.47
Ho	1.28	0.40	0.22	0.87	0.79	0.73	0.75	0.91
Er	3.54	1.08	0.63	2.51	2.27	2.05	2.15	2.60
Tm	0.55	0.17	0.09	0.38	0.36	0.31	0.33	0.39
Yb	3.31	1.05	0.62	2.49	2.21	2.03	2.12	2.51
Lu	0.49	0.16	0.09	0.36	0.33	0.30	0.32	0.37
$^{147}Sm/^{144}Nd$	0.1319	-	-	-	-	-	-	-
$^{143}Nd/^{144}Nd$	0.512878	-	-	-	-	-	-	-
$^{87}Sr/^{86}Sr$	0.704477	-	-	-	-	-	-	-
Th/Nb	0.08	0.27	0.10	0.63	0.09	0.36	0.16	0.18
La/Sm	4.79	4.72	4.40	2.93	2.91	5.46	2.64	2.63
Th/Yb	0.99	2.12	2.53	0.70	0.73	3.16	0.72	0.54
Nb/Yb	12.73	7.76	26.18	1.12	7.92	8.72	4.53	3.03
Nb/U	73.83	58.58	91.21	3.02	32.47	9.22	20.54	13.14
Zr/Y	6.78	4.38	6.50	3.82	4.35	5.57	4.27	3.95
Th/La	0.10	0.20	0.25	0.13	0.13	0.28	0.15	0.11
(La/Yb)N	7.10	7.73	7.15	4.01	3.86	8.23	3.53	3.49
UTME*	505863	506496	507334	518402	509264	509590	510964	510733
UTMN*	6905586	6909510	6908274	6897860	6908762	6908852	6908914	6907511

(La/Yb)N - chondrite normalized values
*Zone 8, NAD 83

	Southern Upper succession								
	Epiclastic rocks				Siliciclastic rocks				
	(aa)	(bb)	(cc)	(dd)	(ee)	(ff)	(gg)	(hh)	(ii)
Lithology SAMPLE	Volcaniclastic RL02-14-7	Volcaniclastic RL02-14-10	Epiclastic rock RL02-17-1	Epiclastic rock RL02-17-4	K-spar Grits RL02-12-5A	Arkosic Grits RL02-12-7	Arkosic Grits RL02-13-5	Green Sandstone RL02-2-10	Green Sandstone RL02-16-1
SiO2 (%)	58.37	57.24	56.05	47.81	64.09	60.53	66.75	82.71	76.42
Al2O3	16.23	15.61	12.32	15.75	15.04	14.54	15.04	7.58	11.71
Fe2O3	8.01	5.98	6.82	10.69	4.58	6.55	3.91	2.54	2.30
MnO	0.17	0.12	0.21	0.15	0.08	0.12	0.06	0.05	0.06
MgO	3.40	2.98	2.00	5.48	1.43	5.61	3.94	1.25	0.82
CaO	4.80	6.21	10.63	10.46	2.15	4.36	0.92	0.96	1.16
Na2O	4.92	4.93	3.66	3.44	1.91	3.12	4.08	1.78	4.83
K2O	0.14	1.25	0.97	0.91	6.67	1.88	2.13	1.11	1.44
TiO2	0.86	0.73	0.79	2.40	0.41	0.73	0.48	0.42	0.51
P2O5	0.22	0.13	0.24	0.44	0.14	0.17	0.14	0.12	0.14
LOI	2.38	4.55	6.60	2.46	3.29	2.72	2.54	1.72	0.77
TOTAL	99.50	99.71	100.29	99.98	99.79	100.32	99.99	100.23	100.15
Cr (ppm)	61	40	-	91	-	225	47	78	31
Ni	53	-	-	65	-	45	31	23	-
Co	19	10	11	29	7	25	12	4	3
V	172	149	123	218	32	156	62	82	35
Zn	133	70	110	116	129	128	131	81	62
Cu	131	93	108	104	84	68	86	69	61
Rb	2	18	24	16	302	56	68	38	44
Ba	102.30	377.70	700.82	129.17	1220.00	830.85	495.83	936.20	706.68
Sr	140	414	544	412	176	365	228	71	110
Ga	17	15	14	17	20	19	18	10	10
Ta	0.20	0.17	0.29	1.59	2.63	0.63	0.78	0.42	0.78
Nb	3.60	2.85	4.99	19.28	34.00	16.43	13.40	6.31	9.77
Hf	3.04	2.09	3.42	5.47	6.08	3.37	3.23	1.72	4.58
Zr	105	72	121	248	255	140	128	72	169
Y	23	15	27	36	21	18	17	11	20
Th	1.96	1.14	2.57	1.99	60.24	8.85	8.55	3.69	13.56
U	0.91	0.61	1.11	0.81	15.88	1.82	1.53	1.31	3.71
Sc	23.50	17.30	17.60	27.80	5.00	20.80	9.30	6.10	6.70
La	10.96	7.82	15.23	19.60	77.43	22.77	19.93	12.80	33.39
Ce	23.27	16.26	30.20	43.81	126.93	40.47	67.86	23.85	63.13
Pr	3.03	2.16	3.82	5.36	11.62	4.19	3.75	2.58	6.68
Nd	14.93	10.79	18.30	25.48	40.28	17.20	15.25	10.76	26.50
Sm	3.86	2.71	4.60	6.45	6.59	3.59	3.37	2.31	5.21
Eu	1.21	0.95	1.33	2.23	1.17	1.05	0.98	0.54	1.05
Gd	3.73	2.63	4.42	6.41	4.34	3.15	2.79	1.87	3.90
Tb	0.68	0.46	0.81	1.16	0.68	0.51	0.52	0.33	0.65
Dy	4.17	2.82	4.84	7.03	3.70	3.01	3.15	1.84	3.74
Ho	0.84	0.56	1.01	1.42	0.71	0.60	0.62	0.37	0.75
Er	2.47	1.59	2.90	3.96	2.06	1.70	1.71	1.04	2.16
Tm	0.38	0.24	0.45	0.59	0.32	0.26	0.24	0.17	0.34
Yb	2.45	1.57	2.90	3.72	2.09	1.71	1.57	1.03	2.17
Lu	0.36	0.24	0.45	0.54	0.31	0.25	0.23	0.15	0.33
$^{147}Sm/^{144}Nd$	-	-	0.1453	-	0.0985	0.1251	-	-	-
$^{143}Nd/^{144}Nd$	-	-	0.512821	-	0.511648	0.512091	-	-	-
$^{87}Sr/^{86}Sr$	-	-	0.705579	-	0.73267	0.720333	-	-	-
Th/Nb	0.54	0.40	0.52	0.10	1.77	0.54	0.64	0.59	1.39
La/Sm	2.84	2.89	3.31	3.04	11.75	6.35	5.92	5.55	6.41
Th/Yb	0.80	0.73	0.89	0.53	28.79	5.18	5.45	3.58	6.24
Nb/Yb	1.47	1.82	1.72	5.19	16.25	9.62	8.54	6.11	4.49
Nb/U	3.96	4.68	4.51	23.92	2.14	9.05	8.73	4.81	2.63
Zr/Y	4.67	4.88	4.42	6.81	11.94	7.85	7.59	6.51	8.56
Th/La	0.18	0.15	0.17	0.10	0.78	0.39	0.43	0.29	0.41
(La/Yb)N	3.21	3.57	3.77	3.78	26.55	9.56	9.11	8.90	11.02
UTME*	511002	511461	523539	524467	514902	514460	516851	521663	522525
UTMN*	6902386	6903602	6896280	6896282	6908367	6908281	6905486	6896648	6896653

(La/Yb)N - chondrite normalized values
*Zone 8, NAD 83

172

Appendix 2 - Analyses of the Little Salmon formation

	Southern Upper succession		
	Siliciclastic rocks		
	(jj)	(kk)	(ll)
Lithology SAMPLE	Green Sandstone RL02-16-2	Green Sandstone RL02-16-3B	Green Sandstone FD02-2-9
SiO2 (%)	82.50	64.81	55.92
Al2O3	7.38	14.62	6.50
Fe2O3	2.57	7.00	2.30
MnO	0.06	0.12	0.55
MgO	1.24	2.30	1.01
CaO	1.19	3.32	16.20
Na2O	2.02	1.08	1.62
K2O	0.85	3.08	0.99
TiO2	0.41	0.73	0.29
P2O5	0.10	0.19	0.06
LOI	1.68	2.79	13.42
TOTAL	99.96	100.04	98.86
Cr (ppm)	61	48	73
Ni	-	36	25
Co	4	12	-
V	63	84	48
Zn	80	149	69
Cu	66	97	69
Rb	29	96	35
Ba	769.13	3340.00	770.38
Sr	76	444	484
Ga	8	19	8
Ta	0.52	0.85	0.30
Nb	6.48	11.10	4.10
Hf	2.14	5.09	1.38
Zr	81	185	56
Y	11	31	14
Th	4.61	12.58	3.36
U	1.42	3.76	0.97
Sc	6.30	14.90	5.30
La	13.15	34.72	13.35
Ce	23.85	67.55	23.72
Pr	2.81	7.37	2.49
Nd	11.52	31.59	10.38
Sm	2.45	6.88	2.22
Eu	0.61	1.59	0.55
Gd	2.03	5.57	1.87
Tb	0.34	0.97	0.33
Dy	2.07	5.78	1.93
Ho	0.42	1.14	0.40
Er	1.21	3.33	1.19
Tm	0.19	0.52	0.18
Yb	1.22	3.38	1.20
Lu	0.18	0.52	0.18
$^{147}Sm/^{144}Nd$	-	-	-
$^{143}Nd/^{144}Nd$	-	-	-
$^{87}Sr/^{86}Sr$	-	-	-
Th/Nb	0.71	1.13	0.82
La/Sm	5.38	5.05	6.01
Th/Yb	3.78	3.72	2.80
Nb/Yb	5.30	3.28	3.42
Nb/U	4.56	2.95	4.21
Zr/Y	7.23	6.04	4.03
Th/La	0.35	0.36	0.25
(La/Yb)$_N$	7.72	7.36	7.99
UTME*	522606	522745	520674
UTMN*	6896866	6896994	6897509

(La/Yb)N - chondrite normalized values
*Zone 8, NAD 83

173

Appendix 3

Analytical method for Nd-Sm and Sr isotopes

Sm and Nd concentrations and Sr and Nd isotopic compositions for this study were determined at the Analytical Geochemistry Group laboratory, Memorial University of Newfoundland, St. John's, Newfoundland, following the methodology[1] described below.

Approximately 0.1 g of rock powder is dissolved in Savilex Teflon beakers using a mixture of concentrate HF – HNO3 acids. A mixed $^{150}Nd/^{149}Sm$ spike is added to each sample prior to acid digestion. Both sample and spike are weighed on a high-precision balance. After five days of digestion, the solution is evaporated to dryness and then taken up in 6N HCl acid for two days. The solution is then dried and taken up in 2.5N HCl and loaded on cationic exchange chromatography using AG50W – X8 resin to collect the REE fractions on one hand and Sr and Rb on the other hand (this chemistry is done twice to purify the Sr). The REE fractions are then purified and Sm and Nd are isolated using a secondary column loaded with Eichrom Ln resin. Sr is separated with the resin Spec Sr. All reagents are purified in order to insure a low contamination level. The measured total chemical blanks range between 40 and 90 pg and are considered negligible.

Sm and Nd concentrations and Sr and Nd isotopic compositions were analyzed using a multicollector Finnigan Mat 262 mass spectrometer in static mode. Nd isotopic ratios are normalized to $^{146}Nd/^{144}Nd = 0.7219$. The reported values were adjusted to the La Jolla Nd standard ($^{143}Nd/^{144}Nd = 0.511860$). During the course of data acquisition, replicates of the standard give a mean value of $^{143}Nd/^{144}Nd = 0.511885 \pm 15$ (2σ, n=25). The in-run precisions on Nd isotopic ratio are given at 95% confidence level. Errors on Nd isotopic compositions are <0.002% and errors on the 147Sm/144Nd ratio are estimated to be lower than 0.1%.

Sr isotopic ratios are normalized to $^{88}Sr/^{86}Sr=8.375209$. Reported Sr values are adjusted to the NBS 987 Standard ($^{87}Sr/^{86}Sr=0.710340$). Replicates of the standard gave a mean value of $^{87}Sr/^{86}Sr=0.710285 \pm 13$ (2σ, N=6). Errors on Sr isotopic compositions are <0.002%.

---

[1] Provided by Dr. Marc Poujol via email on August 26, 2004, Analytical Geochemistry Group, Department of Earth Sciences, 300 Prince Philip Drive, Memorial University of Newfoundland, St. John's NL A1B 3X5 Canada, Tel: +1 709 737 3076, Fax: +1 709 737 2589, Email: mpoujol@esd.mun.ca
Web: http://www.esd.mun.ca/xrficp/ , Personal Web Page: http://www.esd.mun.ca/~mpoujol/

Appendix 4

Klinkit Group rock descriptions

Appendix 4 – Klinkit Group rock descriptions

Butsih Formation[1]
Volcaniclastic member

Volcanic breccia (S-C)

Clasts/Lithics:

- plagioclase-phyric clasts (60% plagioclase crystals in quartzofeldspathic matrix; 3-4 cm φ clasts)
- plagioclase-phyric clasts (20% plagioclase crystals in biotite-rich (80%) quartzofeldspathic matrix)

Crystals:
- Plagioclase crystals (5%)

Matrix:
- The matrix is composed of very fine grained quartzofeldspathic, suggesting devitrified glass.

Unit thickness: 6-8 m total

Coarse crystal/lithic tuff (36-B, S-A1, S-A2, 36-G, 36-H, 33-2, 36-A, S-M12, 36-1A2)

Crystals (up to 45%):
- Plagioclase (subrounded)
- Clinopyroxene (subrounded/partly replaced by hornblende)
- Hornblende (primary?)

Lithics (up to 35%):
- Plagioclase-phyric basaltic clasts (~45%)
- Plagioclase-hornblende-phyric basaltic clasts (~35%)
- Fine grained clasts (~10%)
- Chert (recrystallized quartz) (~3%)
- Biotite-rich clasts (~3%)

Matrix (<10%):
- Very fine grained quartzofeldspathic material in between clasts/crystals, sometime showing biotite overgrowth. Opaque rims around some clasts. The more metamorphosed these tuffs are, the more hornblende- (+/- actinolite), epidote-, and biotite-rich they are.

---

[1] See stratigraphic columns in this appendix for sample location
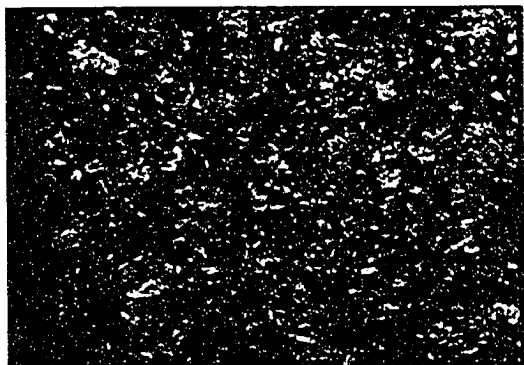
36-1A2 2X, NL (field of view: 5mm)
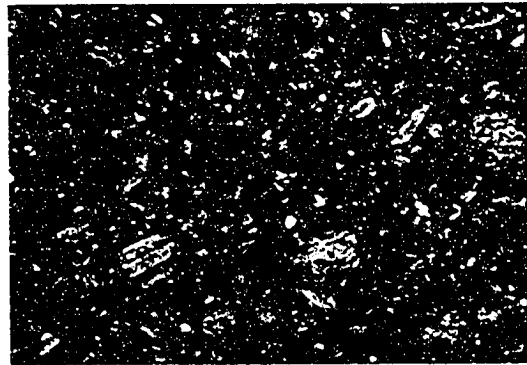
36-1A2 2X, PL (field of view: 5mm)
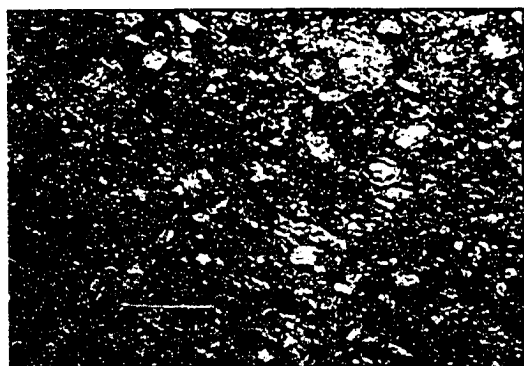
36-A 1X, NL (field of view: 10mm)
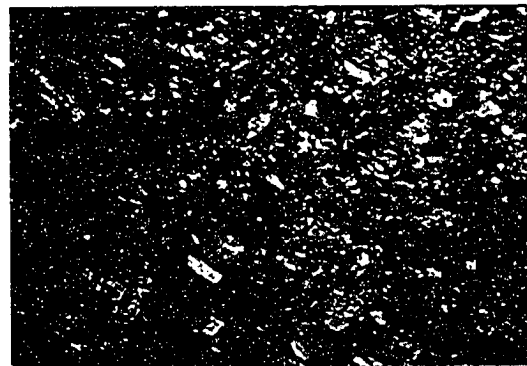
36-A 1X, PL (field of view: 10mm)

36-A 5X, NL (field of view: 2mm)
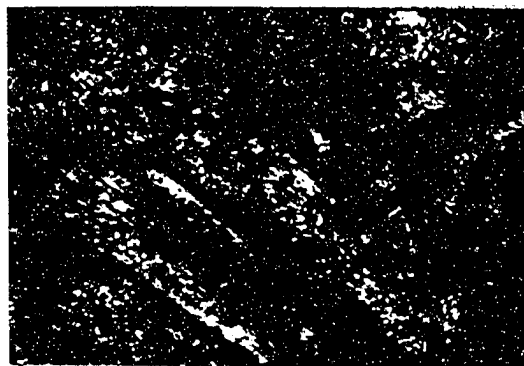
36-A 5X, PL (field of view: 2mm)
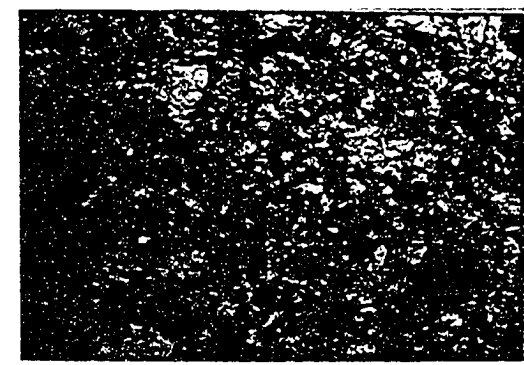
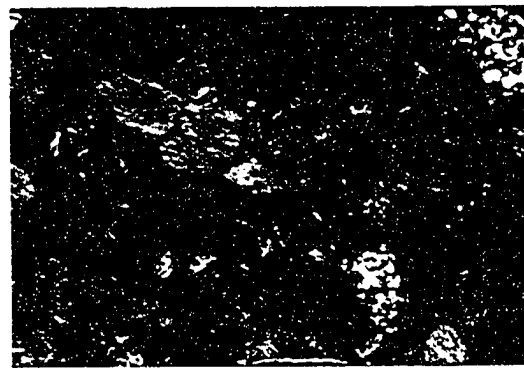S-A2 1X, NL (field of view: 10mm)
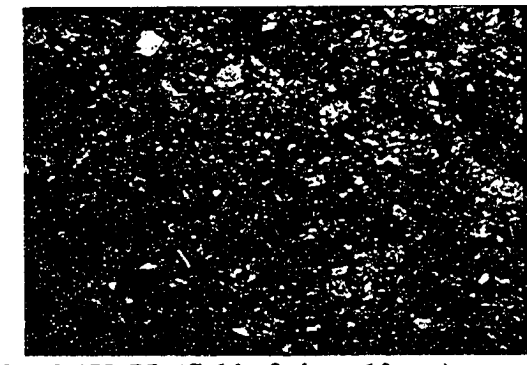
S-A2 1X, PL (field of view: 10mm)

S-A2 5X, NL (field of view: 2mm)

S-A2 5X, PL (field of view: 2mm)

S-M12 5X, NL (field of view: 2mm)
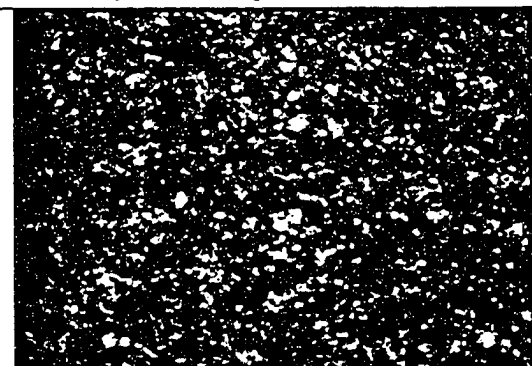

S-M12 5X, NL (field of view: 2mm)

Fine grained crystal/ash tuff (36-C, S-K, S-J, S-H, S-L, S-E, S-D, S-G)

Crystals (up to 25%):
- Very small plagioclase (angular)
- Very small quartz (angular)

Matrix:
- Very fine grained recrystallized quartzofeldspathic matrix with actinolite, epidote, and +/- opaque (devitrified glass?) (5-25% crystals; samples 36-C, S-K, S-J, S-H)
- Some beds show a carbonate-rich +/- quartzofeldspathic matrix with +/- actinolite (0-5% crystals; samples S-L, S-E)
- Others show a biotite-rich +/- quartzofeldspathic matrix (0-5% small broken crystals; samples S-D, S-G)
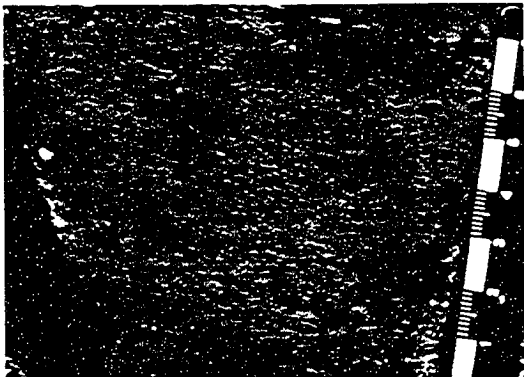

S-K 5X, NL (field of view: 2mm)

S-K 5X, NL (field of view: 2mm)

178
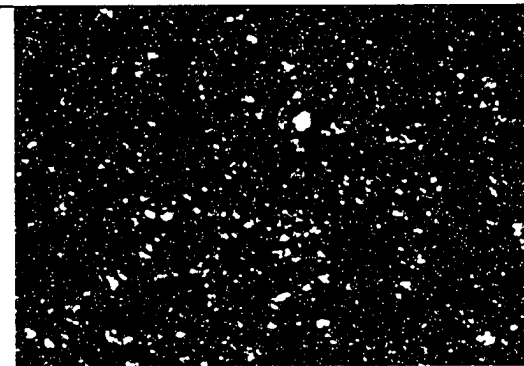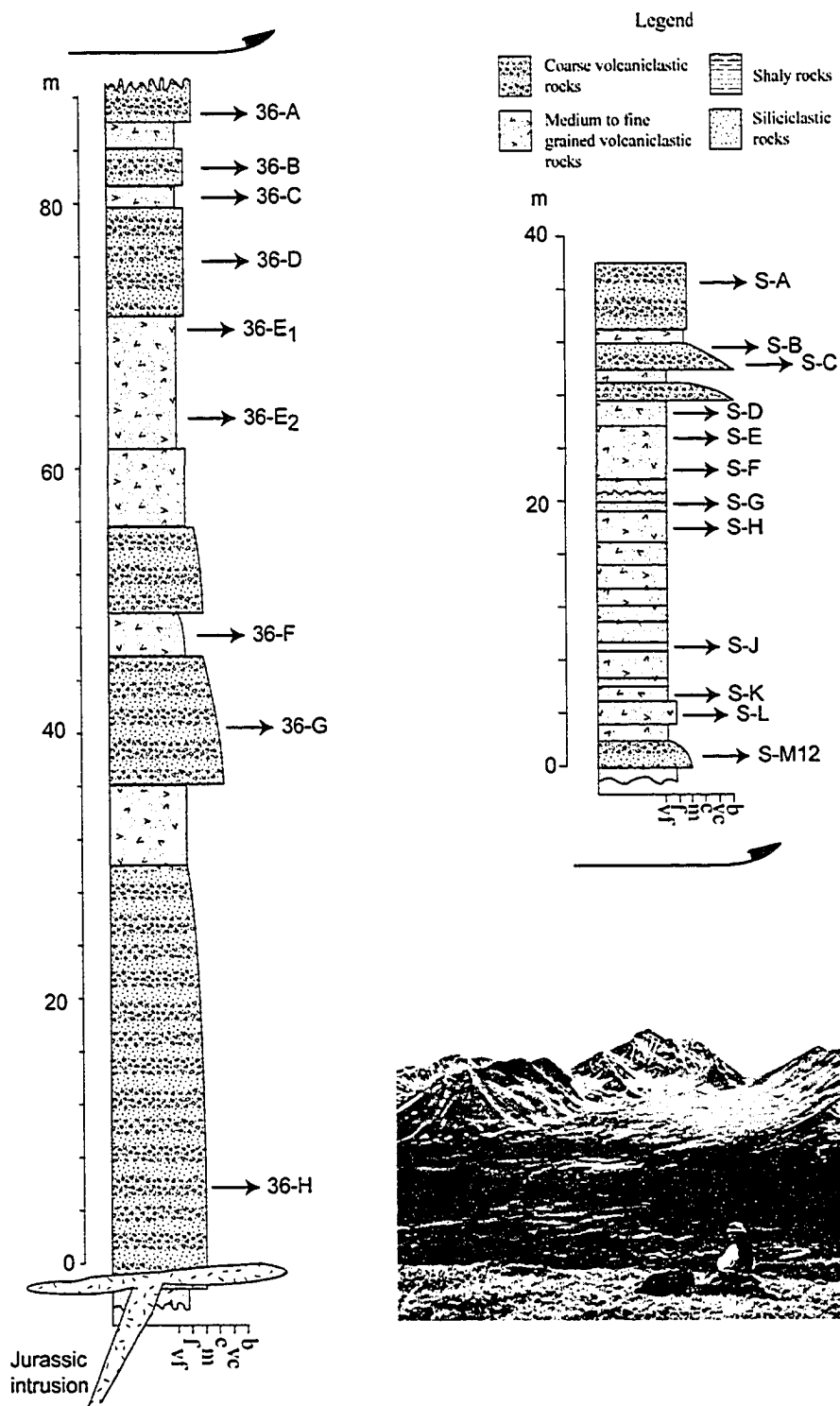
Sample locations on stratigraphic columns from the Butsih Formation. Volcaniclastic Member type area in the Stikine Range. northern British Columbia (W 71°31'58", N 59°35'01"). measured from steep sections on both sides of "Nasty Peak", a prominent peak in the area (peak in the middle on picture above).

Butsih Formation
Upper Clastic Member

Siliciclastic and epiclastic sandstone

Meters-thick sequences of massive and cross-bedded layers of epiclastic and siliciclastic sediments.

Epiclastic very fine grained rock (28-2b, 28-2c)

Grey-green dark very fine grained rock

Clasts/Lihics (ϕ_{moy}<1mm; <10%):
- mafic
- chert

Crystals (ϕ<0.5 mm, <10%):
- Plagioclase (angular fragments)
- Quartz (angular fragments)

Matrix:
- Quartzofeldspathic (?) grennish/brownish matrix covered with very fine biotite (metamorphosed clays?), and chlorite.
- Abundant epidote overgrowth , +/- carbonate

Mount McCleary Formation[2]
Volcaniclastic Member

Coarse crystal/lithic tuff (S-15-4, S-15-3)

Crystals (up to 50%):
- Plagioclase (subrounded)
- Hornblende (primary?, most likely replacing clinopyroxene)

Lithics (up to 60%):
- Quartz grains (rounded; up to 40%)
- Very fine grained clasts (cryptocrystalline; up to 20%)

Matrix (up to 25%):
- Very fine grained quartzofeldspathic material covered by actinolite overgrowth.

Mount McCleary Formation
Alkali-basalt Member

Volcaniclastic beds (S-16-11)

Thinly bedded crystal-tuff

Crystals:
- Plagioclase

Matrix
- Very fine grained quartzofeldspathic matrix, sheared.

Porphyritic lava (S-15-4)

Massive porphyritic lava

Mineralogy

Phenocrysts:
Actinolite, epidote (hornblende or
clinopyroxene relict crystals)

Matrix:
Quartzofeldspathic material, actinolite, epidote, opaque

[2] See following page for Mount McCleary Formation location

Texture
Massive porphyritic lava showing relict shaped Fe-Mg phenocrysts (up to 6 mmϕ; 25%) in a fine grained matrix. No more primary mineralogy preserved. Relict phenocrysts are fairly angular.

Lower clastic member	
Quartz-rich sandstone and siltstone Interbedded quartz-rich sandstone and siltstone couplets.	
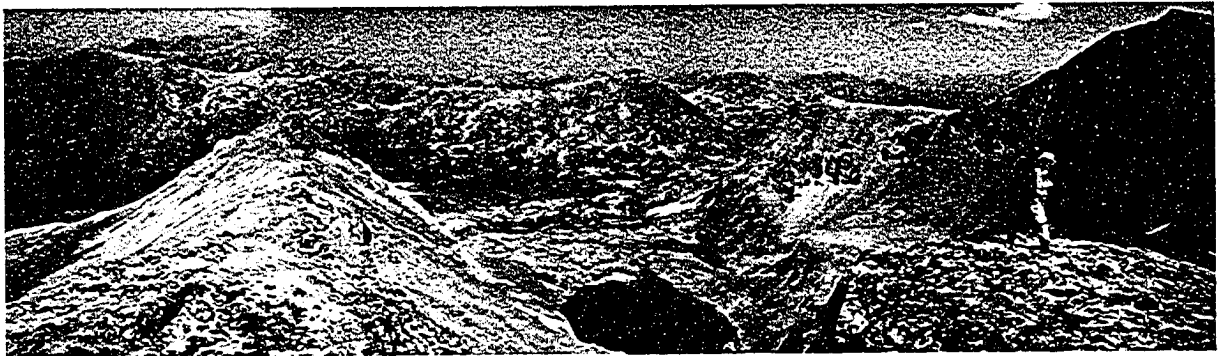
View to the northeast at the type area of Mount McCleary Formation, Englishman Range, southern Yukon (W66°04'26", N60°21'04"). The Mount McCleary Formation (dark cliff on the right, and advancing knob on the left) conformably overlies the English Creek Limestone (light grey rock on the lower right, and underlying the advancing knob on the left). Small rounded lake, 200m across for scale, 300m below the cliff top.

182